Title
Orchestration of Cardiac Gene Expression Mediated by Global Chromatin Architecture

Author
Karbassi, Elaheh

Publication Date
2016

Peer reviewed|Thesis/dissertation

UNIVERSITY OF CALIFORNIA

Los Angeles

Orchestration of Cardiac Gene Expression Mediated by Global Chromatin Architecture

A dissertation submitted in partial satisfaction of the

requirements for the degree Doctor of Philosophy

in Molecular, Cellular, and Integrative Physiology

by

Elaheh Karbassi

2016

ABSTRACT OF DISSERTATION

Orchestration of Cardiac Gene Expression Mediated by Global Chromatin Architecture

by

Elaheh Karbassi

Doctor of Philosophy in Molecular, Cellular, and Integrative Physiology

University of California, Los Angeles, 2016

Professor Thomas M. Vondriska, Chair

The underlying mechanisms by which cell identity is achieved in a cell type-specific manner during development are unknown. In this project, we examine the mechanisms through which genomic architecture is regulated by different protein factors and how these proteins in turn regulate gene expression in the cardiomyocyte. We search for cardiac chromatin structural factors that are important for the establishment of genomic architecture during differentiation. We hypothesized that these candidates would also be implicated in pathological gene expression upon the onset of heart failure. Instead, we found that the expression changes of chromatin structural genes across a panel of different mouse strains were not universal, nor did they correlate with cardiac phenotype after pathological stress. Most of our current knowledge of signaling mechanisms in the heart has stemmed from genetic manipulations in a single mouse strain. Here, we examined well-characterized regulators of cardiac phenotype and showed that the relationships between gene expression and cardiac phenotype are lost when expanding across multiple genetic backgrounds. More importantly, these data demonstrate that there is no single signature gene that drives heart disease (nor is there a single gene whose expression is

a biomarker of the condition), highlighting the role of genetic variability to differentially sculpt the transcriptome in the development and progression of complex diseases. In addition, our findings demonstrate that regulation of gene expression by genetics occurs in a tissue-dependent manner. We previously identified High Mobility Group B2 as an important chromatin structural protein in the heart and showed its involvement in pathological gene expression. These studies suggested this regulation occurs by remodeling global transcriptional activity. To characterize structural organization of cellular transcription, we show that transcriptional activity is compartmentalized into stable factories in the heart that undergo functional changes *in vivo* in response to disease stimuli. We provide evidence of direct reorganization of genomic structure by showing that nuclear positioning of cardiac genes with respect to chromatin environments and transcription factories correlates with changes in their expression. In summary, this project explores the mechanisms of cardiac gene regulation and illustrates multiple levels of regulation, with influences from genetics and chromatin architecture.

The dissertation of Elaheh Karbassi is approved.

Atsushi Nakano

Amy Catherine Rowat

Yibin Wang

Thomas M. Vondriska, Committee Chair

University of California, Los Angeles

2016

TABLE OF CONTENTS

LIST OF FIGURES

LIST OF TABLES

ACKNOWLEDEMENTS

I feel very fortunate and grateful to have been able to conduct my dissertation work and training with my mentor Dr. Tom Vondriska. He has been a figure to aspire to, and I have learned a tremendous amount through his example—from approaches in brainstorming and developing key questions, designing direct experiments, as well as interpreting and presenting data. I am appreciative of his support and encouragement, the learning opportunities that I was presented with, and the resources he has provided me as I prepare for the next steps of my scientific career.

I want to recognize all of the past and present members of the Vondriska lab for their support with this project and creating a positive, enjoyable work environment, in particular: Manuel Rosa Garrido, Emma Monte, Douglas J. Chapski, Shanxi Jiang, Haodong Chen, Todd Kimball, Max Cabaj, Elizabeth Soehalim, Nima Ghorashi and Linqing Wei. I want to thank Manuel for his guidance and example of work ethic and teaching me what it takes to capture a *Nature*-worthy image; Emma for co-leading the analyses of the cardiac transcriptome across genetic diversity (Chapter 5), her enthusiasm and energy; Doug for his help with bioinformatics and statistical analyses and sharing his passion for science; Todd for performing echocardiography and sharing his wisdom; and Haodong for introducing me to and helping me get started with the bioinformatics analyses presented in Chapter 2.

Thank you very much to my committee members Drs. Austin Nakano, Amy Rowat, Yibin Wang and Enrico Stefani. I appreciate their feedback and support, and the opportunities I had to interact with and learn from them, throughout my grad school training. I want to also acknowledge my rotation mentors, Drs. Peipei Ping and Amy Rowat, for exposing me to different approaches and methodologies for studying biological problems; these concepts that I

learned in their labs influenced my perspectives of how we think about gene regulation in this work.

I want to thank the many labs at UCLA that assisted with this project, providing materials and protocols. In particular, I want to acknowledge our collaborators Drs. Jake Lusis, Yibin Wang, Christoph Rau and Jessica Wang who carried out the hybrid mouse diversity panel studies described in Chapter 5. I am very grateful of Drs. Yong Wu and Enrico Stefani for giving me the exciting opportunity of integrating super-resolution microscopy into my project; I appreciate the time they spent with me brainstorming experimental design and approaches for image analysis.

I want to acknowledge Wiley, the American Society for Biochemistry and Molecular Biology and the American Physiological Society for permitting the use of published material presented in this dissertation. I want to recognize the American Heart Association for supporting me with a predoctoral fellowship and the research support of the Vondriska lab from the National Institutes of Health, American Heart Association, David Geffen School of Medicine, Department of Anesthesiology and Perioperative Medicine, and ThermoFisher Scientific.

Lastly, I want to thank my parents, family, and friends for their support and encouragement throughout graduate school.

BIOGRAPHICAL SKETCH

EDUCATION

PhD in Molecular, Cellular, and Integrative Physiology *Expected Fall 2016*
University of California, Los Angeles

Master of Science in Cell and Developmental Biology *September 2010*
University of California, Davis

Bachelor of Arts in Molecular and Cellular Biology *May 2007*
University of California, Berkeley

WORK EXPERIENCE

Quality Control Technician I *02/2011 – 08/2011*
Invivoscribe Technologies San Diego, CA

Research Associate *10/2010 – 01/2011*
Immunovative Clinical Research Carlsbad, CA

Laboratory Technician *10/2007 – 09/2008*
MoBio Laboratories Carlsbad, CA

ORAL PRESENTATIONS

Regulation of Endogenous Chromatin Structure: Insights for Heart Disease. UCLA Molecular, Cellular and Integrative Physiology Retreat. Los Angeles, CA. February 8, 2014

Identification, Quantification and Disease Relevance of Endogenous Cardiac Transcription Factories. UCLA Physiology Department Seminar. Los Angeles, CA. November 14, 2014

Genetic Diversity Operates Through Chromatin Gene Cohorts to Determine Susceptibility to Cardiac Hypertrophy. NHLBI Systems Biology Grantee Meeting. Bethesda, MD. September 11, 2015

Remodeling Chromatin Structure in Heart Disease. UCLA California Nanosystems Institute: Light Sheet Imaging and 3D STED Super-Resolution Microscopy Workshop. Los Angeles, CA. December 8, 2015

POSTER PRESENTATIONS

Karbassi E, Rosa-Garrido M, Vondriska TM. Transcription Factories and Genomic Organization in Cardiovascular Cells. UCLA Department of Molecular Medicine Retreat. Los Angeles, CA. October 19, 2013

Karbassi E, Chapski DJ, Chen H, Jiang S, Kim J, Kimball T, Lopez R, Monte E, Rosa-Garrido M, Shih I, Soehalim E, Vondriska TM. Dynamics of Chromatin Structure Underlying Cardiovascular Health and Disease. UCLA Department of Medicine Research Day. Los Angeles, CA. October 11, 2014

Karbassi E, Monte E, Lopez R, Kim J, Chapski DJ, Rau CD, Wang JJ, Weiss JN, Wang Y, Lusis

AJ, Vondriska TM. Chromatin gene cohorts, not individual cardiac genes, modulate cardiac phenotype in a genetically diverse population. American Heart Association Scientific Sessions. Orlando, FL. November 9, 2015

Karbassi E, Rosa-Garrido M, Chapski DJ, Wu Y, Monte E, Vondriska TM. Structural Reorganization of Cardiac Transcription Factories Mediates Transcriptional Changes in Response to Stress. Basic Cardiovascular Sciences Scientific Sessions. Phoenix, AZ. July 19, 2016

Karbassi E, Rosa-Garrido M, Chapski DJ, Wu Y, Monte E, Vondriska TM. Cardiac Transcription Factories are Dynamic, Mediating Transcriptional Changes in Response to Pathologic Stress. UCLA Cardiovascular Symposium. Los Angeles, CA. September 2, 2016

PEER-REVIEWED PUBLICATIONS

Rosa-Garrido M, **Karbassi E**, Monte E, Vondriska TM. Regulation of chromatin structure in the cardiovascular system. *Circulation J.* 2013. 77:1389-98. PMID: 23575346.

Karbassi E and Vondriska TM. How the proteome packages the genome for cardiovascular development. *Proteomics*. 2014. 14(19):2115-26. PMID: 25074278.

Monte E, Rosa-Garrido M, **Karbassi E**, Chen H, Lopez R, Rau CD, Wang J, Nelson SF, Wu Y, Stefani E, Lusis AJ, Wang Y, Kurdistani SK, Franklin S, Vondriska TM. Reciprocal Regulation of the Cardiac Epigenome by Chromatin Structural Proteins HMGB and CTCF: Implications for Transcriptional Regulation. *J Biological Chemistry*. 2016. 291(30):15428-46. PMID: 27226577.

Karbassi E, Monte E, Chapski DJ, Lopez R, Rosa-Garrido M, Kim J, Wisniewski N, Rau CD, Wang J, Weiss JN, Wang Y, Lusis AJ, Vondriska TM. Relationship of Disease-Associated Gene Expression to Cardiac Phenotype is Buffered by Genetic Diversity and Chromatin Regulation. *Physiological Genomics*. 2016. 48(8):601-15. PMID: 27287924.

Karbassi E, Rosa-Garrido M, Chapski DJ, Wu Y, Stefani E, Wang Y, Monte E, Vondriska TM. Endogenous Structural Reorganization of Cardiac Chromatin Mediates Transcriptional Changes in Response to Hypertrophic Stress. *In preparation.*

HONORS AND AWARDS

Excellence in Science award, UCLA Department of Molecular Medicine Retreat *10/2013*

Best of American Heart Association Specialty Conferences: Basic Cardiovascular Sciences *2016*

RESEARCH SUPPORT

UCLA Molecular, Cellular and Integrative Physiology NIH Institutional Training Grant
5T32GM065823-09, 5T32GM065823-10 *10/2011 – 06/2013*

American Heart Association Predoctoral Fellowship
15PRE22700005 *01/2015 – 12/2016*

Introduction

Heart failure is the condition in which the heart is unable to maintain circulatory function, with multiple etiologies including age. It is responsible for 1 in 9 deaths in the US (1). Some common causes include hypertension, ischemia and cardiomyopathies (2), with top risk factors such as coronary heart disease, smoking, high blood pressure and obesity (1). There is currently no effective cure to directly target heart failure. Present therapies—including angiotensin converting enzyme inhibitors, beta blockers and aldosterone antagonists—are administered during the early stages of the disease when neurohormonal responses are induced, but advanced stages of heart failure demand more complicated procedures, for example implantation of mechanical assist devices and/or require heart transplantation (2). The pathological remodeling on the organ and cellular levels is irreversible. While preventative measures, such as changes in lifestyle, and pharmacologic intervention can help reduce the risks and symptoms, the ultimate goal and challenge remains to develop strategies to reverse these processes upon onset.

Characteristic changes involve thickening of the ventricular walls, increased cell size, impaired calcium handling and contractility, fibrosis and cell death (3). These pathological changes have also been reflected on the level of gene expression in animal models and human patients (4, 5). The global changes in gene expression profile are orchestrated by DNA organization in the nucleus of the cell. While every cell in our body has the same DNA sequence, each cell is unique in that it expresses its own set of genes that give the cell its identity and allow it to serve its function. We now know that different cell types have their own genomic architecture (6, 7). *How does the genome know to package itself in such a way to destine the cell for a particular lineage? What are the key factors involved in this process? What are the structural features of the cardiac genome?* While we have begun to characterize regulators of DNA accessibility and gene expression (most of which have been studied on the nucleosomal level) (8), very little is known

about how these processes are integrated to establish global genomic architecture and phenotype.

The cardiomyocyte is a unique system to study gene regulation. Unlike other cells that undergo dynamic changes in DNA packaging throughout their cell cycle, the myocyte is a fully differentiated post-mitotic cell. Moreover, cardiomyocyte turnover occurs at very low rates (9), implicating that the genome integrity is maintained over the course of the cell's lifetime. This suggests that changes to genome structure due to stress must therefore be targeted events to affect gene expression; the factors in this process have not been identified. The goal of this project is to understand the basic biology behind the regulation of cardiac gene expression and characterize the chromatin structural features and mechanisms by which pathological stress can influence the cardiac transcriptome. Here, we review different chromatin regulators that are essential for cardiac development and present our approaches for identifying candidate chromatin structural regulators that are important for the establishment and maintenance of the gene expression program in cardiomyocytes. We next investigate global chromatin architecture and cardiac transcriptional activity, mediated by chromatin structural proteins HMGB2 and CTCF. Then we examine transcriptome patterns across a genetically diverse panel of mouse strains before and after pathological stress and demonstrate that genetics has partial contribution to gene expression and provide support for chromatin structure as another tier of gene regulation. Finally, we investigate the properties of cardiac transcription factories and show direct evidence of genomic rearrangements in the nucleus upon pressure-overload stress. We hope to characterize features of cardiac chromatin structure that are important for the establishment of gene expression and may be disrupted with stress; these will contribute to our understanding of cellular differentiation and provide input into potential explanations for irreversibility of pathological gene expression that can be implemented in future therapies.

Introduction: References

1. Mozaffarian D, Benjamin EJ, Go AS, Arnett DK, Blaha MJ, Cushman M, Das SR, de Ferranti S, Despres JP, Fullerton HJ, Howard VJ, Huffman MD, Isasi CR, Jimenez MC, Judd SE, Kissela BM, Lichtman JH, Lisabeth LD, Liu SM, Mackey RH, Magid DJ, McGuire DK, Mohler ER, Moy CS, Muntner P, Mussolino ME, Nasir K, Neumar RW, Nichol G, Palaniappan L, Pandey DK, Reeves MJ, Rodriguez CJ, Rosamond W, Sorlie PD, Stein J, Towfighi A, Turan TN, Virani SS, Woo D, Yeh RW, Turner MB, Comm AHAS, Subcomm SS. Heart Disease and Stroke Statistics-2016 Update A Report From the American Heart Association. Circulation. 2016;133(4):E38-E360. doi: 10.1161/Cir.0000000000000350. PubMed PMID: WOS:000369259500002.
2. Pazos-Lopez P, Peteiro-Vazquez J, Carcia-Campos A, Garcia-Bueno L, de Torres JP, Castro-Beiras A. The causes, consequences, and treatment of left or right heart failure. Vasc Health Risk Manag. 2011;7:237-54. doi: 10.2147/VHRM.S10669. PubMed PMID: 21603593; PMCID: PMC3096504.
3. Mann DL, Bristow MR. Mechanisms and models in heart failure: the biomechanical model and beyond. Circulation. 2005;111(21):2837-49. doi: 10.1161/CIRCULATIONAHA.104.500546. PubMed PMID: 15927992.
4. Razeghi P, Young ME, Alcorn JL, Moravec CS, Frazier OH, Taegtmeyer H. Metabolic gene expression in fetal and failing human heart. Circulation. 2001;104(24):2923-31. doi: DOI 10.1161/hc4901.100526. PubMed PMID: WOS:000172701300027.
5. Taegtmeyer H, Sen S, Vela D. Return to the fetal gene program A suggested metabolic link to gene expression in the heart. Ann Ny Acad Sci. 2010;1188:191-8. doi: 10.1111/j.1749-6632.2009.05100.x. PubMed PMID: WOS:000277731600025.

6. Parada LA, McQueen PG, Misteli T. Tissue-specific spatial organization of genomes. Genome Biol. 2004;5(7):R44. doi: 10.1186/gb-2004-5-7-r44. PubMed PMID: 15239829; PMCID: PMC463291.
7. Dixon JR, Jung I, Selvaraj S, Shen Y, Antosiewicz-Bourget JE, Lee AY, Ye Z, Kim A, Rajagopal N, Xie W, Diao Y, Liang J, Zhao H, Lobanenkov VV, Ecker JR, Thomson JA, Ren B. Chromatin architecture reorganization during stem cell differentiation. Nature. 2015;518(7539):331-6. doi: 10.1038/nature14222. PubMed PMID: 25693564; PMCID: PMC4515363.
8. Rosa-Garrido M, Karbassi E, Monte E, Vondriska TM. Regulation of chromatin structure in the cardiovascular system. Circ J. 2013;77(6):1389-98. PubMed PMID: 23575346; PMCID: PMC3704339.
9. Bergmann O, Zdunek S, Felker A, Salehpour M, Alkass K, Bernard S, Sjostrom SL, Szewczykowska M, Jackowska T, Dos Remedios C, Malm T, Andra M, Jashari R, Nyengaard JR, Possnert G, Jovinge S, Druid H, Frisen J. Dynamics of Cell Generation and Turnover in the Human Heart. Cell. 2015;161(7):1566-75. doi: 10.1016/j.cell.2015.05.026. PubMed PMID: 26073943.

Chapter 1: How the Proteome Packages the Genome for Cardiovascular Development

Elaheh Karbassi and Thomas M. Vondriska

[This research was originally published in Proteomics by Karbassi et al. How the proteome packages the genome for cardiovascular development. *Proteomics*. 2014. 14(19):2115-26. PMID: 25074278. © Wiley.]

Abstract

The devastating impact of congenital heart defects has made mechanisms of vertebrate heart and vascular development an active area of study. Because myocyte death is a common feature of acquired cardiovascular diseases and the adult heart does not regenerate, the need exists to understand whether features of the developing heart and vasculature—which are more plastic—can be exploited therapeutically in the disease setting. We know that a core network of transcription factors governs commitment to the cardiovascular lineage, and recent studies using genetic loss-of-function approaches and unbiased genomic studies have revealed the role for various chromatin modulatory events. We reason that chromatin structure itself is a causal feature that influences transcriptome complexity along a developmental continuum, and the purpose of this article is to highlight the areas in which 'omics technologies have the potential to reveal new principles of phenotypic plasticity in development. We review the major mechanisms of chromatin structural regulation, highlighting what is known about their actions to control cardiovascular differentiation. We discuss emergent mechanisms of regulation that have been identified on the basis of genomic and proteomic studies of cardiac nuclei and identify current challenges to an integrated understanding of chromatin structure and cardiovascular phenotype.

Introduction

Cardiac development involves signaling by stage-specific transcription factors that define branching into cellular lineages. Cardiomyocytes arise from the mesoderm (marked by Brachyury and Mesp1), in which cardiac-determined cells of the primary heart fields fuse to form the bilateral cardiac crescent structure (1-4). The bilateral fields of the cardiac crescent merge and differentiate into progenitor cells (marked by Nkx2-5 and Isl1) of the linear heart tube that then mature into cardiomyocytes (marked by Myh6 and Myh7) (1-3, 5). Tissue from the primary heart field will develop into the left ventricle and atria while the precursor cells of the second heart field will contribute to the right ventricle, atria and outflow tract (5, 6); both heart fields have potential to also contribute to the coronary vasculature (7). Later developmental events include cardiac looping, formation of the outflow tract that will give rise to the pulmonary artery and aorta, and atrial-ventricular septation (4). Brachyury-expressing mesoderm cells can differentiate into hematopoietic cells and myocytes (8) while Mesp1-positive pre-cardiac cells are restricted to smooth muscle or cardiomyocyte fate (9). Mesp1 can induce expression of cardiac transcription factors, including Gata4 and Mef2c (9), and is required for heart tube formation (10). Cardiac progenitors can diverge to give rise to cardiomyocytes, cardiac fibroblasts, endothelial cells and smooth muscle (7, 11). Although GATA4, NKX2-5 and TBX5 are necessary transcription factors for myocyte proliferation and cardiac morphogenesis (12, 13), how these signaling pathways regulate chromatin architecture to fine tune global gene expression patterns and the chromatin level factors that determine specialization of cardiomyocytes into atrial, ventricular, and conduction cells remain unknown.

Genome organization in the three-dimensional nuclear space, shaped by temporal and spatial presence of protein factors, underlies differences in cell type-specific transcriptomes. DNA is wound around core histone units (H2A, H2B, H3 and H4) to form the nucleosome, the primary structural unit of chromatin. Chromatin can be loosely packaged into euchromatin, which can allow for gene expression, or tightly packaged into heterochromatin, associated with silenced

regions of the genome. There are stark differences in the packaging of the genome in different cell types and along the same lineage at different stages of development (Figure 1-1). The mechanisms to establish and modify chromatin structure include histone post-translational modifications (PTMs), histone variants, nucleosome positioning (e.g. by ATP-dependent chromatin remodelers), non-nucleosomal chromatin structural proteins, DNA modifications and noncoding RNAs (Figure 1-2). During terminal differentiation of the cardiomyocytes, there is an overall shift from euchromatin to heterochromatin (14) and decrease in transcriptional activity (15) (Figure 1-3). These changes determine cell identity by regulating chromatin packaging in a manner conducive to production of the desired transcriptome—that is, by making the right genes accessible to transcription factors and RNA polymerase. The chromatin structural features of cardiomyocytes remain uncharacterized—furthermore, we have only limited understanding of the mechanisms that establish chromatin structure and delineate phenotype during development. While some aspects of chromatin structure are globally altered with disease, cells do not change from one type to another, implying that a baseline skeleton of the chromatin anatomy is firmly set with development. This baseline skeleton is non-random and reproducible, as determined by global chromosome conformation capture and imaging studies (16, 17). The role of individual chromatin remodeling proteins and histone modifiers has also been recognized in cardiovascular development, yet only recently have studies begun to emerge using genome or proteome-wide studies to characterize this process in an unbiased manner. We summarize herein what is known about the key chromatin structural regulators involved in cardiac development (please see Supplemental Table 1-1 for a comprehensive list of gain/loss of function studies on chromatin regulators in cardiovascular development) and place an emphasis on emergent areas in which proteomics and systems biology can advance our understanding of the epigenetics of development.

Histone Variants and Post-Translational Modifications

Histone methylation and acetylation are the best-studied histone PTMs that, depending on the residue they target, can be indicative of gene repression or activation. Trimethylation of histone H3 at lysine 4 (H3K4me3) is a mark for euchromatin (18) while methylation at lysine 27 (H3K27me3) (19) and lysine 9 (H3K9me3) (20) label heterochromatin, facultative and constitutive respectively. Promoters containing both H3K4me3 and H3K27me3 are labeled poised—meaning they can be selectively activated or silenced in a lineage-specific manner—and are characteristic of regulators of differentiation. Reader proteins that are selective for these histone modifications can further influence accessibility and packaging of the DNA. While a number of other types of histone PTMs have been identified, principally by mass spectrometry (21), the individual functions in chromatin maintenance and regulation of packaging are less established, and how these modifications interact in a coordinate fashion to mediate chromatin architecture during developmental transitions, is yet to be determined.

Although these modifications were originally described in non-cardiovascular cells, many have been shown to be operative in the cardiovascular systems, with the most abundant evidence coming from naturally occurring or experimental disruption of the histone-modifying enzymes. In one recent and unbiased example of the former, examination by exome sequencing of human congenital heart disease patient samples revealed an increased incidence of *de novo* mutations occurring at genes involved in depositing, removing and reading H3K4me3 or H2BK120 ubiquitination marks (22). This study is strong rationale for more ‘omics investigations into how myocyte-specific gene expression is coordinated across the genome: because disruption of any one of various histone modifying enzymes alone is sufficient to induce cardiac development defect, transcriptional circuits in cardiac development can be hypothesized to involve a panoply of histone modifications at various genes—some activating and some inhibiting—in addition to transcription factors. The mutations identified in Zaidi *et al*. occurred in various enzymes in the language of histones (those depositing, reading and removing modifications)—the next step will

be to determine which loci are targeted by these enzymes during development, and whether networks can be built to understand convergent targets amongst the group of altered histone modifiers (e.g. Do the enzymes modified by de novo mutations all target the same genes?).

The Polycomb Repressive Complex 2 (PRC2) is a multiprotein complex involved in depositing H3K27me3. Evaluation of PRC2 in the mouse heart has implicated it in development and maintenance of appropriate gene expression (23). Inactivation of Ezh2, a protein component of PRC2, resulted in hypoplasia, septal defects and atrial dilation in embryos—mice surviving to adulthood had septal defects, hypoplasia, fibrosis and impaired systolic function (23). Chromatin immunoprecipitation sequencing (ChIP-seq) and RNA sequencing (RNA-seq) studies demonstrated that Ezh2 is critical for ventricle-specific gene expression and silencing of non-cardiomyocyte transcription factors during the early stages of heart development (23). At the same time, removal of H3K27me3 is also required for differentiation into cardiovascular cells. JMJD3, a histone demethylase, enables expression of mesoderm marker, *brachyury*, by removing H3K27me3 at its promoter, in differentiating embryonic stem cells (24). Jmjd3 knockout in embryonic stem cells prevents differentiation into mesoderm and cardiomyocytes by disallowing expression of genes necessary for differentiation (i.e. Mesp1, Nkx2-5 and other cardiac structural proteins) (24).

The Smyd family of lysine methyltransferases has been implicated in gene regulation, with Smyd1 shown to be specific to cardiac and skeletal muscle (25). Knockout of Smyd1 is embryonic lethal in mice, in part due to incomplete development of the right ventricle (25). In zebrafish, Smyd1 is important in the maintenance of sarcomere organization (26, 27), perhaps independent of its functions through chromatin. WHSC1 is another histone methyltransferase, shown to establish H3K36me3 marks (28). WHSC1 can also interact with cardiac transcription factor NKX2-5 to suppress expression of cardiac progenitor genes (28), and loss of Whsc1 function leads to

congenital heart defects (28). Furthermore, interactions between different histone methylating complexes are highly coordinated. For example, PHF19, a reader protein, can recognize and bind to H3K36me3 in stem cells to recruit H3K36me3 demethylase NO66, while at the same time recruiting PRC2 to shift from H3K36me3 to H3K27me3 modification (29) and thereby silence Polycomb target genes. JARID2, a transcriptional repressor, has been shown to regulate histone methylation during development via association with PRC2 to promote normal differentiation of mouse embryonic stem cells (30). In addition, stem cell differentiation entails transitioning into a more heterochromatic state through accumulation of H3K9 methylation (14, 31). In the developing heart, JARID2 was found to interact with H3K9 methyltransferase, SETDB1 (32), highlighting another role for JARID2. JARID2 knockout mice had global reduction in H3K9 methylation as well as cardiac developmental impairments, including septal defects and hypertrabeculation (32). It is unclear how JARID2 regulates different histone modifications observed in stem cells and developing heart tissue, and whether its role is specific to the target gene or developmental stage, and/or dependent on other unidentified factors. Histone modification complexes can interact with cardiac transcription factors to co-regulate target genes. JMJD3 closely associates with TBX5 to target promoters and regulate cell fate (33). Overexpression of Isl1 can promote expression of other cardiac transcription factors (Gata4, Nkx2-5 and Mef2c) through increased H3 acetylation at these genes (34). These findings have provided a link between the functions of chromatin structure and tissue-specific transcription factors.

Histone acetylation is another modification required for development. p300 and CBP histone acetyltransferases show peak expression during embryonic development that is reduced in the adult heart (35). Mice with mutated p300 exhibit septal defects and ventricular hypoplasia in addition to other systemic developmental defects (36, 37) and roles in adult heart disease (38). Class I and II histone deacetylases (HDAC) are critical for cardiac chamber development, proliferation and function. HDAC1 and HDAC2 (Class I HDACs) are functionally redundant (39),

but a cardiac-specific double knockout results in inappropriate upregulation of genes associated with stress response, calcium handling and the contractile apparatus (39). Overexpression of HDAC3 (Class I) regulates cardiomyocyte proliferation during development by repressing cell cycle inhibition genes (40). HDAC7 (Class IIa) mutant mice have impaired vascular remodeling by upregulation of matrix metalloproteinase that interferes with vessel integrity during development (41). HDAC5 and HDAC9 (Class IIa) serve redundant functions—suppressing stress-induced genes—and are required for development of ventricular walls and septum formation (42). Class III sirtuins and class IV HDACs are less characterized in the context of chromatin and cardiac development. Some studies have suggested low sirtuin activity correlates with cardiac disease phenotypes (43, 44), whereas other studies have demonstrated their requirement for normal blood vessel formation and the angiogenic response to ischemia (45). The different classes of HDACs with inherent functional redundancy may reflect a mechanism that has evolved for tight control of chromatin structure in a stage-specific manner during development and in a cell type-specific manner in disease.

In addition to covalent modifications of histone tails, histone variants present another level of complexity to chromatin structure by altering DNA packing in the nucleosome, interactions with other core and linker histones, and interactions with DNA repair and transcriptional machinery to regulate nucleosome stability (46). H2A.Z, an H2A variant, is present in nucleosomes near transcription start sites of active genes (47). While associated with nucleosome depletion and open chromatin formation, H2A.Z was also found to be enriched at bivalent promoters, marked with H3K27me3, and in close proximity with transcription start sites of genes that determine cell fate, such as transcription factors, in mouse embryonic stem cells (48). In differentiating neuronal precursor cells, H2A.Z enrichment is associated with active genes, and it is required for differentiation *in vitro* (48). While it is known that H2A.Z is upregulated during cardiac hypertrophy (49), the specific role it plays in regulation of cardiomyocyte differentiation and heart development

has not been established. Other histone variants have not been explored in detail in cardiac development, although the available proteomic literature on the adult indicates that the mouse heart expresses a wide range of variant isoforms for each of the four core histones, as well as for linker histone H1 (50).

One limitation in the histone acetylation/methylation literature in particular has been an absence of genome-wide ChIP-seq studies in cardiovascular cells, in large part due to low endogenous expression of these enzymes and cellular heterogeneity in complex tissues like heart and vasculature. These investigations are needed to determine, in a developmental stage-specific manner, the distribution of individual histone-modifying enzymes as well as their target histone PTMs along the genome. As a result, many loss-of-function studies may reveal phenotypes that are the result of overlapping chromatin-modifying enzymes. Recent studies have made headway in this area with histone marks themselves in isolated cell models of cardiac development (3, 51), as well as in the adult heart (notwithstanding the issues of uncertain cell type contribution when working from endogenous cardiac tissue) during disease (52, 53). *In vitro* differentiation of cardiomyocytes has shown the regulation by histone PTMs at key cardiac genes (51). Genes encoding for cardiac transcription factors are enriched with H3K27me3 marks and poised for activation at early primitive stages (51). During differentiation and concomitant with transcription factor activation, there is a decrease in the silencing H3K27me3 mark and parallel increases in active H3K4me3 and H3K36me3 (associated with transcriptional elongation) marks (51). Meanwhile, cardiac structural genes, when turned on, accumulate H3K4me3 and H3K36me3 and lack the additional level of regulation by H3K27me3 (51). These findings highlight the necessity of appropriate global chromatin remodeling by histone modifications, in addition to expression of master regulators, for the coordinated activation of developmental stage-specific genes. Future studies using ChIP-seq for endogenous histone-modifying enzymes will be required to elucidate

how these proteins coordinate with cardiac transcription factors *in vivo* and at different developmental stages.

ChIP-seq studies for histone PTMs have characterized distal regulatory elements and revealed cardiac-specific enhancers important for developmental and stage-specific regulation of cardiac genes. These enhancers are not static—rather, they serve a temporal role during both differentiation *in vitro* and development (54) with precise coordination of activity with the putative binding and expression of cardiac transcription factors (3). Observations to date have characterized enhancer function by association with the nearest gene on the chromosome without taking endogenous three-dimensional organization into account. As such, structural enhancers—that is, permissive features of chromatin that play a role in endogenous architecture, are distal from the genes they regulate on the DNA strand but near said genes in the endogenous chromatin environment—have not been examined in cardiovascular development. Future studies integrating the current enhancer datasets with three-dimensional chromatin architecture measurements (17) will be important to understand how organization of the genome is coordinated *in vivo* to orchestrate cell fate—whether these enhancers are shared or distinct from those associated with cardiac hypertrophy (52) is another question that, when answered, will advance our understanding of the scales at which cellular programming in disease mimics that in development.

ATP-Dependent Chromatin Remodelers

ATP-dependent chromatin remodelers are critical regulators of DNA accessibility for gene expression and silencing by mediating nucleosome positioning, occupancy and histone variant composition (55, 56). There are four classes of remodelers: SWI/SNF, ISWI, NuRD and INO80. The SWI/SNF complexes have been widely studied in the heart, in both development and disease models. The BAF and PBAF complexes are examples of the mammalian SWI/SNF complex and are composed of multiple subunits, interchanging of which can confer target loci specificity (e.g.

the BAF complex has the BAF250 subunit while the PBAF complex incorporates BAF200 and BAF180 (57)). BAF180 normally co-regulates target genes with nuclear receptors and its deletion results in ventricular wall hypoplasia, whereas BAF250 deletion leads to lethality (58). BAF250a participates in normal cardiac progenitor cell differentiation—loss of BAF250a leads to pervasive cardiac developmental defects and death, acting by inhibiting cellular proliferation. These actions appear to proceed through binding of BAF250a in the promoters of various cardiac transcription factors (59), although global targets of the proteins in the heart remain unknown. BAF250 regulation of Gata4, Mef2c, Nkx2-5 and Bmp10 expression is mediated through increasing DNA accessibility at promoters (59). In agreement with this observation, BAF250a mutations in embryonic stem cells limit pluripotency potential and prevent differentiation into cardiomyocytes (60). In addition to its role in cardiac hypertrophy (61), the ATPase catalytic subunit BRG1 is required for cardiac development (62), and the stoichiometry of interactions amongst BRG1 and TBX transcription factors can mediate transcription of target cardiac genes (62).

BAF60c is specific to the developing heart and, like BRG1, can mediate interactions with cardiac transcription factors to specify cardiac gene expression (63). Specific targeting of remodeling complexes may arise with from readers of histone modifications. DPF3 is a muscle-specific protein that can interact with methylated and acetylated histones as well as members of the BAF complex (64). DPF3 is necessary for zebrafish cardiac development and can localize BAF chromatin remodeling complexes to cardiac-specific genomic loci to regulate gene expression (64). In addition to normal development, there is evidence that chromatin remodelers are important for cardiomyocyte differentiation from an induced pluripotent state. GATA4 requires the presence of BAF60c to act on target genes, and together with TBX5, this complex is sufficient to induce differentiation of non-cardiac mesoderm into beating cardiomyocytes (65).

The roles of the other classes of ATP-dependent remodelers have not been well defined in the heart. The CHD4 of NuRD complex is important for maintenance of vascular integrity *in vivo* by directly regulating expression of extracellular matrix proteases (66). Recently, it was found that BAF250a can interact with NuRD complex to repress transcription in P19 carcinoma cells (67) although the implications for a role of NuRD in cardiac development are unclear. The efficiency of activity of ATP-dependent chromatin remodelers can also depend on association with histones as observed with ISWI. ISWI ATPase activity requires recognition of H4 tails (68), and this interaction and level of ISWI activity are higher in the presence of H2A.Z variants (69). ISWI ATPase Drosophila mutants demonstrate requirement of ATPase activity for chromosome compaction and higher-order structure, which can be mediated through recruitment of linker histones (70). It is anticipated that roles for these remodelers will be tested soon using loss-of-function approaches in the developing heart.

A common theme with ATP-dependent chromatin remodelers is that the combinatorial composition of their subunits can confer specificity of action. Much of the knowledge of subunit composition has been imported to the cardiac field from non-cardiac systems and then tested with loss-of-function approaches, as described in the foregoing paragraphs. A frontier for cardiac-specific chromatin remodeling is the application of interactome mapping targeted at chromatin remodeling complexes in the myocyte. Affinity isolation and proteomic mass spectrometry need to be applied to characterize these complexes in an unbiased manner at different developmental stages, to reveal not only interactions with known cardiac transcription factors, but also with other regulators of activity and gene targeting. Methods like the INTACT approach (71), which uses genetic labeling of specific proteins in a lineage of interest, hold great promise, as they obviate concerns of cell type specificity and recovery of endogenous proteins.

DNA Methylation

DNA methylation is a direct modification of cytosine, associated with gene silencing when present in promoters, enriched at CG-rich regions (CpG islands), and expression when present within gene bodies. There are global increases in DNA methylation during cellular differentiation. *De novo* methylation by DNA methyltransferases, DNMT3a and DNMT3b, is essential for early differentiation in embryonic stem cells (72). Dnmt3b mutations in mice are lethal, showing incomplete ventricular septum formation in addition to other systemic defects interfering with vascular and liver development (73). A model for how DNA methylation contributes to higher-order chromatin structure (between the scale of nucleosome and chromosome) is currently lacking, and it is commonly assumed that this epigenetic mark works in concert with histone modifications to specify chromatin states.

DNA methylation can recruit different sets of protein interacting partners. Methyl-CpG binding protein (MeCP2) is a DNA methylation binding protein that is required for mouse development (74). MeCP2 can serve as a reader of methyl-cytosine to regulate establishment of heterochromatin by recruiting remodeling machinery to modify histones, such as deacetylation of H4 and methylation of H3K9, thereby silencing genes during development (75). In developing cardiomyocytes, there are increases in the expression of Dnmts and methyl-cytosine binding proteins (76), and DNMT activity inhibition in this system can result in net increases in euchromatic histone marks, H3 and H4 acetylation and H3K4me3 (76). An increase in DNA methylation can result in the binucleation and terminal differentiation of cultured fetal cardiomyocytes (77). Changes in methylation states at promoters in genes involved in cardiac development, including EGFR, Tbx5 and Nkx2-5, have been observed in congenital heart disease cases (78). These findings implicate DNA methylation as an important regulator of cardiovascular development worthy of further exploration.

Global methylome studies using bisulfite treatment and DNA sequencing—which would reveal the totality of modified CpGs and shed light on how methylation correlates with chromatin marks and transcription on a global scale—have not been reported for the heart. Studies from adult human tissue in the setting of heart disease indicate global changes in methylation (79), but even in this arena case-control studies are lacking to understand the basal differences in DNA methylation between cells in the cardiovascular lineage. A frontier in this field will be combining DNA methylomics with protein identification—either by looking for interacting partners of known methyl-cytosine binding proteins, or by screening for novel, cardiac-specific methyl-cytosine proteins directly, as has been proposed in other systems (80)—only with this approach will we understand how DNA methylation contributes to high-order chromatin structure, by linking nucleotide modification to protein interaction with chromatin structure as a readout.

Chromatin Structural Proteins

Chromatin structural proteins, which modulate accessibility and local packing independent of direct enzymatic activity, play a role in the establishment and/or maintenance of chromatin architecture and accessibility through direct and indirect mechanisms. Non-nucleosomal structural proteins, linker histone H1 and heterochromatin-associated HP1, have dynamic interactions in stem cell nuclei and become immobile as cells differentiate to establish high-order structure (81), suggesting the proteins participate in setting the chromatin scaffold during development. Levels of histone H1 variants are associated with differentiation of stem cells, with increases in H1.0 variant occupancy at pluripotency genes allowing for silencing of these genes and progression of stem cell differentiation (82, 83). Both linker histones and high mobility group B (HMGB) proteins have been implicated in global increases in transcriptional activity in heart disease (84), although their role in development remains unknown. HMGA2, on the other hand, is an important regulator of cardiomyocyte differentiation and proliferation and can bind to the promoter of Nkx2-5 to directly regulate its expression (85). HMGA proteins are expressed

abundantly during early development, with low expression in mature cells (86). Some genomic territories, like the nucleolus, are associated with specific chromatin-binding proteins (87). Studies from zebrafish have implicated Nucleolin in ribosomal RNA biosynthesis and proper heart formation, a role that may be recapitulated in the setting of disease in mammalian models (88).

The nuclear envelope is an important site for anchoring of repressed genes and accordingly hosts silencing machinery (89, 90). Proteins of the nuclear envelope physically interact with the cellular cytoskeleton enabling communication between cytoplasmic functions and cellular mechanics with nuclear properties and gene expression. There is also significant evidence that specific nuclear envelope proteins silence genes during cardiac lineage commitment, with lamins being a well-characterized example. Lamin A/C has been shown to tether chromatin to the nuclear envelope and reduce the plasticity in differentiated cells (91). Stem cell-derived cardiomyocytes have increased lamin A/C expression, which is undetectable in embryonic stem cells (92). Compared to other mature organs, the heart expresses high levels of lamin A (93). While not required during early mouse development (94), lamin A/C knockout mice develop dilated cardiomyopathy with reduced cardiac function and have shortened lifespan, which can be improved upon reintroduction of lamin A transgene (95). Furthermore, low lamin A levels in dilated cardiomyopathy patients was associated with disrupted nuclear morphology and heterochromatin deposition (96). Lamin A/C knockout results in globally altered chromatin structure to adapt an inverted conversion, such that heterochromatin accumulates in the center of the nucleus (97), demonstrating the role of lamins in genomic-scale organization of heterochromatin at the nuclear envelope.

Differentiation of human myoblasts has provided evidence for global physical restructuring of chromatin and the nucleus (98). Upon differentiation, the nucleus undergoes a reduction in volume and flattens out with dynamic changes in spatial positioning of chromosomes (98) (Figure 1-3). It is understood that the cytoskeleton can influence nuclear properties, but whether and how

chromatin architecture can influence nuclear plasticity and cell function has not been explored in the heart.

A major unanswered question in the field of chromatin structural proteins relates to the basic logic of their function. There have been reports of binding partners for HMG proteins and linker histones, but unlike the chromatin remodeling complexes, transcription factors and histone-modifying enzymes, there is a lack of consensus for the protein complexes in which non-nucleosomal chromatin structural proteins operate. In addition, there have been recent ChIP-seq studies (albeit not from cardiovascular cells) on HMGs (99), CTCF (100) and linker histone proteins (101) suggesting that while some isoforms have apparent consensus sequences that influence their binding, others do not (102, 103). Unlike histones, the extent and functional consequences of PTM on non-nucleosomal proteins is not well understood. Are these proteins non-specific “bricks and mortar” for genome packaging or do they form distinct species of complexes, perhaps with regulation through PTM, and have individual target loci? Answers to these questions will require creative combination of proteomics to map protein complexes with epigenomics to determine which members of said complexes confer specificity.

Noncoding RNAs

Constituting the majority of distinct transcripts when compared to protein-coding RNA, noncoding RNAs (ncRNA) have been implicated in chromatin structure through regulation of histone-modifying enzymes (104, 105), DNA methylation (106), promoter binding (107), as well as alternative splicing and other post-transcriptional processing of mRNA (108). miRNAs have an increasingly recognized role in cardiac development and adult heart regulation (109, 110), acting mostly through regulation of mRNA abundance (111, 112). The individual requirements of miRNAs have been reviewed in greater detail (113, 114). Long noncoding RNAs (lncRNA) have been proposed to regulate interactions between DNA, RNA and proteins via their secondary

structure (108). In such a role, lncRNAs are thought to serve as a scaffold between different sets of molecules to alter chromatin structure and gene expression in a locus-specific manner. Thus, lncRNAs have the potential to solve a major riddle of chromatin biology: how are chromatin remodeling enzymes and structural proteins targeted to the correct genes in a development- and stimulus-responsive manner? lncRNAs, which are expressed at low levels (in comparison to the abundance of protein-coding mRNAs), show a high degree of tissue specificity (115) and can be regulated directly by tissue-specific transcription factors (116). lncRNAs are important for maintaining pluripotency as well as repressing tissue specification programs in mouse embryonic stem cells (117). A large percentage of lncRNAs associate with complexes involved in writing, erasing and reading histone modifications, with H3K27me3 and H3K4me3 being well-established targets (104, 105, 117), and have specifically been shown to positively regulate transcription through recruitment and targeting of H3K4 methyltransferases (105, 118).

lncRNAs, *Braveheart* and *Fendrr*, are specific and critical for cardiac differentiation and examples of lncRNAs that regulate gene silencing machinery. *Braveheart* expression is necessary for the activation of cardiac programming in mouse embryonic stem cells by positively regulating key cardiac transcription factors (e.g. Mesp1, Hand2, Nkx2-5) through interactions with SUZ12 of PRC2 (119). *Fendrr* is expressed in the lateral mesoderm and is a key regulator of cardiac development; *Fendrr*-mutant mouse embryos had impaired cardiac function, septal defects and hypoplasia, proposed to be through altered balance of H3K27me3 and H3K4me3 at promoters of transcription factors (120). lncRNAs are an exciting interface between the transcriptome, genome and proteome for regulating developmental (and adult) phenotypes in part because so much remains unknown about how they function. What are the proteins that guide lncRNAs to the proper histone modifications? Are the lncRNA-protein complexes heterogeneous in a single cell? Are all histone modifications of a given type bound by a given lncRNA in a terminally differentiated cell (e.g. is every nucleosome with H3K27me3 bound by *Braveheart* and/or *Fendrr*)? Are the protein

binding partners for individual lncRNAs dynamic at a single locus and do the complexes change genomic residence during development? Answers to these questions will likely emerge soon as crosslinking and immunoprecipitation sequencing (CLIP-seq) (121) and other RNA localization methods (RNA Antisense Purification and RNA *in situ* hybridization) are combined with proteomic studies in the setting of cardiac development.

Technical Advances and Future Perspectives

Systems approaches have been taken to understand the global dynamics in cellular processes, which have allowed for novel identification of developmental regulators. Mass spectrometry analyses of the mouse cardiac nuclear proteome characterized nuclear proteins associated with different sub-nuclear compartments and identified novel histone variants (50), yet these types of approaches have not been leveraged in the setting of development, primarily due to small sample sizes. To overcome issues of tissue heterogeneity, a very recent study using an *isolation of nuclei tagged in specific cell types* (INTACT) approach employed transgenic methods to selectively label *Xenopus* cardiomyocyte nuclei for proteomic analysis (71). In this system, embryos were introduced with transgenes for a fusion nucleoporin construct and BirA, a biotin ligase specific for the construct, driven by cardiomyocyte *mlc2p* promoter (71). Enrichment of biotinylated nuclei allowed for identification of cardiomyocyte-specific peptides, the complexity of which was lower compared to previous studies performed on whole heart tissue (71). Nascent chromatin capture techniques have been used to identify protein complexes at replication forks to understand transmission of epigenetic memory (122). Another innovative proteomic screening technique that has overcome the issue of cell specificity and limited sample size is the FlipTrap method, which systematically targets endogenous proteins for immunohistochemical tracking or inducible knockout (123).

A well-recognized challenge to 'omics investigations of cardiac development is tissue heterogeneity. When studying proteins in the membrane or mitochondria, for example, it is reasonable to expect that most of the protein mass comes from myocytes in a developing or mature heart. This is not the case in the setting of nuclear proteins and chromatin modifications, because in terms of cell number, myocytes—and therefore myocyte nuclei— constitute 50% or less of the heart. Recent advances in stem cell- and iPS cell-derived cardiomyocyte models have revolutionized the study of the myocyte development, with recent examples including the role of histone modifications in cardiac lineage commitment (3, 51) and the examination of genetic cardiomyopathies in patient-derived myocytes (124). A current frontier is application of quantitative proteomics to these cells, including at intermediate developmental stages, to dissect the stage-specific changes in chromatin bound proteins that determine differential chromatin structure (Figure 1-3) and ultimately control cell fate.

While differentiated cell types display similar chromatin structural features on a large scale, it is unclear how the loci-specific changes occur to give rise to different cell types (Table 1-1). In other words, what dictates the environment for orchestration and targeting of chromatin structural changes during development? Ultimately, the code for development must come from the genome primary sequence—the reading of this code, however, becomes cell type-specific through the repositioning of nucleosomes, their decoration with post-translational modifications, interaction with chromatin structural proteins (and maybe lncRNAs, although in our opinion more evidence is needed to understand the extent to which these molecules regulate chromatin structure in development and adulthood) and by modification of DNA through methylation. We reason many of the cues for cell type specificity may reside in intergenic/non-coding genomic regions that contribute to chromatin structure and thereby gene expression in a cell type-specific and non-intuitive manner (i.e. not by encoding a transcript, but rather by serving as a substrate for unique chromatin features). For transcriptional enhancers this concept has been well defined, but for

regions further away from mRNA coding genes (i.e. functional DNA elements not localized near a gene in the genome) the story is less clear. Dissecting the causal (as well as temporal) relationship amongst transcription factors, chromatin remodelers, chromatin structure and transcriptome makeup is critical to understand the fundamental logic by which one cell becomes another along the developmental continuum. Many congenital heart diseases arise from mutations in cardiac transcription factors and/or chromatin structural regulators. These mutations will allow us to better understand the functions that chromatin structure can play in the establishment of cardiac gene expression during development. While the roles of these structural regulators are becoming clearer, it remains unknown how these mechanisms work in combination to mediate the spatial organization for establishing cardiac-specific gene expression. Future studies will require using global chromosome capture and chromatin interaction analysis by paired-end tag sequencing (ChIA-PET) assays to understand how proteins mediate endogenous three-dimensional structure of the cardiac genome at different stages of development. Since transcriptomes vary widely between differentiated cell types, it is unlikely that chromatin structural measurements in non-cardiac lineage cells will effectively inform on the structural features necessary for cardiac gene expression.

Acknowledgments

Sources of funding: Research in the Vondriska Laboratory is supported by the American Heart Association (IRG18870056) and National Institutes of Health (HL-105699 and HL-115238). E.K. is supported by the NIH Training Grant 5T32GM065823.

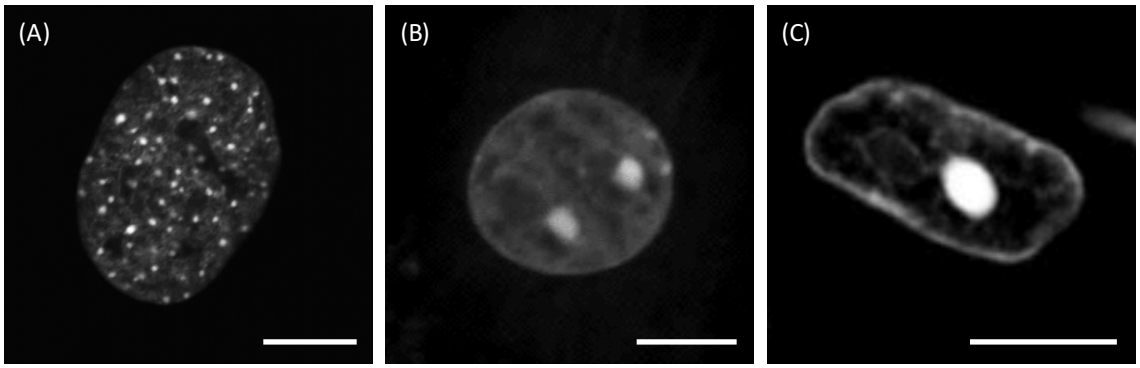

Figure 1-1: Cell-type specific genome organization. DAPI labeling of DNA from mouse embryonic fibroblast (A), neonatal cardiomyocyte (B) and adult cardiomyocyte (C) shows specific chromatin packaging and nuclear structure of the same mouse genome in different cell types and at different developmental stages. Scale bar: 5μm.

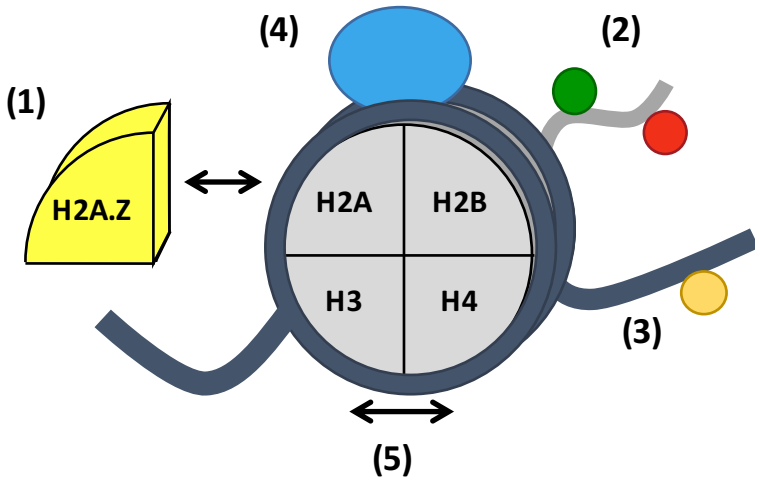

Figure 1-2: Mechanisms of chromatin modification. Levels of genome packaging can be regulated in the following ways: (1) histone variants, (2) histone post-translational modifications (active, *green*, or repressive, *red*), (3) DNA modifications (*e.g.* methylation of cytosine), (4) association with chromatin structural proteins and RNAs (*light blue)* and (5) positioning of nucleosomes along DNA.

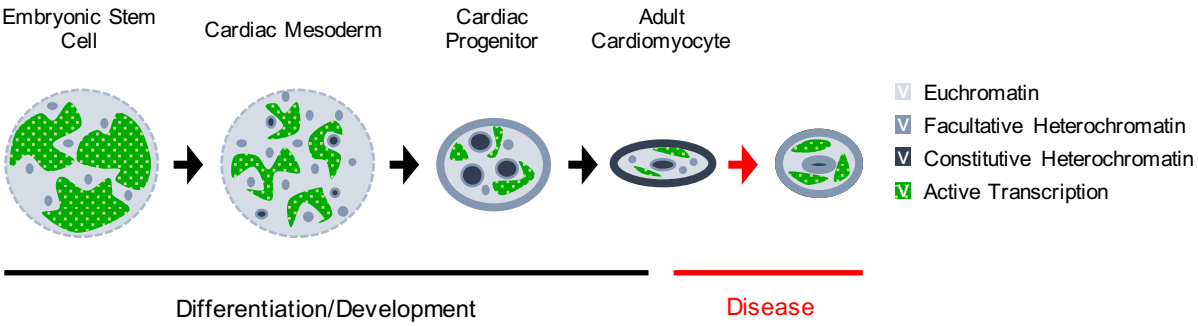

Figure 1-3: Model for chromatin and nuclear architectural changes during development and disease. The cardiac nucleus undergoes dynamic structural changes to create a cell type-specific transcriptome. During differentiation, there is a shift from euchromatin to heterochromatin [14, 31], a decrease in global transcription [15] and an overall compaction of nuclear size [98, 125, 126]. With disease, these features are reverted to resemble earlier developmental stages, including a shift towards euchromatin [84], an increase in RNA production [127] and an increase in nuclear size [128].

Table 1-1: Key Questions Regarding Chromatin Regulation in Cardiovascular Development

Questions	Current Knowledge	Future Directions
How are epigenetic changes coordinated at developmental milestones?	ChIP-seq of individual histone PTMs during cardiomyocyte differentiation	Determine how PTMs correspond to protein localization and specify global transcriptional states
What are the genomic targets of chromatin remodelers (readers, writers & erasers) and how do they control phenotype?	Loss- and gain-of-function for various chromatin enzymes	ChIP-seq for individual histone modifiers; comparison with known modification ChIP-seq datasets; CLIP-seq to prove role in transcription and explore RNA functions
How does the 3D organization of the genome change during development and is this important to specify the cardiovascular lineages?	Chromosome conformation capture analyses of genomes from non-cardiac cells	Chromosome conformation capture and ChIA-PET at various stages of development; comparison with protein localization and transcription

Supplemental Table 1-1: Gain/Loss of Function Studies on Chromatin Mechanisms in Cardiovascular Development

	Gene	Manipulation	Phenotype	Molecular Targets	Reference (PMID)
Histone Methyltransferases	Smyd1	Knockout	Embryonic lethal by E10.5; Enlarged heart due to prominent extracellular matrix; Impaired right ventricular development *Heterozygotes show no noticeable impairments	Downregulation of Hand2 expression	11923873, 16477022, 24068325
		Knockdown (zebrafish)	Impaired cardiac function; Disrupted sarcomeric organization	Upregulation of heat-shock proteins	
	Mll2	Knockout	Embryonic lethal by E14.5; Apoptotic	--	16540515, 23826075
		Point mutation	Embryonic lethal by E11.5; Impaired looping	--	
	Ezh2	Cardiac-specific knockout	Perinatal lethal; Double outlet right ventricle; Underdeveloped endocardial cushion due to decreased proliferation and increased apoptosis; Impaired septal formation, hypertrabeculation; Hypoplasia	Upregulation of negative cell cycle regulators (e.g. Ink4a, Ink4b), non-cardiac transcription factors (Pax6, Six1, Isl1), atrial and conduction gene expression in ventricles (Hcn4, Mlc2a); Downregulation of Tbx2, Hey2 transcription factors	22158708, 22312437
	Whsc1	Knockout	Lethal by P10; Growth defects; Impaired septal formation due to hypoplasia *Heterozygotes display some phenotypes of knockout due to haploinsufficiency	Upregulation of Nkx2-5 dependent genes (e.g. Pdgfra, Isl1)	19483677
Histone Demethylases	Jarid2/Jumonji	Knockout	Perinatal lethal; Thin ventricular walls; Double-outlet right ventricle; Impaired septal formation, hypertrabeculation; Edema; Increased proliferation	Maintained fetal gene expression (increase in βMHC to αMHC ratio, ANF not repressed); Impaired patterning of cardiac gene expression (e.g. ventricular ANF expression maintained, high Mlc2a expression in ventricles and atria); Increase in Notch signaling	10807864, 15870077, 21402699
		Endothelial-specific knockout	Increase in mitotic activity in isolated cardiomyocytes	Upregulation of Cyclin D	
			Perinatal lethal; Thin ventricular wall; Double-outlet right ventricle; Increase endocardium and myocardium spacing; Impaired septal formation, hypertrabeculation; Increased proliferation	Maintained fetal gene expression (no increase in αMHC, ANF not repressed); Increase in Notch signaling	

Supplemental Table 1-1 *(continued)*

	Gene	Manipulation	Phenotype	Molecular Targets	Reference (PMID)
Histone Demethylases	Jmjd3	Knockout	Embryonic lethal by E6.5; Impaired *in vitro* mesoderm and endothelial differentiation in embryonic stem cells	Downregulation of mesoderm and cardiac markers (Brachyury, Mef2c, αMHC, Nppa)	23856522
	UTX	Knockout	Embryonic stem cells cannot differentiate into beating cardiomyocyte *in vitro* Embryonic lethal by E10.5; Impaired looping, cardiomyocyte differentiation	Repression of cardiac markers (ANF, α-cardiac actin, Myh6) Downregulation of cardiac genes (ANF, Mlc2v)	22192413
Histone Acetyltransferases	p300/CBP	p300 knockout CBP knockout Point mutation	Embryonic lethal by E11.5; Impaired growth; Hypotrabeculation; Reduced proliferation *p300 heterozygotes and compound p300/cbp heterozygotes show embryonic lethality Perinatal lethal; Thin ventricular walls; Impaired septal formation; Underdeveloped coronary vasculature, edema, hemorrhaging	Downregulation of cardiac structural protein expression --	9590171, 14517255
Histone Deacetylases	HDAC1, HDAC2	HDAC1 Knockout HDAC2 Knockout Cardiac-specific knockout (HDAC1 or HDAC2) *Functionally redundant—HDAC1/HDAC2 double cardiac knockout neonatal lethal (dilated cardiomyopathy, arrhythmia, apoptosis)	Embryonic lethal by E10.5; Impaired growth and cellular proliferation Perinatal lethal; Decreased heart rate; Right ventricle develops dorsally to left; Reduced chamber size of right ventricle; Thick septum; Hyperplasia No noticeable phenotypes	Upregulation of cell cycle inhibitors (p21, p27) -- -- Upregulation of fetal gene response (increases in ANF, βMHC), calcium channels ($Ca_v3.2$), skeletal muscle contractile genes (α-skeletal actin, TnI)	12032080, 17322895, 17639084
	HDAC3	Knockout Cardiac-specific knockout Cardiac-specific overexpression	Embryonic lethal by E9.5; Gastrulation defects Postnatal lethal by 16wks due to hypertrophy; Altered metabolism (increased lipid accumulation, decrease in mitochondrial function) Thickened septum and ventricular walls due to hyperplasia	-- Upregulation of fetal gene response (increases in ANF, α-skeletal actin), p21 Repression of cell cycle inhibitors (Cdkn1, Cdkn2)	18625706, 18830415

Supplemental Table 1-1 *(continued)*

	Gene	Manipulation	Phenotype	Molecular Targets	Reference (PMID)
Histone Deacetylases	HDAC4	Knockout	No noticeable phenotypes	--	15537544, 17038545
		Overexpression (P19 cells)	Block mesoderm differentiation into cardiomyocyte	Downregulation of cardiac transcription factors (Gata4, Nkx2-5)	
	HDAC5, HDAC9	Knockout	No noticeable phenotypes during early development	--	15367668
			*Functionally redundant: HDAC5/HDAC9 double cardiac knockout perinatal lethal- Impaired growth, septal formation; Increase in heart weight to body weight ratio; Hypoplasia	Upregulation of ANF, BNP	
	HDAC7	Knockout	Embryonic lethal by E11; Dilated chambers; Impaired vascular integrity; Pericardial effusion	Upregulation of MMP10	16873063
		Endothelial-specific knockout	Embryonic lethal by E11.5; Impaired vascular integrity; Pericardial effusion; Dilated chambers	Upregulation of MMP10	
ATP-dependent remodelers	Brg1	Cardiac-specific knockout	Embryonic lethal by E11.5; Impaired looping, no septum formation; Thin ventricular walls due to hypoplasia	Downregulation of Bmp1; Increase in αMHC to βMHC ratio	20596014, 21304516
		Ventricle-specific knockout	Embryonic lethal by E11.5; Double-outlet right ventricle; Decreased ventricular chamber size; Impaired looping, septal formation	Downregulation of cardiac genes (e.g. Nppa, Tbx5, Bmp10)	
			*Neonatal heterozygotes show dilation chambers; impaired septal formation; impaired electrical function		
		Null mutation (zebrafish)	Arrhythmia; Hypoplasia	Differential patterns of cardiac gene expression (e.g. Bmp4, Tbx2)	
	Baf180	Knockout	Embryonic lethal by E15.5; Reduced heart rate; Impaired septal formation; Hypoplasia; Edema	Downregulation of cell growth and proliferation genes; Upregulation of growth arrest-associated genes	15601824
	Baf250a	Knockdown (P19 cells)	--	Upregulation of cardiac markers (e.g. Nkx2-5, Hand1, Acta2)	22621927, 24335282
		Overexpression (P19 cells)	--	Downregulation of cardiac markers (e.g. cTnT, Nkx2-5, Gata4)	
		Cardiac progenitor-specific knockout	Embryonic lethal; Impaired trabeculation of right ventricle, no septum formation, outflow tract; Hypoplasia	Downregulation of cardiac transcription factors (Nkx2-5, Bmp10, Mef2c)	

Supplemental Table 1-1 *(continued)*

	Gene	Manipulation	Phenotype	Molecular Targets	Reference (PMID)
ATP-dependent remodelers	Baf60c	Knockdown	Embryonic lethal by E11; Impaired looping, trabeculation, short outflow tract; Hypoplasia	Differential patterns of cardiac gene expression (e.g. Nkx2-5, Nppa, Hand1, Hand2 affected)	15525990, 17210915
	Dpf3	Knockdown (zebrafish)	Impaired looping; Weak contractility; Disrupted myofibril organization	Upregulation of genes involved in metabolic processes; Downregulation of genes involved in ion/electron transport and cell homeostasis	18765789
	Chd4	Endothelial-specific knockout	Embryonic lethal by E12.5; Impaired vascular integrity, reduced extracellular matrix, hemorrhaging; Hypotrabeculation	Downregulation of extracellular proteins (e.g. Type IV collagen, fibronectin); Differential expression of plasmin regulators to result in activation of matrix metalloproteases	24335282, 24348274
		Knockdown (P19 cells)	--	Upregulation of cardiac genes (e.g. cTnT, Bmp10, Gata4)	
	Chd7	Knockout	Embryonic lethal by E10.5; Interrupted aortic arch	--	17334657, 19855134, 22363697
		Knockdown (zebrafish)	Impaired looping; Pericardial edema	--	
	Reptin	Active mutant (zebrafish)	Impaired contractility; Ventricular hypertrophy due to hyperplasia	--	12464178
	Pontin	Knockdown (zebrafish)	Hyperplasia	--	12464178
DNA Methylation	Dnmt1	Knockout	Embryonic lethal by E11; Underdeveloped heart	--	1606615
	Dnmt3b	Knockout	Embryonic lethal by E16.5; Impaired septum formation; Hemorrhaging	--	16501171
		Targeted point mutations	Normal development, small body size; Thickening of myocardium in some animals	--	
	MeCP2	Cardiac-specific overexpression	Embryonic lethal by E15; Ventricular wall and septal hypertrophy due to hyperplasia	Changes in cardiac genes (e.g. increases in ANF, Mlc2v, Nkx2-5; decreases in βMHC, α-cardiac actin, Tbx5)	20203171
Chromatin Structural Proteins	HMGA2	Overexpression (P19CL6 cells)	Efficient differentiation into cardiomyocytes	Upregulation of cardiac markers (Nkx2-5, ANP, Gata4, Mef2c, Mlc2v)	18425117
		Knockdown (P19CL6 cells)	Blocked cardiomyocyte differentiation	Downregulation of cardiac markers; Mesodermal markers not affected	
		Dominant negative mutation (Xenopus)	Reduced heart size	Downregulation of Nkx2-5	

Supplemental Table 1-1 *(continued)*

	Gene	Manipulation	Phenotype	Molecular Targets	Reference (PMID)
Chromatin Structural Proteins	HMGA2	Knockdown (Xenopus)	--	Downregulation of Nkx2-5	18425117
	Lamin A/C	Knockout	Reduced growth rate (postnatal 2wks); Dilated cardiomyopathy and impaired ventricular contractile function (postnatal 4-6wks)	Upregulation of ANP and BNP; Downregulation of SERCA2a; Elongated nuclear shape, disrupted chromatin structure	14755333
	Nucleolin	Knockdown (zebrafish)	Edema; Small ventricular size; Impaired looping; Decrease in cardiac output	Upregulation of p53; Decreased rRNA expression; Ventricular bmp4 not repressed; Increase in H3K9me3	24077883
		Overexpression (zebrafish)	Edema; Impaired looping, dorsal-ventral axis formation	Upregulation of p53, ventricular Bmp4	

Chapter 1: References

1. Laflamme MA, Murry CE. Heart regeneration. Nature. 2011;473(7347):326-35. doi: 10.1038/nature10147. PubMed PMID: 21593865; PMCID: PMC4091722.
2. Wu SM, Chien KR, Mummery C. Origins and fates of cardiovascular progenitor cells. Cell. 2008;132(4):537-43. doi: 10.1016/j.cell.2008.02.002. PubMed PMID: 18295570; PMCID: PMC2507768.
3. Wamstad JA, Alexander JM, Truty RM, Shrikumar A, Li F, Eilertson KE, Ding H, Wylie JN, Pico AR, Capra JA, Erwin G, Kattman SJ, Keller GM, Srivastava D, Levine SS, Pollard KS, Holloway AK, Boyer LA, Bruneau BG. Dynamic and coordinated epigenetic regulation of developmental transitions in the cardiac lineage. Cell. 2012;151(1):206-20. Epub 2012/09/18. doi: 10.1016/j.cell.2012.07.035. PubMed PMID: 22981692; PMCID: 3462286.
4. High FA, Epstein JA. The multifaceted role of Notch in cardiac development and disease. Nat Rev Genet. 2008;9(1):49-61. doi: 10.1038/nrg2279. PubMed PMID: 18071321.
5. Evans SM, Yelon D, Conlon FL, Kirby ML. Myocardial lineage development. Circ Res. 2010;107(12):1428-44. doi: 10.1161/CIRCRESAHA.110.227405. PubMed PMID: 21148449; PMCID: PMC3073310.
6. Dyer LA, Kirby ML. The role of secondary heart field in cardiac development. Dev Biol. 2009;336(2):137-44. doi: 10.1016/j.ydbio.2009.10.009. PubMed PMID: 19835857; PMCID: PMC2794420.
7. Sturzu AC, Wu SM. Developmental and regenerative biology of multipotent cardiovascular progenitor cells. Circ Res. 2011;108(3):353-64. doi: 10.1161/CIRCRESAHA.110.227066. PubMed PMID: 21293007; PMCID: PMC3073355.
8. Lolas M, Valenzuela PD, Tjian R, Liu Z. Charting Brachyury-mediated developmental pathways during early mouse embryogenesis. Proc Natl Acad Sci U S A. 2014;111(12):4478-83. doi: 10.1073/pnas.1402612111. PubMed PMID: 24616493; PMCID: PMC3970479.

9. Lindsley RC, Gill JG, Murphy TL, Langer EM, Cai M, Mashayekhi M, Wang W, Niwa N, Nerbonne JM, Kyba M, Murphy KM. Mesp1 coordinately regulates cardiovascular fate restriction and epithelial-mesenchymal transition in differentiating ESCs. Cell Stem Cell. 2008;3(1):55-68. doi: 10.1016/j.stem.2008.04.004. PubMed PMID: 18593559; PMCID: PMC2497439.
10. Saga Y, Miyagawa-Tomita S, Takagi A, Kitajima S, Miyazaki J, Inoue T. MesP1 is expressed in the heart precursor cells and required for the formation of a single heart tube. Development. 1999;126(15):3437-47. PubMed PMID: 10393122.
11. Moretti A, Caron L, Nakano A, Lam JT, Bernshausen A, Chen Y, Qyang Y, Bu L, Sasaki M, Martin-Puig S, Sun Y, Evans SM, Laugwitz KL, Chien KR. Multipotent embryonic isl1+ progenitor cells lead to cardiac, smooth muscle, and endothelial cell diversification. Cell. 2006;127(6):1151-65. doi: 10.1016/j.cell.2006.10.029. PubMed PMID: 17123592.
12. McCulley DJ, Black BL. Transcription factor pathways and congenital heart disease. Curr Top Dev Biol. 2012;100:253-77. doi: 10.1016/B978-0-12-387786-4.00008-7. PubMed PMID: 22449847; PMCID: PMC3684448.
13. Srivastava D, Olson EN. A genetic blueprint for cardiac development. Nature. 2000;407(6801):221-6. doi: 10.1038/35025190. PubMed PMID: 11001064.
14. Sdek P, Zhao P, Wang Y, Huang CJ, Ko CY, Butler PC, Weiss JN, Maclellan WR. Rb and p130 control cell cycle gene silencing to maintain the postmitotic phenotype in cardiac myocytes. J Cell Biol. 2011;194(3):407-23. doi: 10.1083/jcb.201012049. PubMed PMID: 21825075; PMCID: PMC3153646.
15. Efroni S, Duttagupta R, Cheng J, Dehghani H, Hoeppner DJ, Dash C, Bazett-Jones DP, Le Grice S, McKay RD, Buetow KH, Gingeras TR, Misteli T, Meshorer E. Global transcription in pluripotent embryonic stem cells. Cell Stem Cell. 2008;2(5):437-47. doi: 10.1016/j.stem.2008.03.021. PubMed PMID: 18462694; PMCID: PMC2435228.

16. Cremer T, Cremer C. Chromosome territories, nuclear architecture and gene regulation in mammalian cells. Nat Rev Genet. 2001;2(4):292-301. doi: 10.1038/35066075. PubMed PMID: 11283701.
17. van Steensel B, Dekker J. Genomics tools for unraveling chromosome architecture. Nat Biotechnol. 2010;28(10):1089-95. doi: 10.1038/nbt.1680. PubMed PMID: 20944601; PMCID: PMC3023824.
18. Strahl BD, Ohba R, Cook RG, Allis CD. Methylation of histone H3 at lysine 4 is highly conserved and correlates with transcriptionally active nuclei in Tetrahymena. Proc Natl Acad Sci U S A. 1999;96(26):14967-72. PubMed PMID: 10611321; PMCID: PMC24756.
19. Cao R, Wang L, Wang H, Xia L, Erdjument-Bromage H, Tempst P, Jones RS, Zhang Y. Role of histone H3 lysine 27 methylation in Polycomb-group silencing. Science. 2002;298(5595):1039-43. doi: 10.1126/science.1076997. PubMed PMID: 12351676.
20. Nakayama J, Rice JC, Strahl BD, Allis CD, Grewal SI. Role of histone H3 lysine 9 methylation in epigenetic control of heterochromatin assembly. Science. 2001;292(5514):110-3. doi: 10.1126/science.1060118. PubMed PMID: 11283354.
21. Arnaudo AM, Garcia BA. Proteomic characterization of novel histone post-translational modifications. Epigenetics Chromatin. 2013;6(1):24. doi: 10.1186/1756-8935-6-24. PubMed PMID: 23916056; PMCID: PMC3737111.
22. Zaidi S, Choi M, Wakimoto H, Ma L, Jiang J, Overton JD, Romano-Adesman A, Bjornson RD, Breitbart RE, Brown KK, Carriero NJ, Cheung YH, Deanfield J, DePalma S, Fakhro KA, Glessner J, Hakonarson H, Italia MJ, Kaltman JR, Kaski J, Kim R, Kline JK, Lee T, Leipzig J, Lopez A, Mane SM, Mitchell LE, Newburger JW, Parfenov M, Pe'er I, Porter G, Roberts AE, Sachidanandam R, Sanders SJ, Seiden HS, State MW, Subramanian S, Tikhonova IR, Wang W, Warburton D, White PS, Williams IA, Zhao H, Seidman JG, Brueckner M, Chung WK, Gelb BD, Goldmuntz E, Seidman CE, Lifton RP. De novo mutations in histone-modifying genes in

congenital heart disease. Nature. 2013;498(7453):220-3. doi: 10.1038/nature12141. PubMed PMID: 23665959; PMCID: PMC3706629.

23. He A, Ma Q, Cao J, von Gise A, Zhou P, Xie H, Zhang B, Hsing M, Christodoulou DC, Cahan P, Daley GQ, Kong SW, Orkin SH, Seidman CE, Seidman JG, Pu WT. Polycomb repressive complex 2 regulates normal development of the mouse heart. Circ Res. 2012;110(3):406-15. doi: 10.1161/CIRCRESAHA.111.252205. PubMed PMID: 22158708; PMCID: PMC3282145.
24. Ohtani K, Zhao C, Dobreva G, Manavski Y, Kluge B, Braun T, Rieger MA, Zeiher AM, Dimmeler S. Jmjd3 controls mesodermal and cardiovascular differentiation of embryonic stem cells. Circ Res. 2013;113(7):856-62. doi: 10.1161/CIRCRESAHA.113.302035. PubMed PMID: 23856522.
25. Gottlieb PD, Pierce SA, Sims RJ, Yamagishi H, Weihe EK, Harriss JV, Maika SD, Kuziel WA, King HL, Olson EN, Nakagawa O, Srivastava D. Bop encodes a muscle-restricted protein containing MYND and SET domains and is essential for cardiac differentiation and morphogenesis. Nat Genet. 2002;31(1):25-32. doi: 10.1038/ng866. PubMed PMID: 11923873.
26. Tan X, Rotllant J, Li H, De Deyne P, Du SJ. SmyD1, a histone methyltransferase, is required for myofibril organization and muscle contraction in zebrafish embryos. Proc Natl Acad Sci U S A. 2006;103(8):2713-8. doi: 10.1073/pnas.0509503103. PubMed PMID: 16477022; PMCID: PMC1531647.
27. Li H, Zhong Y, Wang Z, Gao J, Xu J, Chu W, Zhang J, Fang S, Du SJ. Smyd1b is required for skeletal and cardiac muscle function in zebrafish. Mol Biol Cell. 2013;24(22):3511-21. doi: 10.1091/mbc.E13-06-0352. PubMed PMID: 24068325; PMCID: PMC3826989.
28. Nimura K, Ura K, Shiratori H, Ikawa M, Okabe M, Schwartz RJ, Kaneda Y. A histone H3 lysine 36 trimethyltransferase links Nkx2-5 to Wolf-Hirschhorn syndrome. Nature. 2009;460(7252):287-91. doi: 10.1038/nature08086. PubMed PMID: 19483677.

29. Brien GL, Gambero G, O'Connell DJ, Jerman E, Turner SA, Egan CM, Dunne EJ, Jurgens MC, Wynne K, Piao L, Lohan AJ, Ferguson N, Shi X, Sinha KM, Loftus BJ, Cagney G, Bracken AP. Polycomb PHF19 binds H3K36me3 and recruits PRC2 and demethylase NO66 to embryonic stem cell genes during differentiation. Nat Struct Mol Biol. 2012;19(12):1273-81. doi: 10.1038/nsmb.2449. PubMed PMID: 23160351.
30. Pasini D, Cloos PA, Walfridsson J, Olsson L, Bukowski JP, Johansen JV, Bak M, Tommerup N, Rappsilber J, Helin K. JARID2 regulates binding of the Polycomb repressive complex 2 to target genes in ES cells. Nature. 2010;464(7286):306-10. doi: 10.1038/nature08788. PubMed PMID: 20075857.
31. Wen B, Wu H, Shinkai Y, Irizarry RA, Feinberg AP. Large histone H3 lysine 9 dimethylated chromatin blocks distinguish differentiated from embryonic stem cells. Nat Genet. 2009;41(2):246-50. doi: 10.1038/ng.297. PubMed PMID: 19151716; PMCID: PMC2632725.
32. Mysliwiec MR, Carlson CD, Tietjen J, Hung H, Ansari AZ, Lee Y. Jarid2 (Jumonji, AT rich interactive domain 2) regulates NOTCH1 expression via histone modification in the developing heart. J Biol Chem. 2012;287(2):1235-41. doi: 10.1074/jbc.M111.315945. PubMed PMID: 22110129; PMCID: PMC3256911.
33. Miller SA, Huang AC, Miazgowicz MM, Brassil MM, Weinmann AS. Coordinated but physically separable interaction with H3K27-demethylase and H3K4-methyltransferase activities are required for T-box protein-mediated activation of developmental gene expression. Genes Dev. 2008;22(21):2980-93. doi: 10.1101/gad.1689708. PubMed PMID: 18981476; PMCID: PMC2577798.
34. Yin N, Lu R, Lin J, Zhi S, Tian J, Zhu J. Islet-1 promotes the cardiac-specific differentiation of mesenchymal stem cells through the regulation of histone acetylation. Int J Mol Med. 2014;33(5):1075-82. doi: 10.3892/ijmm.2014.1687. PubMed PMID: 24604334; PMCID: PMC4020474.

35. Chen G, Zhu J, Lv T, Wu G, Sun H, Huang X, Tian J. Spatiotemporal expression of histone acetyltransferases, p300 and CBP, in developing embryonic hearts. J Biomed Sci. 2009;16:24. doi: 10.1186/1423-0127-16-24. PubMed PMID: 19272189; PMCID: PMC2653528.
36. Shikama N, Lutz W, Kretzschmar R, Sauter N, Roth JF, Marino S, Wittwer J, Scheidweiler A, Eckner R. Essential function of p300 acetyltransferase activity in heart, lung and small intestine formation. EMBO J. 2003;22(19):5175-85. doi: 10.1093/emboj/cdg502. PubMed PMID: 14517255; PMCID: PMC204485.
37. Yao TP, Oh SP, Fuchs M, Zhou ND, Ch'ng LE, Newsome D, Bronson RT, Li E, Livingston DM, Eckner R. Gene dosage-dependent embryonic development and proliferation defects in mice lacking the transcriptional integrator p300. Cell. 1998;93(3):361-72. PubMed PMID: 9590171.
38. Haberland M, Montgomery RL, Olson EN. The many roles of histone deacetylases in development and physiology: implications for disease and therapy. Nat Rev Genet. 2009;10(1):32-42. doi: 10.1038/nrg2485. PubMed PMID: 19065135; PMCID: PMC3215088.
39. Montgomery RL, Davis CA, Potthoff MJ, Haberland M, Fielitz J, Qi X, Hill JA, Richardson JA, Olson EN. Histone deacetylases 1 and 2 redundantly regulate cardiac morphogenesis, growth, and contractility. Genes Dev. 2007;21(14):1790-802. doi: 10.1101/gad.1563807. PubMed PMID: 17639084; PMCID: PMC1920173.
40. Trivedi CM, Lu MM, Wang Q, Epstein JA. Transgenic overexpression of Hdac3 in the heart produces increased postnatal cardiac myocyte proliferation but does not induce hypertrophy. J Biol Chem. 2008;283(39):26484-9. doi: 10.1074/jbc.M803686200. PubMed PMID: 18625706; PMCID: PMC2546558.
41. Chang S, Young BD, Li S, Qi X, Richardson JA, Olson EN. Histone deacetylase 7 maintains vascular integrity by repressing matrix metalloproteinase 10. Cell. 2006;126(2):321-34. doi: 10.1016/j.cell.2006.05.040. PubMed PMID: 16873063.

42. Chang S, McKinsey TA, Zhang CL, Richardson JA, Hill JA, Olson EN. Histone deacetylases 5 and 9 govern responsiveness of the heart to a subset of stress signals and play redundant roles in heart development. Mol Cell Biol. 2004;24(19):8467-76. doi: 10.1128/MCB.24.19.8467-8476.2004. PubMed PMID: 15367668; PMCID: PMC516756.
43. Sundaresan NR, Vasudevan P, Zhong L, Kim G, Samant S, Parekh V, Pillai VB, Ravindra PV, Gupta M, Jeevanandam V, Cunningham JM, Deng CX, Lombard DB, Mostoslavsky R, Gupta MP. The sirtuin SIRT6 blocks IGF-Akt signaling and development of cardiac hypertrophy by targeting c-Jun. Nat Med. 2012;18(11):1643-50. doi: 10.1038/nm.2961. PubMed PMID: 23086477; PMCID: PMC4401084.
44. Vakhrusheva O, Smolka C, Gajawada P, Kostin S, Boettger T, Kubin T, Braun T, Bober E. Sirt7 increases stress resistance of cardiomyocytes and prevents apoptosis and inflammatory cardiomyopathy in mice. Circ Res. 2008;102(6):703-10. doi: 10.1161/CIRCRESAHA.107.164558. PubMed PMID: 18239138.
45. Potente M, Ghaeni L, Baldessari D, Mostoslavsky R, Rossig L, Dequiedt F, Haendeler J, Mione M, Dejana E, Alt FW, Zeiher AM, Dimmeler S. SIRT1 controls endothelial angiogenic functions during vascular growth. Genes Dev. 2007;21(20):2644-58. doi: 10.1101/gad.435107. PubMed PMID: 17938244; PMCID: PMC2000327.
46. Maze I, Noh KM, Soshnev AA, Allis CD. Every amino acid matters: essential contributions of histone variants to mammalian development and disease. Nat Rev Genet. 2014;15(4):259-71. doi: 10.1038/nrg3673. PubMed PMID: 24614311; PMCID: PMC4082118.
47. Barski A, Cuddapah S, Cui K, Roh TY, Schones DE, Wang Z, Wei G, Chepelev I, Zhao K. High-resolution profiling of histone methylations in the human genome. Cell. 2007;129(4):823-37. doi: 10.1016/j.cell.2007.05.009. PubMed PMID: 17512414.
48. Creyghton MP, Markoulaki S, Levine SS, Hanna J, Lodato MA, Sha K, Young RA, Jaenisch R, Boyer LA. H2AZ is enriched at polycomb complex target genes in ES cells and is necessary

for lineage commitment. Cell. 2008;135(4):649-61. doi: 10.1016/j.cell.2008.09.056. PubMed PMID: 18992931; PMCID: PMC2853257.

49. Chen IY, Lypowy J, Pain J, Sayed D, Grinberg S, Alcendor RR, Sadoshima J, Abdellatif M. Histone H2A.z is essential for cardiac myocyte hypertrophy but opposed by silent information regulator 2alpha. J Biol Chem. 2006;281(28):19369-77. doi: 10.1074/jbc.M601443200. PubMed PMID: 16687393.
50. Franklin S, Zhang MJ, Chen H, Paulsson AK, Mitchell-Jordan SA, Li Y, Ping P, Vondriska TM. Specialized compartments of cardiac nuclei exhibit distinct proteomic anatomy. Mol Cell Proteomics. 2011;10(1):M110 000703. doi: 10.1074/mcp.M110.000703. PubMed PMID: 20807835; PMCID: PMC3013444.
51. Paige SL, Thomas S, Stoick-Cooper CL, Wang H, Maves L, Sandstrom R, Pabon L, Reinecke H, Pratt G, Keller G, Moon RT, Stamatoyannopoulos J, Murry CE. A temporal chromatin signature in human embryonic stem cells identifies regulators of cardiac development. Cell. 2012;151(1):221-32. doi: 10.1016/j.cell.2012.08.027. PubMed PMID: 22981225; PMCID: PMC3462257.
52. Papait R, Cattaneo P, Kunderfranco P, Greco C, Carullo P, Guffanti A, Vigano V, Stirparo GG, Latronico MV, Hasenfuss G, Chen J, Condorelli G. Genome-wide analysis of histone marks identifying an epigenetic signature of promoters and enhancers underlying cardiac hypertrophy. Proc Natl Acad Sci U S A. 2013;110(50):20164-9. doi: 10.1073/pnas.1315155110. PubMed PMID: 24284169; PMCID: PMC3864351.
53. Kaneda R, Takada S, Yamashita Y, Choi YL, Nonaka-Sarukawa M, Soda M, Misawa Y, Isomura T, Shimada K, Mano H. Genome-wide histone methylation profile for heart failure. Genes Cells. 2009;14(1):69-77. doi: 10.1111/j.1365-2443.2008.01252.x. PubMed PMID: 19077033.
54. May D, Blow MJ, Kaplan T, McCulley DJ, Jensen BC, Akiyama JA, Holt A, Plajzer-Frick I, Shoukry M, Wright C, Afzal V, Simpson PC, Rubin EM, Black BL, Bristow J, Pennacchio LA,

Visel A. Large-scale discovery of enhancers from human heart tissue. Nat Genet. 2011;44(1):89-93. doi: 10.1038/ng.1006. PubMed PMID: 22138689; PMCID: PMC3246570.

55. Mizuguchi G, Shen X, Landry J, Wu WH, Sen S, Wu C. ATP-driven exchange of histone H2AZ variant catalyzed by SWR1 chromatin remodeling complex. Science. 2004;303(5656):343-8. doi: 10.1126/science.1090701. PubMed PMID: 14645854.
56. Fazzio TG, Tsukiyama T. Chromatin remodeling in vivo: evidence for a nucleosome sliding mechanism. Mol Cell. 2003;12(5):1333-40. PubMed PMID: 14636590.
57. Bevilacqua A, Willis MS, Bultman SJ. SWI/SNF chromatin-remodeling complexes in cardiovascular development and disease. Cardiovasc Pathol. 2014;23(2):85-91. doi: 10.1016/j.carpath.2013.09.003. PubMed PMID: 24183004; PMCID: PMC3946279.
58. Wang Z, Zhai W, Richardson JA, Olson EN, Meneses JJ, Firpo MT, Kang C, Skarnes WC, Tjian R. Polybromo protein BAF180 functions in mammalian cardiac chamber maturation. Genes Dev. 2004;18(24):3106-16. doi: 10.1101/gad.1238104. PubMed PMID: 15601824; PMCID: PMC535920.
59. Lei I, Gao X, Sham MH, Wang Z. SWI/SNF protein component BAF250a regulates cardiac progenitor cell differentiation by modulating chromatin accessibility during second heart field development. J Biol Chem. 2012;287(29):24255-62. doi: 10.1074/jbc.M112.365080. PubMed PMID: 22621927; PMCID: PMC3397851.
60. Gao X, Tate P, Hu P, Tjian R, Skarnes WC, Wang Z. ES cell pluripotency and germ-layer formation require the SWI/SNF chromatin remodeling component BAF250a. Proc Natl Acad Sci U S A. 2008;105(18):6656-61. doi: 10.1073/pnas.0801802105. PubMed PMID: 18448678; PMCID: PMC2373334.
61. Hang CT, Yang J, Han P, Cheng HL, Shang C, Ashley E, Zhou B, Chang CP. Chromatin regulation by Brg1 underlies heart muscle development and disease. Nature. 2010;466(7302):62-7. doi: 10.1038/nature09130. PubMed PMID: 20596014; PMCID: PMC2898892.

62. Takeuchi JK, Lou X, Alexander JM, Sugizaki H, Delgado-Olguin P, Holloway AK, Mori AD, Wylie JN, Munson C, Zhu Y, Zhou YQ, Yeh RF, Henkelman RM, Harvey RP, Metzger D, Chambon P, Stainier DY, Pollard KS, Scott IC, Bruneau BG. Chromatin remodelling complex dosage modulates transcription factor function in heart development. Nat Commun. 2011;2:187. doi: 10.1038/ncomms1187. PubMed PMID: 21304516; PMCID: PMC3096875.

63. Lickert H, Takeuchi JK, Von Both I, Walls JR, McAuliffe F, Adamson SL, Henkelman RM, Wrana JL, Rossant J, Bruneau BG. Baf60c is essential for function of BAF chromatin remodelling complexes in heart development. Nature. 2004;432(7013):107-12. doi: 10.1038/nature03071. PubMed PMID: 15525990.

64. Lange M, Kaynak B, Forster UB, Tonjes M, Fischer JJ, Grimm C, Schlesinger J, Just S, Dunkel I, Krueger T, Mebus S, Lehrach H, Lurz R, Gobom J, Rottbauer W, Abdelilah-Seyfried S, Sperling S. Regulation of muscle development by DPF3, a novel histone acetylation and methylation reader of the BAF chromatin remodeling complex. Genes Dev. 2008;22(17):2370-84. doi: 10.1101/gad.471408. PubMed PMID: 18765789; PMCID: PMC2532927.

65. Takeuchi JK, Bruneau BG. Directed transdifferentiation of mouse mesoderm to heart tissue by defined factors. Nature. 2009;459(7247):708-11. doi: 10.1038/nature08039. PubMed PMID: 19396158; PMCID: PMC2728356.

66. Ingram KG, Curtis CD, Silasi-Mansat R, Lupu F, Griffin CT. The NuRD chromatin-remodeling enzyme CHD4 promotes embryonic vascular integrity by transcriptionally regulating extracellular matrix proteolysis. PLoS Genet. 2013;9(12):e1004031. doi: 10.1371/journal.pgen.1004031. PubMed PMID: 24348274; PMCID: PMC3861115.

67. Singh AP, Archer TK. Analysis of the SWI/SNF chromatin-remodeling complex during early heart development and BAF250a repression cardiac gene transcription during P19 cell differentiation. Nucleic Acids Res. 2014;42(5):2958-75. doi: 10.1093/nar/gkt1232. PubMed PMID: 24335282; PMCID: PMC3950667.

68. Clapier CR, Nightingale KP, Becker PB. A critical epitope for substrate recognition by the nucleosome remodeling ATPase ISWI. Nucleic Acids Res. 2002;30(3):649-55. PubMed PMID: 11809876; PMCID: PMC100309.

69. Goldman JA, Garlick JD, Kingston RE. Chromatin remodeling by imitation switch (ISWI) class ATP-dependent remodelers is stimulated by histone variant H2A.Z. J Biol Chem. 2010;285(7):4645-51. doi: 10.1074/jbc.M109.072348. PubMed PMID: 19940112; PMCID: PMC2836070.

70. Corona DF, Siriaco G, Armstrong JA, Snarskaya N, McClymont SA, Scott MP, Tamkun JW. ISWI regulates higher-order chromatin structure and histone H1 assembly in vivo. PLoS Biol. 2007;5(9):e232. doi: 10.1371/journal.pbio.0050232. PubMed PMID: 17760505; PMCID: PMC1951781.

71. Amin NM, Greco TM, Kuchenbrod LM, Rigney MM, Chung MI, Wallingford JB, Cristea IM, Conlon FL. Proteomic profiling of cardiac tissue by isolation of nuclei tagged in specific cell types (INTACT). Development. 2014;141(4):962-73. doi: 10.1242/dev.098327. PubMed PMID: 24496632; PMCID: PMC3912835.

72. Okano M, Bell DW, Haber DA, Li E. DNA methyltransferases Dnmt3a and Dnmt3b are essential for de novo methylation and mammalian development. Cell. 1999;99(3):247-57. PubMed PMID: 10555141.

73. Ueda Y, Okano M, Williams C, Chen T, Georgopoulos K, Li E. Roles for Dnmt3b in mammalian development: a mouse model for the ICF syndrome. Development. 2006;133(6):1183-92. doi: 10.1242/dev.02293. PubMed PMID: 16501171.

74. Tate P, Skarnes W, Bird A. The methyl-CpG binding protein MeCP2 is essential for embryonic development in the mouse. Nat Genet. 1996;12(2):205-8. doi: 10.1038/ng0296-205. PubMed PMID: 8563762.

75. Hashimshony T, Zhang J, Keshet I, Bustin M, Cedar H. The role of DNA methylation in setting up chromatin structure during development. Nat Genet. 2003;34(2):187-92. doi: 10.1038/ng1158. PubMed PMID: 12740577.

76. Kou CY, Lau SL, Au KW, Leung PY, Chim SS, Fung KP, Waye MM, Tsui SK. Epigenetic regulation of neonatal cardiomyocytes differentiation. Biochem Biophys Res Commun. 2010;400(2):278-83. doi: 10.1016/j.bbrc.2010.08.064. PubMed PMID: 20735989.

77. Paradis A, Xiao D, Zhou J, Zhang L. Endothelin-1 promotes cardiomyocyte terminal differentiation in the developing heart via heightened DNA methylation. Int J Med Sci. 2014;11(4):373-80. doi: 10.7150/ijms.7802. PubMed PMID: 24578615; PMCID: PMC3936032.

78. Sheng W, Qian Y, Zhang P, Wu Y, Wang H, Ma X, Chen L, Ma D, Huang G. Association of promoter methylation statuses of congenital heart defect candidate genes with Tetralogy of Fallot. J Transl Med. 2014;12:31. doi: 10.1186/1479-5876-12-31. PubMed PMID: 24479926; PMCID: PMC3915623.

79. Movassagh M, Vujic A, Foo R. Genome-wide DNA methylation in human heart failure. Epigenomics. 2011;3(1):103-9. doi: 10.2217/epi.10.70. PubMed PMID: 22126157.

80. Wu CH, Chen S, Shortreed MR, Kreitinger GM, Yuan Y, Frey BL, Zhang Y, Mirza S, Cirillo LA, Olivier M, Smith LM. Sequence-specific capture of protein-DNA complexes for mass spectrometric protein identification. PLoS One. 2011;6(10):e26217. doi: 10.1371/journal.pone.0026217. PubMed PMID: 22028835; PMCID: PMC3197616.

81. Meshorer E, Yellajoshula D, George E, Scambler PJ, Brown DT, Misteli T. Hyperdynamic plasticity of chromatin proteins in pluripotent embryonic stem cells. Dev Cell. 2006;10(1):105-16. doi: 10.1016/j.devcel.2005.10.017. PubMed PMID: 16399082; PMCID: PMC1868458.

82. Zhang Y, Cooke M, Panjwani S, Cao K, Krauth B, Ho PY, Medrzycki M, Berhe DT, Pan C, McDevitt TC, Fan Y. Histone h1 depletion impairs embryonic stem cell differentiation. PLoS

Genet. 2012;8(5):e1002691. doi: 10.1371/journal.pgen.1002691. PubMed PMID: 22589736; PMCID: PMC3349736.

83. Terme JM, Sese B, Millan-Arino L, Mayor R, Izpisua Belmonte JC, Barrero MJ, Jordan A. Histone H1 variants are differentially expressed and incorporated into chromatin during differentiation and reprogramming to pluripotency. J Biol Chem. 2011;286(41):35347-57. doi: 10.1074/jbc.M111.281923. PubMed PMID: 21852237; PMCID: PMC3195578.
84. Franklin S, Chen H, Mitchell-Jordan S, Ren S, Wang Y, Vondriska TM. Quantitative analysis of the chromatin proteome in disease reveals remodeling principles and identifies high mobility group protein B2 as a regulator of hypertrophic growth. Mol Cell Proteomics. 2012;11(6):M111 014258. doi: 10.1074/mcp.M111.014258. PubMed PMID: 22270000; PMCID: PMC3433888.
85. Monzen K, Ito Y, Naito AT, Kasai H, Hiroi Y, Hayashi D, Shiojima I, Yamazaki T, Miyazono K, Asashima M, Nagai R, Komuro I. A crucial role of a high mobility group protein HMGA2 in cardiogenesis. Nat Cell Biol. 2008;10(5):567-74. doi: 10.1038/ncb1719. PubMed PMID: 18425117.
86. Hock R, Furusawa T, Ueda T, Bustin M. HMG chromosomal proteins in development and disease. Trends Cell Biol. 2007;17(2):72-9. doi: 10.1016/j.tcb.2006.12.001. PubMed PMID: 17169561; PMCID: PMC2442274.
87. Hariharan N, Sussman MA. Stressing on the nucleolus in cardiovascular disease. Biochim Biophys Acta. 2014;1842(6):798-801. doi: 10.1016/j.bbadis.2013.09.016. PubMed PMID: 24514103; PMCID: PMC3972279.
88. Monte E, Mouillesseaux K, Chen H, Kimball T, Ren S, Wang Y, Chen JN, Vondriska TM, Franklin S. Systems proteomics of cardiac chromatin identifies nucleolin as a regulator of growth and cellular plasticity in cardiomyocytes. Am J Physiol Heart Circ Physiol. 2013;305(11):H1624-38. doi: 10.1152/ajpheart.00529.2013. PubMed PMID: 24077883; PMCID: PMC3882469.

89. Towbin BD, Gonzalez-Aguilera C, Sack R, Gaidatzis D, Kalck V, Meister P, Askjaer P, Gasser SM. Step-wise methylation of histone H3K9 positions heterochromatin at the nuclear periphery. Cell. 2012;150(5):934-47. doi: 10.1016/j.cell.2012.06.051. PubMed PMID: 22939621.

90. Kehat I, Accornero F, Aronow BJ, Molkentin JD. Modulation of chromatin position and gene expression by HDAC4 interaction with nucleoporins. J Cell Biol. 2011;193(1):21-9. doi: 10.1083/jcb.201101046. PubMed PMID: 21464227; PMCID: PMC3082185.

91. Rober RA, Weber K, Osborn M. Differential timing of nuclear lamin A/C expression in the various organs of the mouse embryo and the young animal: a developmental study. Development. 1989;105(2):365-78. PubMed PMID: 2680424.

92. Constantinescu D, Gray HL, Sammak PJ, Schatten GP, Csoka AB. Lamin A/C expression is a marker of mouse and human embryonic stem cell differentiation. Stem Cells. 2006;24(1):177-85. doi: 10.1634/stemcells.2004-0159. PubMed PMID: 16179429.

93. Swift J, Ivanovska IL, Buxboim A, Harada T, Dingal PC, Pinter J, Pajerowski JD, Spinler KR, Shin JW, Tewari M, Rehfeldt F, Speicher DW, Discher DE. Nuclear lamin-A scales with tissue stiffness and enhances matrix-directed differentiation. Science. 2013;341(6149):1240104. doi: 10.1126/science.1240104. PubMed PMID: 23990565; PMCID: PMC3976548.

94. Harborth J, Elbashir SM, Bechert K, Tuschl T, Weber K. Identification of essential genes in cultured mammalian cells using small interfering RNAs. J Cell Sci. 2001;114(Pt 24):4557-65. PubMed PMID: 11792820.

95. Frock RL, Chen SC, Da DF, Frett E, Lau C, Brown C, Pak DN, Wang Y, Muchir A, Worman HJ, Santana LF, Ladiges WC, Rabinovitch PS, Kennedy BK. Cardiomyocyte-specific expression of lamin a improves cardiac function in Lmna-/- mice. PLoS One. 2012;7(8):e42918. doi: 10.1371/journal.pone.0042918. PubMed PMID: 22905185; PMCID: PMC3419749.

96. Fidzianska A, Walczak E, Glinka Z, Religa G. Nuclear architecture remodelling in cardiomyocytes with lamin A deficiency. Folia Neuropathol. 2008;46(3):196-203. PubMed PMID: 18825595.

97. Solovei I, Wang AS, Thanisch K, Schmidt CS, Krebs S, Zwerger M, Cohen TV, Devys D, Foisner R, Peichl L, Herrmann H, Blum H, Engelkamp D, Stewart CL, Leonhardt H, Joffe B. LBR and lamin A/C sequentially tether peripheral heterochromatin and inversely regulate differentiation. Cell. 2013;152(3):584-98. doi: 10.1016/j.cell.2013.01.009. PubMed PMID: 23374351.

98. Rozwadowska N, Kolanowski T, Wiland E, Siatkowski M, Pawlak P, Malcher A, Mietkiewski T, Olszewska M, Kurpisz M. Characterisation of nuclear architectural alterations during in vitro differentiation of human stem cells of myogenic origin. PLoS One. 2013;8(9):e73231. doi: 10.1371/journal.pone.0073231. PubMed PMID: 24019912; PMCID: PMC3760906.

99. Cuddapah S, Schones DE, Cui K, Roh TY, Barski A, Wei G, Rochman M, Bustin M, Zhao K. Genomic profiling of HMGN1 reveals an association with chromatin at regulatory regions. Mol Cell Biol. 2011;31(4):700-9. doi: 10.1128/MCB.00740-10. PubMed PMID: 21173166; PMCID: PMC3028635.

100. Cuddapah S, Jothi R, Schones DE, Roh TY, Cui K, Zhao K. Global analysis of the insulator binding protein CTCF in chromatin barrier regions reveals demarcation of active and repressive domains. Genome Res. 2009;19(1):24-32. doi: 10.1101/gr.082800.108. PubMed PMID: 19056695; PMCID: PMC2612964.

101. Li JY, Patterson M, Mikkola HK, Lowry WE, Kurdistani SK. Dynamic distribution of linker histone H1.5 in cellular differentiation. PLoS Genet. 2012;8(8):e1002879. doi: 10.1371/journal.pgen.1002879. PubMed PMID: 22956909; PMCID: PMC3431313.

102. Catez F, Ueda T, Bustin M. Determinants of histone H1 mobility and chromatin binding in living cells. Nat Struct Mol Biol. 2006;13(4):305-10. doi: 10.1038/nsmb1077. PubMed PMID: 16715048; PMCID: PMC3730444.

103. Reeves R. Nuclear functions of the HMG proteins. Biochim Biophys Acta. 2010;1799(1-2):3-14. doi: 10.1016/j.bbagrm.2009.09.001. PubMed PMID: 19748605; PMCID: PMC2818135.

104. Khalil AM, Guttman M, Huarte M, Garber M, Raj A, Rivea Morales D, Thomas K, Presser A, Bernstein BE, van Oudenaarden A, Regev A, Lander ES, Rinn JL. Many human large intergenic noncoding RNAs associate with chromatin-modifying complexes and affect gene expression. Proc Natl Acad Sci U S A. 2009;106(28):11667-72. doi: 10.1073/pnas.0904715106. PubMed PMID: 19571010; PMCID: PMC2704857.

105. Wang KC, Yang YW, Liu B, Sanyal A, Corces-Zimmerman R, Chen Y, Lajoie BR, Protacio A, Flynn RA, Gupta RA, Wysocka J, Lei M, Dekker J, Helms JA, Chang HY. A long noncoding RNA maintains active chromatin to coordinate homeotic gene expression. Nature. 2011;472(7341):120-4. doi: 10.1038/nature09819. PubMed PMID: 21423168; PMCID: PMC3670758.

106. Mohammad F, Pandey GK, Mondal T, Enroth S, Redrup L, Gyllensten U, Kanduri C. Long noncoding RNA-mediated maintenance of DNA methylation and transcriptional gene silencing. Development. 2012;139(15):2792-803. doi: 10.1242/dev.079566. PubMed PMID: 22721776.

107. Schmitz KM, Mayer C, Postepska A, Grummt I. Interaction of noncoding RNA with the rDNA promoter mediates recruitment of DNMT3b and silencing of rRNA genes. Genes Dev. 2010;24(20):2264-9. doi: 10.1101/gad.590910. PubMed PMID: 20952535; PMCID: PMC2956204.

108. Schonrock N, Harvey RP, Mattick JS. Long noncoding RNAs in cardiac development and pathophysiology. Circ Res. 2012;111(10):1349-62. doi: 10.1161/CIRCRESAHA.112.268953. PubMed PMID: 23104877.

109. Dorn GW, 2nd. Therapeutic potential of microRNAs in heart failure. Curr Cardiol Rep. 2010;12(3):209-15. doi: 10.1007/s11886-010-0096-7. PubMed PMID: 20424963.

110. Small EM, Olson EN. Pervasive roles of microRNAs in cardiovascular biology. Nature. 2011;469(7330):336-42. doi: 10.1038/nature09783. PubMed PMID: 21248840; PMCID: PMC3073349.

111. Chen JF, Murchison EP, Tang R, Callis TE, Tatsuguchi M, Deng Z, Rojas M, Hammond SM, Schneider MD, Selzman CH, Meissner G, Patterson C, Hannon GJ, Wang DZ. Targeted deletion of Dicer in the heart leads to dilated cardiomyopathy and heart failure. Proc Natl Acad Sci U S A. 2008;105(6):2111-6. doi: 10.1073/pnas.0710228105. PubMed PMID: 18256189; PMCID: PMC2542870.

112. Saxena A, Tabin CJ. miRNA-processing enzyme Dicer is necessary for cardiac outflow tract alignment and chamber septation. Proc Natl Acad Sci U S A. 2010;107(1):87-91. doi: 10.1073/pnas.0912870107. PubMed PMID: 20018673; PMCID: PMC2806718.

113. van Rooij E, Olson EN. microRNAs put their signatures on the heart. Physiol Genomics. 2007;31(3):365-6. doi: 10.1152/physiolgenomics.00206.2007. PubMed PMID: 17848602.

114. Dorn GW, 2nd. Decoding the cardiac message: the 2011 Thomas W. Smith Memorial Lecture. Circ Res. 2012;110(5):755-63. doi: 10.1161/CIRCRESAHA.111.256768. PubMed PMID: 22383710; PMCID: PMC3294415.

115. Cabili MN, Trapnell C, Goff L, Koziol M, Tazon-Vega B, Regev A, Rinn JL. Integrative annotation of human large intergenic noncoding RNAs reveals global properties and specific subclasses. Genes Dev. 2011;25(18):1915-27. doi: 10.1101/gad.17446611. PubMed PMID: 21890647; PMCID: PMC3185964.

116. He A, Kong SW, Ma Q, Pu WT. Co-occupancy by multiple cardiac transcription factors identifies transcriptional enhancers active in heart. Proc Natl Acad Sci U S A. 2011;108(14):5632-7. doi: 10.1073/pnas.1016959108. PubMed PMID: 21415370; PMCID: PMC3078411.

117. Guttman M, Donaghey J, Carey BW, Garber M, Grenier JK, Munson G, Young G, Lucas AB, Ach R, Bruhn L, Yang X, Amit I, Meissner A, Regev A, Rinn JL, Root DE, Lander ES.

lincRNAs act in the circuitry controlling pluripotency and differentiation. Nature. 2011;477(7364):295-300. doi: 10.1038/nature10398. PubMed PMID: 21874018; PMCID: PMC3175327.

118. Orom UA, Derrien T, Beringer M, Gumireddy K, Gardini A, Bussotti G, Lai F, Zytnicki M, Notredame C, Huang Q, Guigo R, Shiekhattar R. Long noncoding RNAs with enhancer-like function in human cells. Cell. 2010;143(1):46-58. doi: 10.1016/j.cell.2010.09.001. PubMed PMID: 20887892; PMCID: PMC4108080.

119. Klattenhoff CA, Scheuermann JC, Surface LE, Bradley RK, Fields PA, Steinhauser ML, Ding H, Butty VL, Torrey L, Haas S, Abo R, Tabebordbar M, Lee RT, Burge CB, Boyer LA. Braveheart, a long noncoding RNA required for cardiovascular lineage commitment. Cell. 2013;152(3):570-83. doi: 10.1016/j.cell.2013.01.003. PubMed PMID: 23352431; PMCID: PMC3563769.

120. Grote P, Wittler L, Hendrix D, Koch F, Wahrisch S, Beisaw A, Macura K, Blass G, Kellis M, Werber M, Herrmann BG. The tissue-specific lncRNA Fendrr is an essential regulator of heart and body wall development in the mouse. Dev Cell. 2013;24(2):206-14. doi: 10.1016/j.devcel.2012.12.012. PubMed PMID: 23369715; PMCID: PMC4149175.

121. Zhang C, Darnell RB. Mapping in vivo protein-RNA interactions at single-nucleotide resolution from HITS-CLIP data. Nat Biotechnol. 2011;29(7):607-14. doi: 10.1038/nbt.1873. PubMed PMID: 21633356; PMCID: PMC3400429.

122. Alabert C, Bukowski-Wills JC, Lee SB, Kustatscher G, Nakamura K, de Lima Alves F, Menard P, Mejlvang J, Rappsilber J, Groth A. Nascent chromatin capture proteomics determines chromatin dynamics during DNA replication and identifies unknown fork components. Nat Cell Biol. 2014;16(3):281-93. doi: 10.1038/ncb2918. PubMed PMID: 24561620; PMCID: PMC4283098.

123. Trinh le A, Hochgreb T, Graham M, Wu D, Ruf-Zamojski F, Jayasena CS, Saxena A, Hawk R, Gonzalez-Serricchio A, Dixson A, Chow E, Gonzales C, Leung HY, Solomon I, Bronner-

Fraser M, Megason SG, Fraser SE. A versatile gene trap to visualize and interrogate the function of the vertebrate proteome. Genes Dev. 2011;25(21):2306-20. doi: 10.1101/gad.174037.111. PubMed PMID: 22056673; PMCID: PMC3219234.

124. Sallam K, Kodo K, Wu JC. Modeling inherited cardiac disorders. Circ J. 2014;78(4):784-94. PubMed PMID: 24632794.

125. Dahl KN, Ribeiro AJ, Lammerding J. Nuclear shape, mechanics, and mechanotransduction. Circ Res. 2008;102(11):1307-18. doi: 10.1161/CIRCRESAHA.108.173989. PubMed PMID: 18535268; PMCID: PMC2717705.

126. Pajerowski JD, Dahl KN, Zhong FL, Sammak PJ, Discher DE. Physical plasticity of the nucleus in stem cell differentiation. Proc Natl Acad Sci U S A. 2007;104(40):15619-24. doi: 10.1073/pnas.0702576104. PubMed PMID: 17893336; PMCID: PMC2000408.

127. Fanburg BL, Posner BI. Ribonucleic acid synthesis in experimental cardiac hypertrophy in rats. I. Characterization and kinetics of labeling. Circ Res. 1968;23(1):123-35. PubMed PMID: 4232616.

128. Cluzeaud F, Perennec J, de Amoral E, Willemin M, Hatt PY. Myocardial cell nucleus in cardiac overloading in the rat. Eur Heart J. 1984;5 Suppl F:271-80. PubMed PMID: 6241897.

Chapter 2: Structural Regulators for the Establishment of Cardiac Genomic Architecture

DNA packaging, organized by histones and non-nucleosomal structural proteins, is critical for fitting the genome inside the nucleus. Moreover, the degrees of packaging establish a cell-specific landscape allowing for select accessibility of loci for expression. This genomic organization is a dynamic process occurring with differentiation, ensuring appropriate activation and silencing of genes to globally synchronize cellular processes. Chromatin structural proteins are ubiquitously expressed across different tissues and lack a consensus DNA binding sequence. The central question that remains to be addressed is: how do these proteins contribute to cell type-specific chromatin architecture?

Regulation by ATP-dependent remodeling complexes and histone post-translational modifications has been widely studied and shown to play critical roles in maintaining cardiac phenotype both during development and disease (1, 2), and their appropriate expression at defined stages is essential for differentiation (3). While these protein complexes are ubiquitously expressed in different tissue types, their regulation of tissue-specific chromatin structure can be mediated by combinatorial interactions with protein partners, including cardiac transcription factors (3). How cardiac chromatin architecture is specified remains a fundamental question. In this project, we hypothesized that key chromatin structural factors involved in establishing the cardiac transcriptome should be regulated by transcription factors temporally to build on the genomic framework over the course of cellular differentiation. Moreover, alterations to the abundances and/or functions of these key regulators will result in aberrant gene expression to affect disease pathology. Candidate chromatin structural genes may encode for proteins involved in DNA packaging around nucleosomes, nucleosome positioning, higher-order genomic compaction, and/or association with nuclear subcompartments like the nuclear envelope (Figure 2-1).

To search for genes regulated in a cardiac-specific manner, we referenced published ChIP-seq data for five cardiac transcription factors from the HL1 cardiomyocyte cell line (4). The transcription factors used for analysis included: Gata4, Mef2a, Nkx2-5, Srf and Tbx5. The hypothesis is: as transcription factors are turned on with cellular differentiation, they activate chromatin structural genes in a tissue-specific manner to define cell lineage (Figure 2-2). We utilized the ChIP-seq findings to obtain a list of candidates matched with gene ontology terms, chromatin or nucleus, and bound by individual cardiac transcription factors at their promoter (Figure 2-3).

Alternatively, we took a different approach to thoroughly screen for candidate genes. We generated a comprehensive nuclear gene list of putative factors through searching both gene and protein databases. For our gene predictions, we gathered a list of all genes associated with the gene ontology term nucleus, which gave a list of ~4,000 genes. Complementary to compiling a nuclear gene list based on gene ontology, we also searched the mouse proteome (~33,000 proteins) against the Nuclear Protein Database (NPD) to obtain a list of genes based on protein predictions (5). Using the NPD, three different criteria were used: *1)* the NucPred score of ≥0.8, a prediction score for predicting whether the protein spends time in the nucleus (While the outcomes had ~90% accuracy, the coverage was low. As a result, we loosened our requirements by also including the next two criteria.), *2)* a predicted nuclear localization signal with presumed nuclear localization and/or *3)* gene ontology term for nucleus. Any protein meeting at least one of these criteria was used. This list of protein names (~7,000) was converted to gene names (~4,000). By combining the lists of genes from our gene ontology and protein predictions, we retrieved a master list of 6,434 nuclear-associated genes that we used in our subsequent analyses. It should be noted that we wanted to obtain a comprehensive list and many false hits

appear on this list that will be manually filtered. These include many transcription factors that may be unrelated to the context of cardiac development.

We cross-referenced our nuclear gene list to genes with cardiac transcription factor enrichment at their promoters, the regions defined as 2kb upstream of the transcription start sites (4). While a number of the genes obtained from gene ontology and protein predictions overlapped, there were many that might have been missed from a gene ontology search alone (Figures 2-3, 2-4, 2-5A). A number of chromatin factors from the analysis had promoter enrichment of these transcription factors with some examples highlighted (Figure 2-5A). In He *et al.*, cardiac transcription factor ChIP-seq was used to identify new cardiac enhancers based on binding of multiple factors, which would implicate tissue specificity (4). We followed this rationale to find cardiac-specific structural regulators by subsetting the nuclear-associated genes based on the number of transcription factors that were bound at their promoter (one to all five transcription factors) (Figure 2-5B). We found many interesting candidate genes bound by multiple transcription factors from this search, including regulators of histone methylation (e.g. Ehmt2, Smyd1, Whsc1l1) and chromatin structure (e.g. Smarca, Hmgb) (Table 2-1 lists genes with at least 3 transcription factors bound). Jarid2 (bound by Gata4, Srf and Tbx5) and Nucleolin (bound by Gata4, Mef2a, Srf and Tbx5) were identified as putatively regulated by multiple transcription factors; these genes have previously been implicated in cardiac development (6, 7). It is important to note that these experiments were carried out in cultured cells with expression of exogenous forms of these transcription factors. It will be necessary to validate these findings *in vivo* with ChIP-PCR for the endogenous proteins.

To find the genes that are developmentally critical, we focused on genes that are positively regulated over the course of differentiation from embryonic stem cell to cardiomyocyte (Figure 2-2). (We did not include candidate genes that are negatively regulated with differentiation,

downregulated across the time course, but these should be considered in complementary analyses as we try to dissect mechanisms of gene regulation.) We used available RNA-seq datasets for different stages of mouse stem cell to cardiomyocyte differentiation (4954 of the genes from our master nucleus-associated gene list were annotated in the RNA-seq) to retrieve genes that are activated in the process (Figure 2-6) (8). Of the genes that were upregulated (2079 had increased expression comparing stem cells to differentiated cardiomyocytes), the list was further narrowed based on which genes are affected by Gata4 knockout (9). If Gata4 is a positive regulator of a chromatin structural protein's expression, then we expected reduced RNA expression in the Gata4 knockout model. From this list, we then looked at the subset bound by 3, 4 or 5 cardiac transcription factors (4), of which one of the transcription factors is Gata4 (a direct regulator), removed irrelevant genes (non-cardiac transcription factors and cell cycle-related genes) and generated a final list of 15 candidates (Figure 2-6, Table 2-2).

We hypothesized that disruption of cardiac chromatin structure due to stress is responsible for a disease-associated gene expression profile. Therefore, we checked the expression levels of the 15 candidate nuclear-associated structural genes in a pathological setting across a panel of mouse strains that were stressed with isoproterenol (10), the rationale being that isoproterenol-induced transcriptome changes and pathology are universally mediated by altered expression of these chromatin structural factors. We examined the trends in expression (only 12 of the 15 genes were found on the microarray from this study), both at basal states and change in expression after isoproterenol, with changes in normalized heart weight (those that showed significant correlation are shown in Figure 2-7) and other phenotypes (not shown). The majority of gene expressions did not correlate with total heart weight. We examined the complete list of phenotypes measured (10), and individual genes significantly correlated with very few phenotypes (see Chapter 5). Because the genes here were derived based on evidence of direct regulation by Gata4, we examined the relationships between Gata4 and the candidate gene expressions across the panel

of mice and found no trend between changes in Gata4 expression after isoproterenol stress and changes in expression of the candidate genes (Figure 2-8). We do find that Lbh, implicated in heart and limb development (11), to be consistently downregulated across most strains. Strikingly, we found that Gata4 expression response did not show a universal pattern across genetic backgrounds (Figure 2-8), and this inconsistency held true when expanding analyses to the other cardiac transcription factors (Figure 2-9). Cardiac transcription factors have been implicated not only to be critical during development but also regulate gene expression after hypertrophic stress (12, 13). Gata4 overexpression *in vivo* is sufficient to increased heart weight and activate a fetal gene response (14). Based on the reported findings, Gata4 is activated in response to hypertrophic stimuli and regulated post-translationally (12, 15), and Gata4 expression is induced in mice administered isoproterenol (16). However, when examining different mouse strains subjected to the same isoproterenol-induced stress, the responses of change in Gata4 expression differed, highlighting a level of regulation mediated by genetics. On the other hand, Nkx2-5 has been shown to increase expression in C57Bl/6 mice treated with isoproterenol (16), and this trend was consistent across the majority of strains (Figure 2-9). We did not observe significant relationships between levels of expression and heart weight (Figure 2-7A). These observations contributed to the rationale for exploring other expression patterns of cardiac genes across genetic backgrounds and is further discussed in Chapter 5.

In future analyses, we can incorporate additional complementary criteria for how we search for cardiac-specific chromatin structural genes. We can examine the lists of genes located near cardiac enhancers (4, 8, 17, 18), or temporally regulated by histone post-translational modifications over the course of differentiation (8, 19). Additionally, whether a key cardiac chromatin structural gene is affected by pathological stress may be insignificant. The genes involved in establishing cardiac chromatin structure can also be the factors involved in preserving cell type. In other words, when a cardiomyocyte is stressed, it does not convert into another cell

type; its identity is maintained. Thus, chromatin structural candidates may be involved in supporting global cardiac-specific genomic architecture, and other protein factors then locally regulate stress-induced changes in gene expression.

The analyses presented here have focused on protein-coding genes. Recent emergence of noncoding RNAs in tissue-specific gene regulation is another powerful mechanism by which cells can be programmed (20, 21). While chromatin structural proteins are ubiquitous, the tissue-specific noncoding RNAs may be the factors directing these chromatin structural factors to or even coregulating with them at target sites. Furthermore, no single candidate chromatin regulator shows strong correlation with all characteristic features of heart failure in the isoproterenol model (a complete panel of cardiac phenotypes is examined in Chapter 5). We may not be able to identify gene markers because we are looking for single genes to explain a complex trait that are also universal across diverse genetic backgrounds. As described in Chapter 1, the relationship between chromatin structural proteins and cardiac transcription factors is complex, with different tiers of regulation. Here, we examine one relationship, the regulation of expression of chromatin regulatory factors by cardiac transcription factors. Of course, it is important to incorporate the other means of cell type-specific gene regulation, mediated by coregulation and direct interactions of transcription factors and chromatin remodelers as well as the regulation of transcription factors mediated by chromatin structure. The variability in cardiac transcription factor expression changes emphasizes that the networks of genes affected due to pathological stress are not shared between strains. This data provides support for further examination of gene and protein networks and interactions in understanding cardiac development and disease.

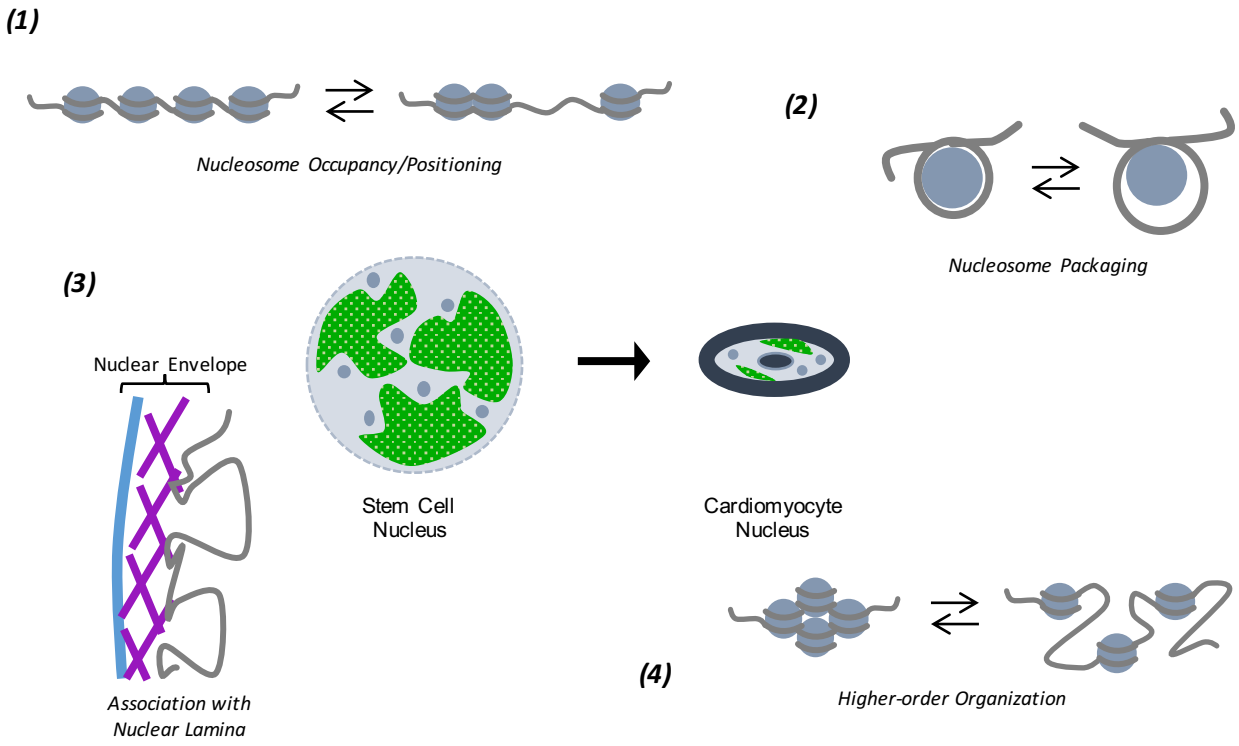

Figure 2-1: Candidate chromatin structural proteins for the establishment of cardiac-specific chromatin architecture. In this project, we aim to search for key chromatin structural factors that are required during the differentiation of a stem cell into a cardiomyocyte by laying out the genomic landscape for cardiac-specific gene expression. Putative gene candidates in this study include regulators of *1)* nucleosome occupancy and positioning (e.g. ATP-dependent chromatin remodelers), *2)* nucleosome packaging (e.g. histone post-translational modifiers), *3)* associations with the nuclear envelope (e.g. lamins) and *4)* regulators of higher-order chromatin structure (e.g. non-nucleosomal chromatin architectural proteins).

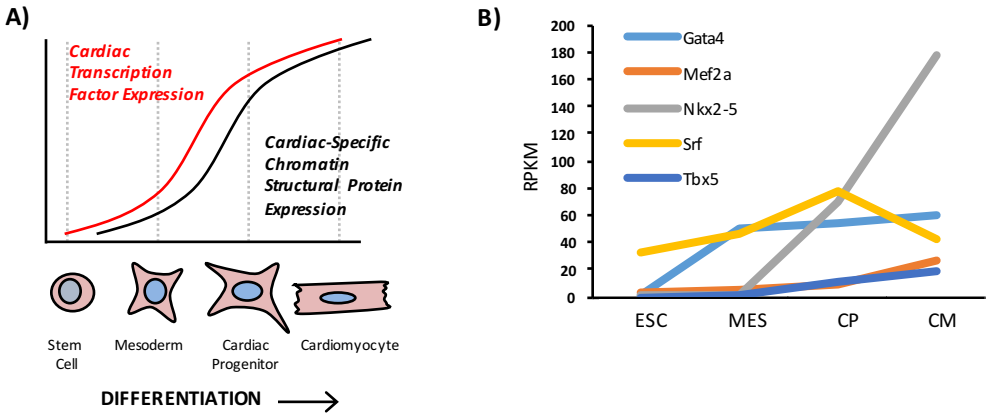

Figure 2-2: Experimental approach to identifying cardiac-specific chromatin structural regulators. A) Cardiac chromatin architecture is important for the establishment of a cell type-specific gene expression profile. Because architecture is regulated by chromatin structural factors that are ubiquitously expressed in different cell types, we hypothesize that cell specificity is mediated through the temporal regulation of these structural factors by transcription factors in the heart. RNA-seq data from different stages of mouse stem cell differentiation into cardiomyocytes will be used to identify chromatin structural genes that are activated in this process [8]. **B)** Expression of cardiac transcription factors is plotted over the course of mouse stem cell differentiation into cardiomyocytes [8]. ESC, embryonic stem cell; MES, mesoderm; CP, cardiac progenitor; CM, cardiomyocyte; RPKM, reads per kilobase of transcript per million mapped reads.

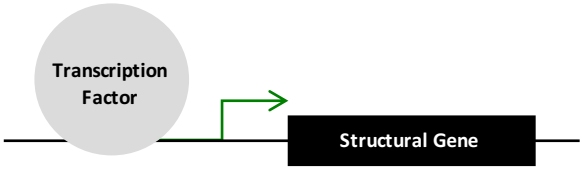

	GO: Chromatin	*GO: Nucleus*
Gata4	26	463
Mef2a	5	102
Nkx2-5	16	329
Srf	82	1363
Tbx5	99	1604
p300	–	6

Figure 2-3: Chromatin structural gene candidates identified by gene ontology. ChIP-seq was performed in HL1 cardiomyocytes, overexpressing cardiac transcription factors (Gata4, Mef2a, Nkx2-5, Srf, Tbx5 and p300) [4]. Gene ontology was used to retrieve a list of candidates with transcription factor binding at their promoter regions (within 2 kilobases upstream of the transcription start site) that are associated with terms chromatin or nucleus. The numbers of identified genes based on gene ontology are shown above.

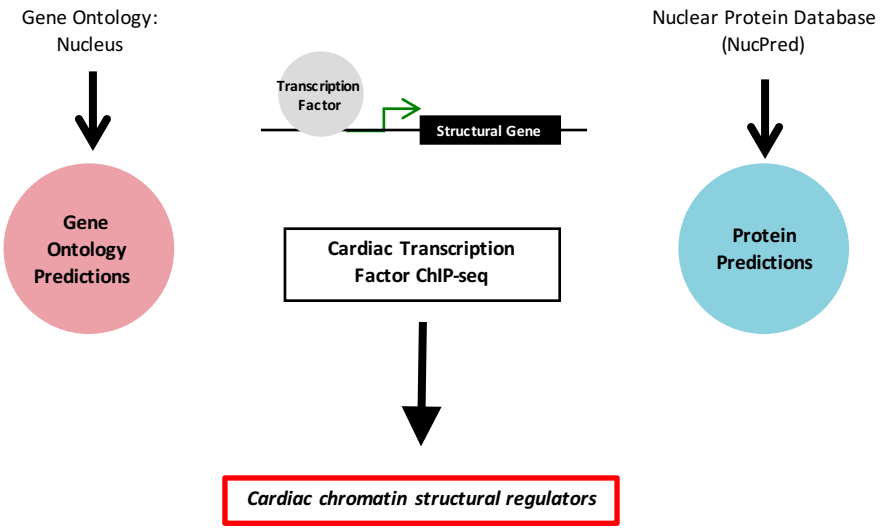

Figure 2-4: Screen for candidate cardiac chromatin structural genes. We generated a comprehensive list of nuclear genes using both gene and protein predictions. Our gene predictions were based on a gene ontology search for the term nucleus. Separately, a gene list using protein predictions was created using the Nuclear Protein Database [5]. The mouse proteome was used to identify those proteins found in the nucleus, have nuclear localization and/or are associated with gene ontology term nucleus; the protein names were converted to gene names. Combining these lists, we retrieved a total of 6,434 nuclear-associated genes that were screened to find ones having enrichment of cardiac transcription factor binding. We termed these cardiac chromatin structural regulators.

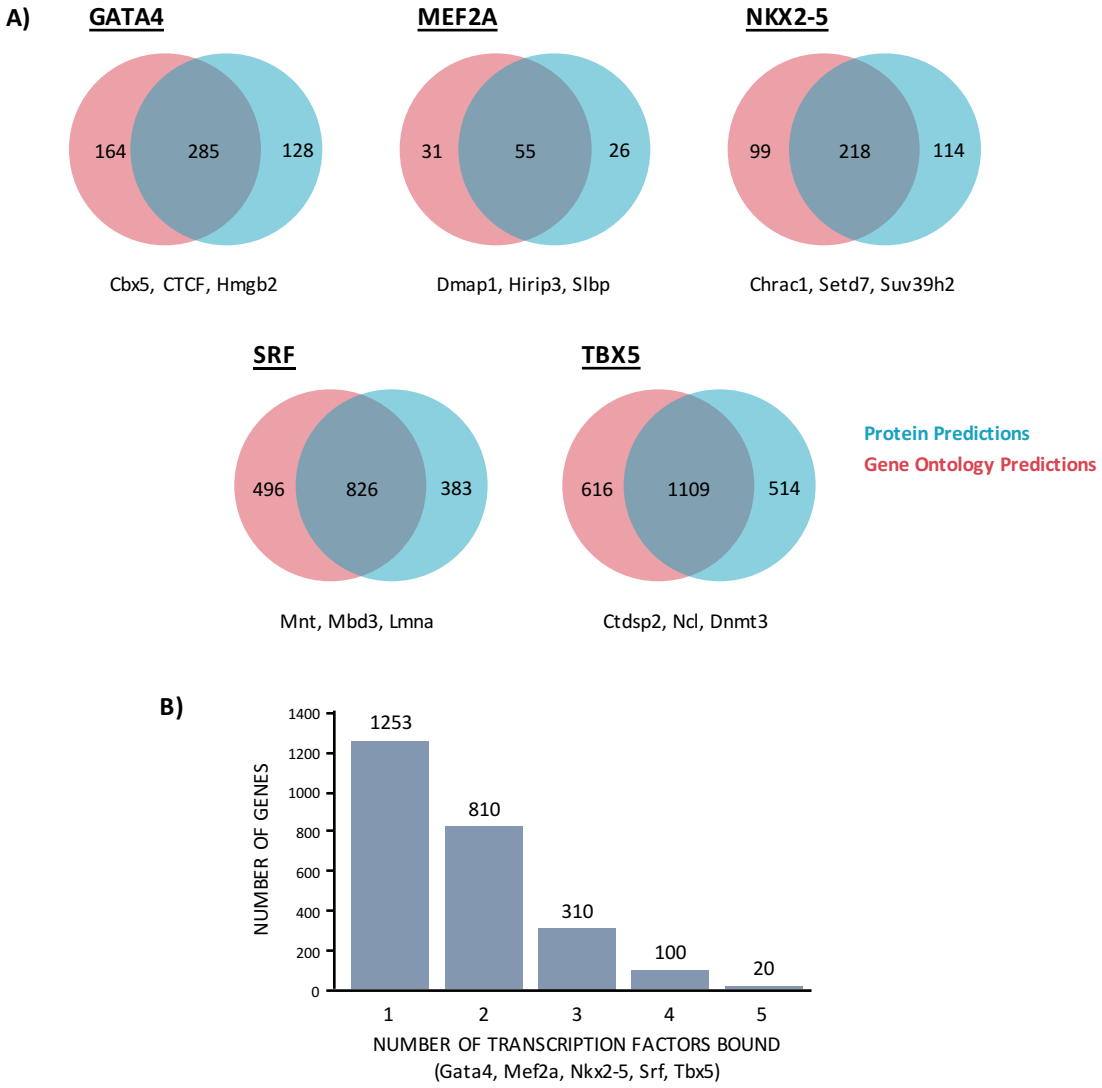

Figure 2-5: Candidate nucleus-associated genes identified as direct targets of cardiac transcription factors. A) Two lists of candidate genes (gene predictions and protein predictions) were combined to generate a master list. Here, the numbers of candidate genes bound by the indicated transcription factor at the promoter (2kb upstream of transcription start site) are shown [4]. Note that while some genes were common to both gene ontology and protein prediction searches, many are unique to each list. Examples of some genes of interest are listed. **B)** The breakdown of the number of genes that have enrichment of one or more cardiac transcription factors within their promoter is shown. We focused our attention on the genes that are potentially regulated by three or more transcription factors, as this may indicate cell specificity (see Table 2-1).

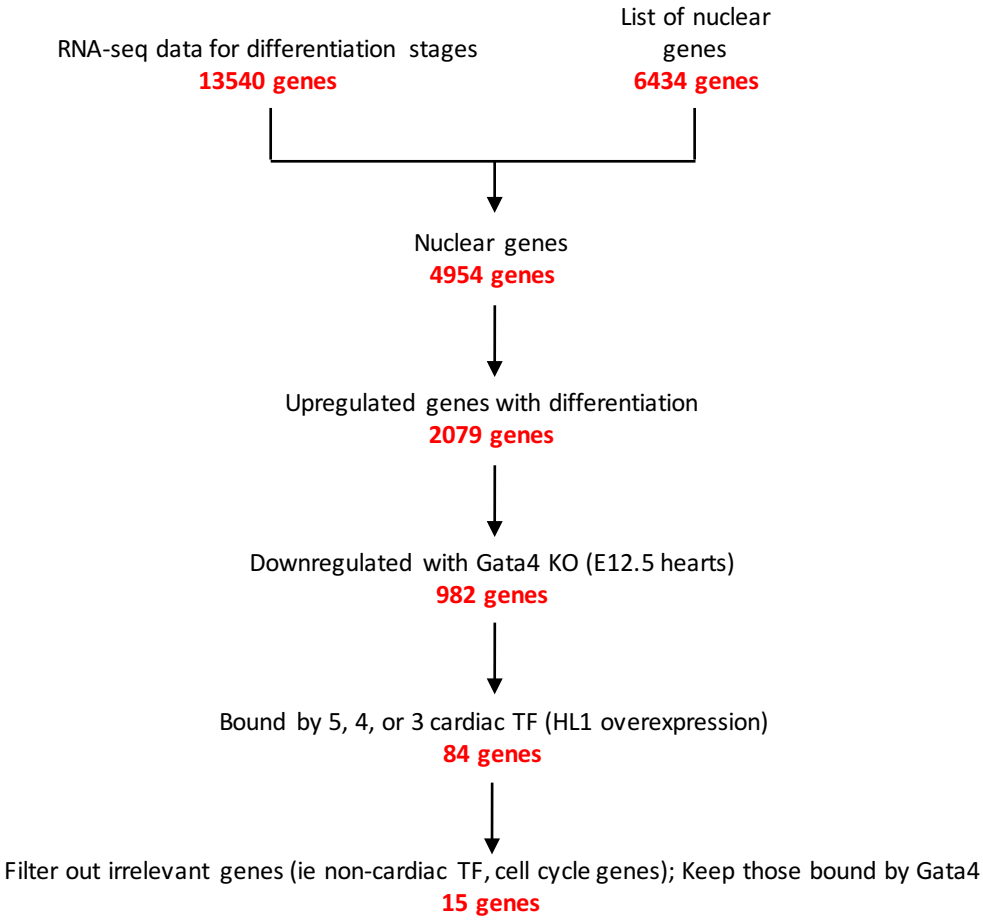

Figure 2-6: Workflow to identify Gata4-regulated chromatin structural genes. To obtain a list of chromatin structural regulators for further analyses, we used RNA-seq data to identify genes that are turned on with differentiation to establish cardiac genomic architecture. Of our 6434 genes, 4954 genes were found on the list of analyzed genes from RNA-seq data [8]. We wanted genes that are upregulated between stem cell and cardiomyocyte stages, giving us 2079 candidates. Because of expression data available after Gata4 knockout in E12.5 mouse hearts [9], we postulated that if Gata4 is a direct regulator, then Gata4-knockout hearts should show reduced expression of these genes (982 fit this criteria). This list of genes was further narrowed by determining which have at least 3 of the cardiac transcription factors bound at their promoter [4], of which one was Gata4. We finally performed a manual screen to remove irrelevant genes (non-cardiac genes, signaling molecules, cell cycle genes) and reached a list of 15 candidates.

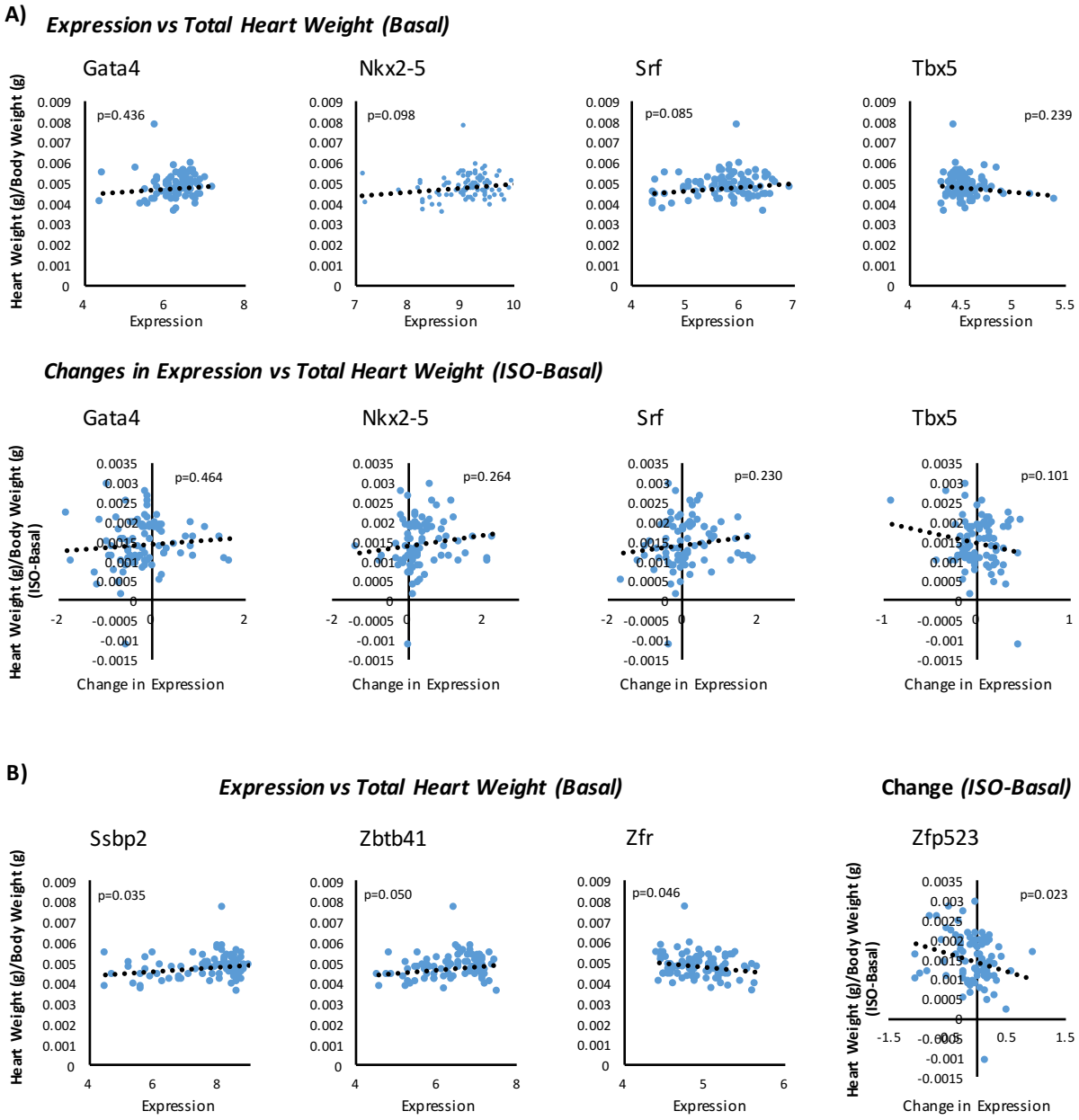

Figure 2-7: Relationships of chromatin structural genes with total heart weight. A) Plots show the relationships between expression levels of each cardiac transcription factor and total heart weight (normalized to body weight) across 84 mouse strains [10]. Top row shows the basal expression versus basal heart weight while bottom row represents the change in expression versus change in heart weight after isoproterenol administration. Cardiac transcription factor expression does not show significant correlation with total heart weight. **B)** The candidate chromatin structural genes were also screened to determine whether abundance of these genes shows association with total heart mass. Here, only the genes/conditions that were significant are shown.

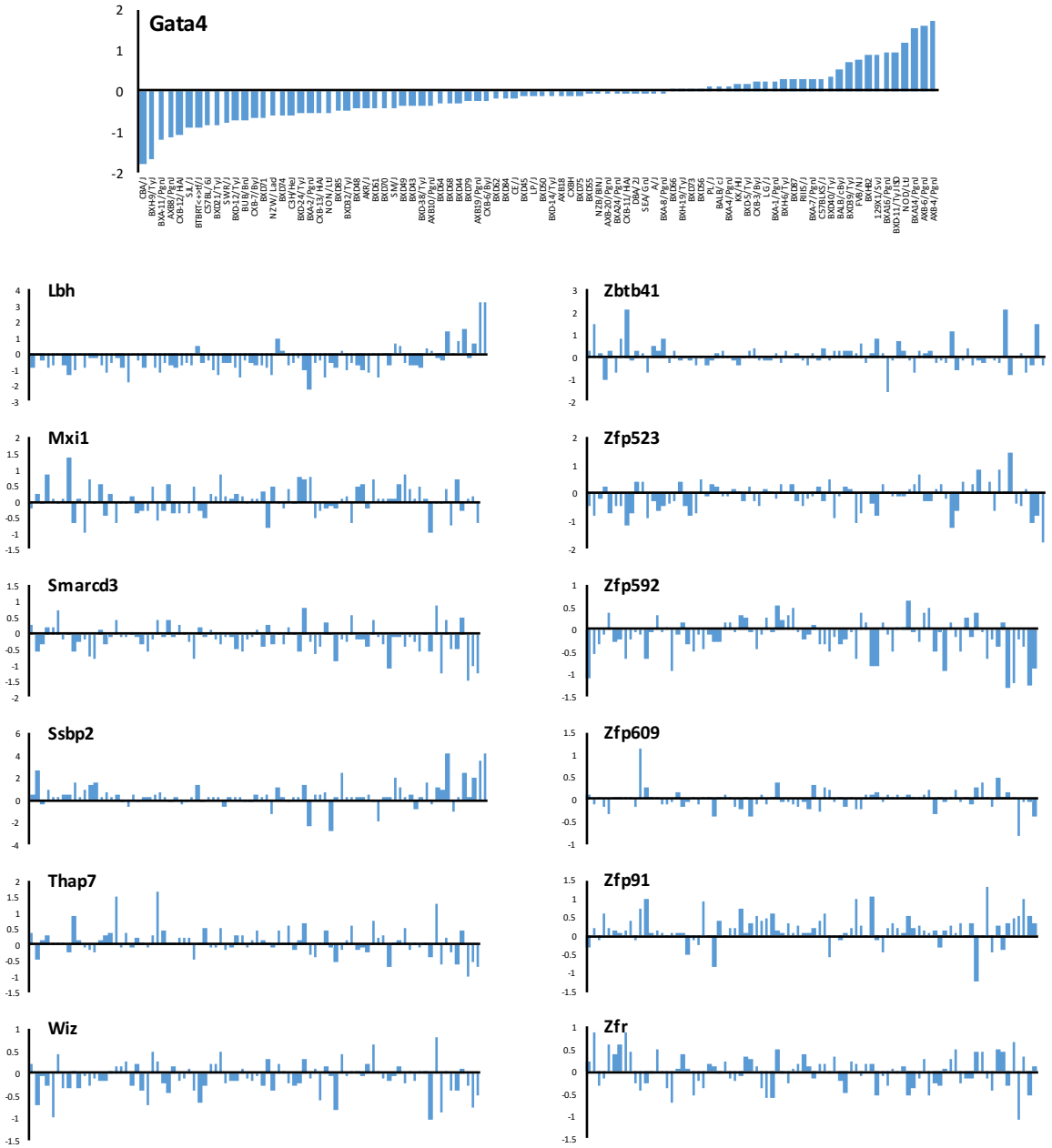

Figure 2-8: Change in expression of Gata4-regulated cardiac structural genes after isoproterenol treatment. 84 mouse strains were administered isoproterenol for 3 weeks [10]. The change in Gata4 expression (ISO-Basal) across the different strains is plotted. Each bar represents a single mouse strain, and strains are ordered based on change in Gata4 expression. Keeping the order of strains the same, below are the changes in expression of the individual candidate genes. There is no noticeable correlation between the expression changes of these genes with changes in Gata4 expression. Interestingly, changes in Gata4 expression are not consistent across the strains.

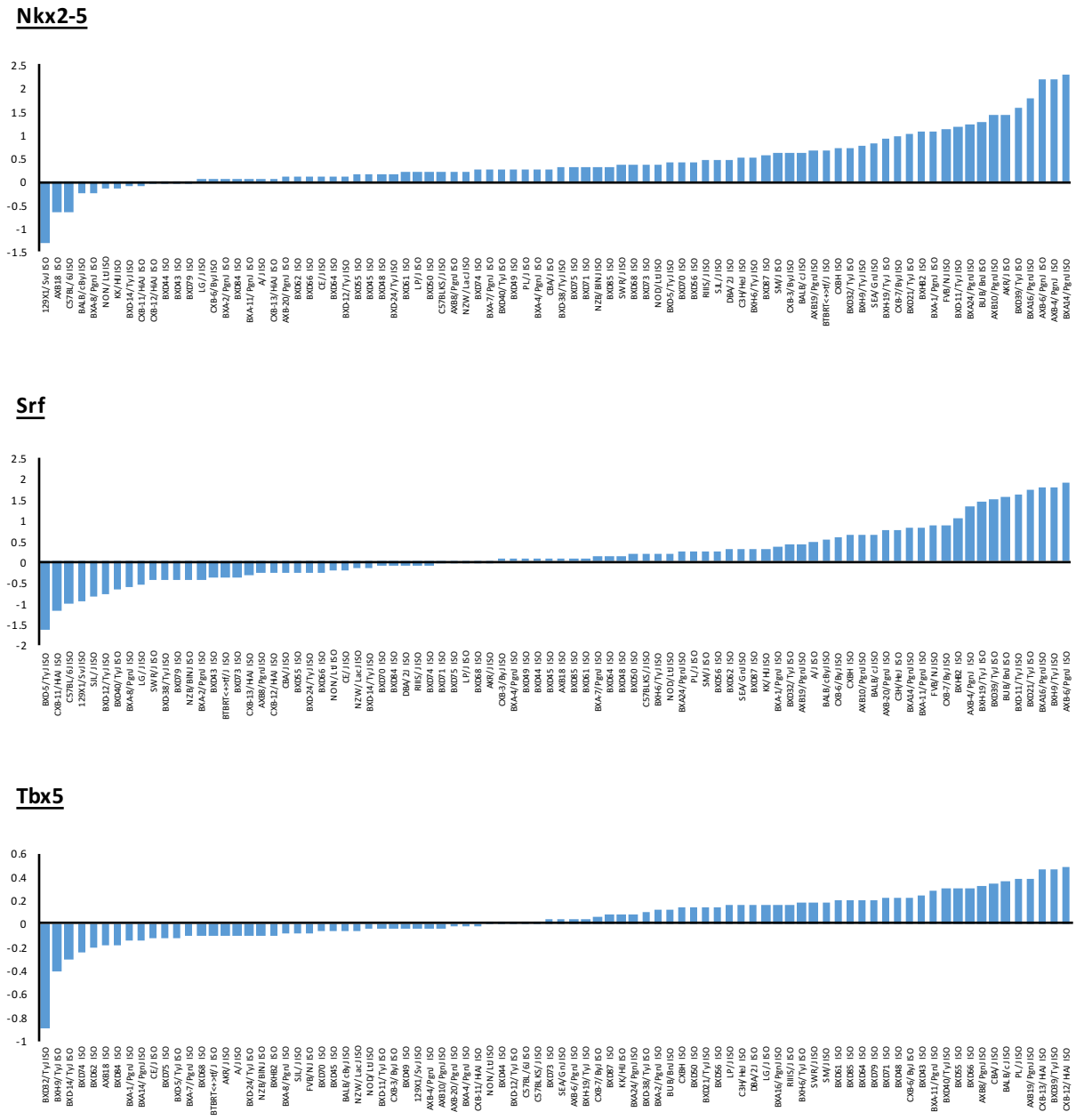

Figure 2-9: Change in cardiac transcription factor expression across mouse strains. The change in expression (ISO-Basal) of 84 different mouse strains is plotted [10]. For each transcription factor, the strains have been sorted by change. As with Gata4, the expression patterns of these transcription factors does not show universal patterns of change across all strains of mice, suggesting a genetic component to the regulation of gene expression. This topic is further explored in Chapter 5.

Table 2-1: Nuclear genes bound by multiple cardiac transcription factors

5 Factors	4 Factors		3 Factors						
0610009D07Rik	5830418K08Rik	Nsl1	1110037F02Rik	Cic	Ik	Nucks1	Rnf38	Tfip11	Zfp687
1700030J22Rik	9530077C05Rik	Nuf2	4632434I11Rik	Crebl2	Ilf3	Nvl	Rnf4	Thap7	Zfp771
6430548M08Rik	Ablim1	Nufip2	9130023H24Rik	Csdc2	Ing1	Osbpl1a	Rpl19	Tjp2	Zfp800
Ankrd1	Adamts1	Pard3	A430005L14Rik	Cse1l	Ints2	Otud4	Rps6kb2	Tkt	Zfp9
Arhgef1	Adk	Per1	Aco2	Cstf3	Ints6	Pank1	Runx1	Tmf1	Zfp91
Egln1	Anapc5	Plekha6	Adm	Ctdsp1	Ipmk	Pax2	Rybp	Tmpo	Zfr
Fanca	Apobec3	Plekha7	Afap1	Cuedc2	Iqgap1	Pcgf2	Sacs	Tnks1bp1	Zhx2
Fbxl19	Arid1a	Polr2j	Agbl5	Daam2	Ivns1abp	Pcm1	Sbds	Tnpo2	Zkscan5
Gse1	Atoh8	Por	Ahdc1	Dab2ip	Jarid2	Pde4dip	Sbno2	Tnpo3	Zranb1
Hnrnpl	Baalc	Ppp1r15b	AI314180	Dazap1	Kcmf1	Pdpk1	Sdccag8	Toe1	Zranb3
Hsbp1	Bcl6	Ppp1r9b	Akap12	Ddit3	Kifap3	Pelo	Serbp1	Tomm70a	
Magi3	Blvrb	Psma6	Amotl2	Dedd	Klf3	Pex3	Sesn3	Tpr	
Mef2a	Bms1	Pspc1	Ankrd23	Dlgap4	Lbh	Phf1	Setd1b	Tra2a	
Palm2	Calm3	Ptges2	Ankrd39	Dmap1	Lgals1	Phf17	Sf1	Trim68	
Pkia	Card10	Rab10	Ap3b1	Dmxl1	Limd1	Phf20l1	Sf3b1	Trim8	
Rhob	Ccar1	Rab11fip3	Arhgef7	Dnajb4	Lipe	Phf23	Sgms1	Trp53bp2	
Slbp	Ccdc88a	Rbl1	Arid5b	Dnajb5	Lmo7	Picalm	Sgol1	Tsc1	
Smarca4	Cdc14a	Rc3h1	Arl2	Dnajb6	Lmod2	Pik3ap1	Sh3gl1	Ttn	
Wbp4	Chd2	Rfc4	Arrb2	Dpp3	Lrrc10	Pik3cb	Sh3pxd2a	Tubb5	
Zfp143	Chka	Sertad2	Asf1a	Dynll1	Lta4h	Pik3r1	Sh3tc2	Tubgcp3	
	Ctdsp2	Sipa1l2	Aspm	Dyrk1a	Luc7l2	Pin1	Shox2	U2af2	
	D19Bwg1357e	Slc25a22	Atad2	Ehmt2	Magi1	Plk1	Shroom3	Ube2i	
	Dnaja3	Slc4a1ap	Atf4	Elf1	Magoh	Pnn	Sipa1l1	Ube3a	
	Dusp16	Snd1	Axin1	Ercc1	Map3k11	Pnrc2	Smarca2	Usp36	
	Ect2	Snrpd3	Baz1b	Esrra	Maz	Polr3k	Smarcd3	Usp37	
	Fos	Socs1	Bcas3	Etv4	Mcm6	Pop7	Smc3	Usp47	
	Fosl2	Sox6	Brms1l	Fbxw11	Mcm7	Ppm1g	Smek2	Vps36	
	Gtf2h4	Spag9	Brpf1	Fgfr3	Med26	Ppp1r12a	Smyd1	Vrk1	
	Hnrnpr	Srpk2	C230081A13Rik	Foxn3	Micall1	Ppp1r3b	Snrpa	Wapal	
	Irs2	St5	Cacybp	Frmd4a	Mllt3	Ppp1r8	Sod1	Wdtc1	
	Jhdm1d	Stag1	Cald1	Fubp3	Mllt4	Ppp3ca	Sorbs3	Wee1	
	Jun	Stim1	Caskin1	Gapdh	Mnat1	Prkce	Specc1	Whsc1l1	
	Khdrbs1	Stk40	Casp8ap2	Gata4	Mrps14	Prrx1	Spred1	Zbtb41	
	Khsrp	Thra	Cbx5	Gcat	Mrvi1	Psmb2	Spty2d1	Zbtb45	
	Krcc1	Thtpa	Ccdc88c	Ghr	Muc1	Psmb3	Srebf2	Zbtb46	
	Lrrfip1	Ttc25	Ccdc96	Grk5	Mus81	Psmb8	Srf	Zc3h11a	
	Maea	Tut1	Ccna2	Grlf1	Nav1	Ptov1	Ssbp2	Zfand2a	
	Marcksl1	Ube2t	Ccnc	Gtf2b	Nf2	Pvr	Ssbp3	Zfand3	
	Marveld1	Uhrf1	Ccnf	Gtpbp4	Nfe2l2	Rab12	Stat1	Zfhx3	
	Mical3	Usp2	Cdc42bpa	H1foo	Nfkbiz	Rab8a	Stk4	Zfml	
	Mlf1ip	Usp30	Cdc73	Hbp1	Nipbl	Rad23b	Suv420h1	Zfp213	
	Mrfap1	Utp3	Cdk5rap2	Hcfc1r1	Noc3l	Rbbp5	Sytl2	Zfp263	
	Mxi1	Wdr77	Cdkn1b	Hes1	Nppa	Rbpj	Syvn1	Zfp36l2	
	Nap1l4	Wiz	Cdkn2c	Hexim1	Nppb	Rbpms	Taf5l	Zfp41	
	Ncl	Zfp207	Celf3	Hirip3	Nr1d1	Rcor2	Tanc2	Zfp428	
	Ncoa1	Zfp526	Cenpc1	Hmgb1	Nr2f2	Rela	Tcea1	Zfp51	
	Nfat5	Zfp568	Chd9	Hmgb2	Nr4a3	Rexo4	Tceb2	Zfp523	
	Nfib	Zfp592	Chek2	Hook2	Ntan1	Rfx1	Tcf3	Zfp553	
	Nip7	Zfp646	Chmp2b	Hspb8	Nub1	Rfx2	Tef	Zfp609	
	Nkx2-5	Zfpm1	Chuk	Ier3	Nubp2	Rgs3	Tfdp1	Zfp62	

Table 2-2: Putative cardiac chromatin-associated genes directly regulated by Gata4

Gene	Protein Annotation	TFs Enrichmed within Promoter
Mxi1	Max interacting protein 1 Gene; Transcriptional repressor. MXI1 binds with MAX to form a sequence-specific DNA-binding protein complex which recognizes the core sequence 5'-CAC[GA]TG-3'. MXI1 thus antagonizes MYC transcriptional activity by competing for MAX. Isoform Short, which lacks a segment, has a much stronger suppressive potential and associates with a SIN3 homologous protein	Gata4, Mef2a, Srf, Tbx5
Ncoa1	nuclear receptor coactivator 1 Gene; Nuclear receptor coactivator that directly binds nuclear receptors and stimulates the transcriptional activities in a hormone-dependent fashion. Involved in the coactivation of different nuclear receptors, such as for steroids (PGR, GR and ER), retinoids (RXRs), thyroid hormone (TRs) and prostanoids (PPARs). Also involved in coactivation mediated by STAT3, STAT5A, STAT5B and STAT6 transcription factors. Displays histone acetyltransferase activity toward H3 and H4; the relevance of such activity remains however unclear. Plays a central role in creati [...]	Gata4, Nkx2-5, Srf, Tbx5
Wiz	widely-interspaced zinc finger motifs Gene; May link EHMT1 and EHMT2 histone methyltransferases to the CTBP corepressor machinery. May be involved in EHMT1-EHMT2 heterodimer formation and stabilization	Gata4, Nkx2-5, Srf, Tbx5
Zfp592	zinc finger protein 207 Gene	Gata4, Mef2a, Srf, Tbx5
Lbh	limb-bud and heart Gene; Modulates the activity of key transcription factors involved in cardiogenesis	Gata4, Srf, Tbx5
Smarcd3	SWI/SNF related, matrix associated, actin dependent regulator of chromatin, subfamily d, member 3 Gene; Plays a role in ATP dependent nucleosome remodeling by SMARCA4 containing complexes. Stimulates nuclear receptor mediated transcription (By similarity)	Gata4, Srf, Tbx5
Ssbp2	single-stranded DNA binding protein 2 Gene	Gata4, Srf, Tbx5
Thap7	THAP domain containing 7 Gene; Chromatin-associated, histone tail-binding protein that represses transcription via recruitment of HDAC3 and nuclear hormone receptor corepressors (By similarity)	Gata4, Srf, Tbx5
Whsc1l1	Wolf-Hirschhorn syndrome candidate 1-like 1 (human) Gene; Histone methyltransferase. Preferentially methylates 'Lys-4' and 'Lys-27' of histone H3. H3 'Lys-4' methylation represents a specific tag for epigenetic transcriptional activation, while 'Lys-27' is a mark for transcriptional repression (By similarity)	Gata4, Srf, Tbx5
Zbtb41	zinc finger and BTB domain containing 41 homolog Gene; May be involved in transcriptional regulation	Gata4, Srf, Tbx5
Zfp523	zinc finger protein 523 Gene; May be involved in transcriptional regulation	Gata4, Mef2a Tbx5
Zfp609	zinc finger protein 609 Gene	Gata4, Srf, Tbx5
Zfp800	zinc finger protein 800 Gene; May be involved in transcriptional regulation	Gata4, Srf, Tbx5
Zfp91	zinc finger protein 91 Gene; May be involved in transcriptional regulation. May play an important role in cell proliferation and/or anti-apoptosis (By similarity)	Gata4, Srf, Tbx5
Zfr	zinc finger RNA binding protein Gene; Involved in postimplantation and gastrulation stages of development. Binds to DNA and RNA. Involved in the nucleocytoplasmic shuttling of STAU2 (By similarity)	Gata4, Srf, Tbx5

* Genes highlighted in blue were not on microarray from isoproterenol study in the HMDP [10].

Chapter 2: References

1. Bruneau BG. Chromatin remodeling in heart development. Current opinion in genetics & development. 2010;20(5):505-11. Epub 2010/08/13. doi: 10.1016/j.gde.2010.06.008. PubMed PMID: 20702085.
2. Han P, Hang CT, Yang J, Chang CP. Chromatin remodeling in cardiovascular development and physiology. Circulation research. 2011;108(3):378-96. Epub 2011/02/05. doi: 10.1161/CIRCRESAHA.110.224287. PubMed PMID: 21293009; PMCID: 3079363.
3. Ho L, Crabtree GR. Chromatin remodelling during development. Nature. 2010;463(7280):474-84. Epub 2010/01/30. doi: 10.1038/nature08911. PubMed PMID: 20110991; PMCID: 3060774.
4. He A, Kong SW, Ma Q, Pu WT. Co-occupancy by multiple cardiac transcription factors identifies transcriptional enhancers active in heart. Proc Natl Acad Sci U S A. 2011;108(14):5632-7. doi: 10.1073/pnas.1016959108. PubMed PMID: 21415370; PMCID: PMC3078411.
5. Dellaire G, Farrall R, Bickmore WA. The Nuclear Protein Database (NPD): sub-nuclear localisation and functional annotation of the nuclear proteome. Nucleic Acids Res. 2003;31(1):328-30. PubMed PMID: 12520015; PMCID: PMC165465.
6. Mysliwiec MR, Carlson CD, Tietjen J, Hung H, Ansari AZ, Lee Y. Jarid2 (Jumonji, AT Rich Interactive Domain 2) Regulates NOTCH1 Expression via Histone Modification in the Developing Heart. Journal of Biological Chemistry. 2012;287(2):1235-41. doi: 10.1074/jbc.M111.315945. PubMed PMID: WOS:000299170300039.
7. Monte E, Mouillesseaux K, Chen H, Kimball T, Ren S, Wang Y, Chen JN, Vondriska TM, Franklin S. Systems proteomics of cardiac chromatin identifies nucleolin as a regulator of growth and cellular plasticity in cardiomyocytes. Am J Physiol Heart Circ Physiol.

2013;305(11):H1624-38. doi: 10.1152/ajpheart.00529.2013. PubMed PMID: 24077883; PMCID: PMC3882469.

8. Wamstad JA, Alexander JM, Truty RM, Shrikumar A, Li FG, Eilertson KE, Ding HM, Wylie JN, Pico AR, Capra JA, Erwin G, Kattman SJ, Keller GM, Srivastava D, Levine SS, Pollard KS, Holloway AK, Boyer LA, Bruneau BG. Dynamic and Coordinated Epigenetic Regulation of Developmental Transitions in the Cardiac Lineage. Cell. 2012;151(1):206-20. doi: 10.1016/j.cell.2012.07.035. PubMed PMID: WOS:000309544200021.
9. He AB, Gu F, Hu Y, Ma Q, Ye LY, Akiyama JA, Visel A, Pennacchio LA, Pu WT. Dynamic GATA4 enhancers shape the chromatin landscape central to heart development and disease. Nature Communications. 2014;5. doi: ARTN 4907 10.1038/ncomms5907. PubMed PMID: WOS:000342984100003.
10. Rau CD, Wang J, Avetisyan R, Romay MC, Martin L, Ren SX, Wang YB, Lusis AJ. Mapping Genetic Contributions to Cardiac Pathology Induced by Beta-Adrenergic Stimulation in Mice. Circ-Cardiovasc Gene. 2015;8(1):40-9. doi: 10.1161/Circgenetics.113.000732. PubMed PMID: WOS:000349873200007.
11. Briegel KJ, Joyner AL. Identification and characterization of Lbh, a novel conserved nuclear protein expressed during early limb and heart development. Dev Biol. 2001;233(2):291-304. doi: 10.1006/dbio.2001.0225. PubMed PMID: 11336496.
12. Akazawa H, Komuro I. Roles of cardiac transcription factors in cardiac hypertrophy. Circ Res. 2003;92(10):1079-88. doi: 10.1161/01.RES.0000072977.86706.23. PubMed PMID: 12775656.
13. Molkentin JD. The zinc finger-containing transcription factors GATA-4, -5, and -6. Ubiquitously expressed regulators of tissue-specific gene expression. J Biol Chem. 2000;275(50):38949-52. doi: 10.1074/jbc.R000029200. PubMed PMID: 11042222.

14. Liang Q, De Windt LJ, Witt SA, Kimball TR, Markham BE, Molkentin JD. The transcription factors GATA4 and GATA6 regulate cardiomyocyte hypertrophy in vitro and in vivo. J Biol Chem. 2001;276(32):30245-53. doi: 10.1074/jbc.M102174200. PubMed PMID: 11356841.
15. Kohli S, Ahuja S, Rani V. Transcription factors in heart: promising therapeutic targets in cardiac hypertrophy. Curr Cardiol Rev. 2011;7(4):262-71. PubMed PMID: 22758628; PMCID: PMC3322445.
16. Saadane N, Alpert L, Chalifour LE. Expression of immediate early genes, GATA-4, and Nkx-2.5 in adrenergic-induced cardiac hypertrophy and during regression in adult mice. Br J Pharmacol. 1999;127(5):1165-76. doi: 10.1038/sj.bjp.0702676. PubMed PMID: 10455263; PMCID: PMC1566134.
17. Papait R, Cattaneo P, Kunderfranco P, Greco C, Carullo P, Guffanti A, Vigano V, Stirparo GG, Latronico MV, Hasenfuss G, Chen J, Condorelli G. Genome-wide analysis of histone marks identifying an epigenetic signature of promoters and enhancers underlying cardiac hypertrophy. Proc Natl Acad Sci U S A. 2013;110(50):20164-9. doi: 10.1073/pnas.1315155110. PubMed PMID: 24284169; PMCID: PMC3864351.
18. May D, Blow MJ, Kaplan T, McCulley DJ, Jensen BC, Akiyama JA, Holt A, Plajzer-Frick I, Shoukry M, Wright C, Afzal V, Simpson PC, Rubin EM, Black BL, Bristow J, Pennacchio LA, Visel A. Large-scale discovery of enhancers from human heart tissue. Nat Genet. 2011;44(1):89-93. doi: 10.1038/ng.1006. PubMed PMID: 22138689; PMCID: PMC3246570.
19. Paige SL, Thomas S, Stoick-Cooper CL, Wang H, Maves L, Sandstrom R, Pabon L, Reinecke H, Pratt G, Keller G, Moon RT, Stamatoyannopoulos J, Murry CE. A Temporal Chromatin Signature in Human Embryonic Stem Cells Identifies Regulators of Cardiac Development. Cell. 2012;151(1):221-32. doi: 10.1016/j.cell.2012.08.027. PubMed PMID: WOS:000309544200022.

20. Saxena A, Carninci P. Long non-coding RNA modifies chromatin: epigenetic silencing by long non-coding RNAs. Bioessays. 2011;33(11):830-9. doi: 10.1002/bies.201100084. PubMed PMID: 21915889; PMCID: PMC3258546.
21. Matkovich SJ, Edwards JR, Grossenheider TC, de Guzman Strong C, Dorn GW, 2nd. Epigenetic coordination of embryonic heart transcription by dynamically regulated long noncoding RNAs. Proc Natl Acad Sci U S A. 2014;111(33):12264-9. doi: 10.1073/pnas.1410622111. PubMed PMID: 25071214; PMCID: PMC4143054.

Chapter 3: Role of High Mobility Group B2 (HMGB2) to Regulate Cardiac Transcription

[This proposal has been funded by the American Heart Association (15PRE22700005).]

1. Specific Aims.

Cardiac hypertrophy entails dynamic structural and metabolic remodeling that is mediated by systemic gene expression changes that revert the transcriptome of the adult heart to one that is reminiscent of the fetal heart (1). The global chromatin structural rearrangements necessary for this remodeling of the cardiac transcriptome are unknown. Interactions of non-nucleosomal chromatin structural proteins can facilitate high-order chromatin packaging and genome architecture—and must do so in a specific manner to establish a cell-specific transcriptome. How the genome is organized to support a cardiac phenotype is not understood—furthermore, the aspects of genomic architecture involved in disease are unknown. I propose that the organization of cardiac-specific "transcription factories", actively transcribed genomic regions enriched with RNA polymerases (2, 3), is structurally and functionally disrupted with disease, leading to global transcriptome changes.

Our lab has identified chromatin structural protein, high mobility group B2 (HMGB2), to be upregulated in hypertrophic mouse hearts. Knockdown of HMGB2 induces an increase in cardiomyocyte size and is sufficient to recapitulate some aspects of the fetal gene program. Here, I will examine the mechanisms by which HMGB2 regulates chromatin structure, using super-resolution microscopy techniques and DNA fluorescence *in situ* hybridization (DNA FISH) to understand how endogenous 3D genome organization set by HMGB2 affects the expression of a subset of cardiac genes. I hypothesize that ***chromatin structural changes due to altered HMGB2 levels disrupt transcription factories, resulting in fetal gene reprogramming in the hypertrophic heart. HMGB2 controls a microenvironment that facilitates cardiac gene***

expression, by regulating access of transcriptional machinery to the gene and/or by regulating localization of the gene itself in a given nuclear domain in situ (Figure 3-1).

Aim 1: I will determine whether changes in cardiac gene expression during hypertrophy induced by pressure overload involve (a) **the physical movement of genes in to and out of stable transcription factories** (labeled by active RNA polymerase II) **and/or** (b) whether transcription factories **dynamically form/disassemble *de novo* around these genes**. Cardiac transcription factories will be imaged using stimulated emission depletion (STED) microscopy to assess number, 3D distribution, and activity in control and hypertrophic adult mouse cardiomyocytes. The distance of DNA FISH signals to the nuclear membrane and with respect to euchromatin and heterochromatin will be measured for the following genes, differentially expressed in hypertrophy models: upregulated (Nppa (4), Myh7 (4), Acta1 (4)); downregulated (Atp2a2 (4), Myh6 (4), Psma4 (5)); remain expressed (Actb, Gapdh (4), Rpl37); remain silenced (Hnf4a, Neurod1, Aqp12); and intergenic regions as controls (1, 6, 7).

Aim 2: I will **determine how HMGB2 affects gene transcription in adult mouse cardiomyocytes by examining effects of transcription factory organization upon knockdown and overexpression**. In addition I will examine a subset of genes affected by HMGB2 knockdown to test whether HMGB2-mediated transcriptional regulation involves redistribution of genes between euchromatin and heterochromatin domains, and/or if HMGB2 locally regulates deposition of histone post-translational modifications on specific loci (ChIP-PCR). I will focus on upregulated (Nppa and Nfkb2), downregulated (Atp2a2 and Dhrs7c), and unaffected genes (Tnni3 and Actb) by knockdown. Our lab has previously shown that these genes change in expression (microarray and PCR) with HMGB2 knockdown in ventricular myocytes and are directly bound by HMGB2 (ChIP-seq).

2. Background and Significance.

Heart disease and fetal gene expression. Cardiovascular disease is the leading cause of death and affects a third of adults in the US (8). Due to pathological stresses, such as high blood pressure and/or heart attack (both of which increase cardiac workload), the heart has to maintain and compensate in function to meet the circulatory demands of the body and as a result undergoes remodeling that leads to the thickening of the ventricular walls *(hypertrophy)* (9). Eventually the heart is no longer able to compensate for increased stress and undergoes an irreversible decline in function *(failure)*, leading to chamber dilation and thinning of the ventricular walls (10). In response to pressure overload, there are global changes in gene expression regulating the metabolism, structure and signaling pathways of cardiomyocytes including: shift from fatty acid to glucose utilization as a more efficient means of energy production, an increase in β-myosin heavy chain (βMHC) to α-myosin heavy chain (αMHC) isoform ratio, impaired calcium handling and an increase in naturietic peptides to decrease blood pressure (11, 12). This acquired transcriptome is similar to that in the fetal heart, also known as “fetal gene reprogramming” (1, 13).

DNA packaging and chromatin structure. DNA is packaged into chromatin structural units, termed nucleosomes, by wrapping around an octamer of core histone proteins (H2A, H2B, H3 and H4). On a larger scale, chromatin structural proteins, including high mobility group proteins and H1 histones, affect the DNA bending and compaction into higher-order structures (14, 15). There exists a spectrum of DNA compaction: euchromatin, associated with loose DNA packaging that can carry active genes; heterochromatin, associated with tight DNA compaction and gene silencing; and intermediate levels of packaging containing DNA poised for expression (16). The transition between euchromatin and heterochromatin can be driven by epigenetic modifications, nucleosome abundance and positioning, and histone variants (17-20). Histone post-translational modifications have served as widespread indicators of chromatin states, due to evidence of their

conserved function across cell types and species; these modifications will be used to demarcate euchromatin and heterochromatin across the genome and at individual target loci in cardiomyocytes. Packaging of the same genome across cell types must be highly organized to specify an active cell-specific transcriptome (21-23).

Transcription factories. Gene transcription occurs at discrete locations known as “transcription factories” (2, 3), concentrated with active RNA polymerases (24). Transcription factories can contain multiple transcribed genes that may be coregulated by the same set of transcription factors and other DNA elements, providing important regulatory contacts for the formation, stability and function of the transcription factory (Figure 3-2) (25). Distinct foci (versus uniform labeling throughout the nucleus) from RNA polymerase II (RNA Pol II) immunofluorescence and pulsed labeling of nascent RNA provides evidence for the existence of transcription factories (Figure 3-2) (3). The ratio of number of active genes to number of RNA Pol II foci suggests that genes must be concentrated at regions of high RNA Pol II abundance (2, 24, 26). Live-cell imaging studies have indicated that there are different populations of RNA polymerases, freely diffusing polymerases and immobile polymerases that are engaged in transcription (27). Meanwhile, higher resolution microscopy techniques have demonstrated that clustering of RNA Pol II is highly dynamic (28). **The properties of transcription factories, whether they form *de novo* or are stable structures, are still debated and have not been explored in the heart**. In this project, I will examine the underlying dynamics of transcription factories (number, distribution and activity) in hypertrophy.

3D gene positioning within the nucleus has been highlighted as a form of transcriptional regulation, with genes that are actively expressed being localized more centrally in the nucleus and at nuclear pore complexes while those that are repressed are situated at the nuclear lamina that hosts silencing machinery (29-31), a process mediated by histone post-translational

modifications (31, 32). I will examine how genes are regulated with respect to colocalization with transcription factories, whether the genes themselves move in to stable transcription factories or whether transcription factories dynamically form *de novo* around genes. ***These studies will be the first of their kind in cardiomyocytes***.

Chromatin structural proteins and high mobility group B2 protein. Histones and non-nucleosomal structural proteins are critical for the packaging of the genome. Furthermore, it is important that genes are activated and silenced appropriately to ensure global coordination of cellular processes. Chromatin structural proteins are ubiquitously expressed throughout different tissues and lack a consensus DNA binding sequence. The central question that remains to be addressed is: how do these proteins contribute to ***cell type-specific chromatin architecture***? Studies on non-nucleosomal proteins have demonstrated the necessity of these proteins in regulating chromatin structure during development and in disease (33, 34). Our lab has revealed an important role for HMGB2, a non-nucleosomal chromatin structural protein that can bind to and bend DNA (35), in maintaining levels of euchromatin and heterochromatin in the heart during hypertrophy (36) and globally regulating transcription levels.

My studies will investigate chromatin features of the cardiomyocyte, a terminally differentiated post-mitotic cell model, whose endogenous genomic architecture has not been yet examined. I reason that the changes in gene expression observed in heart disease must be supported in part by remodeling of chromatin architecture. I hypothesize that HMGB2 maintains the organization of cardiac transcription factories; changes in HMGB2 levels disrupt transcription factories to induce the fetal gene program during the onset of hypertrophy (Figure 3-1).

3. Preliminary Studies.

Previous findings from our lab show a global change in high-order chromatin structure contributes to reprogramming of gene expression in hypertrophic and failing hearts, demonstrated by a shift from heterochromatin towards euchromatin, indicated by increases in trimethylation at lysine 4 of histone H3 (H3K4me3) and concomitant decreases in trimethylation at lysine 9 of histone H3 (H3K9me3) (36). In parallel, there are changes in the abundance of linker histones and other chromatin structural proteins (36). Super-resolution imaging of histone H3 has revealed redistribution of nucleosomes and H3 intensity across the cardiomyocyte nucleus upon isoproterenol treatment (37), providing strong evidence of global 3D rearrangements of chromatin structure. Pulse-labeling experiments from other labs show that total transcriptional activity increases in hypertrophy models (38, 39). I will examine organization of RNA Pol II factories and determine how changes in these factories contribute to increased transcription.

Mass spec data from our lab has shown upregulation of HMGB2 during cardiac hypertrophy in the mouse model (36). More in depth analysis has shown that HMGB2 knockdown can lead to increased cell size, changes in gene expression, reflecting those of the fetal gene program (Figure 3-6), and a shift from heterochromatin to euchromatin in cultured myocytes (36). We have also shown that these changes with HMGB2 knockdown are associated with parallel increases in global transcription as measured by 5'fluorouridine (5'FU) incorporation, a uracil analogue that selectively labels newly synthesized RNA (Figures 3-2, 3-3). Overexpression of HMGB2 leads to an overall silencing of gene transcription indicated by reduced 5'FU labeling (Figure 3-4). These data are the first to our knowledge to measure transcription in the anatomical context of the cardiac nucleus, and to interrogate the molecular function of specific chromatin proteins. The goal of this study is to characterize organization of chromatin within the nucleus to understand nuclear territories *in situ* as well as the role of HMGB2 in maintaining the cardiac transcriptome.

4. Research Design and Methods.

Aim 1: I will determine whether changes in cardiac gene expression during hypertrophy induced by pressure overload involve (a) **the physical movement of genes in to and out of stable transcription factories** (labeled by active RNA polymerase II) **and/or** (b) whether transcription factories **dynamically form/disassemble *de novo* around these genes**. Cardiac transcription factories will be imaged using STED microscopy to assess number, 3D distribution, and activity in control and hypertrophic adult mouse cardiomyocytes. The distance of DNA FISH signals to the nuclear membrane and with respect to euchromatin and heterochromatin will be measured for the following genes, differentially expressed in hypertrophy models: upregulated (Nppa (4), Myh7 (4), Acta1 (4)); downregulated (Atp2a2 (4), Myh6 (4), Psma4 (5)); remain expressed (Actb, Gapdh (4), Rpl37); remain silenced (Hnf4a, Neurod1, Aqp12); and intergenic regions as controls (1, 6, 7).

Hypothesis for Aim 1: A dynamic interplay between transcription factory stability/activity and gene localization establishes cardiac-specific gene expression.

Aim 1A: I will determine whether transcription factories are stable or dynamic structures by immunofluorescence in adult cardiomyocytes from healthy SHAM-operated and transverse aortic constriction (TAC)-induced hypertrophic mouse hearts, an *in vivo* model for pressure overload hypertrophy with which our lab has extensive experience (36, 40, 41). Studies will be carried out in BALB/c adult male mice, 8 weeks of age; analysis will be performed with hearts undergoing hypertrophy, assessed by increase in heart weight to body weight ratio, and failure, determined by reduced ejection fraction according to echocardiography. Because cardiac hypertrophy is reversible while failure is not, I will determine whether these properties are reflected by their respective transcription factories. Previous studies have neglected RNA Pol II activity when performing analyses of transcription factories. *Here, I will specifically look at actively elongating RNA Pol II, phosphorylated at serine 2 of its CTD domain, to map transcription factories.* I will

quantify the number of total active RNA Pol II puncta, marked by serine 2 phosphorylation, and distribution, indicated by concentration of clusters, to map location of polymerases using STED imaging. Due to the high abundance of RNA polymerases in the nucleus, STED will allow us to map out individual clusters of factories that would otherwise not be as apparent by conventional confocal microscopy. I have been working with members of Dr. Enrico Stefani's lab at UCLA to develop the imaging approaches and subsequent analytical techniques (*See letter from Dr. Yong Wu)*. Levels of RNA Pol II, both total and active (serine 2 phosphorylated), will be measured using Western blot. I will confirm antibody specificity using Western in control and tagged RNA Pol II overexpressing cells (probing for both tag and RNA Pol II), in addition to checking for colocalization of CDK9 (kinase that performs phosphorylation at serine 2 to mark transcriptional elongation) (42) and phosphorylated RNA Pol II using immunofluorescence.

I will measure the activity of RNA Pol II transcription factories by measuring the fluorescence intensity of 5'FU incorporation after 5 and 15 minutes of labeling around RNA Pol II clusters using STED (times determined based on preliminary studies to capture detectable signal of nascent transcripts at sites of origin). These cells will be treated with CX5461, an RNA Pol I inhibitor, to differentiate between different RNA polymerase activity (Figure 3-2). The 5'FU intensity from nascent RNA associated with RNA Pol II clusters will be used to calculate the average activity per transcription factory. Using quantification of the number of genes being transcribed based on published RNA sequencing (RNA-seq) data from control and hypertrophic hearts (5, 43), I will estimate the number of transcribed genes per quantitated RNA Pol II transcription factory to understand the flux of genes. In other words taking into account global increases in transcriptional activity (38, 39) and transcriptome complexity (or, the number of different genomic regions that are transcribed) (43), we can determine whether transcribed regions congregate to transcription factories (decrease or show no change in number) or whether increased transcriptional activation results in genes forming new transcription factories (increase in number). With transcriptional

increases in hypertrophy, these results will quantify this effect and map endogenous features of transcription factories.

Aim 1B: I will assess whether genes (focusing on the candidates listed above) physically move in to or out of transcription factories or whether chromatin regulators are recruited to these genes to regulate their transcription using DNA FISH to map out localization in nuclei (modeling control, hypertrophy and failure situations) from SHAM and TAC cardiomyocytes. Control genes were chosen using Tissue-Specific Genes Database (TiSGeD) to find genes expressed or silenced in the adult mouse heart. I will validate the expression of these genes in isolated cardiomyocytes by quantitative PCR. Probes for the individual genes have be designed according to a previously published protocol using http://hdfish.eu (44). I have already mastered analyses of the SERCA2A gene (atp2a2) using a fluorescently labeled probe consisting of 50 PCR-based products tiling the gene body (Figure 3-5). I will measure the distances of the FISH foci to the nuclear envelope, marked by Lamin A/C, using Imaris image analysis software. If a shift in distribution of distances is observed, I will interpret changes in gene expression to associate with the movement of genes to distinct nuclear compartments for regulation. Conversely, if no differences are noted between SHAM and TAC cardiomyocytes, I will interpret this to mean that there is local regulation only in cis (i.e. just upstream of the transcription start site). Using STED microscopy, I will precisely map the location of genes with respect to transcription factories, and 5'FU-positive clusters, in addition to heterochromatin marks (H3K27me3 and H3K9me3) (Figure 3-5).

Controls: I will perform these experiments in 5 separate animals per group, measuring at least 200 cardiomyocytes per animal (colabeling with desmin to demarcate cardiomyocytes). Fibroblasts isolated from the heart will be used as controls.

Expected Outcomes, Interpretations and Alternative Approaches for Aim 1: The endpoints of these studies will provide support for whether genes move in to transcription factories (if no change in distribution) or whether there is *de novo* formation of transcription factories (if distribution changes), as well as map out overall location of cardiac genes within the nucleus. These findings will be analyzed in parallel with a measure of transcriptional complexity to track flux of genes through factories during disease. I will determine how localization of subsets of cardiac genes is regulated with respect to transcriptionally active or silent domains. Subsequently, I will verify loci-specific transcriptional activity using RNA FISH (45). Future studies will utilize chromatin interaction analysis by paired-end tag sequencing (ChIA-PET) in SHAM and TAC cardiomyocytes to map 3D DNA-DNA interactions within RNA Pol II transcription factories, focusing on the candidate genes differentially expressed, to assess whether these 3D microenvironments change between healthy and disease hearts.

Aim 2: I will **determine how HMGB2 affects gene transcription in adult mouse cardiomyocytes by examining effects of transcription factory organization upon knockdown and overexpression**. In addition I will examine a subset of genes affected by HMGB2 knockdown to test whether HMGB2-mediated transcriptional regulation involves redistribution of genes between euchromatin and heterochromatin domains, and/or if HMGB2 locally regulates deposition of histone post-translational modifications on specific loci (ChIP-PCR). I will focus on upregulated (Nppa and Nfkb2), downregulated (Atp2a2 and Dhrs7c), and unaffected genes (Tnni3 and Actb) by knockdown. Our lab has previously shown that these genes change in expression (microarray and PCR) with HMGB2 knockdown in ventricular myocytes and are directly bound by HMGB2 (ChIP-seq).

Atp2a2 is one of the genes that we have started to analyze that has strong enrichment of HMGB2 at its promoter (Figure 3-6). We hypothesize that the shift towards more euchromatin by HMGB2

knockdown can trigger fetal gene programming, and thereby reducing *atp2a2*/SERCA2A expression, by destabilization of chromatin structure and transcription factories while HMGB2 overexpression promotes high-order packaging and formation of heterochromatin, evidenced by a global reduction in transcription and downregulation trend of cardiac genes (Figures 3-4, 3-6). Findings will help determine if HMGB2 knockdown and overexpression influence *atp2a2* through common mechanisms.

Hypothesis for Aim 2: Coordinated expression of HMGB2 is critical for appropriate cardiac gene transcription. Changes in HMGB2 expression, as may be involved in hypertrophy, will disrupt organization of transcription factories and thereby alter the cardiac transcriptome.

Aim 2A: I will evaluate the global effect of HMGB2 on chromatin structural regulation of RNA Pol II transcription factory number, activity and distribution using STED imaging. Studies from our laboratory indicate that HMGB2 knockdown results in a shift from heterochromatin to euchromatin to result in globally increased transcription (Figure 3-3). Moreover, HMGB2 overexpression leads to a decrease in transcription (Figure 3-4). I will determine the structural basis for changes in RNA Pol II-mediated transcription, carried out using adenoviral knockdown and overexpression of HMGB2 in adult mouse cardiomyocytes—the viruses for these experiments are already being used in the lab. I will test whether transcriptional increases by HMGB2 knockdown are the result of: (1) increased RNA Pol II activity by quantifying fluorescence intensity of 5'FU labeling around RNA Pol II clusters using microscopy as well as performing Western blot for active forms of RNA Pol II (both phosphorylation of serine 5, which marks initiation, and of serine 2, which indicates elongation); or, (2) the result of increased number of transcription factories, quantified using Imaris analysis software. These analyses will be carried out with HMGB2 overexpression to determine if trends of reduced transcription are due to destabilization of transcription factories.

Aim 2B: I will determine nuclear 3D distribution of candidate genes using DNA FISH to assess if differential gene expression in HMGB2 knockdown and overexpression is due to transitioning between heterochromatin (marked by H3K9me3 and H3K27me3) and euchromatin (marked by RNA Pol II and H3K36me3) domains, as well as measure the distance to the nuclear envelope, using immunofluorescence. In the case of overexpression, where select genes are shown to be generally downregulated (Figure 3-6), I will determine whether these genes share a common mechanism of regulation by HMGB2—for example, does HMGB2 overexpression result in anchoring of genes to specific sites (e.g. nuclear envelope)?

Aim 2C: I will assess the enrichment of histone post-translational modifications indicative of heterochromatin (H3K9me3 and H3K27me3) and euchromatin (H3K4me3) and RNA Pol II at promoters of candidate genes using ChIP-PCR in HMGB2 knockdown and overexpressing cardiomyocytes. Because HMGB2 knockdown results in both up- and downregulation of different genes, I hypothesize that individual expression changes can be a result of loci-specific configurations in architecture.

Controls: I will perform these experiments in 5 separate animals per group, measuring at least 200 cardiomyocytes per animal (colabeling with desmin to demarcate cardiomyocytes). Fibroblasts isolated from the heart will be used as controls. Empty vector transfections will be used as controls, and HMGB2 knockdown and overexpression will be verified by Western blot.

Expected Outcomes, Interpretations and Alternative Approaches for Aim 2: In Aim 2, I will study the functional role of HMGB2 in establishing cardiac transcription factories and whether changes in transcription of specific genes are due to chromatin architecture remodeling around the proximity of the gene, measured by the enrichment of euchromatin and heterochromatin histone marks, or movement of genes between transcriptionally silent and active domains. If the

latter case is true, I may or may not see changes in chromatin marks at promoters of these genes by ChIP-PCR, but rather the localization of the gene near other DNA regions with transcription factories will dictate whether it can be transcribed. HMGB2 knockdown and overexpression experiments in hypertrophic cardiomyocytes will provide further understanding for HMGB2's role on transcriptional regulation in disease. Parallel studies in the lab examining other non-nucleosomal proteins including additional HMGB isoforms, CTCF and linker H1 histones will provide insight into why certain genes are more susceptible to HMGB2 changes—whether these proteins interact or compete for binding—and also a more comprehensive overview of the structural events occurring at individual genes.

I will identify features of chromatin structure that specialize the cardiac nucleus to drive cell-specific phenotype. **The experiments in this aim are complementary (microscopy and ChIP-PCR)**, allowing me to thoroughly investigate HMGB2 function in adult cardiac cells. ***From these studies I will gain fundamental knowledge regarding transcriptional regulation with focus on HMGB2 function, revealing key endogenous chromatin structural features that govern cardiac cell phenotype.***

5. Ethical Aspects of the Proposed Research. See Vertebrate Animal Subjects section.

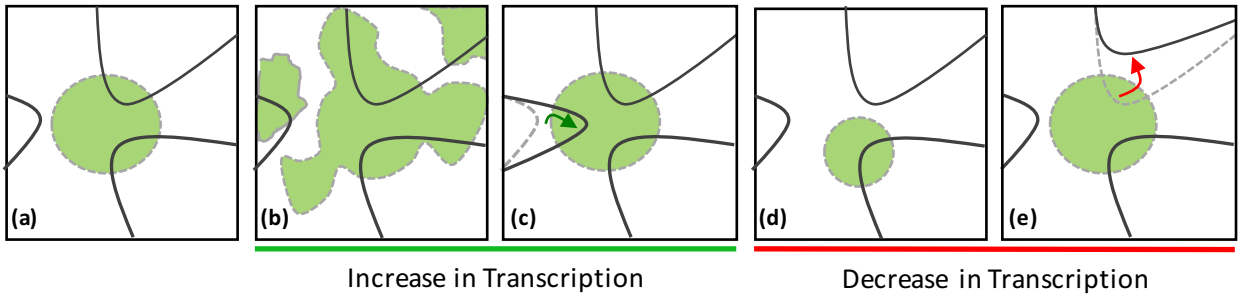

Figure 3-1: High Mobility Group B2 (HMGB2) protein is necessary for the maintenance of cardiac transcription factories. *Hypothesis:* Changes in HMGB2 abundance disrupt the structure and function of transcription factories to affect the cardiac transcriptome and induce fetal gene reprogramming during the onset of cardiac hypertrophy. I will address two potential mechanisms for HMGB2-mediated gene regulation: (1) regulation of the formation, stabilization and activity of transcription factories; and/or, (2) movement of genes to and from transcription factories. Based on our preliminary observations, I will test the following models (the control state represented in *(a)*): the global increases in transcription upon HMGB2 knockdown are due to increased activity of existing and/or formation of new transcription factories (green) *(b)*, or net movement of genes (lines) into transcription factories *(c)*; overexpression of HMGB2 can destabilize transcription factories *(d)*, or facilitate genes out of transcription factories to more heterochromatin-rich nuclear domains *(e)*. It is possible that a combination of these mechanisms may occur, or no change may be observed, for which I will use ChIP-PCR for euchromatin and heterochromatin histone marks to characterize loci-specific chromatin structural changes. *(EK, unpublished hypothesis)*

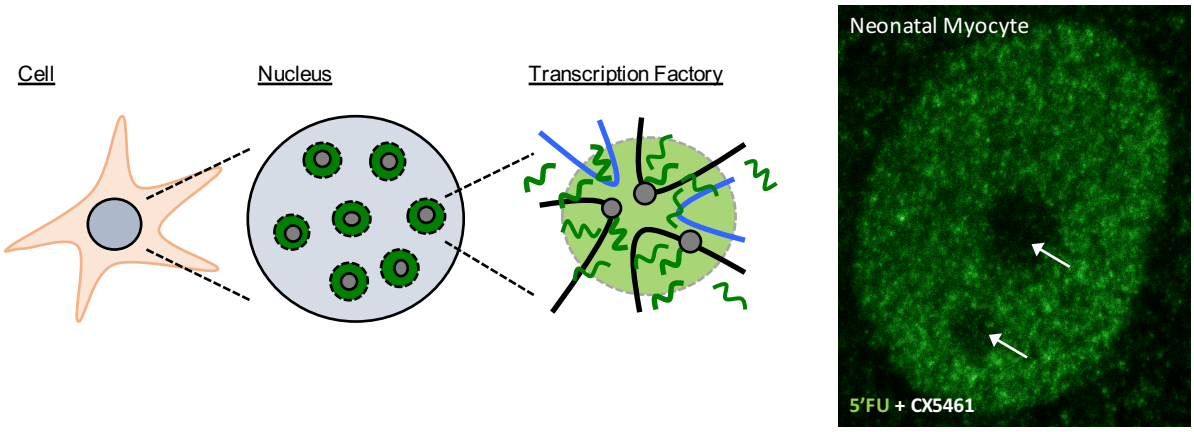

Figure 3-2: RNA polymerase II-mediated transcription is organized into factories. *Left:* Schematic zooms in on the nucleus (blue circle) of a cell. Sites of active transcription (RNA Pol II, gray circle; RNA, green lines) are concentrated at distinct transcription factory compartments (light green area) within the nucleus. These factories contain expressed genes (black lines) and other regulatory genomic elements (blue lines). *Right:* Cardiac transcripts are pulse-labeled by 5'fluorouridine (5'FU) incorporation (30min) into nascent RNA and revealed by super-resolution stimulated emission depletion (STED) microscopy. Cardiomyocytes were pretreated with CX5461, an RNA polymerase I inhibitor, to selectively label for RNA polymerase II transcripts. Note the absence of 5'FU labeling in the nucleolus, the site of ribosomal RNA transcription (indicated by arrows). *(EK, MRG & TV, unpublished model and observations)*

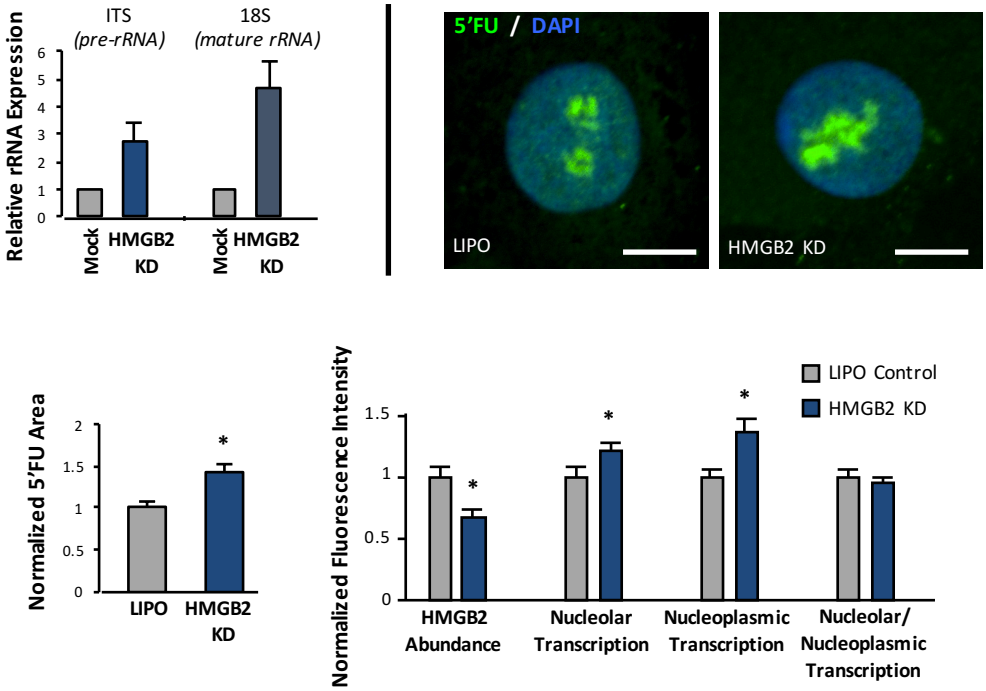

Figure 3-3: HMGB2 knockdown increases ribosomal RNA transcription in neonatal cardiomyocytes. *Top left:* qPCR analyses indicate increased abundance of pre and mature rRNA transcripts. *Top right:* Representative nuclei images of HMGB2 knockdown in cardiomyocytes show increases in ribosomal RNA transcriptional area as labeled with 5'FU (4mM, 30min). *Bottom left:* Area occupied by ribosomal transcripts labeled with 5'FU was quantitated and normalized to total nuclear area. *Bottom right:* Analyses of imaged cardiomyocyte nuclei show increased levels of nascent transcripts in the nucleolar and nucleoplasmic compartments upon HMGB2 knockdown, based on 5'FU fluorescence intensity. * *indicates p<0.05. Scale bar: 5μm. (EK, EM, MRG & TV, unpublished observations)*

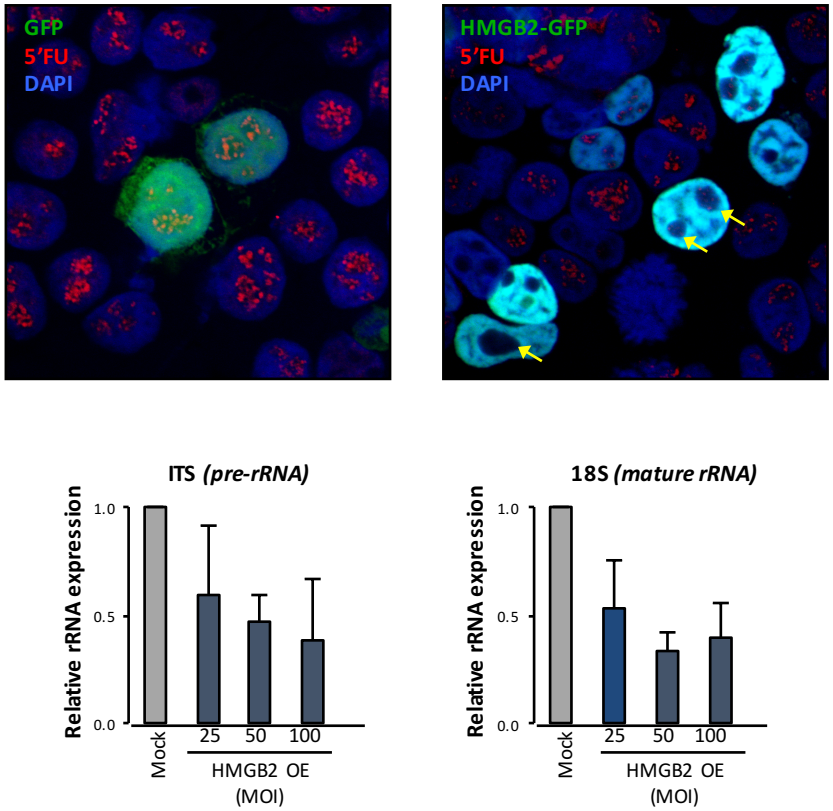

Figure 3-4: HMGB2 overexpression suppresses ribosomal transcription. *Top:* 293T cells were transfected with HMGB2-GFP or GFP alone. Extent of HMGB2 overexpression (green) negatively correlates with global transcription levels as measured by 5'FU incorporation (15min; red). Yellow arrows point to absence of 5'FU signal in nucleolus, site of rRNA transcription, of HMGB2-overexpressing cells. *Bottom:* Neonatal ventricular myocytes, overexpressing HMGB2, show reduced rRNA expression as measured by qPCR. *(EK, MRG & TV, unpublished observations)*

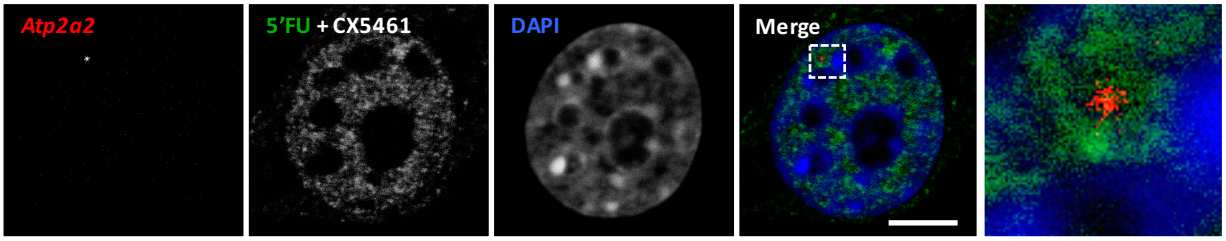

Figure 3-5: SERCA2A gene *(atp2a2)* is mapped to transcription factories by DNA FISH. *Atp2a2* location (red) is mapped with respect to RNA Pol II transcription factories labeled with 5'FU (30min; green) in 3T3 fibroblasts pretreated with RNA Pol I inhibitor, CX5461. *Atp2a2* does not colocalize with RNA Pol II transcripts (bottom panel zooms in on one *atp2a2* locus from boxed area in merged image). *Scale bar: 5μm. (EK, MRG & TV, unpublished observations)*

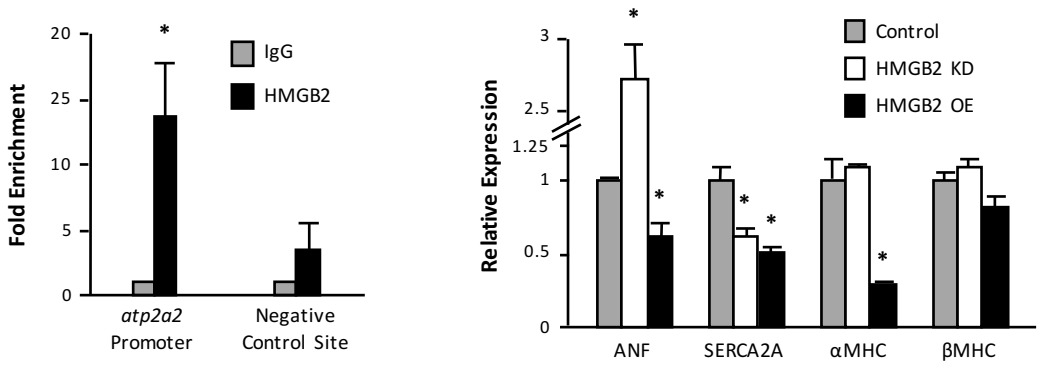

Figure 3-6: HMGB2 is enriched at the promoter of the SERCA2A gene (*atp2a2*) and regulates cardiac gene expression. <u>*Left:*</u> ChIP-PCR validates our previous findings of ChIP-seq of HMGB2 enrichment at the promoter of *atp2a2* with enrichment 864bp upstream of the transcription start site (TSS). No significant enrichment was found at our negative intergenic control site 5kbp upstream of the *atp2a2* TSS. Data represents average from three different chromatin immunoprecipitations for HMGB2. <u>*Right:*</u> HMGB2 knockdown recapitulates some aspects of the fetal gene program (Franklin *et al. MCP.* 2012) while overexpression of HMGB2 results in downregulation of cardiac genes. * *indicates p<0.05. (EK, EM, MRG & TV, unpublished observations)*

Chapter 3: References

1. Rajabi M, Kassiotis C, Razeghi P, Taegtmeyer H. Return to the fetal gene program protects the stressed heart: a strong hypothesis. Heart failure reviews. 2007;12(3-4):331-43. Epub 2007/05/23. doi: 10.1007/s10741-007-9034-1. PubMed PMID: 17516164.
2. Iborra FJ, Pombo A, Jackson DA, Cook PR. Active RNA polymerases are localized within discrete transcription "factories' in human nuclei. Journal of cell science. 1996;109 (Pt 6):1427-36. Epub 1996/06/01. PubMed PMID: 8799830.
3. Chakalova L, Fraser P. Organization of transcription. Cold Spring Harbor perspectives in biology. 2010;2(9):a000729. Epub 2010/07/30. doi: 10.1101/cshperspect.a000729. PubMed PMID: 20668006; PMCID: 2926752.
4. Patrizio M, Musumeci M, Stati T, Fasanaro P, Palazzesi S, Catalano L, Marano G. Propranolol causes a paradoxical enhancement of cardiomyocyte foetal gene response to hypertrophic stimuli. British journal of pharmacology. 2007;152(2):216-22. Epub 2007/06/27. doi: 10.1038/sj.bjp.0707350. PubMed PMID: 17592507; PMCID: 1978260.
5. Papait R, Cattaneo P, Kunderfranco P, Greco C, Carullo P, Guffanti A, Vigano V, Stirparo GG, Latronico MV, Hasenfuss G, Chen J, Condorelli G. Genome-wide analysis of histone marks identifying an epigenetic signature of promoters and enhancers underlying cardiac hypertrophy. Proceedings of the National Academy of Sciences of the United States of America. 2013;110(50):20164-9. Epub 2013/11/29. doi: 10.1073/pnas.1315155110. PubMed PMID: 24284169; PMCID: 3864351.
6. van den Bosch BJ, Lindsey PJ, van den Burg CM, van der Vlies SA, Lips DJ, van der Vusse GJ, Ayoubi TA, Doevendans PA, Smeets HJ. Early and transient gene expression changes in pressure overload-induced cardiac hypertrophy in mice. Genomics. 2006;88(4):480-8. Epub 2006/06/20. doi: 10.1016/j.ygeno.2006.04.012. PubMed PMID: 16781840.

7. Komuro I, Yazaki Y. Control of cardiac gene expression by mechanical stress. Annual review of physiology. 1993;55:55-75. Epub 1993/01/01. doi: 10.1146/annurev.ph.55.030193.000415. PubMed PMID: 8466185.
8. Go AS, Mozaffarian D, Roger VL, Benjamin EJ, Berry JD, Blaha MJ, Dai S, Ford ES, Fox CS, Franco S, Fullerton HJ, Gillespie C, Hailpern SM, Heit JA, Howard VJ, Huffman MD, Judd SE, Kissela BM, Kittner SJ, Lackland DT, Lichtman JH, Lisabeth LD, Mackey RH, Magid DJ, Marcus GM, Marelli A, Matchar DB, McGuire DK, Mohler ER, 3rd, Moy CS, Mussolino ME, Neumar RW, Nichol G, Pandey DK, Paynter NP, Reeves MJ, Sorlie PD, Stein J, Towfighi A, Turan TN, Virani SS, Wong ND, Woo D, Turner MB. Heart disease and stroke statistics--2014 update: a report from the american heart association. Circulation. 2014;129(3):e28-e292. Epub 2013/12/20. doi: 10.1161/01.cir.0000441139.02102.80. PubMed PMID: 24352519.
9. Jessup M, Brozena S. Heart failure. The New England journal of medicine. 2003;348(20):2007-18. Epub 2003/05/16. doi: 10.1056/NEJMra021498. PubMed PMID: 12748317.
10. Kehat I, Molkentin JD. Molecular pathways underlying cardiac remodeling during pathophysiological stimulation. Circulation. 2010;122(25):2727-35. Epub 2010/12/22. doi: 10.1161/CIRCULATIONAHA.110.942268. PubMed PMID: 21173361; PMCID: 3076218.
11. Harvey PA, Leinwand LA. The cell biology of disease: cellular mechanisms of cardiomyopathy. The Journal of cell biology. 2011;194(3):355-65. Epub 2011/08/10. doi: 10.1083/jcb.201101100. PubMed PMID: 21825071; PMCID: 3153638.
12. Dorn GW, 2nd, Robbins J, Sugden PH. Phenotyping hypertrophy: eschew obfuscation. Circulation research. 2003;92(11):1171-5. Epub 2003/06/14. doi: 10.1161/01.RES.0000077012.11088.BC. PubMed PMID: 12805233.
13. Razeghi P, Young ME, Alcorn JL, Moravec CS, Frazier OH, Taegtmeyer H. Metabolic gene expression in fetal and failing human heart. Circulation. 2001;104(24):2923-31. Epub 2001/12/12. PubMed PMID: 11739307.

14. Stros M. HMGB proteins: interactions with DNA and chromatin. Biochimica et biophysica acta. 2010;1799(1-2):101-13. Epub 2010/02/04. doi: 10.1016/j.bbagrm.2009.09.008. PubMed PMID: 20123072.
15. Happel N, Doenecke D. Histone H1 and its isoforms: contribution to chromatin structure and function. Gene. 2009;431(1-2):1-12. Epub 2008/12/09. doi: 10.1016/j.gene.2008.11.003. PubMed PMID: 19059319.
16. Crossley M. Genome packaging and expression. Genome biology. 2002;3(5):reports4014. Epub 2002/06/07. PubMed PMID: 12049660; PMCID: 139357.
17. Allfrey VG, Faulkner R, Mirsky AE. Acetylation and Methylation of Histones and Their Possible Role in the Regulation of Rna Synthesis. Proceedings of the National Academy of Sciences of the United States of America. 1964;51:786-94. Epub 1964/05/01. PubMed PMID: 14172992; PMCID: 300163.
18. Struhl K, Segal E. Determinants of nucleosome positioning. Nature structural & molecular biology. 2013;20(3):267-73. Epub 2013/03/07. doi: 10.1038/nsmb.2506. PubMed PMID: 23463311; PMCID: 3740156.
19. Skene PJ, Henikoff S. Histone variants in pluripotency and disease. Development. 2013;140(12):2513-24. Epub 2013/05/30. doi: 10.1242/dev.091439. PubMed PMID: 23715545.
20. Franklin S, Zhang MJ, Chen H, Paulsson AK, Mitchell-Jordan SA, Li Y, Ping P, Vondriska TM. Specialized compartments of cardiac nuclei exhibit distinct proteomic anatomy. Molecular & cellular proteomics : MCP. 2011;10(1):M110 000703. Epub 2010/09/03. doi: 10.1074/mcp.M110.000703. PubMed PMID: 20807835; PMCID: 3013444.
21. Solovei I, Joffe B. Inverted nuclear architecture and its development during differentiation of mouse rod photoreceptor cells: a new model to study nuclear architecture. Genetika. 2010;46(9):1159-63. Epub 2010/11/10. PubMed PMID: 21058510.

22. Parada LA, McQueen PG, Misteli T. Tissue-specific spatial organization of genomes. Genome biology. 2004;5(7):R44. Epub 2004/07/09. doi: 10.1186/gb-2004-5-7-r44. PubMed PMID: 15239829; PMCID: 463291.
23. Lieberman-Aiden E, van Berkum NL, Williams L, Imakaev M, Ragoczy T, Telling A, Amit I, Lajoie BR, Sabo PJ, Dorschner MO, Sandstrom R, Bernstein B, Bender MA, Groudine M, Gnirke A, Stamatoyannopoulos J, Mirny LA, Lander ES, Dekker J. Comprehensive mapping of long-range interactions reveals folding principles of the human genome. Science. 2009;326(5950):289-93. Epub 2009/10/10. doi: 10.1126/science.1181369. PubMed PMID: 19815776; PMCID: 2858594.
24. Jackson DA, Iborra FJ, Manders EM, Cook PR. Numbers and organization of RNA polymerases, nascent transcripts, and transcription units in HeLa nuclei. Molecular biology of the cell. 1998;9(6):1523-36. Epub 1998/06/17. PubMed PMID: 9614191; PMCID: 25378.
25. Li G, Ruan X, Auerbach RK, Sandhu KS, Zheng M, Wang P, Poh HM, Goh Y, Lim J, Zhang J, Sim HS, Peh SQ, Mulawadi FH, Ong CT, Orlov YL, Hong S, Zhang Z, Landt S, Raha D, Euskirchen G, Wei CL, Ge W, Wang H, Davis C, Fisher-Aylor KI, Mortazavi A, Gerstein M, Gingeras T, Wold B, Sun Y, Fullwood MJ, Cheung E, Liu E, Sung WK, Snyder M, Ruan Y. Extensive promoter-centered chromatin interactions provide a topological basis for transcription regulation. Cell. 2012;148(1-2):84-98. Epub 2012/01/24. doi: 10.1016/j.cell.2011.12.014. PubMed PMID: 22265404; PMCID: 3339270.
26. Osborne CS, Chakalova L, Brown KE, Carter D, Horton A, Debrand E, Goyenechea B, Mitchell JA, Lopes S, Reik W, Fraser P. Active genes dynamically colocalize to shared sites of ongoing transcription. Nature genetics. 2004;36(10):1065-71. Epub 2004/09/14. doi: 10.1038/ng1423. PubMed PMID: 15361872.
27. Kimura H, Sugaya K, Cook PR. The transcription cycle of RNA polymerase II in living cells. The Journal of cell biology. 2002;159(5):777-82. Epub 2002/12/11. doi: 10.1083/jcb.200206019. PubMed PMID: 12473686; PMCID: 2173384.

28. Cisse, II, Izeddin I, Causse SZ, Boudarene L, Senecal A, Muresan L, Dugast-Darzacq C, Hajj B, Dahan M, Darzacq X. Real-time dynamics of RNA polymerase II clustering in live human cells. Science. 2013;341(6146):664-7. Epub 2013/07/06. doi: 10.1126/science.1239053. PubMed PMID: 23828889.
29. Akhtar A, Gasser SM. The nuclear envelope and transcriptional control. Nature reviews Genetics. 2007;8(7):507-17. Epub 2007/06/06. doi: 10.1038/nrg2122. PubMed PMID: 17549064.
30. Cabal GG, Genovesio A, Rodriguez-Navarro S, Zimmer C, Gadal O, Lesne A, Buc H, Feuerbach-Fournier F, Olivo-Marin JC, Hurt EC, Nehrbass U. SAGA interacting factors confine sub-diffusion of transcribed genes to the nuclear envelope. Nature. 2006;441(7094):770-3. Epub 2006/06/09. doi: 10.1038/nature04752. PubMed PMID: 16760982.
31. Towbin BD, Gonzalez-Aguilera C, Sack R, Gaidatzis D, Kalck V, Meister P, Askjaer P, Gasser SM. Step-wise methylation of histone H3K9 positions heterochromatin at the nuclear periphery. Cell. 2012;150(5):934-47. Epub 2012/09/04. doi: 10.1016/j.cell.2012.06.051. PubMed PMID: 22939621.
32. Zullo JM, Demarco IA, Pique-Regi R, Gaffney DJ, Epstein CB, Spooner CJ, Luperchio TR, Bernstein BE, Pritchard JK, Reddy KL, Singh H. DNA sequence-dependent compartmentalization and silencing of chromatin at the nuclear lamina. Cell. 2012;149(7):1474-87. Epub 2012/06/26. doi: 10.1016/j.cell.2012.04.035. PubMed PMID: 22726435.
33. Hock R, Furusawa T, Ueda T, Bustin M. HMG chromosomal proteins in development and disease. Trends in cell biology. 2007;17(2):72-9. Epub 2006/12/16. doi: 10.1016/j.tcb.2006.12.001. PubMed PMID: 17169561; PMCID: 2442274.
34. Monzen K, Ito Y, Naito AT, Kasai H, Hiroi Y, Hayashi D, Shiojima I, Yamazaki T, Miyazono K, Asashima M, Nagai R, Komuro I. A crucial role of a high mobility group protein HMGA2 in

cardiogenesis. Nature cell biology. 2008;10(5):567-74. Epub 2008/04/22. doi: 10.1038/ncb1719. PubMed PMID: 18425117.

35. Thomas JO, Travers AA. HMG1 and 2, and related 'architectural' DNA-binding proteins. Trends in biochemical sciences. 2001;26(3):167-74. Epub 2001/03/14. PubMed PMID: 11246022.
36. Franklin S, Chen H, Mitchell-Jordan S, Ren S, Wang Y, Vondriska TM. Quantitative analysis of the chromatin proteome in disease reveals remodeling principles and identifies high mobility group protein B2 as a regulator of hypertrophic growth. Molecular & cellular proteomics : MCP. 2012;11(6):M111 014258. Epub 2012/01/25. doi: 10.1074/mcp.M111.014258. PubMed PMID: 22270000; PMCID: 3433888.
37. Mitchell-Jordan S, Chen H, Franklin S, Stefani E, Bentolila LA, Vondriska TM. Features of endogenous cardiomyocyte chromatin revealed by super-resolution STED microscopy. Journal of molecular and cellular cardiology. 2012;53(4):552-8. Epub 2012/08/01. doi: 10.1016/j.yjmcc.2012.07.009. PubMed PMID: 22846883; PMCID: 3704345.
38. Cutilletta AF. Muscle and nonmuscle cell RNA polymerase activities in early myocardial hypertrophy. The American journal of physiology. 1981;240(6):H901-7. Epub 1981/06/01. PubMed PMID: 6454350.
39. Fanburg BL, Posner BI. Ribonucleic acid synthesis in experimental cardiac hypertrophy in rats. I. Characterization and kinetics of labeling. Circulation research. 1968;23(1):123-35. Epub 1968/07/01. PubMed PMID: 4232616.
40. Paulsson AK, Franklin S, Mitchell-Jordan SA, Ren S, Wang Y, Vondriska TM. Post-translational regulation of calsarcin-1 during pressure overload-induced cardiac hypertrophy. Journal of molecular and cellular cardiology. 2010;48(6):1206-14. Epub 2010/02/23. doi: 10.1016/j.yjmcc.2010.02.009. PubMed PMID: 20170660; PMCID: 2866759.
41. Mitchell-Jordan SA, Holopainen T, Ren S, Wang S, Warburton S, Zhang MJ, Alitalo K, Wang Y, Vondriska TM. Loss of Bmx nonreceptor tyrosine kinase prevents pressure overload-

induced cardiac hypertrophy. Circulation research. 2008;103(12):1359-62. Epub 2008/11/08. doi: 10.1161/CIRCRESAHA.108.186577. PubMed PMID: 18988895; PMCID: 2735252.

42. Ghamari A, van de Corput MP, Thongjuea S, van Cappellen WA, van Ijcken W, van Haren J, Soler E, Eick D, Lenhard B, Grosveld FG. In vivo live imaging of RNA polymerase II transcription factories in primary cells. Genes & development. 2013;27(7):767-77. Epub 2013/04/18. doi: 10.1101/gad.216200.113. PubMed PMID: 23592796; PMCID: 3639417.
43. Song HK, Hong SE, Kim T, Kim do H. Deep RNA sequencing reveals novel cardiac transcriptomic signatures for physiological and pathological hypertrophy. PloS one. 2012;7(4):e35552. Epub 2012/04/24. doi: 10.1371/journal.pone.0035552. PubMed PMID: 22523601; PMCID: 3327670.
44. Bienko M, Crosetto N, Teytelman L, Klemm S, Itzkovitz S, van Oudenaarden A. A versatile genome-scale PCR-based pipeline for high-definition DNA FISH. Nature methods. 2013;10(2):122-4. Epub 2012/12/25. doi: 10.1038/nmeth.2306. PubMed PMID: 23263692; PMCID: 3735345.
45. Raj A, van den Bogaard P, Rifkin SA, van Oudenaarden A, Tyagi S. Imaging individual mRNA molecules using multiple singly labeled probes. Nature methods. 2008;5(10):877-9. Epub 2008/09/23. doi: 10.1038/nmeth.1253. PubMed PMID: 18806792; PMCID: 3126653.

Chapter 4: Chromatin Structural Regulation of Cardiac Transcription

[This research was originally published in the Journal of Biological Chemistry by Monte et al. Reciprocal Regulation of the Cardiac Epigenome by Chromatin Structural Proteins HMGB and CTCF: Implications for Transcriptional Regulation. *J Biological Chemistry*. 2016. 291(30):15428-46. PMID: 27226577. © the American Society for Biochemistry and Molecular Biology.]

For the proposed project in Chapter 3, we examined the properties of cardiac RNA polymerase II transcription factories in control and failing mouse hearts. We measured changes in transcriptional activity indicated by 5'fluorouridine incorporation that maps increases in total, nucleolar and nucleoplasmic RNA production in hypertrophic cardiomyocytes. Our findings provide support for the changes in structure and function of these factories. Using super-resolution imaging, we quantitate the anatomical distribution of active RNA polymerase II clusters as well as mean intensity of factories in cardiomyocyte nuclei. These results corroborate the existence of transcription factories and demonstrate the recruitment and engagement of RNA polymerase II molecules to specific sites in the nucleus to enhance transcriptional activity in stressed myocytes. Furthermore, we analyze the relationships of expression levels with nuclear gene positioning *in vivo* for the endogenous gene loci of *Atp2a2*, *Nppa*, *Gapdh* and *Nefl*. This project is described in further detail in Chapter 6.

To further investigate prospective regulators of cardiac transcription factories, we investigated chromatin structural protein, HMGB2, previously identified by our lab to regulate cardiomyocyte hypertrophy and cardiac gene expression (1). In a recent study, we found HMGB2 influences global transcriptional activity in cultured cardiomyocytes (2). As demonstrated with 293T cells, we find that overexpression of HMGB2 in cultured cardiomyocytes suppresses global RNA synthesis as measured by mean nuclear 5'fluorouridine intensity while nuclear area remains unaffected

(Figure 4-1). When HMGB2 is knocked down in cardiomyocytes, we observed a decrease in ribosomal RNA transcription without changes to nuclear or nucleolar dimensions (Figure 4-2). The mechanism behind how HMGB2 influences this transcriptional activity has yet to be investigated. One potential hypothesis is that HMGB2 is important for the stabilization of RNA polymerase I transcription factories.

Furthermore, we found that HMGB2 expression is inversely correlated with CTCF levels (2), another chromatin structural protein that is important in the maintainence of heterochromatin/euchromatin domains and an important mediator of genome looping and interactions (3, 4). Unlike HMGB2 whose overexpression has negative impacts on transcriptional activity, CTCF overexpression has no detectable impact on global transcriptional activity (Figure 4-1A). On the other hand, CTCF knockdown disrupts global transcription in neonatal cardiomyocytes and affects also nuclear area and nucleoli number (Figure 4-3) (2). Comparisons of HMGB2 ChIP-seq from our lab to published CTCF data demonstrate that CTCF and HMGB2 are enriched at common sites in the genome (2). Furthermore, HMGB2 and CTCF do not colocalize *in situ*, suggesting that they do not cooccupy these shared genomic sites at the same time, evidenced using both super-resolution imaging as well as conventional confocal microscopy (Figure 4-4) (2). The quantitative measurements of super-resolution images show minimal overlap between HMGB2 and CTCF, with only 9% colocalization (protein-protein distances of <50nm is equivalent to colocalization based on microscope resolution) (2). These analyses used cardiomyocytes at the basal state and should be expanded to include the disease condition to understand whether this association is still maintained and to better uncover how HMGB2 and CTCF cooperatively function to influence heart pathology. Interestingly, the ratio of CTCF to HMGB2 directly correlates with the heart mass across different strains of mice (2). This concept of expression stoichiometry is further discussed in Chapter 5 where we examine transcriptome

patterns across a panel of genetically distinct mice to understand the relationships between genetics, gene expression and heart physiology.

How HMGB2 affects transcription factories needs to be further investigated. We characterize cardiac transcription factories in Chapter 6. Studies investigating whether HMGB2 levels can affect this organization using quantitative transcription factory analysis as later presented can help us better understand the global observations in changes of transcriptional activity. Examination of the effects of perturbations to HMGB2 levels to global transcription factory number, distribution and activity will provide insights into the fundamental biology of how HMGB2 can regulate transcription. Furthermore, the analyses presented here examined total transcriptional activity, the sum of RNA polyermases I, II and III, with RNA polymerases I and III having the predominant contribution (5). By using coimmunoprecipitation and imaging approaches to measure and visualize interactions with RNA polymerases, we can quantify the selective effects of HMGB2 on the different RNA polyermerase transcription factories, and measure and characterize activity levels of individual transcription factories. Additional analyses using dual color super-resolution imaging measuring associations between HMGB2 and RNA polymerase II factories in the heart, in control and failing conditions, will help elucidate the relationships of these proteins. In Chapter 6, we assess nuclear localizations of *Atp2a2* and *Nppa*, two genes that change expression in disease and are also affected by HMGB2 knockdown, and in the case of *Atp2a2*, also directly regulated by HMGB2 (Figure 3-6). Future analyses may include examining whether HMGB2 can mediate changes in nuclear positioning of these genes. CTCF is enriched at borders of lamin-associating domains (2, 6, 7), and HMGB2-enriched regions can also overlap at these boundaries (2). The mechanisms of gene regulation may involve the interplay of CTCF and HMGB2 at the nuclear periphery, such that when HMGB2 is depleted, CTCF binding to the *Atp2a2* promoter may stabilize the gene to the nuclear envelope for silencing. More importantly, how these ubiquitously expressed proteins regulate 3D genomic architecture in a cell type-specific manner

is still poorly understood—a mechanism most likely involving coordination with cell-specific transcription factors that recruit these proteins to target sites to bridge distal regulatory regions and control expression. By comparing the organizations of transcription factories in two models of cardiac hypertrophy (hypertrophic agonist versus HMGB2 knockdown), we can identify chromatin structural features that are important for the induction of pathological gene expression and progression towards heart failure.

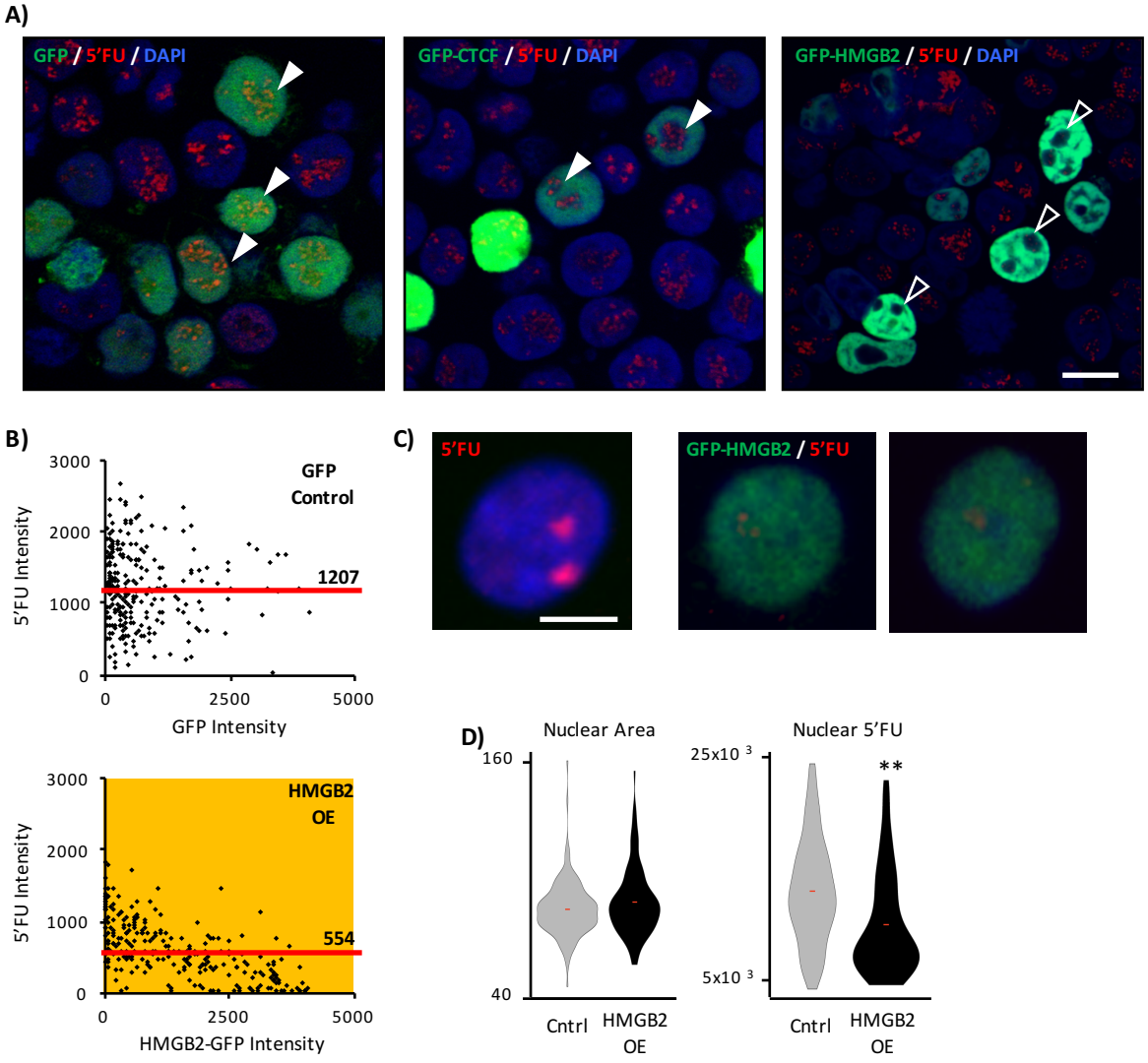

Figure 4-1: HMGB2 overexpression suppresses global transcriptional activity. A) 293T cells overexpressing HMGB2 or CTCF were labeled with 5'fluorouridine (5'FU) for 15min to mark transcriptional activity. Representative images show that overexpression of GFP-HMGB2 negatively regulates rRNA synthesis while GFP-CTCF and GFP expression have no detectable effects, indicated by arrows. *Scale bar: 10μm.* **B)** Quantification of GFP versus 5'FU intensities shows a negative correlation between HMGB2 overexpression and global transcriptional activity (*bottom plot;* p<0.001, yellow plot), which is not evident in the GFP-expressing controls *(top plot)*. **C)** HMGB2 overexpression in neonatal rat ventricular cardiomyocytes (NRVM) also suppresses global transcriptional activity indicated by 30min of 5'FU labeling. Control nucleus is shown on *left* with two representative nuclei of GFP-HMGB2 overexpression on *right*. Note the minimal red signal in the HMGB2-overexpressing nuclei. *Scale bar: 5μm.* **D)** HMGB2 overexpression in NRVMs does repress transcriptional activity, marked by reduced 5'FU signal in the nucleus, without affecting nuclear area. ** *indicates p<0.0001.* [2]

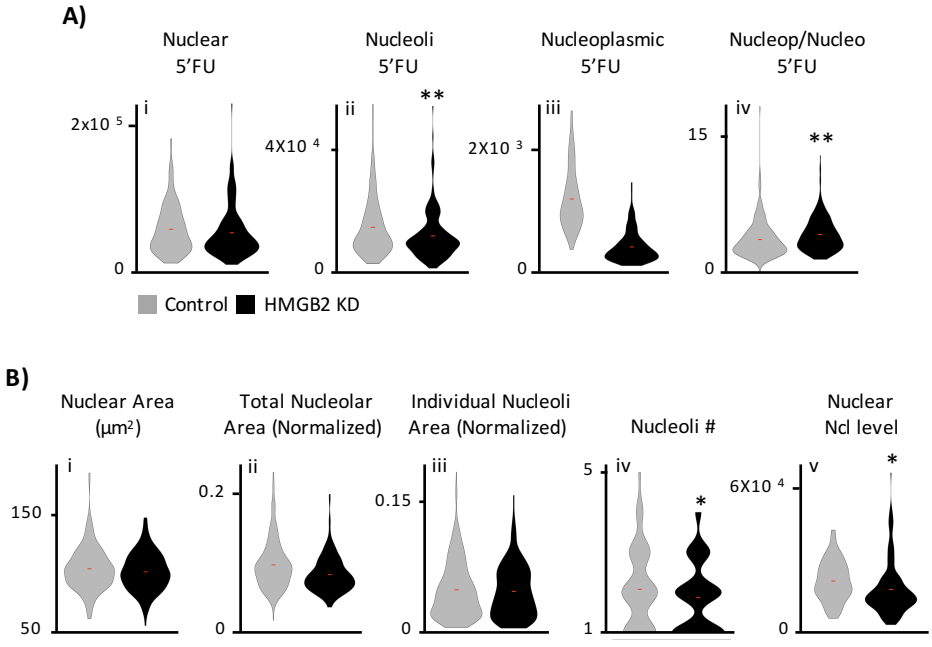

Figure 4-2: HMGB2 knockdown in cardiomyocytes reduces transcriptional activity without affecting nuclear properties. A) Cultured cardiomyocytes, control and with HMGB2 knockdown, were treated with 5'FU for 30min to label nascent RNA. Knockdown did not impair total nuclear transcriptional activity, measured by 5'FU intensity (i). When comparing nuclear anatomical changes, there was a significant decrease in 5'FU signal in the nucleoli (ii), which corresponded to a significant increase in the nucleoplasmic to nucleolar intensity detected (iv). ** *indicates p<0.01.* **B)** Knockdown of HMGB2 did not affect structure of the nucleus or nucleolar organization (total nucleolar area normalized to nuclear size; i-iv) although nucleolin (Ncl) levels were affected (determined by a decrease in fluorescence intensity; v). * *indicates p<0.05.*

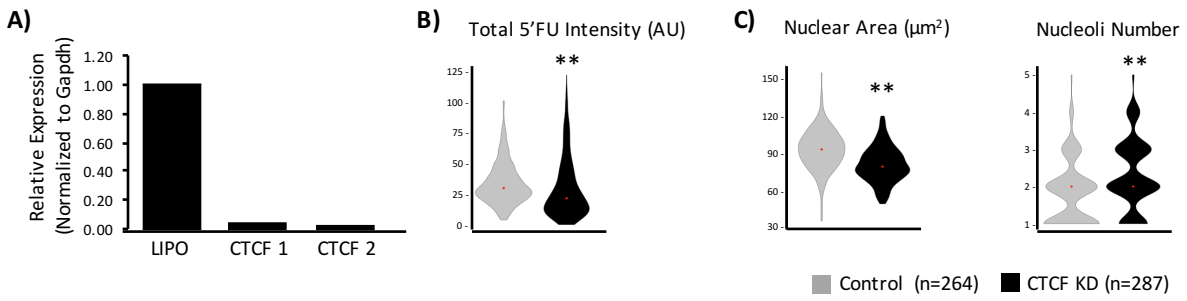

Figure 4-3: CTCF knockdown affects transcriptional activity and nuclear structure in cardiomyocytes. A) CTCF knockdown was confirmed in NRVMs using 2 different primer sets for the gene. A subset of cells from the same dish was then used to assess global transcriptional activity. **B)** 5'FU incorporation (30min) is reduced by 11% in cells with CTCF knockdown, indicating disruption of transcriptional activity. **C)** Nuclear area was reduced in cells with CTCF knockdown and average nucleoli number per nucleus increased. ** *indicates p<0.001.* [2]

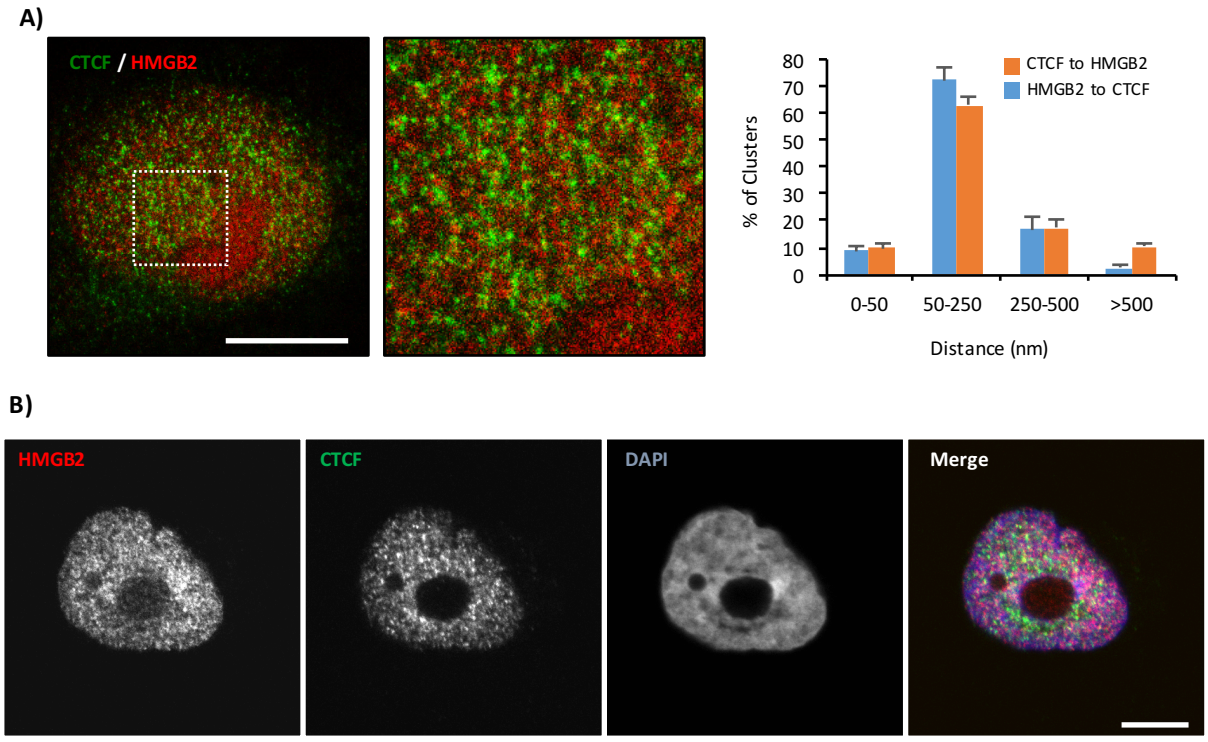

Figure 4-4: HMGB2 and CTCF do not colocalize in cardiomyocyte nuclei. A) Control NRVMs were labeled with CTCF and HMGB2 and imaged using super-resolution STED microscopy. Quantitative analyses measuring the closest distance of neighboring protein cluster are shown on right. We defined colocalization to be distances of <50nm, determined based on the resolution of the STED microscope. From these measurements, we find <9% of HMGB2 and CTCF clusters colocalize. These findings are consistent with ChIP-reChIP experiments that also demonstrate that HMGB2 and CTCF do not co-occupy genomic sites at the same time. *Scale bar: 5μm.* [2] **B)** These results are consistent in 293T cells imaged by confocal microscopy (note the absence of detectable colocalization), suggesting a cell type independent relationship of chromatin structural regulation mediated by HMGB2 and CTCF. *Scale bar: 5μm.*

Chapter 4: References

1. Franklin S, Chen H, Mitchell-Jordan S, Ren S, Wang Y, Vondriska TM. Quantitative analysis of the chromatin proteome in disease reveals remodeling principles and identifies high mobility group protein B2 as a regulator of hypertrophic growth. Mol Cell Proteomics. 2012;11(6):M111 014258. doi: 10.1074/mcp.M111.014258. PubMed PMID: 22270000; PMCID: PMC3433888.
2. Monte E, Rosa-Garrido M, Karbassi E, Chen H, Lopez R, Rau CD, Wang J, Nelson SF, Wu Y, Stefani E, Lusis AJ, Wang Y, Kurdistani SK, Franklin S, Vondriska TM. Reciprocal Regulation of the Cardiac Epigenome by Chromatin Structural Proteins Hmgb and Ctcf: IMPLICATIONS FOR TRANSCRIPTIONAL REGULATION. J Biol Chem. 2016;291(30):15428-46. doi: 10.1074/jbc.M116.719633. PubMed PMID: 27226577; PMCID: PMC4957031.
3. Kim S, Yu NK, Kaang BK. CTCF as a multifunctional protein in genome regulation and gene expression. Exp Mol Med. 2015;47. doi: ARTN e166 10.1038/emm.2015.33. PubMed PMID: WOS:000358594800001.
4. Dixon JR, Selvaraj S, Yue F, Kim A, Li Y, Shen Y, Hu M, Liu JS, Ren B. Topological domains in mammalian genomes identified by analysis of chromatin interactions. Nature. 2012;485(7398):376-80. doi: 10.1038/nature11082. PubMed PMID: WOS:000304099100044.
5. Paule MR, White RJ. Transcription by RNA polymerases I and III. Nucleic Acids Research. 2000;28(6):1283-98. doi: DOI 10.1093/nar/28.6.1283. PubMed PMID: WOS:000085897000001.
6. Guelen L, Pagie L, Brasset E, Meuleman W, Faza MB, Talhout W, Eussen BH, de Klein A, Wessels L, de Laat W, van Steensel B. Domain organization of human chromosomes revealed by mapping of nuclear lamina interactions. Nature. 2008;453(7197):948-U83. doi: 10.1038/nature06947. PubMed PMID: WOS:000256632000050.

7. Zullo JM, Demarco IA, Pique-Regi R, Gaffney DJ, Epstein CB, Spooner CJ, Luperchio TR, Bernstein BE, Pritchard JK, Reddy KL, Singh H. DNA Sequence-Dependent Compartmentalization and Silencing of Chromatin at the Nuclear Lamina. Cell. 2012;149(7):1474-87. doi: 10.1016/j.cell.2012.04.035. PubMed PMID: WOS:000305753800014.

Chapter 5: Relationship of Disease-Associated Gene Expression to Cardiac Phenotype is Buffered by Genetic Diversity and Chromatin Regulation

Elaheh Karbassi, Emma Monte, Douglas J. Chapski, Rachel Lopez, Manuel Rosa Garrido, Joseph Kim, Nicholas Wisniewski, Christoph D. Rau, Jessica J. Wang, James N. Weiss, Yibin Wang, Aldons J. Lusis, Thomas M. Vondriska

[This research was originally published in Physiological Genomics by Karbassi et al. Relationship of Disease-Associated Gene Expression to Cardiac Phenotype is Buffered by Genetics Diversity and Chromatin Regulation. *Physiological Genomics*. 2016. 48(8):601-15. PMID: 27287924. © the American Physiological Society.]

Abstract

Expression of a cohort of disease-associated genes, some of which are active in fetal myocardium, is considered a hallmark of transcriptional change in cardiac hypertrophy models. How this transcriptome remodeling is affected by the common genetic variation present in populations is unknown. We examined the role of genetics, as well as contributions of chromatin proteins, to regulate cardiac gene expression and heart failure susceptibility. We examined gene expression in 84 genetically distinct inbred strains of control and isoproterenol-treated mice, which exhibited varying degrees of disease. Unexpectedly, fetal gene expression was not correlated with hypertrophic phenotypes. Unbiased modeling identified 74 predictors of heart mass after isoproterenol-induced stress, but these predictors did not enrich for any cardiac pathways. However, expanded analysis of fetal genes and chromatin remodelers as groups correlated significantly with individual systemic phenotypes. Yet, cardiac transcription factors and genes shown by gain-/loss-of-function studies to contribute to hypertrophic signaling did not correlate with cardiac mass or function in disease. Because the relationship between gene expression and phenotype was strain specific, we examined genetic contribution to expression. Strikingly, strains

with similar transcriptomes in the basal heart did not cluster together in the isoproterenol state, providing comprehensive evidence that there are different genetic contributors to physiological and pathological gene expression. Furthermore, the divergence in transcriptome similarity versus genetic similarity between strains is organ specific and genome-wide, suggesting chromatin is a critical buffer between genetics and gene expression.

Introduction

Investigations of the mechanisms underpinning complex physiological phenotypes generally take one of two approaches: either a given pathway (new or previously observed in another cell) is interrogated using gain-/loss-of-function approaches or omics-based discovery experiments are used to determine groups of molecules involved in a phenomenon. Particularly when one approach is marshaled as validation for the other, these dichotomous methods have revealed the molecular basis for various disease processes. The advent of systems genetics in mouse models (an example in the latter category), in which multiple inbred mouse strains with characterized genetic diversity are systematically phenotyped in response to a stress, concomitant with gene expression analysis, allows for genome-wide association analyses (1) and data-driven discovery of genetic networks (2). In the present study, we utilize systems genetics to test hypotheses regarding the differential onset of cardiac disease and to discover novel principles of gene expression. The disease in question is cardiac hypertrophy and the biological process is chromatin-dependent regulation of transcription.

In response to chronic stresses and/or acute injuries, the mammalian heart hypertrophies, increasing the size of individual myocytes. This compensatory response plays a beneficial role *in vivo* but is also a common precursor to the deleterious condition of heart failure. The following three pieces of rationale related to this disease condition serve as the basis for the present investigation: *1*) multiple models of cardiac hypertrophy have been shown to be accompanied by

"fetal gene reprogramming," in which adult diseased muscle expresses genes/isoforms associated with an earlier developmental state (3); *2*) an extensive cadre of genes has been implicated in cardiac hypertrophy on the basis of knockout and overexpression studies in cells and mice (4); and *3*) human and mouse studies indicate that cardiac hypertrophy and failure have large genetic components of unexplained mechanism (i.e., they are heritable, but we do not know how the heritability manifests at the molecular level) (5, 6). In this study, we test hypotheses that incorporate these three distinct observations. Specifically, we examine whether the panel of genes altered in a single genetic background behaves similarly when examined in the real-world scenario of common genetic variation. Second, we ask how genes known to be capable of modulating cardiac phenotype in gain-/loss-of-function studies correlate with cardiac phenotype in the setting of naturally occurring genetic and phenotypic diversity. Lastly, we investigate how chromatin proteins and transcription factors are affected by common genetic variation, and the relationship in turn between the transcriptomes of these molecules and cardiac phenotype.

Material and Methods

All experiments involving animals conform to the National Institutes of Health Guide for the Care and Use of Laboratory Animals and were approved by the UCLA Animal Research Committee.

Analysis of data from the hybrid mouse diversity panel.

Microarray [RNA isolated from left ventricle (LV)] and phenotypic data from 84 classical inbred and recombinant strains of mice in the basal state or after treatment with isoproterenol (ISO) were analyzed. Isoproterenol was administered continuously at 30 mg/kg/day for 3 wk via osmotic minipump to 8-10 wk old female mice. N=2 for microarray (RNA from 2 mice/strain/condition were combined and analyzed on a single microarray). N=2 for control phenotype and n=4 for ISO phenotype (7). Additional microarray data were obtained from macrophages before and after LPS stimulation (16 wk, male) (8), bone marrow (16 wk, male) (9), striatum, and hippocampus (8 wk,

male) (10). Microarrays were performed as follows: cardiac and brain tissue, Illumina ref 8v2; macrophages, Affymetrix mouse 430a; bone marrow, Illumina ref 6v1. Change in expression with isoproterenol was calculated as the difference between the normalized, log2 transformed values for isoproterenol and basal. Cardiac mass and echocardiography parameters were used to classify mice into four phenotype categories based on their response to isoproterenol. Resistant mice were defined as exhibiting minimal change in response to isoproterenol (as compared with the entire panel). Hypertrophic and failing mice were classified based on measurements of their state after isoproterenol and in the change (ISO-Basal) in parameters in response to isoproterenol. Strains whose traits were congruent with different conditions or that resembled different phenotypes when we considered their isoproterenol state versus their ISO-Basal state were left unclassified.

We used a stepwise process, incorporating multiple morphological and functional phenotypes, to classify the response of mice to cardiac stress. Strains were ranked from smallest to largest percent change in normalized total heart weight, a range that spanned 85% to 164% [ISO as a percentage of basal heart weight/body weight (HW/BW)]. Strains with ISO heart sizes close to basal heart sizes (102% to 118%; representing 14% of strains) were subset for later consideration as either resistant or failing based on other parameters (only one strain, CXB-13/HiAJ, had a heart smaller after ISO). Strains with yet larger hearts after ISO (135-164%; representing 38% of strains) were subset for consideration as either hypertrophic or failing. These thresholds of 118 and 135% were determined based on the values of AXB-4/PgnJ and C3H/HeJ, respectively, which we had previously classified as resistant and failing according to a less systematic approach based solely on mass. Next, strains were ranked based on changes in normalized LV weight after ISO (giving an LV/BW range of 75 to 171% of basal size), and strains with minimal change in LV size (100-110%; representing 8% of strains) were subset to be potentially classified as resistant; those with LV 130% of basal after ISO were subset as failing or hypertrophic (130-

138% as potentially failing; 140% as potentially hypertrophic or failing, representing 52% of strains). For left ventricular internal diameter in diastole (LVIDd; which gave a range of 85 to 136% of basal after ISO), strains with small diameters (85-103%, 17% of strains) were subset as potentially hypertrophic, whereas strains with LVIDd 104% (7% of strains) were subset as either hypertrophic or resistant, those unchanging (105-107% of basal after ISO, 17% of strains) subset as potentially resistant, and those with enlarged diameters (117-136% of basal after ISO, 18% of strains) were subset as potentially failing. For posterior wall thickness (PWTH; ranging from 24% to 293% of basal after ISO), strains with thinner walls (24% to 79%; 24% of strains) were subset as potentially failing, those with minimal change in PWTH (97-107%, 20% of strains) were subset as potentially resistant and those with increased PWTH (120-293%, 32% of strains) were subset as potentially hypertrophic (although PWTH 135% was allowable in a strain to be classified as resistant, provided the other metrics did not warrant classification as hypertrophic). Lastly, for ejection fraction (EF; ranging from 56 to 138% of basal after ISO), strains with depressed EF (56-86% of basal after ISO, 15% of strains) were subset as potentially failing, those with minimal change in EF (97-109%, 32% of strains) were subset as potentially resistant and those with improved EF (109-138%, 35% of strains) were subset as potentially hypertrophic.

Based on the above parameters, we assigned strains to a single category. For each strain, we counted the number of phenotypes that matched the resistant, hypertrophic, or failing category and assigned said strain to the most appropriate group, provided there were not multiple conflicting classifications. For example, a strain would not be assigned resistant, even if the majority of parameters were labeled resistant, if there were multiple examples of parameters being classified otherwise. As a result, a strain's classification would be based not on a single parameter. Finally, we repeated this analysis using the ISO only values (as opposed to change between ISO and basal, as described above) and adjusted strain classifications if the results of the ISO phenotype data strongly conflicted with the change in expression data. Our objective was

a core set of strains that were confidently identifiable as hypertrophic, failing, or resistant. The cost was that we left almost 50% of strains unclassified, but what we gained was the ability to reliably make conclusions about the expression patterns of the other three categories, since we had stringently defined phenotype groups. The purpose of this entire classification exercise was to study the syndrome of cardiac pathology more closely to how it presents in the clinic, which is as a spectrum of phenotypes across a population of humans, rather than as a single morphological or functional endpoint.

Identification of genes with consistent response to isoproterenol within phenotype group.

All 25,697 probes on the microarray were classified as upregulated (ISO-Basal > 1), downregulated (ISO-Basal < -1) or unchanged (-1 < ISO-Basal < 1) in each hypertrophic, failing, or resistant strain after isoproterenol. We next searched for probes that were either up- or downregulated in the majority of strains within at least one phenotype group. Majority required 77% of failing (10 of 13 strains), 77% of hypertrophic (17 of 22 strains), or 75% of resistant strains (6 of 8 strains) to have the same response. In total, 21 probes met this condition. By contrast, 24,887 were unchanged in the majority of all three phenotype groups, with 12,257 probes unchanged in all strains. We confirmed that all 21 of these genes are expressed [fragments per kilobase of transcript per million mapped reads (FPKM) ranges from 2 to 13, median of 6] in the adult mouse heart by comparing our data to RNA-seq data from ENCODE (ENCFF742HJE).

Correlation of gene expression change with disease phenotype.

We generated comprehensive lists of different functional subsets of genes that have been implicated based off of manual curation of the literature to be involved in cardiac remodeling during hypertrophy and failure: fetal genes (representing not just genes expressed in development, but specifically demonstrated to change in hypertrophy and be used as biomarkers of hypertrophy in the literature); cardiac transcription factors; hypertrophic regulators (based on

previous gain- and loss-of-function studies in the heart); and chromatin regulators. Genes from other subsets that were functionally validated in mice were also included as hypertrophic regulators. For the purpose of the hypertrophic regulator gene list, we focused on the disease outcome, not etiology, identifying genes associated with cardiac hypertrophy or failure based on published mouse models. We examined the Pearson correlation of expressions (basal, isoproterenol, or change with isoproterenol) of these subsets of cardiac genes with 49 phenotypes (basal, isoproterenol, or change with isoproterenol) across hybrid mouse diversity panel (HMDP) mouse strains. We also computed correlations between each gene's expression and the total number of genes up- or downregulated after isoproterenol treatment (ISO-Basal > 1.5 or < -1.5) for each strain.

To determine whether any gene subsets (fetal genes, cardiac transcription factors, hypertrophic regulators, chromatin regulators) were enriched with genes that were correlated to phenotype, we discretized the correlation of individual genes into "significant" and "nonsignificant" based on a significance threshold of alpha 0.05 and performed a hypergeometric test on the group followed by a false discovery rate (FDR) correction using fdrtool (11, 12).

To examine whether changes in expression of individual genes correlate with overall disease state, we used our strain categorization to plot change in expression across strains that are resistant, undergoing hypertrophy, or in failure. The Kruskal-Wallis test was used to quantify statistical significance of the differences between changes in individual gene expression across disease states, and we corrected for multiple testing using the FDR (fdrtool).

Histone clusters and expression in the different phenotype groups.

Change in expression of histones was used to cluster the hypertrophic, failing, and resistant strains using hierarchical ordered partitioning and collapsing hybrid (HOPACH), generating five

clusters of strains. HOPACH was developed in part to optimize clustering samples based on gene subsets by combining hierarchical and partitioning clustering (13). We tested for contribution of population structure to our clustering by comparing the kinship coefficients of strains within a group to the coefficients between groups and found no significant difference for any of our clusters. Enrichment of the three disease states (hypertrophic, failing, or resistant) in each histone cluster was determined by the binomial test. Separately, change in expression with isoproterenol was calculated for each histone variant across all strains in a disease state (hypertrophic, failing, or resistant). Presence of significant differences between the three disease states was determined for each variant using the Kruskal-Wallis test. For those variants with significant differences between the groups, the Mann-Whitney test was used to determine which disease states exhibited the difference.

Linear regression modeling of expression versus phenotype.

We used the R package glmnet (14) to identify microarray probes that may be better predictors of cardiac phenotypes when taken together. The difference between log2 transformed isoproterenol and basal expression of all microarray probes in 82 strains of mice was scaled and used as the pool of potential predictors. Response was change in normalized total heart weight (isoproterenol HW/BW minus basal HW/BW). The cvfit function was set to nfold 10 such that a model is built on 90% of the strains and validated on 10% and this process repeated 10 times. We used default parameters of cvfit with s="lambda.min" and increasing values of alpha to empirically determine the appropriate alpha to generate ~100 predictors for analysis. For each alpha 0.1–1 (increments of 0.1), we ran cvfit 1,000 times and found alpha=0.2 generated 98 predictors (microarray probes) that were present in 800 of the 1,000 models (with each model representing 10 fold cross-validation). The 98 predictors were then subsetted and used to rerun cvfit, resulting in 74 probes in the final model. The accuracy of this model was validated by its ability to accurately predict the difference in total heart weight of the 82 strains. The 74 returned

predictors were searched using Princeton University GO Term Finder (15) and DAVID Bioinformatics (16, 17). Neither generated a Gene Ontology (GO) term with enrichment after Benjamini correction. Motif enrichment for the promoter regions of these genes [2 kb upstream of transcription start site (TSS)] was determined using CentriMo in the MEME suite, using the vertebrate motif database. We then attempted a similar analysis using EF instead of HW/BW as the outcome to predict. However, the glmnet algorithm did not generate an optimized model with our input parameters when using cross-validation. Instead, the model was highly strain dependent, and we therefore did not feel confident drawing conclusions from the model without further optimization.

Multiple organ clustering.

To explore features across organs, we analyzed the 37 strains with microarray data from all tissues (heart, macrophage, bone marrow, striatum and hippocampus). Cluster, a package for R, was used to cluster strains into a predetermined number of groups (k=5) with partitioning around medoids using the Euclidean metric. Clustering was performed on microarray data for all core histone variant probes on the array in the tissue being analyzed. Separately, clustering was performed using the entire transcriptome or using the panel of chromatin regulators. The Euclidean distance between each strain-by-strain comparison was converted to a rank from the most-closely related strain pair to the least-similar pair. Rankings were used to cluster organs based on similar “expression relatedness” between strains and genetic relatedness [based on kinship matrix derived from single nucleotide polymorphisms (SNPs)] using heatmap.2, a function of gplots. The kinship matrix was derived using EMMA (18), and serves to generate a kinship coefficient for each pairwise comparison between strains that estimates the proportion of the genome that is identical between two strains due to common ancestry (19).

Results

Expression of individual genes does not correlate with disease severity.

A recent genome-wide association study (GWAS) on mice treated with the beta-adrenergic agonist isoproterenol revealed significant genetic loci, and new genes, associated with cardiac hypertrophy across a panel of inbred mouse strains (20). This study provided a unique opportunity to subclassify cardiac pathology based on the various phenotypes measured in these mice; for the present analysis, we have done this classification based on *in vivo* measurements of cardiac function, to mimic the clinical situation in which patients with comparable environmental risk present distinct extent of disease and in some cases, no disease. We chose phenotypes related to heart size and function recorded after 3 wk of isoproterenol infusion and measured by echocardiography (21), combined with postmortem measurements of heart mass (20), and divided strains into four disease states: hypertrophic (mass increased but function was preserved, n=22); failing (mass increased and function deteriorated, n=13); resistant (minimal change in mass or function, n=9); or unclassified (mass, function and other disease measurements were not in agreement with each other and the spectrum of phenotypes in the animal thus included some that appeared diseased and others that appeared healthy, n=40). The distribution of strains between these groups for six measurements of cardiac size and function is shown in Figure 5-1A. Population structure did not contribute significantly to disease state classifications, as determined by genetic similarities within groups versus between groups (measured by kinship coefficients).

Cardiac disease in animal models is often associated with characteristic alterations in gene expression, called a “fetal gene program,” because the change in gene expression mimics aspects of earlier developmental stages of the heart. (As an aside, it is noteworthy that there are many differences in the transcriptomes of fetal, adult, and diseased hearts, and the term “fetal genes,” used to refer to a small cohort that may behave in the diseased adult heart more similarly to the healthy fetal heart, is thus somewhat of a misnomer. We use the term fetal genes to

distinguish the canonical marker genes measured as indicators of hypertrophy from what we refer to herein as “hypertrophic regulators,” which in this study include genes whose genetic manipulation in mouse studies implicate them as components of hypertrophic signaling.) Some human studies have shown similar gene expression changes in heart failure patients (22, 23). However, the role of common genetic variation to influence this gene expression change is unknown. We tested the hypothesis that this gene expression program would be conserved across genetic backgrounds as a common mechanism of disease pathology. To test this, we examined a representative subset of genes often used experimentally to evaluate this phenomenon: alpha myosin heavy chain (α-MHC, predicted to decrease with disease), beta myosin heavy chain (β-MHC, predicted to increase), atrial natriuretic factor (ANF, predicted to increase) and the sarcoplasmic reticulum calcium ATPase (SERCA, predicted to decrease). Because of the differential disease susceptibility across the panel of mice, we were able to examine fetal gene expression in different disease states, despite having microarray data from only two time points (basal and after 3 wk of ISO). To our surprise, these fetal genes were poor predictors of cardiac pathology across genetically distinct mice (Figure 5-1B), with only α-MHC displaying the expected trend, in which most of the animals with disease exhibited a decrease in expression. Notably, commonly used strains including BALB/cJ and C57BL/6J were inconsistent, whereas FVB/NJ and DBA/2J were consistent, with the expected changes in expression of these fetal genes (Figure 5-1B, right panels).

Complementary to the aforementioned manual classification, we also used two computational approaches to cluster strains. The first was unsupervised hierarchical clustering of Euclidean distances based on the percent change in phenotype after ISO for the same six phenotypes used to manually group strains. This scenario generated five clusters of strains, which we examined for their expression of ANF, SERCA, α-MHC, and β-MHC, asking if 50% of strains followed the

expected trend (up- or downregulated) for individual genes. Only one cluster had at least two genes meeting this minimal criteria (n=23/41 strains upregulating ANF and n=34/41 strains downregulating α-MHC). This cluster also contained 18 of the 22 strains we had manually classified as hypertrophic. The second method we used was also an unsupervised clustering approach (called partitioning around medoids), using as input a different set of phenotypes (normalized total HW, normalized LV weight, normalized lung weight, LVIDd, and EF; expressed as the ISO value minus that in basal state) to produce five clusters of mice. In this scenario as well, ANF, SERCA, and β-MHC all failed to show consistent up- or downregulation in any of these clusters. One of the groups had over 50% of strains upregulating ANF (57% of strains upregulated), while two groups had SERCA downregulated in 50% of strains (60% of strains in one group, 58% of strains in the second group). No group had β-MHC upregulated in over 37% of strains, and all groups had α-MHC downregulated in ~71% of strains. Thus, two unsupervised clustering methods and one manual clustering approach all failed to produce groups of mice whose ostensible susceptibility to cardiac pathology was accompanied by the canonical changes in fetal gene expression. Switching back to the phenotype classifications shown in Figure 5-1, then, we examined all microarray probes to determine if other genes serve as better markers of response to isoproterenol treatment across genetic backgrounds (Figure 5-2). The limited size of this list (21 probes) suggests that single genes serve as poor predictors of cardiac disease state.

We wanted to further explore this observation by probing genes as a group as well as considering individual phenotypes as opposed to overall disease states. We expanded the list of fetal genes examined from four to 37 and also tested additional cohorts of genes: regulators of hypertrophic signaling (as determined from knockout and/or transgenesis experiments in mice, n=142, see Supplemental Table 5-1 for citations and phenotype information from previous mouse studies), cardiac transcription factors (with known effects on cardiac phenotype, n=31), and chromatin

regulators (see Table 5-1 for a list of genes in all these groups). Because many of the changes in gene expression (and phenotype) across genetic backgrounds cannot be explained through the actions of SNPs acting in cis (i.e., the variant base is situated in or near the modified gene), we reasoned that alterations in the expression of chromatin modifiers could be a mechanistic explanation for some of these differences in gene expression. To test this, we also included a list of genes for epigenetic and chromatin structural modifiers (referred to as chromatin regulators, n=124; Table 5-1) in our analyses. We examined the expression of these genes in the basal setting, after isoproterenol and the difference between these points as three independent measurements, rather than looking only at the difference as in Figure 5-1B.

Unlike the previous analysis looking for genes consistently up- or downregulated across strains, here we looked for linear correlations between the level of gene expression and the severity of the cardiac phenotypes. Using expression data for probes representing each gene cohort and individual phenotypes for all strains, we derived Pearson correlations for the relationships between gene expression and phenotypes. We took the fraction of probes for each gene cohort that were deemed significantly correlated with the given phenotype (percentages are indicated for cardiac mass and function parameters in Figure 5-3A) and measured enrichment by comparing to the fraction of significantly correlated probes from the entire microarray (Table 5-2 lists P values for enrichment for the complete set of phenotypes examined in this study). While individual genes remained poor predictors of cardiac disease (few genes show significant correlation, indicated by $P<0.05$, for any given phenotype), when examined as groups, the fetal gene subset and chromatin regulator subset were significantly enriched in genes correlated with multiple cardiac phenotypes compared with the correlation exhibited by all genes detected on the microarray (Figure 5-3A and Table 5-2). Microarray probes for the fetal genes showed significant enrichment for correlations with left atrial mass (enriched 2.97-fold compared with entire transcriptome), change in total heart mass (3.14-fold), and change in LV mass (3.81-fold) after

isoproterenol. Individually, considering the seven heart mass and function phenotypes in three conditions (ISO, basal, change with ISO), 65% of the fetal genes correlate with at least three of the 21 comparisons, an enrichment over the correlation of all genes in the genome. Expression of chromatin remodelers correlated with right ventricular mass under both basal and isoproterenol conditions (1.36-fold and 1.42-fold, respectively) and fractional shortening (1.50-fold) with isoproterenol.

When we investigated relationships in the expression of individual genes among the different disease states, trends did emerge for some of the cardiac transcription factors, the expanded fetal gene list, hypertrophic regulators, and chromatin modifiers, but these were not significant (Figure 5-3B), highlighting again that individual genes do not correlate well with overall state. From these observations we made two hypotheses. First, genetic variation buffers the expression of individual genes, such that the effect of a gene's absolute mRNA abundance on phenotype is dependent on its stoichiometry with other interacting genes and therefore is a poor indicator of phenotype when analyzed individually. Second, part of the buffering effect of genetic variation to influence cardiac phenotype may be mediated by chromatin. To test this second hypothesis further, we examined genes encoding chromatin proteins in more detail, focusing on histone variants, which we previously found to exhibit altered stoichiometry in a mouse model of cardiac hypertrophy and failure (24).

Specific histone variants are consistently regulated by disease state.

Of the chromatin remodeling genes, 58 are histone-modifying enzymes, of which, 43% are correlated with at least three of the seven cardiac size and function phenotypes in any of the conditions (ISO, basal, change with ISO). To investigate whether histone variants in addition to histone modification may be regulating susceptibility to cardiac pathology, we performed the antithetic clustering analysis: rather than cluster strains by disease state and examine histone

expression, we organized strains according to histone expression (basal value subtracted from isoproterenol value) and observed whether phenotype patterns emerged. Figure 5-4A shows the five clusters of strains that emerge based on histone variant expression; the rows are histone variants and the shading of the cells corresponds to the change in expression. We checked for contribution of population structure and found no genetic bias between strains within clusters. When each of these clusters was examined for the distribution of disease states, cluster 4 (marked by minimal change in histone expression; Figure 5-4A) was significantly enriched in hypertrophic mice and depleted of resistant mice (Figure 5-4B); however, the other histone clusters did not discriminate between phenotypic outcome to isoproterenol, suggesting only weak correlation between histone stoichiometry and susceptibility to isoproterenol. To test this, we examined histone variants as groups between the disease states. No differences were observed in the contribution of variant families to the overall stoichiometry of histones between the different phenotypes (Figure 5-4C); however, when individual histone variants were examined, three showed significant expression differences between disease states (Figure 5-4D). This is in contrast to the fetal genes, cardiac transcription factors, hypertrophic regulators, and chromatin regulators, for which there was no single gene with significant difference in expression between disease states. (Note, the analyses in Figures 5-3B and 5-4D use lower thresholds than that of the consistently changing genes in Figure 5-2, in that Figure 5-2 requires 75% of strains in a disease state to exhibit the same trend, while these figures require only a significant difference in trends between disease states.) Together, this suggests that like the other gene groups analyzed, a general relationship between histone stoichiometry and disease outcome does not exist across different genetic backgrounds despite histones having been implicated in hypertrophy in individual strains (25).

Because we had previously characterized, using mass spectrometry, histone variant and chromatin protein expression in another model of cardiac hypertrophy and failure induced by

pressure overload hypertrophy (24), we sought to determine whether the modules of proteins identified with altered chromatin association in this study were recapitulated in the transcriptome data. In short, none of the chromatin protein modules identified by quantitative proteomics exhibited conserved transcriptome regulation in the present study (data not shown), a not completely unexpected observation, given the tiers of cellular regulation between gene expression and protein occupancy on chromatin.

Unbiased identification of disease predictors do not share common ontology.

We next asked if we could identify genes better correlated with cardiac phenotype. We used linear regression modeling to identify genes whose expressions are predictive of change in normalized total heart weight with isoproterenol. This exercise identified 74 probes that were present in 80% of our models and successfully predicted phenotype but found that they shared no common pathways or functions (based on no significant GO results), suggesting that the relevance of important cardiac signaling pathways may be masked by genetic diversity in the transcriptional response to isoproterenol such that the changes in stoichiometry of key genes within functional modules are genotype dependent (Table 5-3). We compared our data to RNA-seq data from the adult mouse heart (ENCODE, ENCFF742HJE): 34 of the genes were expressed with an FPKM>1. GO analysis of these 34 also returned no significant terms. Furthermore, motif analyses of the promoters (2 kb upstream of TSS) of these 34 genes revealed no enriched vertebrate motifs.

Cardiac transcriptome patterns are not reflective of genetics.

In addition to dissecting the genetically conserved expression changes that predict cardiac phenotype, we next tested if expression, both conserved and strain specific, was in fact correlated with genetics by expanding our analysis to expression data for the HMDP from bone marrow (9), macrophages (8), striatum, and hippocampus (10). We asked: if two strains have similar gene

expression in one organ (due to genetics), do they also share similar transcriptomes in other organs? When two organs cluster in the dendrogram (such as control macrophages and hippocampus; Figure 5-5A, left), it indicates that strains with similar expression in one organ also have similar expression in the other organ. Dendrograms were made with expression data for chromatin regulators, histones, or all genes (Figure 5-5A).

For each organ we ranked strain-by-strain transcriptome comparisons from the most similar strain pair (1, green) to the most different (667, red), and generated a heatmap to display how these rankings vary by organ (Figure 5-5B). Surprisingly, similar transcriptomes between strains in the basal heart did not predict similar expression after isoproterenol (control and ISO hearts do not cluster, Figure 5-5B), suggesting the genetic determinants of physiological and pathological gene expression are different. By contrast, basal and LPS-stimulated macrophages do cluster. We also included a ranking of genetic similarity using kinship matrices based on SNPs. The similarity between the transcriptomes of two strains was only weakly dependent on the genes analyzed, as all gene subsets clustered together for a given organ. Secondly, the relatedness between strains as calculated by gene expression was markedly different from the genetic relatedness determined by SNPs (with the exception of macrophages), though gene expression of all genes was consistent with chromatin gene expression. Together these two patterns suggest that the relationship between genetics and gene expression is buffered by a mechanism that is both organ dependent and globally acting across multiple genes. We postulate this is due to the effects of cell/organ-specific epigenetic programming.

Discussion

Previous studies have shown a diversity of cardiac phenotype across distinct mouse strains (26, 27) and linked them to gene expression differences (28). Here we have expanded these analyses to look across a larger panel of strains to determine whether these differences can still be

attributed to the changes in a single set of genes. We found that, unexpectedly, the majority of cardiac-associated genes implicated with cardiac disease do not share consistent expression changes across strains with similar phenotypes. Instead, our results highlighted the roles of gene cohorts, including those involved with chromatin regulation.

Genetics and chromatin combine to influence gene expression patterns and phenotype, although the mechanisms are incompletely understood (Figure 5-6), in no small part because animal studies often examine only a single genetic background. Here, we show that phenotype cannot be predicted solely by expression of individual genes when a genetically diverse population is examined. Neither genes that have been implicated in regulating hypertrophic signaling nor the fetal genes associate with overall disease state after isoproterenol. In a comparable study using C57BL/6J and DBA/2J administered ISO for 2 wk, both strains displayed significant increases in HW, fractional shortening, and EF (29). These phenotypes are consistent with what we observe, as are the changes in α-MHC expression (no change in the C57BL/6J strain and decrease in DBA/2J). In contrast to our observations, this study reported an increase in ANF in C57BL/6, a difference that may be attributable to variation in the time course of the study.

We further find that the genetic drivers of gene expression are different after isoproterenol. Strains with similar expression patterns in the basal heart no longer share expression similarities after stimulus. A similar observation is seen when comparing gene expression similarities across organs. Our analyses suggest that chromatin, in addition to environmental stimulus, is an important independent modifier of the genetic contribution to gene expression.

The HMDP demonstrates that strains that are most closely related genetically do not always exhibit the most similar transcriptional responses to pathogenic stimuli. To identify the source of this discrepancy, we report three separate findings that point to chromatin as the mechanism.

Firstly, we show that the discrepancy between shared genetics and shared transcriptomes is due to a mechanism that has a strong organ-dependent component. Secondly, we show that the genetic relationships act similarly to control the expression of different gene subsets, suggesting a genome-wide mechanism. Finally, our analyses of gene subsets demonstrate that genetic buffering diminishes the correlation between a single gene and cardiac phenotype, and yet, we still find examples of histone variants with conserved expression changes across disease states and show that chromatin regulators as a group correlate with several disease phenotypes. Although not highlighted in our analyses, DNA methylation serves as another regulator for gene expression and was included in our analyses of chromatin regulators. We find that modulators of DNA methylation, including DNA methyltransferases and methylation binding proteins, correlate with aspects of cardiac hypertrophy. This matches our previous observation that there is differential cardiac DNA methylation in the HMDP (30).

We see two explanations for the lack of correlation between mRNA expression and phenotype, disease state, and genetics. The first is that there are posttranscriptional events that result in a disconnect between mRNA abundance and functional protein levels. Future studies are needed to test these relationships at the protein level. Coexpression modules from microarray have been shown to be inconsistent with protein interaction networks from the heart (31), whereas recent detailed bioinformatics analyses indicate that transcriptome and proteome levels are often quite similar (32). This question can only be resolved experimentally for each protein. Previous studies have indicated that for select genes, the protein levels are very good indicators of heart failure in humans. BNP and NTproBNP, for example, have been shown to be effective biomarkers for ruling out heart failure in patients referred for suspected heart failure by their general practitioner (33). In these cases, differences between tissue mRNA levels (not measured in humans) and circulating plasma protein levels could arise due to the multiple regulatory steps between transcription and subsequent secretion. However, we also propose that for some genes, genetics

is playing a major role in disrupting the correlation between the expression of disease-causing genes and phenotype.

Previous work on the HMDP has been successful using GWAS analysis to identify 24 significant or suggestive loci regulating cardiac hypertrophy and fibrosis (20). None of the 24 candidate genes in these loci showed a significant linear correlation with either total HW or LV weight, with only one (Srpx, P=0.049) showing modest correlation with fibrosis due to isoproterenol treatment. Independently, we found 579 genes (3% of genes detectable on the microarray) showed significant correlation with fibrosis in the isoproterenol state, including Col3a1, Ctgf, and Postn (genes implicated in cardiac fibrosis), which also showed significant correlations with total heart and LV masses. One major implication from our work is that analysis of individual genes should be complemented with future studies that include a middle-ground approach that takes into account many interacting SNPs (as we do here with kinship matrices) while still examining individual SNPs with functional roles (as in GWAS). Such approaches are being developed, wherein large cohorts of SNPs (in this case all SNPs on a single chromosome or in the entire genome) are related to phenotype and have proven more successful at explaining the majority of the heritability of common traits (34).

The low level of causative SNPs identified by GWAS for heart failure (35) has been attributed to the theory that an interaction between multiple SNPs, each with small effect size, is necessary to explain certain complex traits (36). This theory is in line with our observation that gene subsets serve as better predictors of cardiac traits than do individual genes. Importantly, GWAS analysis by the CHARGE consortium also demonstrates that the genetic determinants of heart failure incidence are different between ethnicities (35). Here we attempted to ask a similar question in mice, that is: are hypertrophic or failing mice sick due to the same pathological transcriptome, independent of genetics? In other words, can the same genes serve as predictors of cardiac

phenotype across the HMDP? We were surprised to find poor correlation between abundance of individual genes and specific cardiac phenotypes. In light of this, we attempted to further subdivide strains based on overall disease state, re-examining the data for potential relationships between gene expression and phenotype. This step was taken to address the fact that the different strains may be at different stages of disease progression (i.e., a variation in temporal onset of disease), in addition to being overall more or less resistant to pathology (i.e., variation in severity of disease). This classification inherently induces bias, and thus it is possible that the grouping of strains we performed does not reflect the type of distribution in a human population. It may be that more precise classification strategies exist that would reveal cohorts of animals that have better correlation for the classes of genes tested herein. For the subdivision we present here, however, we find poor correlation between specific genes and overall disease state. This refutes the hypothesis that all mouse strains show altered cardiac size upon isoproterenol by similar transcriptional changes and supports a model where different gene stoichiometry can result in similar phenotypes (37).

It is known that both the incidence of cardiovascular risk factors, such as hypertension, and the incidence of advanced-stage disease outcomes, including heart failure, differ by race (38, 39). Understanding genetic differences in cardiovascular disease is necessary to better assess risk and tailor treatment to individual patients. We show that in addition to differences in heart failure susceptibility, mice of diverse genetic backgrounds also undergo diverse transcriptional responses to achieve a similar phenotypic outcome. One ramification of this is that fetal genes, as well as the entire transcriptome, are poor predictors of cardiac phenotype when analyzed individually across different genetic backgrounds. In our study, chromatin emerges as a mediator of the response to isoproterenol, integrating genetic variation with environmental stress.

Grants

This study was supported by National Heart, Lung, and Blood Institute (NHLBI) Grants HL-105699 (T. M. Vondriska), HL-115238 (T. M. Vondriska), HL-129639 (T. M. Vondriska, Y. Wang), HL-28481 (A. J. Lusis), HL-123295 (A. J. Lusis, Y. Wang), and HL-114437 (J. N. Weiss). E. Karbassi, E. Monte, M. Rosa Garrido, R. Lopez, and C. D. Rau were supported by American Heart Association Fellowships. D. J. Chapski was supported by NHLBI Training Grant T32 HL-69766.

Disclosures

No conflicts of interest, financial or otherwise, are declared by the author(s).

Author Contributions

E.K., E.M., J.N.W., Y.W., A.J.L., and T.M.V. conception and design of research; E.K., E.M., R.L., M.R.G., J.K., C.D.R., and J.J.W. performed experiments; E.K., E.M., D.J.C., M.R.G., N.W., C.D.R., J.J.W., and T.M.V. analyzed data; E.K., E.M., D.J.C., N.W., and T.M.V. interpreted results of experiments; E.K., E.M., D.J.C., and T.M.V. prepared figures; E.K., E.M., and T.M.V. drafted manuscript; E.K., E.M., and T.M.V. edited and revised manuscript; E.K., E.M., D.J.C., R.L., M.R.G., J.K., N.W., C.D.R., J.J.W., J.N.W., Y.W., A.J.L., and T.M.V. approved final version of manuscript.

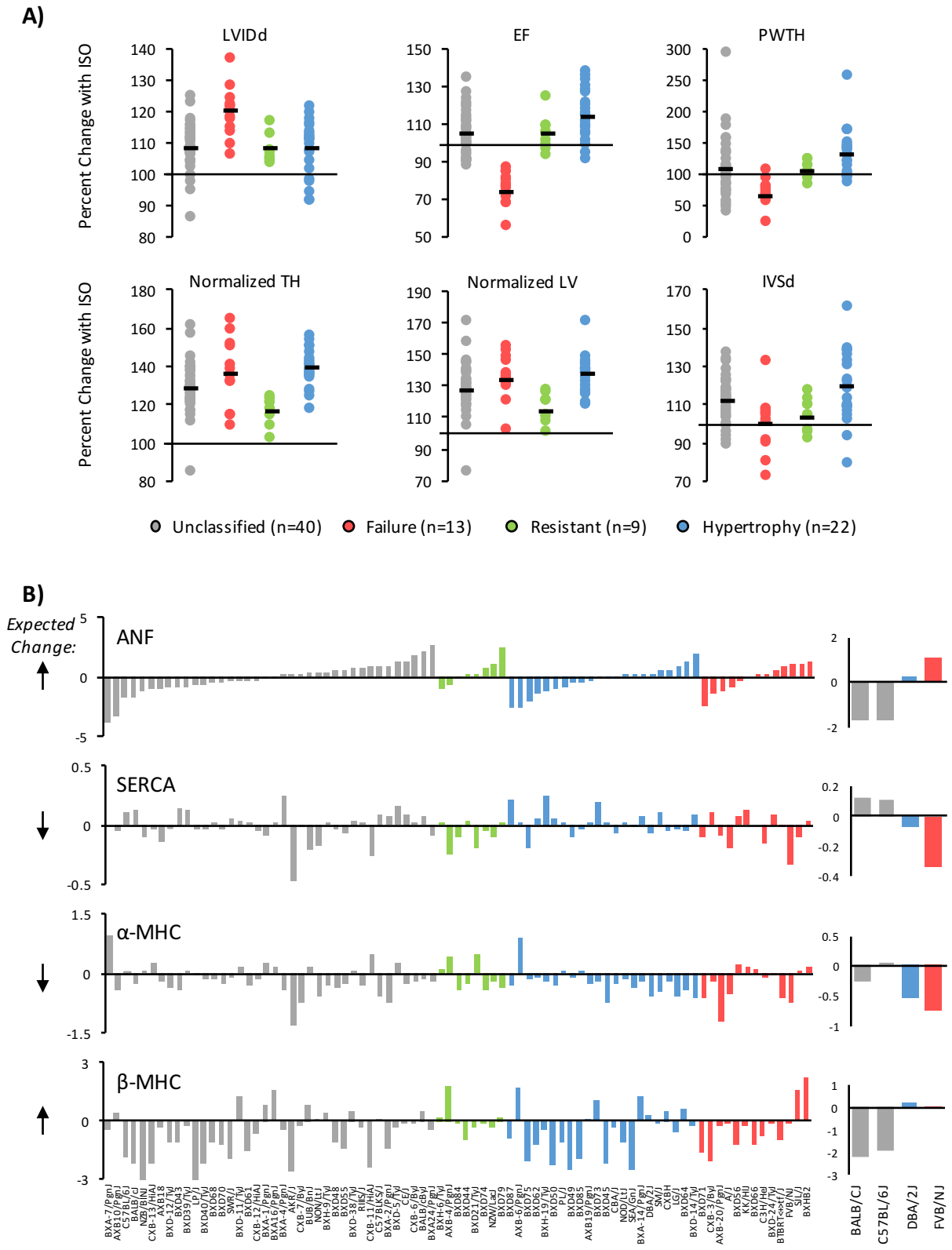
A)
LVIDd
EF
PWTH
Normalized TH
Normalized LV
IVSd
Percent Change with ISO
Unclassified (n=40)
Failure (n=13)
Resistant (n=9)
Hypertrophy (n=22)
B)
Expected Change:
ANF
SERCA
α-MHC
β-MHC
BALB/CJ
C57BL/6J
DBA/2J
FVB/NJ

Figure 5-1: The fetal gene program does not coincide with cardiac hypertrophy in diverse genetic backgrounds. A) 84 inbred strains of mice were phenotyped after treatment with the beta-adrenergic agonist isoproterenol. Mice were categorized as hypertrophic or failing if the majority of their traits matched human clinical measurements of these conditions. Mice with minimal change after isoproterenol were classified as resistant. Strains whose traits were congruent with different conditions were left unclassified. Each dot represents a strain. Bar represents group mean. LVIDd, left ventricular internal diameter in diastole; EF, ejection fraction; PWTH, posterior wall thickness; normalized TH, total heart weight/body weight; LV, left ventricular weight/body weight; IVSd, interventricular septum thickness at diastole. **B)** Cardiac microarray data from the same 84 strains of mice were used to analyze change in expression of the fetal genes. With the exception of alpha myosin heavy chain, there was an equal number of strains upregulating or downregulating the fetal genes, even when controlling for disease state, suggesting they are not good markers of isoproterenol-induced hypertrophy across genetic backgrounds. Each bar represents a strain. Expected direction of change in expression is represented by the black arrows to the left. The commonly studied mouse strains BALB/cJ and C57BL/6J do not display expected trends in expression patterns, while DBA/2J and FVB/NJ do (right panels). ANF, atrial natriuretic factor; SERCA, sarcoplasmic reticulum calcium ATPase.

Illumina	Gene	Resistant	Hypertrophy	Failure	Human
ILMN_1218235	Gnb3		-1.272		Up in ICM (PMID: 24429688)
ILMN_1239726	Snai3	-1.430	-1.762	-1.561	
ILMN_1226472	Retnla			-1.280	
ILMN_1223317	Lgals3	1.735		1.795	
ILMN_2909808	Lrrc52	0.646			
ILMN_2805375	Itgb6	-0.939	-1.246		
ILMN_1232261	Ctnnal1	0.933			
ILMN_2950622	Arhgdig	1.231		1.134	Up in ICM, Up in DCM (PMID:25528681)
ILMN_2769918	Timp1	2.225		2.026	Up in ICM, Down in DCM (PMID: 25528681)
ILMN_3103896	Timp1	2.194		2.020	
ILMN_1246800	Serpina3n	2.006		2.207	
ILMN_2705628	Clec4d	1.312		1.714	
ILMN_1251894	Dct	1.405		1.867	
ILMN_2625279	Pacrg	1.134			
ILMN_2687014	Cyp2e1	-0.448			
ILMN_2764036	Ahsg	0.245			
ILMN_2993745	Ahsg	0.124			
ILMN_1224014	Tmem100	0.450			Up in ICM (PMID:25528681)
ILMN_2666312	Tmem82	-0.994			
ILMN_3005431	2610028H24Rik	1.668		2.241	
ILMN_2654624	AI593442	1.456		2.027	

Figure 5-2: Genes with shared expression response within phenotype groups. We identified genes that showed the same expression response to isoproterenol in at least 75% of strains within any one phenotype group and cross-referenced the genes with patient heart failure expression data. Colored boxes represent genes were at least 75% of strains within a phenotype group showed a consistent gene expression response (green is up-regulated, ISO-basal >1; red is down-regulated, ISO-basal <1; yellow is no change, ISO-basal between -1 and 1). White boxes represent genes where, for that phenotype, there was not a consistent response. The value represents the mean ISO-basal value. Note that the mean is not always representative of the majority of strains due to outliers: the trend of the majority is indicated by the color. ICM, ischemic cardiomyopathy; DCM, dilated cardiomyopathy.

A)

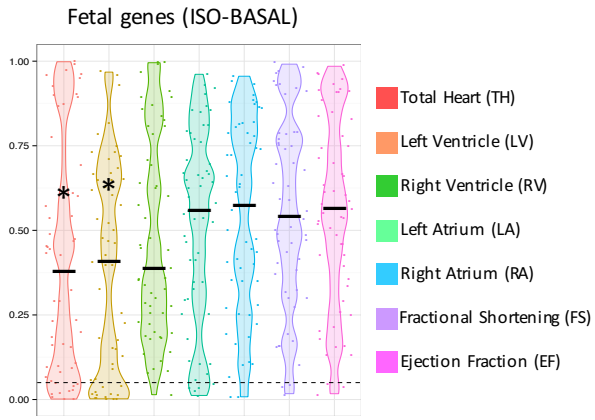

BASAL (% probes)					
PHENOTYPE	ALL	TF	CHR	FETAL	HYP
TH	11.5	13.0	14.1	12.7	14.5
LV	11.4	18.5	13.7	12.7	12.7
RV	23.7	16.7	32.2	32.7	31.4
LA	3.4	1.9	2.4	0.0	2.3
RA	5.4	11.1	4.4	5.5	7.3
FS	5.7	5.6	5.4	9.1	6.4
EF	5.3	3.7	3.9	10.9	5.9
Probes	25697	54	205	55	220

ISO (% probes)					
PHENOTYPE	ALL	TF	CHR	FETAL	HYP
TH	6.2	5.6	7.8	12.7	2.7
LV	7.7	5.6	10.2	10.9	6.4
RV	15.1	13.0	21.5	20.0	19.5
LA	8.6	7.4	7.8	25.5	7.7
RA	1.9	1.9	1.0	3.6	1.8
FS	12.3	13.0	18.5	16.4	14.1
EF	12.0	13.0	17.1	20.0	13.2
Probes	25697	54	205	55	220

ISO-BASAL (% probes)					
PHENOTYPE	ALL	TF	CHR	FETAL	HYP
TH	5.8	5.6	6.8	18.2	5.5
LV	6.2	7.4	7.3	23.6	6.4
RV	3.4	1.9	2.9	1.8	4.1
LA	3.5	5.6	1.5	9.1	5.5
RA	1.8	1.9	2.9	3.6	2.7
FS	2.9	1.9	2.9	5.5	3.2
EF	3.1	1.9	3.4	5.5	3.6
Probes	25697	54	205	55	220

B)

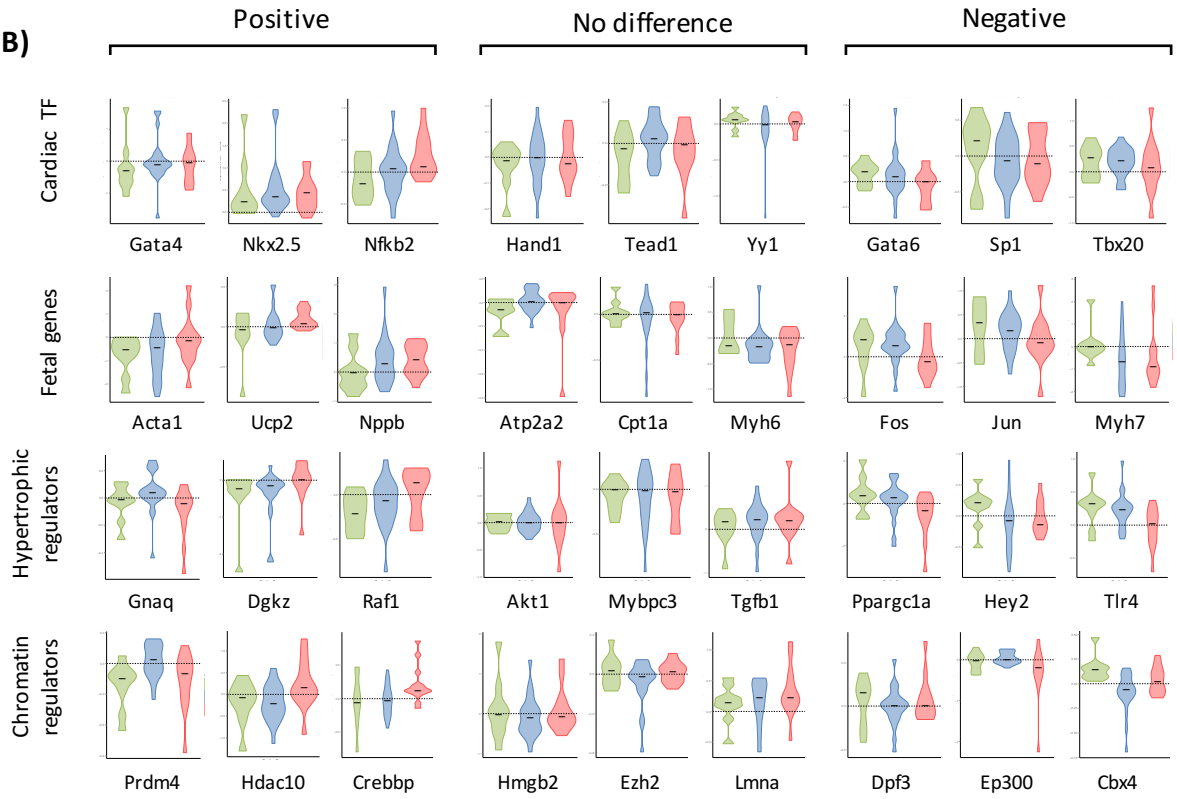

Figure 5-3: Gene groups, but not individual fetal genes, correlate with cardiac hypertrophy across diverse genetic backgrounds. A) mRNA abundance for individual probes on the microarray were compared to cardiac parameters across all 84 strains and plotted to identify genes whose expression, or change in expression, was significantly correlated with a trait in either basal or isoproterenol-treated hearts (Pearson correlation, $p<0.05$). Plotted are the distribution of p-values for individual probes. Tables show the percentage of probes within a subset of genes that demonstrate significance. Gene subsets that were enriched for probes that were correlated with phenotype were determined by normalizing to the level of correlation across all probes on the microarray. * or red indicates $p<0.05$ for enrichment of gene subset with respect to the entire array. **B)** The changes in expression after isoproterenol for individual cardiac transcription factors (TF) (n=31), fetal genes (n=37), hypertrophic regulators (n=142) and chromatin regulators (n=124) reveal no significant difference between resistant, hypertrophic or failing mice. Shown are examples of genes with nonsignificant positive and negative trends across these groups. Red indicates failing, green resistant and blue hypertrophic, strains. Horizontal lines represent change of 0.

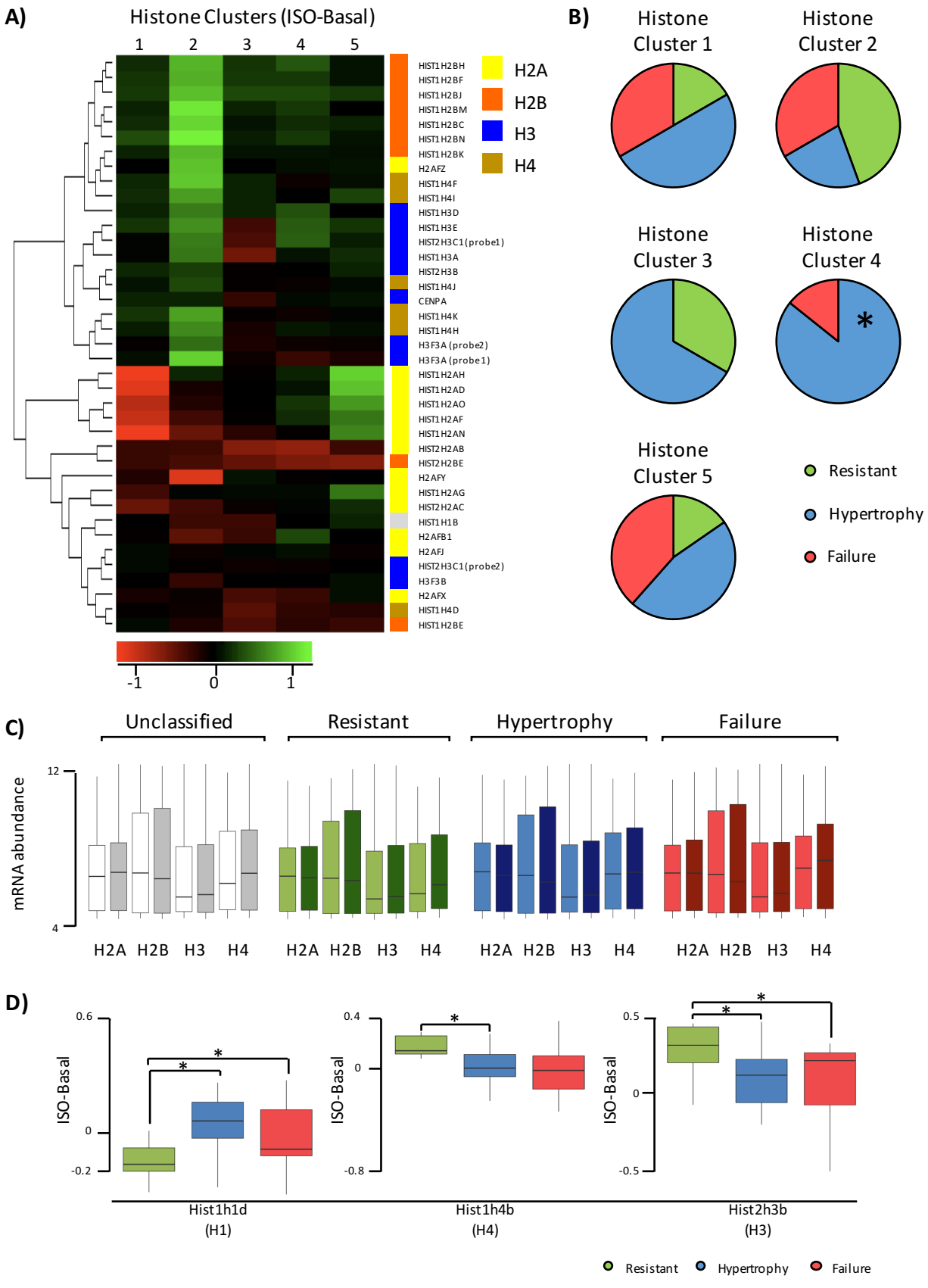
A)
Histone Clusters (ISO-Basal)
1
2
3
4
5
HIST1H2BH
HIST1H2BF
HIST1H2BJ
HIST1H2BM
HIST1H2BC
HIST1H2BN
HIST1H2BK
H2AFZ
HIST1H4F
HIST1H4I
HIST1H3D
HIST1H3E
HIST2H3C1(probe1)
HIST1H3A
HIST2H3B
HIST1H4J
CENPA
HIST1H4K
HIST1H4H
H3F3A (probe2)
H3F3A (probe1)
HIST1H2AH
HIST1H2AD
HIST1H2AO
HIST1H2AF
HIST1H2AN
HIST2H2AB
HIST2H2BE
H2AFY
HIST1H2AG
HIST2H2AC
HIST1H1B
H2AFB1
H2AFJ
HIST2H3C1(probe2)
H3F3B
H2AFX
HIST1H4D
HIST1H2BE
H2A
H2B
H3
H4
-1
0
1
B)
Histone Cluster 1
Histone Cluster 2
Histone Cluster 3
Histone Cluster 4
Histone Cluster 5
*
Resistant
Hypertrophy
Failure
C)
Unclassified
Resistant
Hypertrophy
Failure
mRNA abundance
12
4
H2A
H2B
H3
H4
D)
ISO-Basal
0.6
0
-0.2
0.4
-0.8
0.5
-0.5
*
Hist1h1d
(H1)
Hist1h4b
(H4)
Hist2h3b
(H3)
Resistant
Hypertrophy
Failure

Figure 5-4: Clustering mice by histone expression reveals patterns of change associated with phenotype. A) Hierarchical Ordered Partitioning And Collapsing Hybrid (HOPACH) clustered strains into 5 groups based on histone expression change with isoproterenol. Rows indicate individual histone variants while shading represents changes in expression. (n=12, cluster 1; n=9, cluster 2; n=3, cluster 3; n=7, cluster 4; n=13, cluster 5) **B)** For each histone cluster, the composition of phenotype group is shown. Cluster 4 is significantly enriched (enriched 2.57-fold, p=0.0068) for hypertrophic mice and depleted for resistant mice (p=0.0585, not significant). **C)** Abundance of all variants for each of the core histones was pooled across strains in the basal (light) or isoproterenol-treated (dark) hearts, revealing no gross differences between phenotypic groups. **D)** Three histone variants were differentially regulated by isoproterenol between phenotype groups (* indicates $p<0.05$).

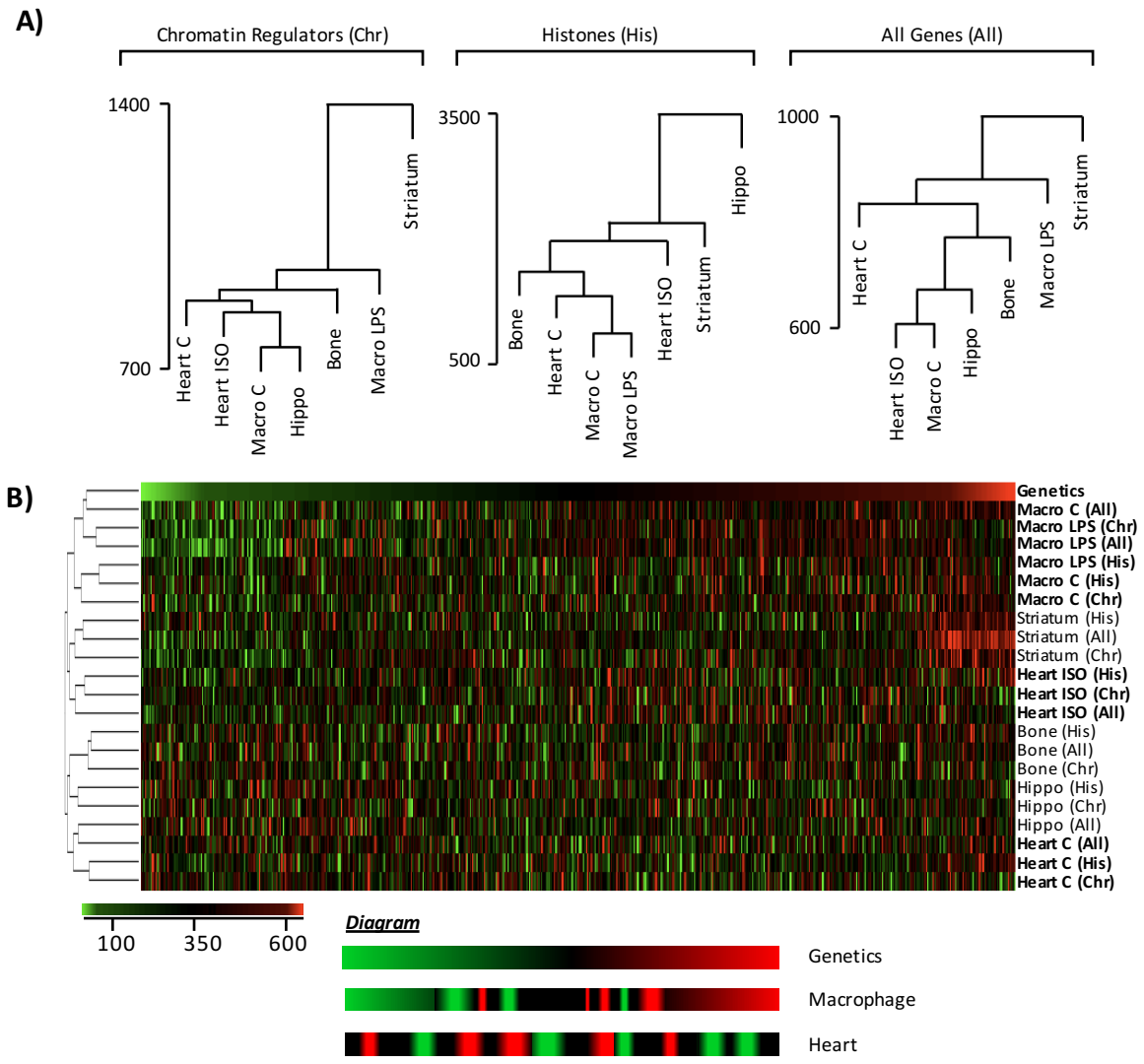

Figure 5-5: The role of genetics in chromatin gene expression is organ specific. A) We asked if two strains showing similar expression in one organ are also closely associated in another organ. We clustered 37 strains with microarray data in 5 tissues based on histone expression (middle). The relatedness in expression between each strain-by-strain comparison was compared across organs. Strains with similar histone expression in basal macrophages also show similar expression after LPS treatment (control and LPS-treated are neighbors); this is not the case for the heart before and after isoproterenol stimulation. This analysis was repeated using expression of chromatin regulators (left) or of all genes (right) to cluster strains. **B)** Heatmap x-axis represents each strain-by-strain comparison. Scale is the ranking of Euclidean distance in the organ and gene subset from 1 (green, most-closely related strain pair) to 667 (red, most-distant strain pair). "Genetics" indicates relatedness based on kinship matrix derived from single nucleotide polymorphisms. Diagram below represents observations from macrophage and heart expression datasets (in bold) with respect to genetic similarities between strains. As in the dendrograms, we see that LPS stimulus of macrophages does not disrupt co-expression relatedness between strains, but isoproterenol stimulation of the heart does. Similarly, macrophages exhibit the greatest overlap between expression relatedness and genetic relatedness.

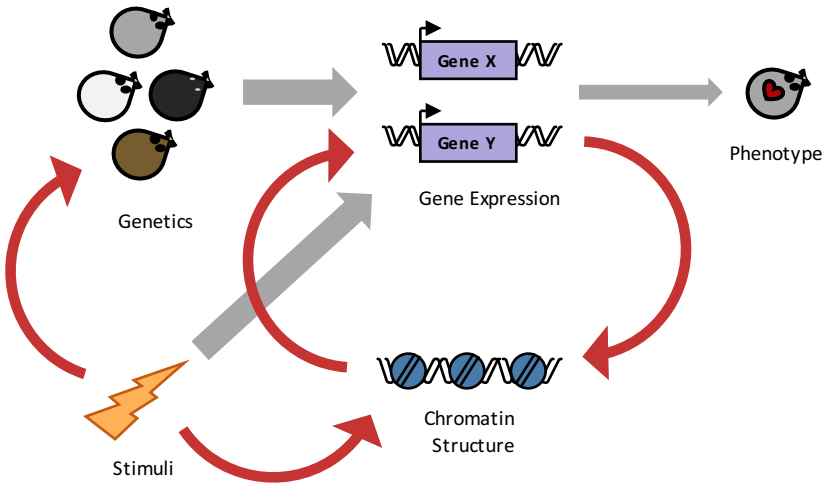

Figure 5-6: Chromatin proteins modulate the relationship between genetics and gene expression. The existing framework (gray arrows) for explaining cardiac phenotype is that genetics and environmental stimulation are the driving regulators of gene expression, which in turn determines phenotype. Our data supports this model, showing that cardiac gene expression does not correlate with phenotype across all genetic backgrounds due to contributions by chromatin regulatory inputs. Additionally, we build on this model (red arrows) showing that chromatin protein levels feed back to influence gene expression, based on our observation that gene expression "relatedness" is organ dependent. We further posit that there is a direct interaction between environmental stimuli and genetics, based on our observation that different genetic components are responsible for basal or isoproterenol-induced gene expression in the heart.

Table 5-1: List of genes analyzed for each gene subset

Cardiac TF	Chromatin Regulators				Fetal Genes		Hypertrophy Regulators				
Gata4	Aicda	Ezh1	Jmjd2b	Rnf40	Acadm	Slc2a4	Adrb1	Frap1	Map3k1	Pdpk1	Slc9a1
Gata5	Arid1a	Ezh2	Jmjd2c	Ruvbl1	Acta1	Slc8a1	Adrbk1	Gata4	Map3k7	Pik3ca	Smad1
Gata6	Arid2	Hat1	Jmjd2d	Ruvbl2	Acta2	Smad3	Agtr1a	Gata6	Mapk1	Plcb1	Smad2
Hand1	Arid3a	Hdac10	Jmjd3	Set	Actc1	Ucp2	Agtr1b	Gdf15	Mapk10	Pln	Smad3
Hand2	Arid3b	Hdac11	Jmjd4	Setd1a	Adss	Ucp3	Agtr2	Gna11	Mapk14	Ppara	Smad6
Irx4	Arid3c	Hdac2	Jmjd5	Setd1b	Ankrd1	Vdac1	Akt1	Gnaq	Mapk3	Pparg	Smad7
Isl1	Arid4a	Hdac3	Jmjd6	Setd2	Atp2a2		Atp2a2	Gsk3a	Mapk7	Ppargc1a	Smarca4
Mef2b	Arid4b	Hdac4	Kat5	Setd3	Ckm		Bnip3	Gsk3b	Mapk8	Ppargc1b	Sp1
Mef2c	Arid5a	Hdac5	Lmna	Setd4	Col1a2		Brd4	Hand1	Mapk9	Ppp2ca	Tbx20
Mef2d	Arid5b	Hdac6	Lmnb1	Setd5	Col3a1		Cacna1c	Hand2	Mb	Ppp3ca	Tead1
Mesp1	Bmi1	Hdac7	Lmnb2	Setd6	Cpt1a		Cacna1g	Hdac2	Mef2c	Ppp3cb	Tgfb1
Myocd	Brd4	Hdac8	Mecp2	Setd7	Cpt1b		Calm1	Hdac3	Mef2d	Ppp3cc	Tlr4
Nfat5	Carm1	Hdac9	Mst1	Setd8	Ctgf		Camk2d	Hdac4	Mmp2	Prkca	Tmod1
Nfatc1	Cbx2	Hmga1	Ncl	Setdb1	Fhl1		Camk2g	Hdac5	Mmp9	Prkcb	Tpm2
Nfatc2	Cbx3	Hmga2	Pbrm1	Setdb2	Fos		Camta2	Hdac6	Mov10l1	Prkcd	Trpc6
Nfatc3	Cbx4	Hmgb1	Prdm1	Sirt1	Gnas		Cdc42	Hdac9	Mtpn	Prkce	Vegfa
Nfatc4	Cbx5	Hmgb2	Prdm10	Sirt2	Gys1		Cib1	Hey2	Mybpc3	Prkcm	Yy1
Nfkb1	Cbx6	Hmgb2l1	Prdm14	Sirt6	Hspa8		Ckm	Hif1a	Myl2	Pten	Zfpm2
Nfkb2	Cbx7	Hmgb3	Prdm16	Sirt7	Jun		Crebbp	Hmga1	Myl4	Ptk2	
Nkx2-3	Cbx8	Hmgb4	Prdm4	Smarca4	Mlycd		Csrp3	Hopx	Myocd	Ptpn11	
Nkx2-5	Chd4	Hmgn1	Prdm5	Smarcd3	Myc		Ctf1	Il6	Myoz2	Rac1	
Nkx2-6	Crebbp	Hmgn2	Prdm6	Smc1a	Myh6		Ctgf	Il6ra	Nfatc2	Raf1	
Smad1	Ctcf	Hmgn3	Prdm9	Smc3	Myh7		Ctnnb1	Il6st	Nfatc3	Rasa1	
Smad6	Dnmt1	Jarid1b	Prmt2	Smyd1	Myl7		Ctsk	Irx4	Nfatc4	Rhoa	
Sp1	Dnmt3a	Jarid1c	Prmt3	Suv39h1	Ndufb10		Dgkz	Jmjd2a	Nfkb1	Rock1	
Srf	Dnmt3b	Jarid1d	Prmt5	Suv39h2	Nppa		Dscr1	Lif	Nfkb2	Rock2	
Tbx20	Dnmt3l	Jarid2	Prmt6	Suv420h1	Nppb		Ep300	Map2k1	Nkx2-5	Rps6kb1	
Tbx5	Dpf3	Jmjd1a	Prmt7	Suv420h2	Pdk2		Fgf16	Map2k3	Nppa	Ryr2	
Tead1	Ehmt1	Jmjd1b	Prmt8	Suz12	Pdk4		Fgf2	Map2k4	Parp1	S100a1	
Xbp1	Ehmt2	Jmjd1c	Rad1	Utx	Ppara		Foxo1	Map2k5	Paxip1	Sirt1	
Yy1	Ep300	Jmjd2a	Rnf20	Wiz	Slc2a1		Foxo3	Map2k6	Pde5a	Sirt3	

Table 5-2: P-values for enrichment of correlation of gene groups with cardiac parameters for basal, isoproterenol and change with isoproterenol state

	BASAL				ISO				ISO - BASAL			
Phenotype	Cardiac TF	Chr	Fetal	Hyp	Cardiac TF	Chr	Fetal	Hyp	Cardiac TF	Chr	Fetal	Hyp
Total Heart	0.51	0.41	0.44	0.31	0.47	0.32	0.0058	0.40	0.36	0.58	0.039	0.36
Left Ventricle	0.41	0.33	0.43	0.27	0.54	0.27	0.028	0.31	0.32	0.52	3.53E-04	0.28
Right Ventricle	0.53	0.09	0.28	0.020	0.60	0.06	0.017	0.16	0.48	0.43	0.32	0.06
Left Atrium	0.50	0.12	0.51	0.62	0.43	0.64	6.93E-04	0.32	0.19	0.65	0.042	0.07
Right Atrium	0.63	0.57	0.036	0.64	0.36	0.60	0.20	0.17	0.29	0.28	0.14	0.21
Lung	0.0069	0.46	0.63	0.28	0.66	0.45	0.0061	0.52	0.05	0.64	0.27	0.14
Liver	0.43	0.64	0.44	0.32	0.54	0.57	0.09	0.07	0.19	0.49	0.31	0.31
Adrel	0.38	0.60	0.63	0.35	0.43	0.26	0.57	0.51	0.59	0.51	0.59	0.64
Normalized TH	0.36	0.22	0.38	0.19	0.46	0.27	0.09	0.66	0.43	0.32	0.0048	0.50
Normalized LV	0.14	0.26	0.37	0.33	0.55	0.19	0.26	0.59	0.34	0.31	4.59E-04	0.44
Normalized RV	0.63	0.021	0.15	0.031	0.54	0.042	0.24	0.12	0.52	0.52	0.53	0.32
Normalized LA	0.53	0.59	0.63	0.61	0.50	0.55	0.0018	0.56	0.24	0.65	0.07	0.16
Normalized RA	0.11	0.57	0.41	0.20	0.36	0.60	0.21	0.45	0.35	0.19	0.19	0.22
Normalized Lung	0.65	0.61	0.61	0.63	0.13	0.61	0.050	0.37	0.0044	0.65	0.27	0.13
Normalized Liver	0.24	0.46	0.54	0.21	0.18	0.49	0.27	0.11	0.14	0.54	0.07	0.35
Normalized Adrel	0.48	0.63	0.48	0.63	0.32	0.13	0.66	0.57	0.47	0.65	0.61	0.65
Fibrosis (score)	0.55	0.61	0.55	0.39	0.61	0.61	0.0093	0.52	0.46	0.64	0.023	0.60
TG	0.37	0.41	0.61	0.53	0.61	0.63	0.28	0.66	0.66	0.60	0.26	0.62
Cholesterol	0.61	0.63	0.19	0.19	0.63	0.43	0.043	0.43	0.63	0.36	0.59	0.60
HDL	0.61	0.50	0.10	0.14	0.63	0.27	0.21	0.39	0.58	0.20	0.51	0.52
UC	0.55	0.52	2.04E-04	0.41	0.59	0.62	0.13	0.46	0.60	0.50	0.53	0.61
FFA	0.27	0.12	0.59	0.22	0.64	0.36	0.06	0.63	0.22	0.046	0.30	0.0042
Glucose	0.64	0.49	0.11	0.66	0.38	0.56	0.51	0.020	0.44	0.36	0.45	0.57
Fibrosis (area)	0.21	0.61	0.06	0.35	0.59	0.52	0.06	0.36	0.52	0.40	0.050	0.31
Heart Rate	0.27	0.63	0.18	0.49	0.54	0.64	0.31	0.43	0.37	0.22	0.24	0.20
IVSd	0.40	0.33	0.06	0.47	0.31	0.07	0.52	0.53	0.10	0.48	0.57	0.36
LVIDd	0.39	0.56	0.10	0.24	0.62	0.60	0.0022	0.36	0.55	0.66	0.09	0.55
PWd	0.66	0.13	0.06	0.29	0.54	0.21	0.44	0.0045	0.54	0.58	0.30	0.024
IVSs	0.61	0.0033	0.050	0.13	0.31	0.0045	0.56	0.030	0.52	0.62	0.52	0.39
LVIDs	0.36	0.61	0.16	0.31	0.56	0.34	0.016	0.26	0.62	0.36	0.20	0.32
PWs	0.65	0.60	0.40	0.62	0.58	0.0068	0.59	0.0026	0.18	0.20	0.41	0.0018
ET	0.65	0.29	0.52	0.61	0.55	0.67	0.17	0.32	0.35	0.30	0.49	0.35
E	0.63	0.29	0.59	0.52	0.39	0.65	0.20	0.31	0.27	0.12	0.27	0.27
A	0.59	0.040	0.05	0.13	0.45	0.022	0.53	0.11	0.15	0.46	0.45	0.62
E/A	0.39	0.0040	0.28	0.20	0.41	0.05	0.56	0.28	0.21	0.21	0.57	0.64
A/E	0.46	0.0014	0.28	0.10	0.61	0.27	0.56	0.56	0.13	0.64	0.22	0.44
FS	0.43	0.50	0.21	0.36	0.41	0.032	0.26	0.30	0.48	0.43	0.19	0.38
IVS/PWd	0.60	0.44	0.60	0.56	0.31	0.66	0.58	0.62	0.34	0.61	0.51	0.35
IVS/PWs	0.26	0.0017	0.15	0.0053	0.31	0.61	0.31	0.54	0.36	0.53	0.61	0.20
RWTd	0.24	0.32	0.19	0.16	0.42	0.19	0.43	0.12	0.64	0.65	0.44	0.23
PWTH	0.59	0.15	0.13	0.15	0.64	0.63	0.31	0.63	0.06	0.31	0.47	0.36
Vold	0.32	0.61	0.12	0.43	0.61	0.62	0.010	0.56	0.56	0.67	0.09	0.35
Vols	0.27	0.57	0.17	0.32	0.36	0.31	0.012	0.48	0.61	0.63	0.48	0.30
EF	0.52	0.60	0.11	0.36	0.39	0.07	0.11	0.35	0.50	0.37	0.21	0.33
LVM	0.57	0.39	0.19	0.26	0.65	0.32	0.0015	0.16	0.43	0.046	0.06	0.54
LVMc	0.57	0.39	0.19	0.26	0.65	0.32	0.0015	0.16	0.43	0.047	0.06	0.54
Vcf	0.23	0.60	0.35	0.22	0.32	0.0069	0.58	0.11	0.61	0.53	0.32	0.31
MNSER	0.31	0.51	0.46	0.21	0.36	0.027	0.60	0.24	0.62	0.60	0.34	0.43
Upreg Genes	0.47	0.30	0.31	0.16	0.19	0.31	0.66	0.41	0.19	0.16	0.27	0.010
Downreg Genes	0.61	0.21	0.29	0.12	0.20	0.012	0.46	5.30E-06	0.033	0.028	0.43	0.15

Subset of probes representing cardiac transcription factors (TF), chromatin regulators, fetal gene program and hypertrophic regulators were analyzed using Pearson correlation to determine significance with association to phenotype. Here, enrichment of these gene groups was compared with respect to all probes that had detectable expression on the microarray. Measured phenotypes include: mass of heart and indicated chambers and other tissues (these were, in addition, normalized to body weight); fibrosis, measured independently by visual scoring and area quantification; plasma triglycerides (TG), cholesterol, HDL cholesterol, unesterified cholesterol (UC), glucose, free fatty acids (FFA); echocardiogram parameters including heart rate, diastolic and systolic interventricular septal thickness (IVSd, IVSs), left ventricular internal diameter (LVIDd, LVIDs), posterior wall thickness (PWd, PWs), ejection time (ET), early and late ventricular filling velocities (E, A) and their ratios, fractional shortening (FS), diastolic relative wall thickness (RWTd), posterior wall thickening (PWTH), end diastolic and systolic end volume (Vold, Vols), ejection fraction (EF), left ventricular mass (LVM) and LVW corrected for growth (LVMc), mean velocity of circumferential fiber shortening (Vcf), and mean normalized systolic ejection rate (MNSER). Additionally, the numbers of up- and down regulated genes after isoproterenol treatment for each strain (Upreg and Downreg) were measured to determine whether overall changes in transcription are correlated to gene groups. Significant enrichment is indicated in red.

Table 5-3: Gene predictors of heart mass are not members of a single biological process

Illumina	Gene	Coefficient	Illumina	Gene	Coefficient
ILMN_2934549	BC055324	-6.79E-05	ILMN_2444594	Cdh3	-2.17E-05
ILMN_2816271	Dcpp2	6.22E-05	ILMN_2890915	EG331493	-2.15E-05
ILMN_2687716	4930433I11Rik	-5.99E-05	ILMN_2751822	Dsg1b	2.11E-05
ILMN_3072147	Foxo6	-5.77E-05	ILMN_2509644	Tpk1	2.10E-05
ILMN_2482494	Trim16	5.75E-05	ILMN_2795644	Tlr11	-2.06E-05
ILMN_2977849	Fank1	-4.57E-05	ILMN_1253791	Kcnv2	-2.05E-05
ILMN_1234692	1300007F04Rik	4.29E-05	ILMN_2719803	Stap1	1.82E-05
ILMN_2780323	Tkt	4.27E-05	ILMN_2859908	Olfr335	-1.79E-05
ILMN_2792089	Srebf1	-4.21E-05	ILMN_2686924	Epha1	1.78E-05
ILMN_1213351	Gsdma1	4.10E-05	ILMN_3162671	EG432555	-1.75E-05
ILMN_1238397	Olfr126	-4.01E-05	ILMN_2824954	OTTMUSG00000000421	-1.65E-05
ILMN_2742887	Scrib	3.89E-05	ILMN_2540726	Olfr670	-1.60E-05
ILMN_3072427	Il1rn	3.70E-05	ILMN_2703720	Bclaf1	1.55E-05
ILMN_2965612	Abca6	-3.55E-05	ILMN_2701712	Plcxd3	-1.48E-05
ILMN_1223335	Ano10	-3.52E-05	ILMN_1254646	Sox6	-1.48E-05
ILMN_2734661	Hagh	3.49E-05	ILMN_2806235	Gm813	1.44E-05
ILMN_1240675	Rbm12b	3.43E-05	ILMN_2911123	Itga2b	-1.40E-05
ILMN_1214602	Sfrp2	3.12E-05	ILMN_3062163	Rab11fip5	1.38E-05
ILMN_2642418	Mest	-3.10E-05	ILMN_2675623	Mrfap1	-1.32E-05
ILMN_1245040	9030617O03Rik	-3.02E-05	ILMN_1218034	Tmco4	1.31E-05
ILMN_2898062	Olfr108	2.96E-05	ILMN_1239583	Wins2	-1.29E-05
ILMN_1213265	2610208M17Rik	2.96E-05	ILMN_2863437	1110038F14Rik	-1.19E-05
ILMN_2833993	4921501E09Rik	-2.91E-05	ILMN_3048689	Rffl	-1.19E-05
ILMN_2779272	Olfr313	-2.86E-05	ILMN_2805051	Upk3a	1.18E-05
ILMN_2708142	Xkr6	2.82E-05	ILMN_2693946	Olfr1347	-9.91E-06
ILMN_2753867	Scgb3a2	2.76E-05	ILMN_2742311	Cyp39a1	-9.27E-06
ILMN_2670398	Eif4ebp1	2.70E-05	ILMN_1214065	Slco1a6	-8.32E-06
ILMN_2900653	Gadd45b	2.69E-05	ILMN_1223591	Zfp202	-7.79E-06
ILMN_2938373	Tas2r116	-2.68E-05	ILMN_2601758	Gsto2	-6.97E-06
ILMN_2682493	Bmp5	2.57E-05	ILMN_2678714	Id4	6.61E-06
ILMN_1259759	Olfr672	2.57E-05	ILMN_2657207	Hey2	-5.61E-06
ILMN_2527490	LOC381375	2.51E-05	ILMN_2661495	Tmem44	3.59E-06
ILMN_1242281	Txndc2	2.43E-05	ILMN_2726837	Nppb	3.50E-06
ILMN_1221960	Gtf2ird1	-2.38E-05	ILMN_2700468	Pcdhgc4	-3.37E-06
ILMN_2790241	Herpud1	-2.28E-05	ILMN_2705242	Wee2	2.22E-06
ILMN_2630521	Hist1h1a	-2.24E-05	ILMN_2863849	C1qtnf3	2.19E-06
ILMN_1223384	Nadsyn1	2.20E-05	ILMN_2596998	Lypd6b	1.67E-06

Linear regression analysis, using the glmnet package, was performed on change in expression with isoproterenol for all probes on the microarray to predict change in normalized total heart mass in 82 strains. We used 10-fold cross-validation to build each model, and a total of 1000 models were performed to identify 98 probes with predictive capacity in 800 of the 1000 models. The model incorporates 74 of these probes and fits the actual data for the 82 strains with an r-squared of 0.99. Coefficient indicates weight of the contribution in final model. GO analysis on these genes returned no significant enrichment for biological processes or cellular components.

Supplemental Table 5-1: Summary of studies of genes implicated as regulators of pathological hypertrophy by gain and/or loss of function

Gene	Model	Phenotype	PMID
Adrb1	OE	Increased contractility, development of myocyte hypertrophy followed by failure	10359838
Adrbk1	OE	Blocks ISO-induced enhanced contractility	7761854
	IN	Enhanced contractility in presence and absence of ISO; improved cardiac function in calsequestrin overexpression and MLP-/- models	7761854 9618528 11331748
Agtr1a	KO	Reduced AngII-mediated fibrosis	10330427
	AC	Sensitive to AngII infusion, develop fibrosis and impaired relaxation (no signs of hypertrophy)	17607364
Agtr1b	OE	Develop hypertrophy and fibrosis, upregulation of ANF expression (enhanced with AngII)	16276415
Agtr2	KO	Resistant to AngII-induced hypertrophy, fibrosis and impaired relaxation but still able to develop hypertrophy without impaired function in response to abdominal aortic constriction	11457756 10930448
Akt1	AC	Develop hypertrophy and increased wall thickness, reduced function	11909972
Atp2a2	KO	Development of heart failure	22824267
	OE	Enhanced contractility and relaxation	21278384 9851937
Bnip3	OE (In vitro)	Increase in cell size, upregulation of ANF and BNP	20852920
Brd4	IN	Blocks TAC-induced hypertrophy and wall thickening, fetal gene program activation and functional impairment	23939492 23911322
Cacna1c	OE	Develop hypertrophy and dilatation, enhanced contractility, upregulation of ANF expression	10419451
Cacna1g	KO	Blocks TAC- and AngII- induced cardiac hypertrophy but develop increased fibrosis and activation fetal gene program	19122177
	IN	Blocks TAC-and AngII-induced hypertrophy	19122177
Calm1	OE	Induces hypertrophy	8319584
Camk2d	KO	Protects against hypertrophy, fibrosis, cell death, upregulation of fetal genes (ANP, BNP, βMHC) and development of failure in response to TAC	19179290 19381018
	OE	Induces cardiac hypertrophy and dilation, reduced cardiac function and contractility, fibrosis, upregulation of ANF, βMHC, and α-skeletal actin, and downregulation of αMHC, Serca2a, PLB	11694533 12676814
	IN	Protects against impaired cardiac function and dilation after MI or ISO; block PE-induced ANF expression	9388275 15793582
	OE (In vitro)	Induces expression of ANF reporter	9388275
Camk2d Camk2g	Double KO	Develops TAC- and ISO-induced hypertrophy and fetal gene program activation but protected from TAC- and ISO-induced fibrosis and function impairments	25124496
Camta2	KO	Attenuated hypertrophy and suppress fetal gene program in response to TAC and ISO	16678093
	OE	Develop hypertrophy, upregulation of fetal genes (ANF, BNP, βMHC)	16678093
Cdc42	KO	Enhanced hypertrophy, decreased function, fibrosis and development of heart failure in response to TAC and AngII/PE	19741299
Cib1	KO	Reduced hypertrophy, fibrosis, functional impairment and upregulation of ANF after TAC	20639889
	OE	Enhanced hypertrophy in response to TAC and PE	20639889
Ckm	KO	Increase in LV mass	15639481
Crebbp	KD (In vitro)	Blocks PE-induced increase in cell size, protein synthesis and ANF expression	12477714
	OE (In vitro)	Increase in cell size and protein synthesis, upregulation of ANF	12477714
Csrp3	KO	Develop dilated cardiomyopathy and failure, increase in HW/BW, upregulation of ANF	9039266
Ctf1	--	Induces increase in cell size and upregulation of ANF with treatment in cardiomyocytes	8621626
Ctgf	OE	Develop hypertrophy, dilation and cardiac functional impairments in aged animals (without upregulation of ANF or BNP); upregulation of ANF and BNP but maintain function in response to AngII; blunted hypertrophy and upregulation of ANF, BNP and skeletal α-actin in response to TAC	19707545
Ctnnb1	HET	Reduced hypertrophy but enhanced upregulation of ANF, BNP and βMHC in response to TAC	17673255
Ctsk	KO	Reduced hypertrophy and wall thickening, impaired contraction and fibrosis, as well as blocked activation of fetal gene program after abdominal aortic constriction	23529168
	KD (In vitro)	Blocks PE-induced increase in cell size and protein synthesis	23529168
	OE (In vitro)	Upregulated Gata4 and protein synthesis, which can be blocked by rapamycin	23529168
Dgkz	OE	Resistant to AngII- and PE-mediated hypertrophy and upregulation of ANF	16380548
Dscr1	OE	Suppresses hypertrophy, development of dilated cardiomyopathy and activation of fetal genes as well as restores function in ISO and calcineurin transgenic models	11248078
Ep300	OE	Develop of hypertrophy and impaired function	18697823 12724418
	HET	Reduced extent of hypertrophy and upregulation of fetal genes induced by TAC	18697823
	DN (In vitro)	Prevents PE-induced increase in cell size	12724418 12477714
Fgf16	KO	Increased HW/BW and fibrosis; enhanced hypertrophy and fibrosis and upregulation of ANF, BNP and βMHC in response to AngII	23600527
Fgf2	KO	Blunts hypertrophy and fibrosis with ISO	21274419
	OE	Enhanced hypertrophy, fibrosis and functional impairment with ISO	21274419
FoxO1	OE (In vitro)	Blocks AngII-induced protein synthesis, increase in cell size and ANF upregulation	16952979
FoxO3	IA	Develops hypertrophy and upregulates MCIP1.4 expression	16952979
	OE (In vitro)	Blocks calcineurin phosphatase activity and decreases MCIP1.4 expression	16952979

Supplemental Table 5-1 *(continued)*

Gene	Model	Phenotype	PMID
Frap1	KO	Development of dilated cardiomyopathy and heart failure	20644257 21357822
	IA	Impaired cardiac function	18326485
Gata4	KO	Impaired function and development of dilation; blocks hypertrophy with enhanced functional impairment after TAC	20705924 16514068
	OE	Develop hypertrophy, fibrosis, reduced function, upregulation of ANF and BNP expression	11356841
	DN (In vitro)	Blocks increase in cell size and protein synthesis, blocks ANF expression and BNP reporter activation by PE	11356841
	OE (In vitro)	Activates BNP reporter (further enhanced with PE), increases in cell size and protein synthesis	11356841
Gata6	KO	Blocks hypertrophy and impaired function but upregulates ANF and skeletal α-actin in response to TAC and AngII/PE	20705924
	OE	Increase in HW/BW; enhanced hypertrophy after TAC	20705924
	OE (In vitro)	Activates BNP reporter (further enhanced with PE), increases in cell size and protein synthesis	11356841
Gdf15	OE	Resistant to TAC-induced hypertrophy and upregulation of ANF, skeletal α-actin and βMHC; adenoviral delivery blocks ventricular dilation and failure in MLP-/- model	16397142
	KO	Enhanced hypertrophy and functional impairment in response to TAC with same extent of upregulation of ANF, skeletal α-actin and βMHC as wild-type	16397142
	OE (In vitro)	Blunted PE/AngII- and NE-induced increase in cell area and protein synthesis	16397142 24554716
Gna11	KO	Blocks TAC-induced hypertrophy, wall thickening and functional impairment in Gαq-null model	11689889
Gnaq	OE	Develop hypertrophy, upregulation of ANF, skeletal α-actin and βMHC and impaired contractility	9223325 10403750
Gsk3a	OE	Reduced LV mass/BW and myocyte area; reduced hypertrophy, exacerbated functional impairment, increased fibrosis and cell death while having suppressed induction of ANF in response to TAC	17855351
	IA (Knock-in)	Exacerbated hypertrophy, functional impairment and increase in cell death due to TAC	19106302
	KD (In vitro)	Increase in cell size and protein synthesis, reduced apoptosis	17855351
Gsk3b	IA (Knock-in)	Blocks hypertrophy, cell death and change in ejection fraction in response to TAC	19106302
Hand1	IA	Develop hypertrophy and fibrosis, reduced contractility and function, upregulation of ANF, BNP and βMHC expression	21559426
Hand2	KO	Suppresses hypertrophy and fetal gene upregulation (ANF, BNP, skeletal α-actin and βMHC), preserves function and contractility after TAC	24161931
	OE	Develop dilatation, decrease in LV mass/BW, impaired contraction, upregulation of ANF, BNP and βMHC	24161931
	KD (In vitro)	Blocks calcineurin- and PE-induced increase in cell size	24161931
	OE (In vitro)	Increase in cell area, upregulation of ANF expression	24161931
Hdac2	KO or IN	Protects against ISO- and TAC-induced hypertrophy and activation of fetal gene program	17322895
	OE	Increased HW/BW, reactivation of fetal gene program	17322895
Hdac3	KO	Develop hypertrophy and impaired function, upregulation of fatty acid metabolic genes, upregulation of ANF, BNP, skeletal α-actin and p21	18830415
	OE	Increase in HW/BW after ISO (similar to wild-type)	18625706
Hdac4	KO	Upregulation of ANF expression though no effect on cardiac function	23434587
	IA (In vitro)	Blocks increase in protein synthesis induced by PE	16767219
Hdac5	KO	Develop hypertrophy and upregulate ANF, BNP and βMHC (enhanced with TAC and ISO)	15367668
Hdac6	KO or IN	Develop hypertrophy and fibrosis (similar to wild-type) but maintain cardiac function in response to AngII and TAC	24858848
Hdac9	KO	Increase in HW/BW (enhanced increase with TAC)	12202037
Hey2	KO	Enhanced increase in ventricular mass and decrease in ejection fraction after TAC	22408025
	OE	Increase in ventricular mass but had preserved function and minimal fibrosis after TAC; resistant to PE-induced hypertrophy and fetal gene program activation	20001863 16603706
Hif1a	KO	Enhanced hypertrophy, impaired function, fibrosis and apoptosis in response to TAC	22403061
	OE	Blocks cardiomyocyte hypertrophy and fibrosis induced by streptozotocin	20566749
Hmga1	KO	Develop hypertrophy, reduced function, upregulation of ANF and βMHC	16510570
Hopx	OE	Develop hypertrophy and fibrosis	18926829
Il6	--	Develop hypertrophy and fibrosis and upregulate IL6 and TNFα expression after infusion	20606113
Il6st	DN	Attenuates hypertrophy, increase in wall thickness and upregulation of BNP and downregulation of Serca2a expression after abdominal aortic constriction	11262406
Irx4	KO	Impaired cardiac function and increased wall thickening in aged animals	11238910
Jmjd2a	KO	Attenuates hypertrophy and upregulation of fetal genes in response to TAC	21555854
	OE	Enhanced development of hypertrophy and upregulation of fetal genes in response to TAC	21555854
Lif	--	Increase in cell size and protein synthesis, upregulation of c-fos and ANF expression in LIF-treated cardiomyocytes	8884986 12644003
Map2k1	AC	Develop hypertrophy and increased wall thickness, increased function and upregulation of ANF, BNP, skeletal α-actin and βMHC	11101507
	AC (In vitro)	Increase in cell size, upregulation of ANF expression	11101507
Map2k3	DN	Increase in HW/BW and dilation, impaired function, increase in fibrosis, upregulation of ANF and BNP (effects further enhanced with TAC, AngII, ISO and PE)	12750397
Map2k4	KO	Enhanced response to TAC-mediated hypertrophy, fibrosis, cell death and upregulation of ANF, BNP, RCAN1.4	19265040
Map2k5	AC	Develop ventricular dilation and decrease in myocyte area (no change in ventricular mass/TL), reduced cardiac function, activation of fetal genes	11387209
	DN (In vitro)	Blocks PE and LIF-mediated increase in cell size, upregulation of ANF, BNP, and skeletal α-actin	11387209
	AC (In vitro)	Enhanced upregulation ANF, BNP and skeletal α-actin in response to PE	11387209

Supplemental Table 5-1 *(continued)*

Gene	Model	Phenotype	PMID
Map2k6	OE or AC	Upregulation of ANF reporter (further enhanced with PE, LIF or ET1 treatment)	9584192
	DN	Increase in HW/BW, upregulation of ANF and BNP, impaired function (further enhanced TAC, AngII, ISO or PE)	12750397
Map3k1	KO	Develop failure and have enhanced increase in lung weight and cell death after TAC; blocks hypertrophy and functional impairments in transgenic-Gαq mice	11891332 12122119
Map3k7	AC	Increase in HW/BW and wall thickness, impaired function, fibrosis, upregulation of ANF and βMHC	10802712
Mapk1	KO	Blocks hypertrophy and upregulation of ANP, BNP, Col1a2, Col3a1, Cgtf but susceptible to failure after TAC or ISO	24631771
	IN	Develop heart failure, increased fibrosis and cell death after TAC	17709754
Mapk10	KO	Increase in HW/BW after TAC (similar to wild-type)	16579967
Mapk14	DN	Develop hypertrophy, dilation, impaired function, increase in fibrosis and upregulation of ANF and BNP (further enhanced with TAC, AngII, ISO and PE)	12750397 12639989
	OE (In vitro)	Upregulation of ANF reporter (further enhanced with PE, LIF, or ET1)	9584192
	IN (In vitro)	Blocks ET1- and LIF- induced increase in cell size	9584192
Mapk3	KO	Increase in HW/BW after TAC (similar to wild-type)	17709754
	IN	Develop heart failure, increased fibrosis and cell death after TAC	17709754
Mapk7	KO	Blunts hypertrophy and increase in wall thickness, fibrosis and fetal gene upregulation (ANF, skeletal α-actin, βMHC) while having increased apoptosis and worsening of function after TAC	20075332
	AC	Develop ventricular dilation and wall thinning, decrease in function, activation of fetal gene program	11387209
	KD (In vitro)	Blocks ISO-mediated upregulation of fetal genes and increased protein synthesis	20075332
Mapk8	KO	Develop hypertrophy (similar to wild-type) but have greater functional impairment, fibrosis and cell death after TAC	16579967
	OE (In vitro)	Negatively regulates ANF reporter expression in response to PE, LIF, or ET1 (expression of inactive form has reciprocal effects)	9584192
Mapk9	KO	Increase in HW/BW after TAC (similar to wild-type)	16579967
Mb	KO	Impaired contractility after ISO	20145201
Mef2c	KD	Blocks hypertrophy and wall thickness, collagen deposition and upregulation of ANF after TAC	20041152
	OE	Develop dilated cardiomyopathy, increase in ventricular mass/BW, decreased function, activation of fetal gene program	16469744
Mef2d	KO	Blunts hypertrophy, impaired function and activation of fetal gene program in response to TAC and ISO	18079970
	OE	Develop fibrosis, activate fetal gene program	18079970
Mmp2	KD or IN	Blocks AngII-induced hypertension though no effects on hypertrophy or fibrosis	21079048
Mmp9	KO	Blocks MI-induced LV dilatation and implicated to protect against volume overload impaired cardiac contractility	10880048 17552869
Mov10l1	OE (In vitro)	Suppressed hypertrophy and activation of fetal gene program induced by PE	11854500
Mtpn	OE	Develop hypertrophy, fibrosis, impaired function, upregulation of ANF, βMHC and proto-oncogenes	14970239
Mybpc3	KO	Increase in HW/BW, wall thickness and fibrosis, decrease in function, upregulation of ANF, BNP, βMHC and skeletal α-actin	11909824
Myocd	DN (In vitro)	Blocks PE-induced expression of fetal genes (ANF, BNP, βMHC, skeletal α-actin, SRF)	16556869
	OE (In vitro)	Increase in cell size, upregulation of ANF, BNP, βMHC, skeletal α-actin, SRF	16556869
Myoz2	OE	Reduced increase in hypertrophy, increase in contractility and upregulation of ANF, BNP and MCIP1 with AngII	18025526
	IA	No changes in structure or contractility but had reduced function, upregulated ANF, BNP, MCIP1.4; develop hypertrophy and further upregulation of ANF, BNP, MCIP1.4 after TAC	15543153
	OE (In vitro)	Blocks AngII-, PE-, ET1-mediated hypertrophy and upregulation of ANF and MCIP1.4	18025526
Nfatc2	IA	Blocks hypertrophy, fibrosis, functional impairment and upregulation of ANF, BNP and βMHC mediated by AngII, TAC, and calcineurin signaling	18477567
Nfatc3	IA	Blocks hypertrophy but does not rescue function or upregulate ANF, BNP and βMHC mediated by AngII, TAC, and calcineurin signaling	12370307
Nfatc4	AC	Develop hypertrophy and fibrosis	9568714
	IA	Increase in HW/TL after TAC or AngII infusion (no effect on hypertrophy development)	12370307
	DN (In vitro)	Blocks hypertrophy and upregulation of ANF expression induced by ET1, constitutively active calcineurin expression, or cardiotrophin-1	12226086
Nfkb1	KO	Increase in HW/BW and fibrosis, upregulation of BNP	22210479
Nkx2-5	DN	Decrease in function, increased fibrosis, no change in fetal gene expression or heart mass	11889119
Nppa	KO	Increase in LV mass and wall thickness in response to volume overload	14985074
Parp1	KO	Blunted hypertrophy, no fibrosis or upregulation of ANF, BNP, βMHC in response to TAC	15374823
	IN	Blocks hypertrophy, collagen production and decrease in contractile function induced by TAC	15523000
	IN	Preserves LV mass/BW and function, reduces fibrosis in spontaneously hypertensive rat model	19443425
	OE (In vitro)	Cell death	15374823
Pde5a	IN	Improves AngII-induced hypertrophy, functional impairments and cell death	23117837
	KD (In vitro)	Blocks PE-induced increase in protein synthesis	18790048
	OE (In vitro)	Enhances ANF expression induced by PE	18790048
Pdpk1	KO	Develop heart failure, thinning of ventricular walls	12970179
Pik3ca	DN	Decrease in HW/BW, wall thickness and chamber size but have increased ANF expression	10835352
	AC	Increase in HW/BW, wall thickness, chamber size, shift from αMHC to βMHC	10835352
Plcb1	OE (In vitro)	Increase in cell size and protein synthesis, upregulation of ANF	19564249
Pln	KO	Not responsive to ISO-mediated induction of contractility	9124439
	OE	Reduced contractility and function, which were reversed with ISO treatment	8567978

Supplemental Table 5-1 *(continued)*

Gene	Model	Phenotype	PMID
Ppara	KO	Develop fibrosis and impaired contractility observed at basal and after ISO	16461373
	OE	Develop ventricular hypertrophy, activation of fetal gene program, decreased function	11781357
Pparg	KO	Develop hypertrophy but maintain function, upregulation of ANF and βMHC	16051889
	OE	Development of dilated cardiomyopathy, increased expression of fatty acid oxidation genes	17823655
Ppargc1a	KO	Decrease in HW/BW and function, upregulation of ANF, βMHC, and skeletal α-actin with dobutamine treatment; reduced mitochondrial activity	15760270 18487436
	OE	Increase in heart size, development of dilated cardiomyopathy	11018072
	OE (In vitro)	Induced mitochondria biogenesis, impaired contractility	11018072
Ppargc1b	KO	No change in LV mass, function or structure; develop heart failure in Ppargc1a-/- background	18628400
Ppp2ca	DN	Develop dilated cardiomyopathy, increased HW/BW, impaired function, increase in βMHC expression	10993798
Ppp3ca Ppp3cb Ppp3cc	AC	Development of hypertrophy and wall thickening	9568714
	DN	Suppressed hypertrophy, fibrosis and fetal gene activation after TAC	11435345
	IN	Blocks hypertrophy, development of dilated cardiomyopathy and upregulation of fetal genes (ANF, skeletal α-actin, βMHC) due to TAC, AngII, ISO and genetic mouse models	9733519 11904392
	IN (In vitro)	Blocks AngII- and PE-induced increase in cell size and upregulation of ANF expression	9568714 10655507
Prkca	DN (In vitro)	Resistant to PMA-induced hypertrophy	15271671
	OE (In vitro)	Increase in cell size, protein synthesis and upregulation of ANF	11864993 15271671
Prkcb	KO	No change in phenotype and similar response as wild-type to TAC	11299230
	OE	Show impaired relaxation	9410895
Prkcd	DN (In vitro)	Blocks stretch-induced increase in cell size and protein synthesis	15316932
Prkce	DN (In vitro)	Does not block increase in cell size or protein synthesis mediated by ET1	11158975
	AC (In vitro)	Resistant to increase in cell size and protein content while upregulating ANF and βMHC expression	11158975
Prkcm	KO	Blunts response to hypertrophy, fibrosis, impaired function and fetal gene upregulation (ANF, BNP, βMHC) induced by TAC, AngII or ISO	18287012
	OE	Ventricular wall thinning and chamber dilation, decreased function, upregulation of ANF, BNP, skeletal α-actin and βMHC	16648482
	KD (In vitro)	Reduces increase in cell size and ANF secretion induced by PE	16648482
Pten	KO	Increase in LV mass/TL (further increased with AngII infusion); protects against hypertrophy, ventricular dilation, reduced function, fibrosis and upregulation of ANF and BNP in response to TAC	18281373
	DN (In vitro)	Increase in cell area and protein synthesis, upregulation of ANF	11448956
Ptk2	OE	Increase in LV mass/TL	22056317
	DN (In vitro)	Blocks increase in cell size and upregulation of ANF induced by ET1 or PE	10749882 10775151
Ptpn11	DN	Develop hypertrophy and wall thickening, fibrosis, impaired contractility	22058153
Rac1	KO	Reduces hypertrophy response and activation of fetal gene program due to AngII	16651530
	AC	Induces cardiac dilation and hypertrophy, activation of fetal gene program, enhanced contractility	10749567
	DN (In vitro)	Blocks PE-mediated increase in cell area	12672819
	AC (In vitro)	Increase in protein synthesis	12672819
Raf1	KO	Impaired cardiac function, dilatation and apoptosis	15467832
	DN	Poor survival, no development of hypertrophy, resistant to fetal gene program activation in response to TAC	15289381
Rasa1	AC	Induces hypertrophic signaling	19880762
	IN (In vitro)	Blocks NE-induced increase in cell size and protein synthesis	19880762
Rhoa	KO	Enhances dilation and ventricular wall thinning, increased chamber size and impaired contractility but reduced fibrosis in response to TAC	25336613
	OE	LV dilation, impaired LV contractility	10377168
Rock1	KD	Develop hypertrophy but with reduced fibrosis and apoptosis in response to TAC; blocks LV dilation and contractile impairments in Gαq-overexpression model	18178218 16675849
Rock2	KO	Blunted hypertrophy, fetal gene activation, fibrosis and apoptosis in response to AngII or TAC	23271052
Rps6kb1	IN	Suppresses increase in LV mass/BW induced by TAC	15367823
Ryr2	IA	Increase in HW/BW, upregulation of ANF expression (further enhanced with TAC)	23666671
	AC	Enhanced hypertrophy after TAC	20157052
S100a1	KO	Impaired contractility in response to ISO and TAC	11909974
	OE	Increased contractility which is further enhanced with ISO treatment	12777394
	AC	Reduces LV hypertrophy, preserves cardiac function and contractility induced by MI	16168714
Sirt1	HET	Resistant to hypertrophy in response to TAC	22055503
	OE (In vitro)	Prevents increase in cell area and repression of fatty acid oxidation genes in response to PE	21115502
Sirt3	KO	Develop LV thickening, decrease in fractional shortening	19652361
	OE	Resistant to increase in HW/BW, fibrosis, as well as upregulation of ANF and βMHC in response to AngII; resistant to LV thickening and functional impairments in response to ISO	19652361
	OE (In vitro)	Lessens protein synthesis in response to PE	19652361
Slc9a1	IN	Resistant to LV hypertrophy and functional impairments after coronary artery occlusion	25216745
	AC	Develop hypertrophy and fibrosis, impaired fibrosis, upregulation of ANF (hypertrophy and ANF upregulation enhanced with PE)	21359875 20460605
	IN (In vitro)	Resistant to increase in cell area and induction of ANF in response to PE	25216745

Supplemental Table 5-1 ***(continued)***

Gene	Model	Phenotype	PMID
Smad1	OE	Protects against I/R-mediated apoptosis	15911698
	IN (In vitro)	Blocks GDF15-mediated increase in protein synthesis and hypertrophy	20232299
Smad2	IN	Blunts hypertrophy, impaired function, increase in lung weight and downregulation of Serca2a in response to TAC	22049534
	OE (In vitro)	Blocks increase in cell size induced by AngII and PE	16397142
Smad3	KO	Enhances hypertrophy and LV thickness but reduces fibrosis after TAC	19919989
Smad6	IA	Develop endocardium thickening and vascular ossification that compromises function	10655064
	OE (In vitro)	Reverses GDF15-mediated suppression of cell size increase	16397142
Smad7	KO	Enhances response to AngII including impaired function and increase in LV mass, fibrosis	23894614
Smarca4	KO	Blunts hypertrophy and development of fibrosis, upregulates αMHC and downregulates βMHC after TAC	20596014
Sp1	OE (In vitro)	Enhances upregulation of ANF after PE treatment	20874724
Tbx20	HET	Develop dilated cardiomyopathy, decreased wall thickness and impaired function	15843414
Tead1	OE	Decrease in function, increase in βMHC expression	20194497
Tgfb1	KO	Resistant to AngII-induced hypertrophy	11901187
	OE	Develop severe hypertrophy, fibrosis, upregulation of ANF	12181157
Tlr4	KO	Block development of hypertrophy in response to TAC	15967420
Tmod1	OE	Develop dilated cardiomyopathy, increase in HW/BW, impaired function, increase in ANF and βMHC expression	9421465
Tpm2	OE	No effects on histology, structure, or function but show impaired relaxation	8530495
Trpc6	OE	Increase in HW/BW and impaired function in response to TAC	17099778
Vegfa	KO	Thinning of septal and LV walls (dilated hearts), impaired function	11331753
Yy1	KD (In vitro)	Increase in cell size, activation of fetal gene program	18632988
	OE (In vitro)	Blocks cellular hypertrophy and reactivation of fetal genes	18632988
Zfpm2	KO	Develop heart failure (dilation and impaired function), fibrosis, upregulation of ANF and BNP	19411759

Genes that have been implicated as part of hypertrophic signaling pathways have been summarized in mouse studies or other model systems as indicated. Family members of these genes and other suggested genes not tested in gain or loss of function in the heart were also included in HMDP analyses (see Table 2 for complete list of genes). This list represents the genes in the “hypertrophic regulators” subset. OE, overexpression; KO, knockout; DN, dominant negative mutant; AC, active mutant; IN, inhibition; KD, knockdown; HET, heterozygous; IA, inactive mutant; ISO, isoproterenol; PE, phenylephrine; AngII, angiotensin II; ET1, endothelin 1; NE, norepinephrine; TAC, transverse aortic constriction; MI, myocardial infarction; LV, left ventricle; HW, heart weight; BW, body weight; TL, tibia length.

Chapter 5: References

1. Ghazalpour A, Rau CD, Farber CR, Bennett BJ, Orozco LD, van Nas A, Pan C, Allayee H, Beaven SW, Civelek M, Davis RC, Drake TA, Friedman RA, Furlotte N, Hui ST, Jentsch JD, Kostem E, Kang HM, Kang EY, Joo JW, Korshunov VA, Laughlin RE, Martin LJ, Ohmen JD, Parks BW, Pellegrini M, Reue K, Smith DJ, Tetradis S, Wang J, Wang Y, Weiss JN, Kirchgessner T, Gargalovic PS, Eskin E, Lusis AJ, LeBoeuf RC. Hybrid mouse diversity panel: a panel of inbred mouse strains suitable for analysis of complex genetic traits. Mamm Genome. 2012;23(9-10):680-92. doi: 10.1007/s00335-012-9411-5. PubMed PMID: 22892838; PMCID: PMC3586763.
2. Rau CD, Wisniewski N, Orozco LD, Bennett B, Weiss J, Lusis AJ. Maximal information component analysis: a novel non-linear network analysis method. Front Genet. 2013;4:28. doi: 10.3389/fgene.2013.00028. PubMed PMID: 23487572; PMCID: PMC3594742.
3. Rajabi M, Kassiotis C, Razeghi P, Taegtmeyer H. Return to the fetal gene program protects the stressed heart: a strong hypothesis. Heart Fail Rev. 2007;12(3-4):331-43. doi: 10.1007/s10741-007-9034-1. PubMed PMID: 17516164.
4. van Berlo JH, Maillet M, Molkentin JD. Signaling effectors underlying pathologic growth and remodeling of the heart. J Clin Invest. 2013;123(1):37-45. doi: 10.1172/JCI62839. PubMed PMID: 23281408; PMCID: PMC3533272.
5. Dorn GW, 2nd. Genetics of common forms of heart failure. Curr Opin Cardiol. 2011;26(3):204-8. doi: 10.1097/HCO.0b013e328345d336. PubMed PMID: 21464711.
6. Monte E, Vondriska TM. Epigenomes: the missing heritability in human cardiovascular disease? Proteomics Clin Appl. 2014;8(7-8):480-7. doi: 10.1002/prca.201400031. PubMed PMID: 24957631; PMCID: PMC4267468.
7. Rau CD, Wang J, Avetisyan R, Romay MC, Martin L, Ren S, Wang Y, Lusis AJ. Mapping genetic contributions to cardiac pathology induced by Beta-adrenergic stimulation in mice.

Circ Cardiovasc Genet. 2015;8(1):40-9. doi: 10.1161/CIRCGENETICS.113.000732. PubMed PMID: 25480693; PMCID: PMC4334708.

8. Orozco LD, Bennett BJ, Farber CR, Ghazalpour A, Pan C, Che N, Wen PZ, Qi HX, Mutukulu A, Siemers N, Neuhaus I, Yordanova R, Gargalovic P, Pellegrini M, Kirchgessner T, Lusis AJ. Unraveling Inflammatory Responses using Systems Genetics and Gene-Environment Interactions in Macrophages. Cell. 2012;151(3):658-70. doi: 10.1016/j.cell.2012.08.043. PubMed PMID: WOS:000310529300020.
9. Farber CR, Bennett BJ, Orozco L, Zou W, Lira A, Kostem E, Kang HM, Furlotte N, Berberyan A, Ghazalpour A, Suwanwela J, Drake TA, Eskin E, Wang QT, Teitelbaum SL, Lusis AJ. Mouse Genome-Wide Association and Systems Genetics Identify Asxl2 As a Regulator of Bone Mineral Density and Osteoclastogenesis. Plos Genetics. 2011;7(4). doi: ARTN e1002038 10.1371/journal.pgen.1002038. PubMed PMID: WOS:000289977000032.
10. Park CC, Gale GD, de Jong S, Ghazalpour A, Bennett BJ, Farber CR, Langfelder P, Lin A, Khan AH, Eskin E, Horvath S, Lusis AJ, Ophoff RA, Smith DJ. Gene networks associated with conditional fear in mice identified using a systems genetics approach. Bmc Syst Biol. 2011;5. doi: Artn 43 10.1186/1752-0509-5-43. PubMed PMID: WOS:000291876500002.
11. Strimmer K. fdrtool: a versatile R package for estimating local and tail area-based false discovery rates. Bioinformatics. 2008;24(12):1461-2. doi: 10.1093/bioinformatics/btn209. PubMed PMID: WOS:000256756800008.
12. Strimmer K. A unified approach to false discovery rate estimation. Bmc Bioinformatics. 2008;9. doi: Artn 303 10.1186/1471-2105-9-303. PubMed PMID: WOS:000257832700001.
13. van der Laan MJ, Pollard KS. A new algorithm for hybrid hierarchical clustering with visualization and the bootstrap. J Stat Plan Infer. 2003;117(2):275-303. PubMed PMID: WOS:000185490400008.
14. Friedman J, Hastie T, Tibshirani R. Regularization Paths for Generalized Linear Models via Coordinate Descent. J Stat Softw. 2010;33(1):1-22. PubMed PMID: WOS:000275203200001.

15. Boyle EI, Weng SA, Gollub J, Jin H, Botstein D, Cherry JM, Sherlock G. GO::TermFinder - open source software for accessing Gene Ontology information and finding significantly enriched Gene Ontology terms associated with a list of genes. Bioinformatics. 2004;20(18):3710-5. doi: 10.1093/bioinformatics/bth456. PubMed PMID: WOS:000225786600064.
16. Huang DW, Sherman BT, Lempicki RA. Bioinformatics enrichment tools: paths toward the comprehensive functional analysis of large gene lists. Nucleic Acids Research. 2009;37(1):1-13. doi: 10.1093/nar/gkn923. PubMed PMID: WOS:000262335700001.
17. Huang DW, Sherman BT, Lempicki RA. Systematic and integrative analysis of large gene lists using DAVID bioinformatics resources. Nat Protoc. 2009;4(1):44-57. doi: 10.1038/nprot.2008.211. PubMed PMID: WOS:000265781800006.
18. Kang HM, Zaitlen NA, Wade CM, Kirby A, Heckerman D, Daly MJ, Eskin E. Efficient control of population structure in model organism association mapping. Genetics. 2008;178(3):1709-23. doi: 10.1534/genetics.107.080101. PubMed PMID: WOS:000254921600050.
19. Lynch M, Ritland K. Estimation of pairwise relatedness with molecular markers. Genetics. 1999;152(4):1753-66. PubMed PMID: WOS:000081889600046.
20. Rau CD, Wang J, Avetisyan R, Romay MC, Martin L, Ren SX, Wang YB, Lusis AJ. Mapping Genetic Contributions to Cardiac Pathology Induced by Beta-Adrenergic Stimulation in Mice. Circ-Cardiovasc Gene. 2015;8(1):40-9. doi: 10.1161/Circgenetics.113.000732. PubMed PMID: WOS:000349873200007.
21. Wang JJC, Rau C, Avetisyan R, Ren SX, Romay MC, Stolin G, Gong KW, Wang YB, Lusis AJ. Genetic Dissection of Cardiac Remodeling in an Isoproterenol-Induced Heart Failure Mouse Model. Plos Genetics. 2016;12(7). doi: ARTN e1006038 10.1371/journal.pgen.1006038. PubMed PMID: WOS:000381050100002.

22. Razeghi P, Young ME, Alcorn JL, Moravec CS, Frazier OH, Taegtmeyer H. Metabolic gene expression in fetal and failing human heart. Circulation. 2001;104(24):2923-31. doi: DOI 10.1161/hc4901.100526. PubMed PMID: WOS:000172701300027.
23. Taegtmeyer H, Sen S, Vela D. Return to the fetal gene program A suggested metabolic link to gene expression in the heart. Ann Ny Acad Sci. 2010;1188:191-8. doi: 10.1111/j.1749-6632.2009.05100.x. PubMed PMID: WOS:000277731600025.
24. Franklin S, Chen HD, Mitchell-Jordan S, Ren SX, Wang YB, Vondriska TM. Quantitative Analysis of the Chromatin Proteome in Disease Reveals Remodeling Principles and Identifies High Mobility Group Protein B2 as a Regulator of Hypertrophic Growth. Molecular & Cellular Proteomics. 2012;11(6). doi: ARTN M111.014258 10.1074/mcp.M111.014258. PubMed PMID: WOS:000306408500019.
25. Chen IY, Lypowy J, Pain J, Sayed D, Grinberg S, Alcendor RR, Sadoshima J, Abdellatif M. Histone H2A.z is essential for cardiac myocyte hypertrophy but opposed by silent information regulator 2 alpha. Journal of Biological Chemistry. 2006;281(28):19369-77. doi: 10.1074/jbc.M601443200. PubMed PMID: WOS:000238847000052.
26. Barnabei MS, Palpant NJ, Metzger JM. Influence of genetic background on ex vivo and in vivo cardiac function in several commonly used inbred mouse strains. Physiol Genomics. 2010;42A(2):103-13. doi: 10.1152/physiolgenomics.00071.2010. PubMed PMID: 20627938; PMCID: PMC2957793.
27. Waters SB, Diak DM, Zuckermann M, Goldspink PH, Leoni L, Roman BB. Genetic background influences adaptation to cardiac hypertrophy and Ca2+ handling gene expression. Front Physiol. 2013;4. doi: ARTN 11 10.3389/fphys.2013.00011. PubMed PMID: WOS:000346774000011.
28. Auerbach SS, Thomas R, Shah R, Xu H, Vallant MK, Nyska A, Dunnick JK. Comparative Phenotypic Assessment of Cardiac Pathology, Physiology, and Gene Expression in C3H/HeJ,

C57BL/6J, and B6C3F1/J Mice. Toxicol Pathol. 2010;38(6):923-42. doi: 10.1177/0192623310382864. PubMed PMID: WOS:000286315700006.

29. Kiper C, Grimes B, Van Zant G, Satin J. Mouse Strain Determines Cardiac Growth Potential. Plos One. 2013;8(8). doi: ARTN e70512 10.1371/journal.pone.0070512. PubMed PMID: WOS:000324465000079.
30. Chen HD, Orozco LD, Wang J, Rau CD, Rubbi L, Ren SX, Wang YB, Pellegrini M, Lusis AJ, Vondriska TM. DNA Methylation Indicates Susceptibility to Isoproterenol-Induced Cardiac Pathology and Is Associated With Chromatin States. Circulation Research. 2016;118(5):786-97. doi: 10.1161/Circresaha.115.305298. PubMed PMID: WOS:000371747700007.
31. Camargo A, Azuaje F. Linking Gene Expression and Functional Network Data in Human Heart Failure. Plos One. 2007;2(12). doi: ARTN e1347 10.1371/journal.pone.0001347. PubMed PMID: WOS:000207459600029.
32. Li JJ, Biggin MD. Statistics requantitates the central dogma. Science. 2015;347(6226):1066-7. PubMed PMID: WOS:000350354200018.
33. Zaphiriou A, Robb S, Murray-Thomas T, Mendez G, Fox K, McDonagh T, Hardman SMC, Dargie HJ, Cowie MR. The diagnostic accuracy of plasma BNP and NTproBNP in patients referred from primary care with suspected heart failure: Results of the UK natriuretic peptide study. European Journal of Heart Failure. 2005;7(4):537-41. doi: 10.1016/j.ejheart.2005.01.022. PubMed PMID: WOS:000229723900016.
34. Yang J, Manolio TA, Pasquale LR, Boerwinkle E, Caporaso N, Cunningham JM, de Andrade M, Feenstra B, Feingold E, Hayes MG, Hill WG, Landi MT, Alonso A, Lettre G, Lin P, Ling H, Lowe W, Mathias RA, Melbye M, Pugh E, Cornelis MC, Weir BS, Goddard ME, Visscher PM. Genome partitioning of genetic variation for complex traits using common SNPs. Nature Genetics. 2011;43(6):519-U44. doi: 10.1038/ng.823. PubMed PMID: WOS:000291017000007.

35. McNamara DM, London B. GWAS Applied to Heart Failure Bigger Will Be Better ... Eventually. Circ-Cardiovasc Gene. 2010;3(3):226-8. doi: 10.1161/Circgenetics.110.957324. PubMed PMID: WOS:000278799900002.
36. Manolio TA, Collins FS, Cox NJ, Goldstein DB, Hindorff LA, Hunter DJ, McCarthy MI, Ramos EM, Cardon LR, Chakravarti A, Cho JH, Guttmacher AE, Kong A, Kruglyak L, Mardis E, Rotimi CN, Slatkin M, Valle D, Whittemore AS, Boehnke M, Clark AG, Eichler EE, Gibson G, Haines JL, Mackay TFC, McCarroll SA, Visscher PM. Finding the missing heritability of complex diseases. Nature. 2009;461(7265):747-53. doi: 10.1038/nature08494. PubMed PMID: WOS:000270547500027.
37. Weiss JN, Karma A, MacLellan WR, Deng M, Rau CD, Rees CM, Wang J, Wisniewski N, Eskin E, Horvath S, Qu ZL, Wang YB, Lusis AJ. "Good Enough Solutions" and the Genetics of Complex Diseases. Circulation Research. 2012;111(4):493-504. doi: 10.1161/Circresaha.112.269084. PubMed PMID: WOS:000307308700015.
38. Bahrarni H, Kronmal R, Bluemke DA, Olson J, Shea S, Liu K, Burke GL, Lima JAC. Differences in the Incidence of Congestive Heart Failure by Ethnicity - The Multi-Ethnic Study of Atherosclerosis. Arch Intern Med. 2008;168(19):2138-45. doi: DOI 10.1001/archinte.168.19.2138. PubMed PMID: WOS:000260332400012.
39. Jones DW, Hall JE. Racial and ethnic differences in blood pressure - Biology and sociology. Circulation. 2006;114(25):2757-9. doi: 10.1161/Circulationaha.106.668731. PubMed PMID: WOS:000243522300004.

Chapter 6: Endogenous Structural Reorganization of Cardiac Chromatin Mediates Transcriptional Changes in Response to Hypertrophic Stress

Elaheh Karbassi, Manuel Rosa Garrido, Douglas J. Chapski, Yong Wu, Enrico Stefani, Yibin Wang, Emma Monte, Thomas M. Vondriska

Abstract

Pathological stress in the heart has been shown to result in increases in transcriptional activity and induce gene expression changes. Genomic organization is an important determinant of gene expression, and regulation of DNA accessibility can mediate whether transcriptional machinery can be recruited to loci for expression. While on the nucleosomal scale, factors regulating gene expression have been characterized, the structural arrangements at the nuclear level have not been explored in the heart. We hypothesize that structural rearrangements of chromatin mediate the pathological changes in gene expression observed with disease. We evaluated global transcriptional activity using a run-on assay and show an increase in transcriptional activity (total and RNA polymerase-specific) in hypertrophic cardiomyocytes and further provide evidence that activity is compartmentalized into transcription factories. Using super-resolution imaging, we analyzed the nuclear organization of RNA polymerase II transcription factories in both neonatal rat ventricular cardiomyocytes and adult heart sections. The spatial organization of these factories is not affected with pressure-overload stress although the data suggests that RNA polymerase II molecules are recruited to factories to meet the transcriptional demands of the stressed cardiomyocyte. Furthermore, we examine the regulation of subsets of cardiac genes and demonstrate that nuclear positioning with respect to chromatin environment is associated with expression. Atp2a2 downregulation corresponds with a shift towards silent nuclear territories while Nppa activation has reduced presence at the nuclear envelope. This study is the first to show direct evidence of genomic reorganization in the heart and characterize the tissue-specific genomic structural features.

Introduction

The genome is intricately packaged in the nucleus of the cell to regulate transcriptional activity in a cell-specific manner. Levels of packaging, which can be categorized into heterochromatin or euchromatin, can determine the accessibility and recruitment of protein factors and transcriptional machinery to regulate given loci. This accessibility is regulated by epigenetic factors, including histone and DNA modifications and noncoding RNAs (1), and by non-nucleosomal chromatin structural proteins that facilitate high order packaging (2, 3). In the failing heart, there is a shift from heterochromatin to euchromatin, indicated by changes in global abundances of histone marks (2), which corresponds to increases in transcriptional activity (4).

There have been a range of studies examining cell lineage-specific features of chromatin architecture, through DNA accessibility and 3D genomic interactions (5-7), yet these studies lack spatial information with respect to nuclear structure. It is known that the nucleus is arranged into structural and functional compartments (8, 9). Structurally, the genome itself is specifically organized into chromosome territories (10, 11) and on the sub-chromosomal scale into topologically associating domains (12). Transcription factories are functional nuclear subcompartments that are enriched with active RNA polymerases (13). These units allow for efficient organization and execution of polymerase activity. The nucleolus is a well-established example of a nuclear compartment that houses transcription factories for RNA polymerase I (14). RNA polymerase II factories have been demonstrated with live cell imaging using fluorescence loss in photobleaching (FLIP) and/or fluorescence recovery after photobleaching (FRAP) experiments, demonstrating that RNA polymerase molecules are not freely diffusing, but supporting that there is a subset of the population of RNA polymerases that are engaged (15). Labeling of nascent RNA shows that transcription occurs at distinct puncta that have increasing intensity with time (16, 17). Furthermore, these factories are functional; genes have been shown to translocate to transcription factories, marked by RNA polymerase upon activation (18). On the

other hand, a more recent study contradicts the existence of factories by demonstrating that RNA polymerases do not cluster and exist as single molecules using super-resolution imaging and quantitative analyses (19). These studies have used overexpression approaches in cultured cells to track RNA polymerases irrespective of activity, and the establishment of transcription factories *in vivo* has yet to be determined.

3D DNA fluorescence *in situ* hybridization has served as a powerful tool to uncover features of global gene regulation on a single-cell basis and to demonstrate that gene positioning with respect to nuclear anatomy is an additional contributor of gene regulation. Imaging approaches have utilized reporter genes to complement DamID analyses, which have mapped genomic interactions with the nuclear lamina (20), and demonstrated gene silencing occurs at the nuclear envelope, with anchoring mechanisms mediated by histone methylation and deacetylation (21-23). In the cardiomyocyte, overexpression of histone deacetylase, HDAC4, has been shown to decrease the expression of a subset of genes, which were also linked to their displacement from the nuclear pores (24); these provide support for the importance of 3D physical arrangements in mediating regulation of gene expression in the heart.

Our lab has previously shown that there is global structural reorganization of nucleosomes, from imaging of histone proteins, in the hypertrophic cardiomyocyte (25). How this structural change influences gene expression is unknown. We hypothesize that the coordination of gene expression changes that occur with the development of heart failure are mediated by structural reorganization of transcription factory/gene interactions. Here, we will examine features of endogenous transcription factories and cardiac-specific genes to learn more about how the cardiomyocyte nucleus maintains transcriptional function. We characterize the structural properties of the nuclei of cardiomyocytes, a post-mitotic cell-type, to understand features unique to cell type, focusing on cardiac transcription factories and gene positioning to better understand how these affect and

correlate with transcriptome changes measured in the failing heart. Our results provide support for the compartmentalization of gene expression into transcription factories and demonstrate that gene expression is a function of genomic architecture.

Materials and Methods

Animal Models

Adult male C57/Bl6 mice (8weeks of age, Jackson Lab) were subjected to transverse aortic constriction hypertrophy (TAC) surgery to induce heart failure. Analysis was performed on animals in the heart failure state (~6weeks post surgery), as indicated by cardiac dimensions and functional parameters measured by echocardiography. Whole hearts and corresponding liver tissue from the same mice were fixed with formalin and paraffin-embedded to be used for imaging. For a subset of samples, isolated cardiomyocytes and homogenized brain and liver tissues were used for gene expression analyses.

Cell Culture

Neonatal rat ventricular myocytes (NRVMs) were isolated using enzymatic digestion, collected and plated with DMEM supplemented with 17% M199, 1x Penicillin-Streptomycin-Glutamine (Gibco 10778016), 10% Horse Serum (Gibco 26050070) and 5% Newborn Calf Serum (Gibco 26010066). After 24hr, media was switched to serum-free (1% Penicillin/Streptomycin [Gibco 15140122] and 1:1000 ITS [BD 354351] in DMEM). The next day cells were treated with 10μM phenylephrine for 48hr to induce hypertrophy. For NRVM imaging, cells were plated on coverslips coated with laminin (10μg/ml in PBS, Sigma L2020).

Adult Mouse Cardiomyocyte Isolation

Adult mouse cardiomyocytes were isolated using a Langendorff system. Mice were injected with heparin to block blood clotting and then anesthetized with pentobarbital, after which hearts were excised and cannulated. Hearts were perfused with Tyrode's calcium-free solution (13mM NaCl, 0.54mM KCl, 0.06mM NaH_2PO_4, 0.1mM $MgCl_2$, 1mM HEPES, 10mM glucose, pH 7.37) for 5min, digested with 0.1mg/ml Protease (Sigma P5147)/0.7mg/ml Collagenase, Type 2 (Worthington LS004177) prepared in Tyrode's solution for 20-30min, then washed with KB solution (25mM KCl, 10mM KH_2PO_4, 2mM $MgSO_4$, 5mM HEPES, 20mM glucose, 20mM taurine, 5mM creatine, 100mM glutamic acid-potassium salt, 10mM aspartic acid, 0.5mM EGTA, pH 7.18). Atria were removed, and ventricular myocytes were gently released into solution. Cells were spun at 1500rpm for 5min and washed with PBS. Cell pellets were distributed for subsequent RNA, protein and ChIP analyses.

Cell and Nuclear Size Analyses

For cell/nuclear size measurements, NRVMs were fixed with formalin (10min, Sigma HT501128) and then washed with PBS (3x5min) and 0.1% Triton X-100/PBS (5min). Cells were then stained with 1:40 Phalloidin (Molecular Probes A12379)/1:500 DAPI (Molecular Probes D3571)/PBS for 30min at room temperature, washed with PBS (3x5min) and mounted using Prolong Gold (Molecular Probes P36934). Area measurements were performed using FIJI/ImageJ and statistical analyses were performed using Mann-Whitney test. For correlations, statistical significance was determined using Pearson correlation coefficient.

Transcriptional Run-on Assay

Transcriptional run-on assay with 5'fluorouridine (5'FU, Sigma F5130) was performed to label nascent RNA (26). NRVMs were treated in culture with 4mM 5'FU for the indicated times after which, the cells were rinsed with 1xHEPEM (65mM PIPES, 30mM HEPES, 2mM $MgCl_2$-$6H_2O$, 10mM EGTA, pH 6.9). Cells were fixed and permeabilized (3.7% formaldehyde/1xHEPEM /0.5%

Triton X-100) for 15min, underwent a series of washes (1xHEPEM, 2x5min; PBS, 5min; 0.05% Tween20/PBS, 5min), then incubated with primary BrdU (1:50 in PBS, Sigma B8434) overnight at 4C. The cells were then washed with PBS (2x5min) and 0.05% Tween20/PBS (5min), incubated with secondary antibody/DAPI/PBS (1:100) for 1 hour at room temperature, washed with PBS (3x5min) and mounted with Prolong Gold.

To examine RNA polymerase II/III activity, NRVMs were supplemented with 2μM CX-5461 (Selleckchem S2684), an RNA polymerase I inhibitor (27), for 15min prior to the addition of 5'FU. The addition of 4mM 5'FU also included CX-5461. To differentiate nucleolar versus nucleoplasmic transcription, cells were colabeled with nucleolin to mark the nucleolus. 5'FU intensity analyses were carried out using FIJI/ImageJ software. Mann-Whitney tests were used for statistical analyses for comparing control and hypertrophic cardiomyocytes.

RNA and protein preparation

Isolated cardiomyocytes were resuspended in either Trizol (Ambion 15596018) for RNA or lysis buffer (50mM Tris pH 7.4/10mM EDTA/1% SDS/0.1mM PMSF/0.2mM sodium orthovanadate/0.1mM sodium fluoride/10mM sodium butyrate/protease inhibitor cocktail tablets [Roche]). RNA was isolated using chloroform extraction, and preparation of cDNA was carried out using iScript cDNA Synthesis kit (Biorad 1725201), followed by quantitative PCR. For protein, lysates were sonicated and then spun at maximum speed to remove cellular debris. Protein concentration of supernatant was quantitated using a BCA assay (Thermo Scientific 23225), and samples were diluted in Laemmli buffer for westerns.

Generation of DNA FISH probes

For labeling of genes, we generated DNA FISH probes as previously published, using hdfish.nl (28). Gene coordinates (mm10 mouse genome) were used to obtain a list of PCR primers to be

used to generate DNA products of ~200bp that will span the region of interest. For shorter genes, coordinates were expanded to upstream and downstream, such that the probe covered at least 20kb. The following genomic sites were targeted: Nppa, gene Chr4:148,000,745-148,002,067, primers Chr4:147,997,910-148,021,634 (64 primer sets); Atp2a2, gene Chr5:122,453,512-122,502,225, primers Chr5:122,453,757-122,499,765 (51 primer sets); Gapdh, gene Chr6:125,161,851-125,165,773, primers Chr6:125,148,520-125,176,210 (60 primer sets); Nefl, gene Chr14:68,083,883-68,087,737, primers Chr14:68,069,935-68,102,872 (62 primer sets). After semi-quantitative PCR, products of primers that successfully produced specific amplicons of ~200bp were pooled, fluorescently labeled with AlexaFluor 647 using Ulysis Nucleic Acid Labeling Kit (Molecular Probes U21660) and underwent column purification to remove excess label (Biorad 732-6223). Labeled probes were reconstituted at 1ng/μl in hybridization buffer (1.7xSSC [saline sodium citrate buffer], 70% formamide, 50mM phosphate buffer [Na_2HPO_4/NaH_2PO_4], 10% dextran sulfate, 5x Denhardt's solution, pH 7.5) for cells or 2ng/μl for tissue (probes for tissue also included 20ng/μl mouse cot-1 DNA [Invitrogen 18440-016] and 8ng/μl salmon sperm DNA [Ambion AM9680]).

3D-DNA Fluorescence In Situ Hybridization (DNA FISH): Cells

DNA FISH experiments in cultured cells (mouse embryonic fibroblasts and mouse neonatal cardiomyocytes) were carried out as described (29). Cells were fixed with 4% formaldehyde (10min, room temperature, with the addition of 0.5% Triton X-100/PBS at 9 minutes) and then washed with 0.05% Triton X-100/PBS (3x5min). Permeabilization was performed with 0.5% Triton X-100 (10min) and incubation with 20% glycerol/PBS (60min), followed by repeated freeze/thaw of coverslips with liquid nitrogen (total of 6 times). Coverslips were washed (0.05% Triton X-100/PBS, 3x5min) and then rinsed with 0.1N HCl, followed by incubation with 0.1N HCl (10min). Cells were washed again with 0.05% Triton X-100/PBS (3x5min), equilibrated with 2xSSC (5min)

and then incubated with 50% formamide/2xSSC for 30min. Immunostaining, if applicable, was performed after the Triton X-100 permeabilization step and prior to incubation with 20% glycerol/PBS. Coverslips were then transferred to a small drop of fluorescent probe, sealed with rubber cement and allowed to hybridize for at least 48hr at 37C in a humid chamber. Cells were then washed with the following: 2xSSC (3x10min, 37C), 0.1xSSC (2x5min, 60C), rinsed with 2xSSC and equilibrated with PBS (5min). After post-fixation with 2% formaldehyde (10min), samples were counterstained with DAPI/PBS (1:100, 5min), washed with PBS (5min) and mounted with Prolong Gold. Chromosome 5 labeling was performed according to manufacturer's instructions (Cytocell AMP5G).

3D-DNA Fluorescence In Situ Hybridization: Tissue

Formalin-fixed, paraffin-embedded tissue sections were deparaffinized and rehydrated with serial washes: xylene (2x5min), 100% ethanol (3x3min), 95% (2x3min), 70% (3min), dH_2O (5min), PBS (2x5min). Samples were heated in Pretreatment Reagent (Cytocell LPS100) for 20min using a vegetable steamer, allowed to cool (20min) and washed with 2xSSC (2x5min). Tissue was denatured with 60% formamide/2xSSC (70C, 2min on heat block). Concurrently, FISH probes were denatured (75C, 7min) and incubated at 37C for at least 1hr to pre-anneal. After pre-annealing, probes were added to tissue, sealed with rubber cement and allowed to hybridize at 37C (at least 24hr).

For FISH labeling only, tissues were washed with 50% formamide/2xSSC (42C, 2min) and 2xSSC (4x2min) and then counterstained with DAPI and WGA (Molecular Probes W849, 1:100 in PBS, 10min), washed with PBS (2x5min) and mounted. For FISH and immunostaining, steps were as follows: 50% formamide/2xSSC (42C, 2min), 2xSSC (4x2min), PBS (3x5min), block with 5% BSA/PBS (1hr) and incubation with primary antibodies (1:100 in 2.5% BSA/0.1% Triton X-100/PBS) overnight at 4C. The next day, samples were washed with PBS (3x5min), incubated

with secondary antibodies (1:100 antibody, DAPI, WGA in 2.5% BSA/0.1% Triton X-100/PBS) for 1hr at room temperature, washed with PBS (2x5min) and mounted with Prolong Gold.

Chromatin Immunoprecipitation

For chromatin immunoprecipitation (ChIP) experiments, isolated adult mouse cardiomyocytes were fixed with 1% formaldehyde (10min) and quenched with 125mM glycine (10min). Cells were then lysed using a dounce homogenizer and sonicated using both probe and bath sonication to obtain DNA fragments averaging ~500bp. Sonicates from 6 animals were pooled, and ChIP was performed using the ChIP-IT High Sensitivity kit (Active Motif 53040), with 30μg chromatin for each IP reaction and input. Quantitation was determined by quantitative PCR by first normalizing to input and then determining fold enrichment from IgG.

Immunolabeling (Tissue)

Formalin-fixed paraffin embedded tissues were deparaffinized (xylene 2x5min; 100% ethanol 3x3min; 95% 2x3min; 70% 3min; dH_2O 5min; PBS 2x5min), underwent heat-mediated antigen retrieval in 10mM sodium citrate/0.05% Tween20 buffer (30min, vegetable steamer), then allowed to cool to room temperature. For immunofluorescence, samples were washed with PBS (3x5min), blocked with 5% BSA/PBS for at least 1hr and then incubated with primary antibody (prepared with 2.5% BSA; 1:100 dilution) overnight. Tissue was then washed with 0.05% Tween20/PBS (3x5min), incubated with secondary antibody (1:100 in PBS) for 1hr, washed with PBS (3x5min) and mounted using Prolong Gold.

Microscopy

Confocal imaging was carried out using a Nikon A1R system using 60x objective (100x was used for DNA FISH images). For DNA FISH imaging, we acquired single stacks. Nuclei from tissue were assessed by scanning across the z axis and and selecting the plane giving the strongest

FISH signal. For transcription factory imaging, we used a 2-color in-house built stimulated emission depletion (STED) microscope. Samples were labeled with Atto647N (Active Motif) and Oregon Green 488 (Life Technologies) fluorophore-conjugated secondary antibodies and imaged using a 100x objective. We used 635nm excitation and 750nm depletion lasers for Atto647 visualization and 485nm excitation and 592nm depletion lasers for Oregon Green 488 labels.

Image Analysis

For transcription factory distance and intensity quantitations, images were processed by the following: application of a Gaussian filter, subtracting background noise and removing objects less than 50nm (based on microscope resolution). Imaris software (Bitplane) was then used to designate clusters and measure closest distances of center of the clusters with respect to each other as well as with the nuclear periphery using distance transformation. To determine the nuclear distribution of transcription factories for each nucleus, the minimum and maximum cluster distances to the nuclear periphery were used to determine the total range. This range was divided by 5 to generate bins, and clusters were then assigned their corresponding bin based on their distance to the periphery for analyses.

For DNA FISH analyses, we carried out quantitation of nuclear gene positioning as described (30) to segment nuclei into 5 equal concentric areas and determine localization with respect to the nuclear periphery. For distance quantifications, Imaris software was used to create surfaces to demarcate the nucleus or heterochromatin (determined based on DAPI intensity). The closest distance from the center of the FISH signal to the nuclear periphery (inside of surface) or distance to heterochromatin (outside of surface) was calculated.

For statistical analyses of mean intensities or distances, a Mann-Whitney test was used to determine significance while a Chi-squared test was used to assess comparisons of distributions between control and treated groups.

Antibodies

ANF (Abcam ab91250); BrdU (Sigma B8434): Desmin (Sigma D1033); Gapdh (Millipore MAB374); IgG (Santa Cruz sc2027); Lamin A/C (Abcam ab8984); Nucleolin (Abcam ab22758); RNA polymerase II (Active Motif 102660); RNA polymerase II Ser2P (Abcam ab5095); RNA polymerase II Ser5P (Abcam ab5131); Serca2 (Abcam ab2861); secondary AlexaFluor antibodies (Life Technologies)

Results

Increased transcriptional activity in hypertrophic cardiomyocytes

Our goal is to characterize properties of cardiac chromatin architecture and identify the features that may impact function. From a global standpoint, we asked whether there were any changes to nuclear structure with cardiac hypertrophy. Phenylephrine-treated NRVMs were stained to obtain cell and nuclear area measurements (Figure 6-1A). Hypertrophic cardiomyocytes showed both significant increases in cell and nuclear sizes by 60% and 8% respectively (Figure 6-1B). To determine whether there was a proportional increase, we find that the ratio of nuclear to cell areas decreases, suggesting that the growth of the cell occurs to a greater extent that nuclear growth. We show that there is no difference in nuclear shape, indicated by the circularity. These results hold consistent when cells are subsetted based on nuclei number (Figure 6-1C). In control cells, the nuclear area versus cell area relationships between mononucleated and binucleated cells are significant and hold consistent, with slopes of 8.22 ($r=0.655$, $p<0.001$) and 7.321 ($r=0.506$, $p=0.023$) while with phenylephrine this changes to 11.20 ($r=0.563$, $p<0.001$) and 4.691 ($r=0.233$, $p=0.272$) (Figure 6-1D). While the relationship between cell and nuclear area is maintained but

different between control and phenylephrine-treated mononucleated cells (significant correlations but different slopes), it is lost in binucleated cells with phenylephrine treatment. We can compare these changes to perturbations in global chromatin structure in mouse embryonic fibroblasts to better decipher potential epigenetics contributors, histone acetylation and DNA methylation, that affect nuclear size though in opposite manners (Figure 6-2). Treatment with sodium butyrate, an HDAC inhibitor, reduces nuclear area while inhibiting DNA methylation with 5-aza-CdR increases nuclear area.

To decipher structural features of the cardiac genome, we approached this by mapping transcriptionally active regions. We used 5'fluorouridine (5'FU), a uracil analogue, to selectively label nascent RNA (26), and with immunofluorescence, we can then detect sites of incorporation, or active transcription (Figures 6-3, 6-4, 6-5). We examined 5'FU incorporation in NRVMs in control and hypertrophy (induced by phenylephrine). Based on 5'FU intensity, hypertrophic cardiomyocytes have increased total RNA production (by all 3 RNA polymerases; 16% increase) as well as RNA polymerase I-mediated transcription found in the nucleolus (23% increase), the site of ribosomal RNA synthesis (marked by nucleolin labeling) (Figure 6-6A). To examine nucleoplasmic transcription, we blocked RNA polymerase I activity with CX-5461 (27) and find total transcription and that mediated by RNA polymerases II and III also is increased in hypertrophic cells (Figures 6-6B,C). Though not significant, we found a 23% increase in nucleoplasmic 5'FU intensity. These results confirm previous studies demonstrating increases in transcriptional activity with cardiac hypertrophy in myocytes (4, 31, 32) and complement them by providing an anatomical dissection of this process. Furthermore, due to the punctate nature of the labeling patterns, this data provides support for the organization of transcription factories in cardiomyocytes.

Mapping and characterization of cardiac transcription factories in hypertrophy

RNA polymerase II transcription factories have been characterized with imaging of tagged RNA polymerase II molecules, monitoring polymerase dynamics of exogenous molecules *in vitro* using FLIP/FRAP tools (33). While polymerase molecules are mobile, there are a subset that are engaged and active (33). Furthermore, RNA synthesis occurs in a punctate manner in cells (34, 35), consistent with what we observe (Figure 6-6A,B). We wanted to compare the patterns of RNA labeling with that of RNA polymerase II protein to assess organization and activity of RNA polymerase II transcription in hypertrophic cardiomyocytes. Due to the abundance of RNA polymerases and the reported sizes of transcription factories in the nucleus (<200nm, below the resolution of conventional confocal) (13), we used super-resolution STED imaging to obtain a high resolution map of endogenous active, elongating RNA polymerase II molecules (marked by serine 2 phosphorylation) and nascent RNA transcripts (marked by 5'FU) in neonatal rat ventricular myocytes in control and hypertrophic states (Figure 6-7A,B). Analysis of polymerase clusters reveals no change in the number of clusters when normalizing the absolute number of clusters detected (~1000 clusters in control and ~1400 in hypertrophic cells) to nuclear area (Figure 6-7C). Furthermore, the mean intensity of clusters does not change (Figure 6-7C), nor do the intensity ranges (minimum and maximum intensities) differ although a modest increase is suggested (Figure 6-7D).

While features of individual RNA polymerase II clusters do not appear to change with hypertrophic stress, we asked whether there is a structural reorganization of factories across the nucleus. The distance between individual polymerase II clusters did not change, with average distance of ~140nm between clusters (Figure 6-8A), nor does the distance with respect to the nuclear periphery (Figure 6-8B). While there is an increase in absolute distance from the periphery (1625nm to 2036nm), this effect is minimized due to the enlargement of nuclear area with phenylephrine treatment (Figure 6-7C). An alternative approach to characterizing RNA polymerase II with respect to nuclear anatomy was to generate bins based on the possible range

of absolute distance to the periphery (maximum and minimum distance difference) and characterize the transcription factories for each bin; this approach also allowed us to normalize for nuclear size (Figure 6-8C). The distribution of clusters in each bin did not differ, nor did the mean intensity of clusters with phenylephrine (Figure 6-8D). Interestingly, we do observe more clusters found at the peripheral bins. This can be explained by the presence of the nucleolus that occupies the center of the nucleus. Also, the bins were generated based on distance, and we have disregarded their areas. Analysis of the top most intense clusters also shows that there is an increase in distance from the nuclear periphery with phenylephrine (Figure 6-8E,F); the very intense clusters accumulate more centrally.

5'FU analyses in these nuclei show an increase in absolute number of nascent RNA puncta and reduced cluster intensity (Figure 6-9A,B). Because RNA needs to be transported out of the nucleus, one possible explanation for the reduced intensity may relate to the diffusion of the molecules. Consistent with the RNA polymerase II measurements, the distances between closest neighboring clusters does not change (Figure 6-9C) and the distance to the nuclear periphery increases (Figure 6-9D). Again this agrees with the RNA polymerase results (Figure 6-8B), which suggest that active polymerase molecules shift towards more central nuclear positions. Because of the increases in transcription with hypertrophy (Figure 6-6), we hypothesized that active RNA polymerases would have increased association with 5'FU molecules, but we find no difference in the distance of closest 5'FU to RNA polymerase II cluster (Figure 6-9E). We also found no association when comparing RNA polymerase II and 5'FU signals using a Pearson correlation ($r=0.206$ in control and $r=0.199$ with phenylephrine treatment, $p=0.697$). The absence of change we observe in RNA polymerase distribution in NRVMs suggests that transcription factories are fixed compartments.

Reorganization of cardiac transcription factories in the failing heart

To characterize cardiac transcriptional activity *in vivo*, we performed *in situ* labeling of nascent RNA in heart tissue to obtain a direct readout of transcriptional activity (Figure 6-10). We injected mice with 5'FU to allow for systemic incorporation, collected and fixed tissue and then used immunofluorescence to visualize nascent RNA production. We found signal in nuclei, some binucleated cells showed successful labeling in both nuclei while some had one nucleus transcriptional active and the other silent (Figure 6-10A). However, we also found signal in the nuclei of our negative controls, which were not injected with 5'FU (Figure 6-10B). Due to false positives, we opted to mark transcription factories with active RNA polymerase II.

We subjected C57/Bl6 mice to transverse aortic constriction surgery to induce pressure-overload mediated heart failure (Figure 6-11) and then performed labeling of RNA polymerase II in tissue sections (Figure 6-12). In NRVMs, there is a 30% increase in the activated form of RNA polymerase II (marked by serine 5 phosphorylation) and 53% increase in elongating RNA polymerase II (serine 2 phosphorylation) (Figure 6-12A), suggesting enhanced polymerase activation. Unlike the NRVM analyses, the nuclear area in the population of adult cardiomyocytes used for analysis did not differ, nor did nucleoplasmic area (Figure 6-12D). Nucleoplasmic area was defined by regions positive of RNA polymerase II signal (Figure 6-12C). Because the cardiomyocyte nucleus contains a large heterochromatic chromocenter (see Figure 1-1) and nucleolus that would lack RNA polymerase II, these regions would affect the transcription factory counts, so nucleoplasmic area was also used. In the failing heart, there was no difference observed in cluster number (absolute and when normalized to area) (Figure 6-13A). However, there is an increase in cluster size (by 12%) and mean intensity (40% increase), and this increase in intensity is reflected across the nucleus (Figure 6-13A-C). We also measure a subtle but significant increase in distance between RNA polymerase II neighbors from 123.5nm to 125.8nm (Figure 6-13D). We do not however notice any changes in distance to the nuclear periphery, and the distribution of clusters is not altered with pressure-overload stress (Figure 6-13E). When

subsetting the cluster populations into the top and bottom 20% based on intensity (Figure 6-14), we show a global increase in mean cluster intensity (up by 50%) that occurs uniformly across the nucleus (Figure 6-14A-C). The spacing between closest neighboring clusters increases (115nm to 119nm) when focusing on the most intense clusters (Figure 6-14D). While the overall distribution of clusters is unaffected, this suggests the breakdown of a subpopulation of transcription factories to redistribute to more transcriptionally demanding sites, possibly containing stress-activated genes. On the other hand, the least intense clusters are not affected (Figure 6-14E). This data supports the engaged nature of RNA polymerase molecules and suggests that with pathological stress, RNA polymerase II molecules are recruited to factories to enhance transcriptional responses. Future analyses identifying the genetic components of transcription factories will better dissect these structural arrangements.

Correlation of gene expression with nuclear positioning

We next wanted to better understand how this reorganization of cardiac transcription factories affects pathological gene expression. We selected genes to represent four different categories of responses to stress (upregulated, downregulated, remain active and remain silent): well-established genes, Nppa and Atp2a2, known to be differentially expressed in heart failure models (36); Gapdh, a housekeeping gene, that remains active after stress; and Nefl, a neuronal-specific intermediate filament gene that is silent in the heart (37). The expression patterns of these genes were confirmed at the level of RNA and protein (Figure 6-15).

Based on prior studies examining gene expression with respect to the nuclear envelope and demonstrating gene silencing occurs at the nuclear lamina (20, 38), we wanted to test the relevance of these models in the cardiomyocyte. We generated high definition DNA FISH probes (28) to target the four genes (using the mouse genome) and confirmed the specificity of labeling (Figures 6-16, 6-17). In early experiments using mouse fibroblasts, we colabeled gene loci with

other nuclear markers, including nuclear lamins as well as sites of active transcription (Figure 6-18). Because of our limitations to working with isolated cells in our transcriptional run-on assays and development of mouse-specific FISH probes, we pursued analyses in isolated mouse neonatal cardiomyocytes to address whether gene positioning is affected with hypertrophic stress (Figure 6-19). We successfully isolated and labeled Atp2a2 in neonatal mouse myocytes treated with different hypertrophic agonists, isoproterenol and phenylephrine, and found no change in the distribution of genes after agonist treatment (Figure 6-19C). Though there was no change in nuclear positioning of these loci, we began to test localization with respect to transcriptionally active regions with 5'FU (Figure 6-19E). We later learned that it was previously reported that neonatal mouse and neonatal rat ventricular myocytes behave differently (39). Unlike NRVMs that can be used to model cardiac hypertrophy, neonatal mouse myocytes are still developing and shown to be unresponsive to hypertrophic agonists and were not an appropriate model.

Alternatively, we switched over to use our mouse FISH probes in the adult animal, a more suitable model of disease, to assess gene positioning *in vivo* (Figures 6-20, 6-21). Adult mice were subjected to TAC surgery to induce heart failure (Figure 6-11). Gene positioning was assessed in the heart tissue sections collected (Figure 6-21). For quantitative analyses of gene positioning with respect to the nuclear membrane, DAPI labeling was used to mark the nucleus and then segment the nucleus into 5 annuli of equal areas (Figure 6-21A) (30). This approach provides a given locus an equal probability of falling within each bin. Further, it serves as a method to normalize for nuclear size and shape. Mature cardiomyocyte nuclei tend to be ellipsoid shape, therefore we could not use radial distances for normalization. Additionally, because we were using tissue sections in these studies, nuclear orientation varied in different parts of the tissue (Figure 6-12B). In the heart, Atp2a2, Nppa and Gapdh tended to preferentially localize in the center of the nucleus (Figure 6-22A,B,C). On the other hand, Nefl loci were evenly distributed across nuclear area (Figures 6-22D). After TAC surgery, Atp2a2 (downregulated in failure) had a

significantly different distribution from its sham counterpart, with increased association at the nuclear periphery (0% to 4% in bin 1) and decreased association with the center (46.5% to 35.7% in bin 5) (Figure 6-22A). Activation of Nppa was not reflected in changes in overall locus distribution, although there was reduced associated with the periphery (5.8% to 1.7%). Also, Nppa positioning was established towards the center of the nucleus and may be a mechanism that allows to gene to be readily activated upon stress. These results may also suggest that there might be a stronger mechanism in place in the mature cardiomyocyte for gene silencing since we see more significant shifts in positioning of the Atp2a2 locus than for the activation of genes (although this may also be a function of gene length and chromatin environment). Gapdh and Nefl distributions do not change with stress (Figure 6-22C,D).

Because of the heterogeneity in nuclear architecture, we also assessed distances to heterochromatin regions (indicated by DAPI intensity) (Figures 6-21B, 6-23). Atp2a2 loci increase association with heterochromatin (average distance of 158nm in sham to 102nm in TAC with a shift from 33% of loci colocalizing with heterochromatin to 48%) and also move closer to the nuclear periphery (1.24μm to 1.17μm). We hypothesized that the opposite would be true with Nppa, though we find that its average distance to heterochromatin does not change, but its absolute distance from the the nuclear periphery does increase (1.06μm to 1.31μm) (Figure 6-23B). Gapdh distance to and colocalization with heterochromatin significantly increases (334nm to 463nm) and decreases (27.5% to 11.5% colocalization) respectively while absolute distance to the nuclear periphery does not change (Figure 6-23C). This reduced association with heterochromatin is consistent with expression results that show increases in Gapdh expression after pressure-overload stress (Figures 6-15Aiv). Nefl is not affected by TAC-induced stress and remains in close proximity to heterochromatin when compared to other genes (Figure 6-23D).

Gene association with cardiac transcription factories

To determine whether gene expression is associated with cardiac transcription factories, we looked at RNA polymerase II occupancy at these genes using published ChIP-seq data after acute stress (four days post-TAC) in the whole heart (40) (Figure 6-24, *left panels*). We find that at four days there is an increase in occupancy of active RNA polymerase II at and around the Nppa gene, minimal changes at Atp2a2 and slight increase at Gapdh. We performed ChIP-PCR to validate these findings in isolated cardiomyocytes from the failing heart (Figure 6-24, *right panels*). Our findings show enrichment of RNA polymerase at the Nppa promoter and gene body. For Atp2a2 and Gapdh, RNA polymerase II occupancy is reduced while Nefl has no enrichment of RNA polymerase II. These differences between the published data and our data can be attributed to time points used for analysis (acute versus chronic stress) as well contributions of cell type (published dataset used heart tissue while we used isolated adult cardiomyocytes).

Tissue-specific establishment of genomic architecture

To understand the tissue-specific establishment of chromatin architecture, we used DNA FISH examine the localization of these cardiac genes in liver tissue from the TAC mice. The liver shows a different genomic pattern (compare DAPI labeling patterns to that of heart, Figure 6-21) and does not express these genes, with the exception of Gapdh (Figure 6-15). The distribution of gene positioning in the liver was not affected by TAC (Figure 6-25), nor are the distances to heterochromatin and nuclear periphery affected (Figure 6-26). Overall positioning of Gapdh in the liver is shifted towards the center of the nucleus (Figure 6-25C). Interestingly, we find that Nppa positioning is also shifted towards the center with 36% of loci found in bin 5 (Figure 6-25B). Nefl distance to heterochromatin increased in response to TAC (226nm to 456nm with reduced colocalization, 39% to 21%) (Figure 6-26D). We thought that while the genes themselves (Nppa and Nefl) are not expressed, it is possible that the genes are situated near hepatic genes that are on or were affected by heart failure. Heart failure has been associated with liver dysfunction (41),

which could be reflected by changes in expression of nearby hepatic genes. We used the UCSC genome browser to pull up RNA polymerase II ChIP-seq and RNA-seq tracks in basal liver and heart tissues to compare and explore the regions surrounding these genes that cannot be resolved by microscopy (Figure 6-27). For the Nppa locus in the liver (Figure 6-27B), we do observe relatively low signal RNA-seq outside the Nppa gene, though it is not clear whether this low signal is enough to associate the gene with the center of the nucleus. Furthermore, when we examine the Nefl gene (Figure 6-27D), there are no annotated genes within ~200kb window. At this level, we did not find hepatic genes that could be affected with heart failure development and are in close proximity to the regions that were targeted by FISH. Because these data are analyzing these loci at a local scale, these sites may in fact be interacting with hepatic genes, which are actively expressed, in three dimensions in topologically associating domains (that are on the order of megabases, a much greater scale than what we examine here), and/or these targeted sites could be serving as regulatory loci for distal hepatic genes.

Discussion

In this study, we show direct evidence of chromatin structural changes *in vivo* in a disease setting. We utilized imaging approaches to characterize the anatomy of the cardiomyocyte nucleus. Our data supports the existence of transcription factories and suggests that these are stable compartments that have differential levels of activity upon pathological stress. Furthermore, genes are positioned in the nucleus in a tissue-specific manner which regulate their expression.

We show that cardiomyocyte nuclei undergo an increase in area. Whether this is due to or reflective of changes in chromatin packaging or just a result of alterations in cellular architecture due to growth is unknown. Our data in fibroblasts shows differential contribution of epigenetic perturbations; affecting DNA methylation or histone acetylation (both favoring a more open, active state) result in opposite changes in nuclear size (Figure 6-2). These experiments should be

replicated in cardiomyocytes to determine whether nuclear area is still affected in the same manner, and whether simply changing the epigenetic state is sufficient to induce changes in cellular area. Acute treatment with trichostatin A, another HDAC inhibitor, in NRVMs resulted in an increase in nuclear area (42). How these physical changes in nuclear area influence transcription rates needs to be elucidated. It has been shown that RNA transcriptional activity is proportional to cell size (43), and by regulating transcriptional activity, cell growth can be limited (44). Another study has shown *in vivo* that hypertrophic skeletal muscle myocytes have increased RNA synthesis, but the relationship with cell size is lost (45). These studies suggest that targeting transcriptional activity may alleviate cell growth due to stress. In the heart, targeting of TFIIB, important for the recruitment of RNA polymerase II, can prevent pathological hypertrophy (46). The concern that needs to be addressed is what are the long-term consequences of blocking a compensatory stress response.

Our findings show that the increases in cell and nuclear sizes also correspond to increases in transcriptional activity (Figure 6-6). In human heart failure, there is evidence of higher transcriptional activity, indicated by increased abundances of phosphorylated forms of RNA polymerase II (47). To understand the organization of transcriptional regulation, we examined the organization endogenous active forms of RNA polymerase II in cell and animal models. In hypertrophic NRVMs, the organization of factories, based on multiple criteria (cluster density, intensity, spacing between clusters and distance to the nuclear periphery), has been evidenced to be static (Figures 6-7, 6-8). Though not significant, it is suggested that puncta intensity increases (Figure 6-7D) as well as association with 5'FU clusters (Figure 6-9E), indicative of increases in activity at those sites. Due to the punctate pattern of nascent RNA labeling and static nature of RNA polymerase II molecules, we provide support for transcription factories in cardiomyocytes. Interestingly in the adult heart, the distribution of RNA polymerase II molecules does not change, rather the intensities of the clusters increase (Figure 6-13). This change may

be reflective of the severity of stress imposed on the cardiomyocytes. These results can be interpreted to favor a model in which RNA polymerases are recruited to existing factories. To understand this dynamic nature, future experiments using live cell imaging and performing FRAP would address RNA polymerase II properties in response to hypertrophic stress (Figure 6-28).

We then examined regulation of cardiac genes that are differentially expressed in the failing heart (Figure 6-22). Atp2a2 downregulation correlated with a shift towards the nuclear periphery. When examining the nuclear positioning analyses, it is important to be aware that being close to the nuclear periphery is much different from interacting with the nuclear lamina. Because RNA polymerase II molecules are present across the nucleus, a given gene can still be active while in close proximity to the nuclear periphery. In the case of Atp2a2, localization at the nuclear periphery also corresponds with reduced RNA polymerase II occupancy at the gene (Figure 6-24). On the other hand, Nppa is situated towards the center of the nucleus. When activated with stress, this positioning was maintained with significant decrease in association with the nuclear periphery. HDAC4 overexpression in NRVMs has been shown to shift the gene locus for Nppb (which is in close proximity to the Nppa locus, Figure 6-27B) to the nuclear center and has been implicated in regulating interactions with the nuclear membrane (24). This may suggest a mechanism that is in place in the adult heart and involved in displacement of the Nppa gene from the nuclear envelope upon stress. The prominent central positioning of the Nppa locus may be a feature that is established with development to situate the gene in an environment where it can readily be activated. We do see increased enrichment of RNA polymerase II at the Nppa gene body by ChIP-PCR though it does not appear striking, at least not to the extent of its upregulation.

In the heart, changes in association with the nuclear periphery show correlation with expression, but these changes only account for a small percentage of loci measured. Furthermore, association with heterochromatic regions (not just the nuclear envelope) account for another

mechanism of silencing. Even so, with these analyses, there is heterogeneity with regards to the distribution of positioning, which also emphasizes the other mechanisms in place for gene regulation at a local level. In this project, we quantitate distance to silencing compartments. Using DNA FISH alongside RNA polymerase II labeling, we are currently analyzing the converse, to quantitate distances to active regions. By assessing these measurements, we can lay out the contributions of association with active versus inactive regions to gene expression. For the liver, we had hypothesized that the majority of cardiac loci would be found at the periphery. Instead, a more uniform distribution is observed. This can be attributed to the number of heterochromatin centers dispersed across the liver nucleus, but in the case of Nefl in the heart, we also observe this pattern (here, we would have expected association with heterochromatin at either periphery or center based on the DNA organization). These results and our ChIP observations support a model in which gene association with active regions may outweigh association with heterochromatin. Though, this may depend on the context of where the gene is situated with respect to other genomic regions in three dimensions. When we examine the surrounding ~250kb regions of Nppa and Atp2a2, we find that there is a very low but present RNA polymerase II enrichment and RNA-seq signal (compared to Nefl, our negative control gene), which may contribute to the central positioning of these genes in the liver (versus being anchored to the periphery). These surrounding genomic regions may have a stronger impact in where the gene is situated and may be a function of length (the larger the silenced regions, the greater the effect; Nppa is a relatively small gene therefore its activation may not have much of an influence in nuclear localization compared to a larger gene like Atp2a2). Moreover, HiC analyses examining the 3D genomic interactions have proposed that the genome is divided into either A or B compartments, with topologically associating domains in A associated with active or open chromatin and those in B more tightly packaged (11). It may be that the compartment type is a determinant of spatial positioning and changes in compartment assignment (A to B or B to A) affect whether there is a location reassignment. Ongoing HiC analyses in our lab of isolated

cardiomyocytes from sham and TAC hearts will address this. Though we only examine 2 examples of genes differentially regulated, it appears that cardiac gene positioning can have a larger role in the repression of genes than activation, suggested by the greater shift we observe with Atp2a2 downregulation than with Nppa activation. The anchoring of genes to nuclear landmarks, such as the nuclear lamina or heterochromatin, may explain the incomplete reversion of gene expression profiles after mechanical unloading as in the case of LVADs (48), or incomplete maturation of stem cell-derived cardiomyocytes (49), and it would be interesting to explore the genomic architecture in these cases.

One of the limitations of the FISH experiments was the low labeling efficiency. We chose to maintain structural integrity of the tissue/nuclei instead of increase tissue digestion with enzymes that would enhance labeling efficiency but compromise tissue structure (Figure 6-20). This is a tradeoff, but we assume that with the less stringent digestion that the probability of a given loci to get labeled by DNA FISH remains the same—that there wasn't selective or preferential labeling of loci located in euchromatin or more accessible environments. Using a CRISPR/Cas-directed system would be a more precise approach to specifically tag loci of interest confidently with GFP in adult tissue (that also tends to have high background due to autofluorescence) and also allow us to examine gene dynamics during development and in response to stress (50).

These findings provide a global map of how the genome is organized. Further analyses at single base pair resolution are needed to complement this information by dissecting the critical 3D genomic interactions. Chromatin interaction analysis with paired end-tag sequencing (ChIA-PET) can identify the genes associated with RNA polymerase II factories and identify the genomic regions, such as enhancers, important for the regulation and stabilization of these factories (51). In the case of HUVEC cells, the interactions between TNFα-activated genes were shown to be critical for the expression of all the genes in the transcription factory (52). By disrupting one of the

genes, the expressions of other genes in that contact were also impaired (52), thus highlighting the importance of identifying the components, DNA and protein, of transcription factories. The cardiac loci may share same transcription factor binding sites that coordinate cardiac-specific gene expression and recruitment to factories, and disruptions in these structural components can provide the basis for global transcriptome changes.

The genome organization is not random and chromosomes are organized into territories (10). Furthermore, there is preferential localization of chromosomes to either the periphery or center of the nucleus (53). Integration of spatial data, using imaging approaches, with high resolution sequencing methodologies will be key to obtaining a detailed picture of how genomic structure is translated into function. Our analyses provide a correlation between expression and chromatin structure. Single cell analyses using RNA FISH or colabeling with RNA polymerase II using super-resolution imaging would validate these associations and better correlate expression with positioning. We have tried confocal analysis of gene colocalization with RNA polymerase II (Figure 6-29). Due to the low resolution of RNA polymerase imaging (limited by confocal resolution, small size of nucleus and large abundance of RNA polymerase molecules), combination of FISH and polymerase analyses require super-resolution microscopy and are ongoing.

We still do not understand the factors involved in maintaining these factories. Beta-actin is required for RNA polymerase II activity through stabilization of pre-initiation complexes (54). We have also demonstrated a potential role for HMGB2 in regulating cardiac transcription (3). Bridging how these different proteins interact along with tissue-specific transcription factors will be key to understanding the establishment of transcription factories unique to cell type. We also do not understand the mechanisms genes use to regulate positioning or the factors that are involved in guiding this process. In rod cells, it has been illustrated that the nuclear architecture

is important not only to orchestrate transcription in the cell, but it serves also as a key component of cellular function to focus light (55). Exploring other properties and functions of the cardiomyocyte nucleus will provide additional insight into how and why it is organized the way it is for the functioning of the cell.

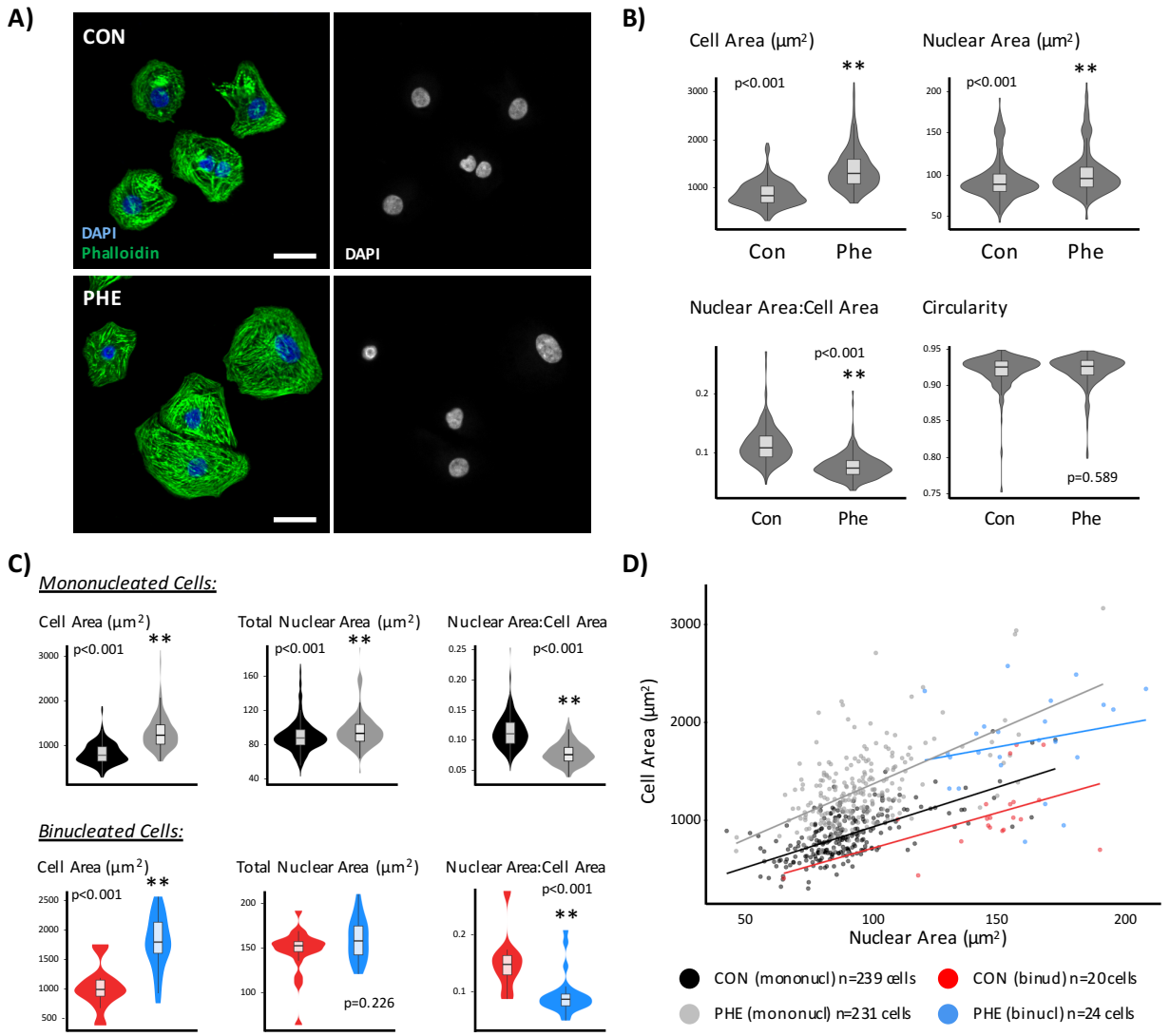

Figure 6-1: Nucleus:cell size ratios are not maintained in hypertrophic cardiomyocytes. A) Neonatal rat ventricular myocytes were treated with 10µM phenylephrine for 48hr, after which they were fixed and labeled with Phalloidin and DAPI for cell and nuclear size measurements. *Scale bar = 25µm.* **B)** Quantifications of cell and nuclear size show significant increases in cell (60% increase) and total nuclear (8% increase) areas. The ratio of total nuclear area to cell area was significantly reduced in the hypertrophic cardiomyocytes, highlighting greater growth of the cell versus nucleus (nuclear occupancy is reduced to 8% of cell from 12%). The increase in nuclear size does not affect nuclear shape, indicated by circularity (a perfect circle has circularity value of 1). **C)** Measurements were subsetted based on nuclei number. The increase in cell and nuclear areas, as well as reduction in nuclear:cell area ratio, was consistent in the mononucleated cell population. Binucleated cell populations had larger cell areas in hypertrophic cardiomyocytes, but total nuclear area did not differ. **D)** The nuclear versus cell sizes were plotted for the different cell populations. Mononucleated cells show significant correlation between nuclear versus cell sizes (control: r=0.655, p<0.001; phenylephrine: r=0.563, p<0.001). On the other hand, binucleated cells lost this association when treated with phenylephrine (control: r=0.506, p=0.023; phenylephrine: r=0.233, p=0.272); ** *p<0.001 [Mann-Whitney].*

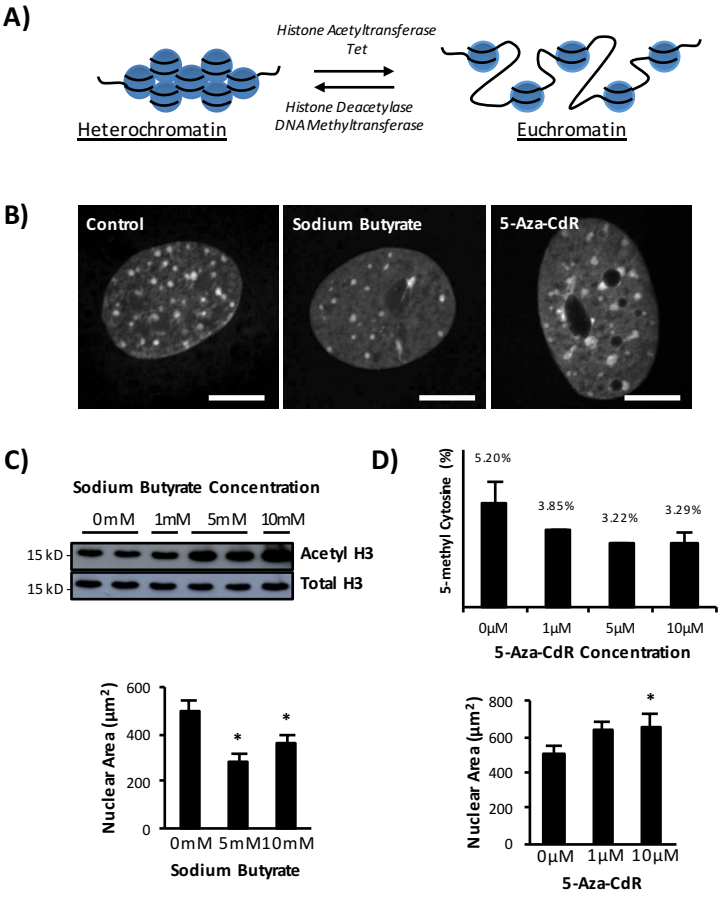

Figure 6-2: Epigenetic perturbations of chromatin structure in mouse fibroblasts differentially affect nuclear size. A) Levels of DNA packaging can be mediated by epigenetic modifications like histone acetylation and DNA methylation. **B)** Representative images of nuclei treated with sodium butyrate (HDAC inhibitor; 10mM) and 5-aza-2'-deoxycytidine (5-Aza-CdR, DNA methyltransferase inhibitor; 10µM) show effects on global DNA patterns by DAPI staining. Sodium butyrate-treated nuclei have fewer and smaller puncta while 5-Aza-CdR-treated nuclei show a smeared pattern. *Scale bar: 5µm.* **C)** Treatment with sodium butyrate results in increased levels of acetylated H3 shown by Western and a decrease in nuclear area. *Molecular weights for H3 and acetylated H3 ~17kDa.* **D)** 5-Aza-CdR treatment conditions were confirmed by multiple reaction monitoring mass spec quantitation showing reduction of total 5-methyl cytosine. Treatment results in an increase in nuclear area. * *p<0.05 [Mann-Whitney].*

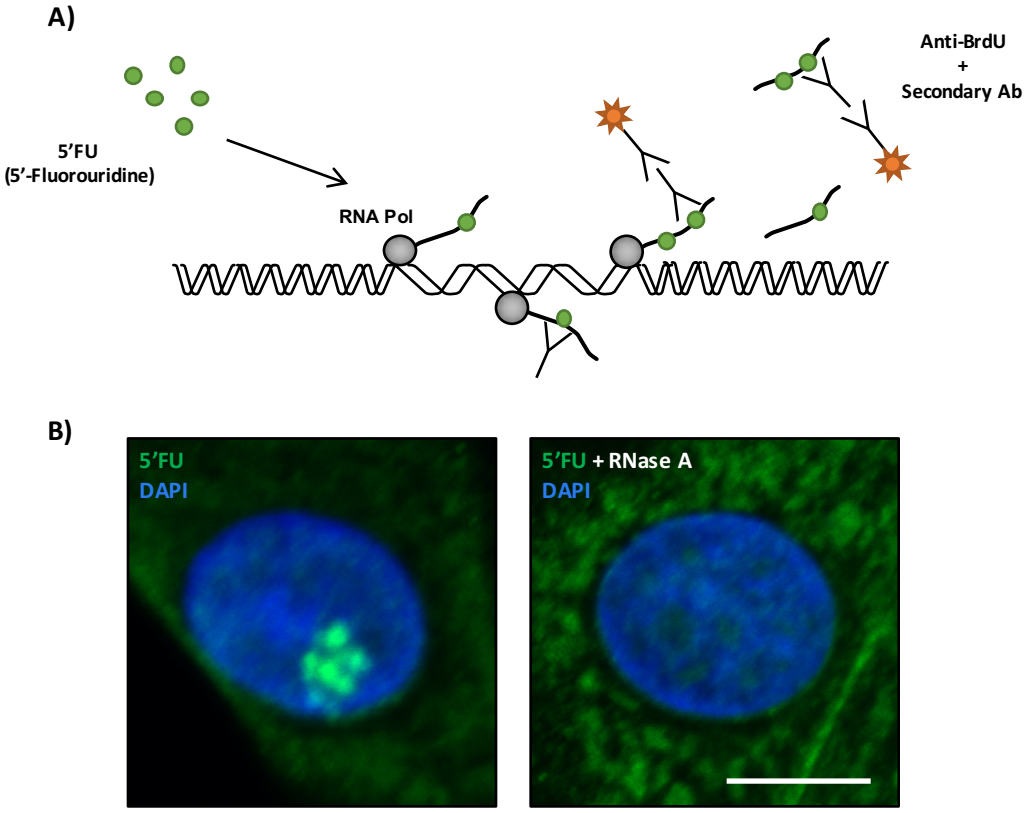

Figure 6-3: In situ visualization of transcriptional activity. A) 5'Fluorouridine (5'FU) is a uracil analogue that can permeate live cells and be incorporated into synthesizing RNA. Sites of 5'FU incorporation can then be detected using immunofluorescence. **B)** Representative image of neonatal rat ventricular myocytes treated with 4mM 5'FU for 30min is shown on *left.* RNase A treatment post-5'FU incorporation shows absence of 5'FU signal, demonstrating specificity of labeling to RNA *(right). Scale bar: 5μm.*

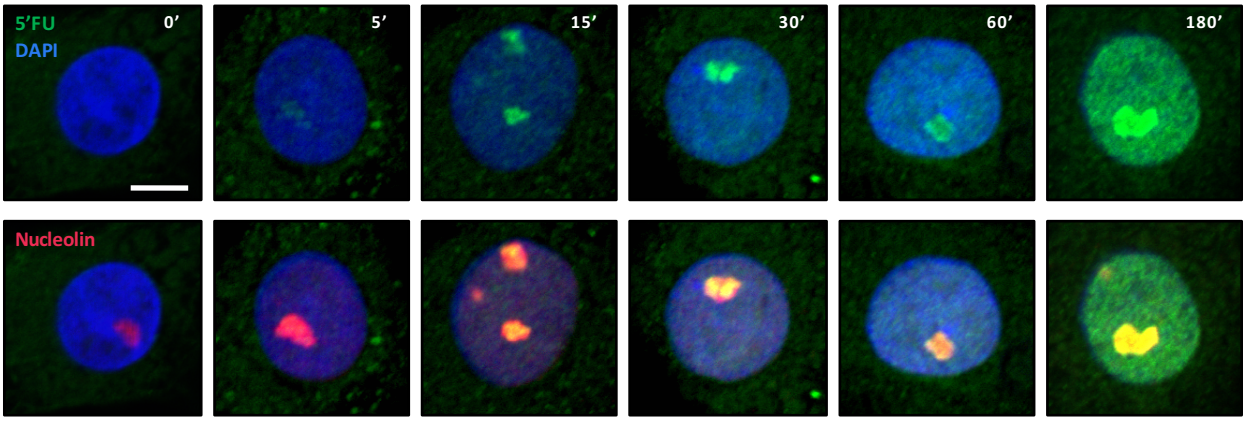

Figure 6-4: Time course of 5'fluorouridine labeling. Rat ventricular cardiomyocytes were treated with 5'fluorouridine for the indicated times. There is a large enrichment of signal in the nucleolus (marked by nucleolin) that increases with time. The nucleolus is occupied by RNA polymerase I molecules, which carry out ribosomal RNA transcription and quench the 5'fluorouridine due to a high transcriptional rate; signal is detected in the nucleolus within 5min of 5'fluorouridine treatment. *Scale bar = 5μm.*

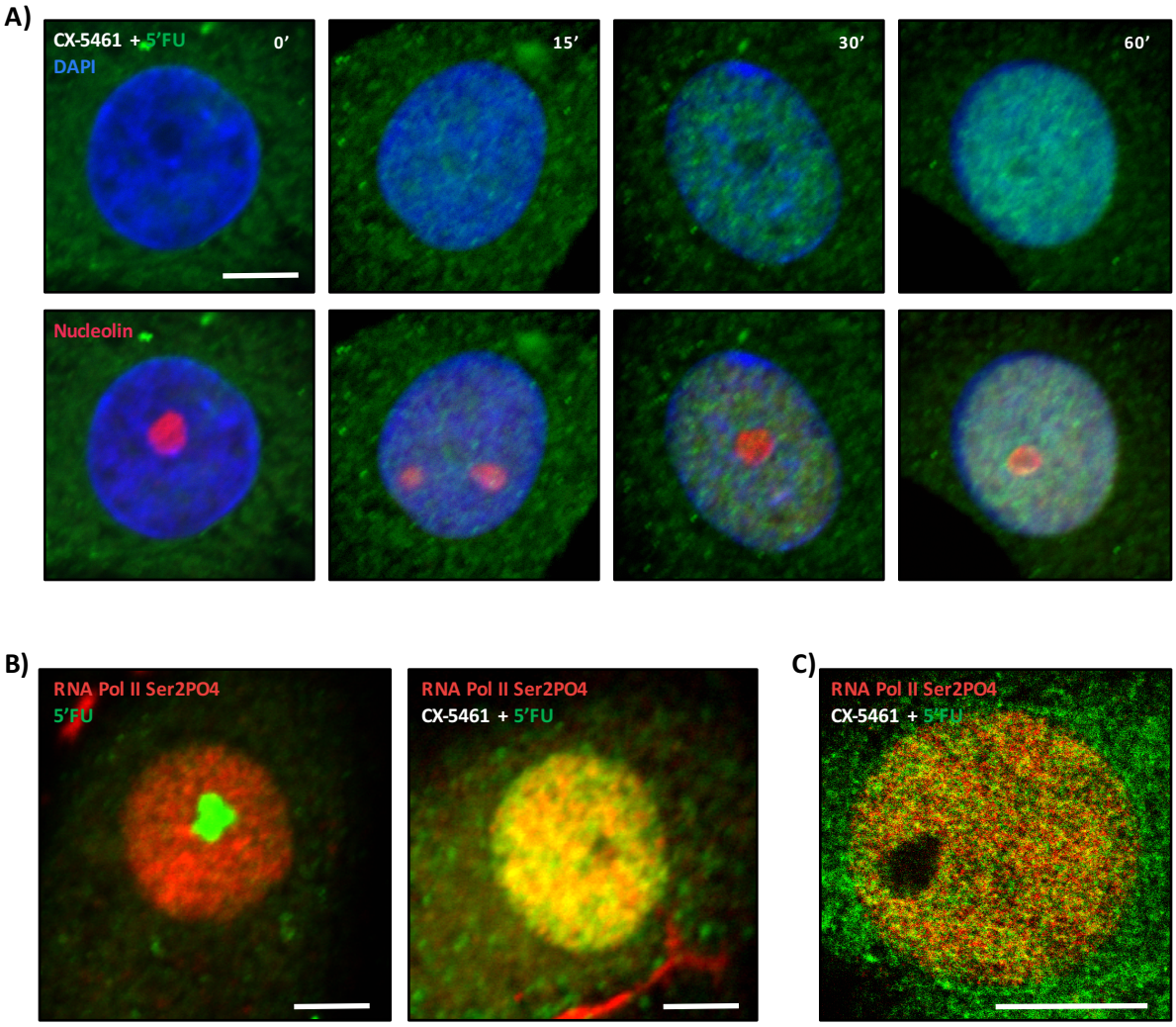

Figure 6-5: Selective labeling of RNA polymerase activity. A) Neonatal cardiomyocytes were treated with CX-5461, an RNA polymerase I inhibitor (2μM, 15min), prior to the addition of 5'fluorouridine. Thus, 5'fluorouridine labeling is reflective of RNA polymerase II and III activity. Note the absence of signal in the nucleolus, marked by nucleolin. **B)** RNA polymerase I activity quenches 5'fluorouridine signal into the nucleolus while treatment with CX-5461 allows for selective labeling of transcriptional activity in the nucleoplasm, which is associated with sites of active RNA polymerase II (phosphorylated at serine 2) occupancy, indicated by colocalization (yellow). **C)** This association between RNA polymerase II and 5'fluorouridine-labeled transcripts is also reflected by super-resolution STED imaging. *Scale bar = 5μm.*

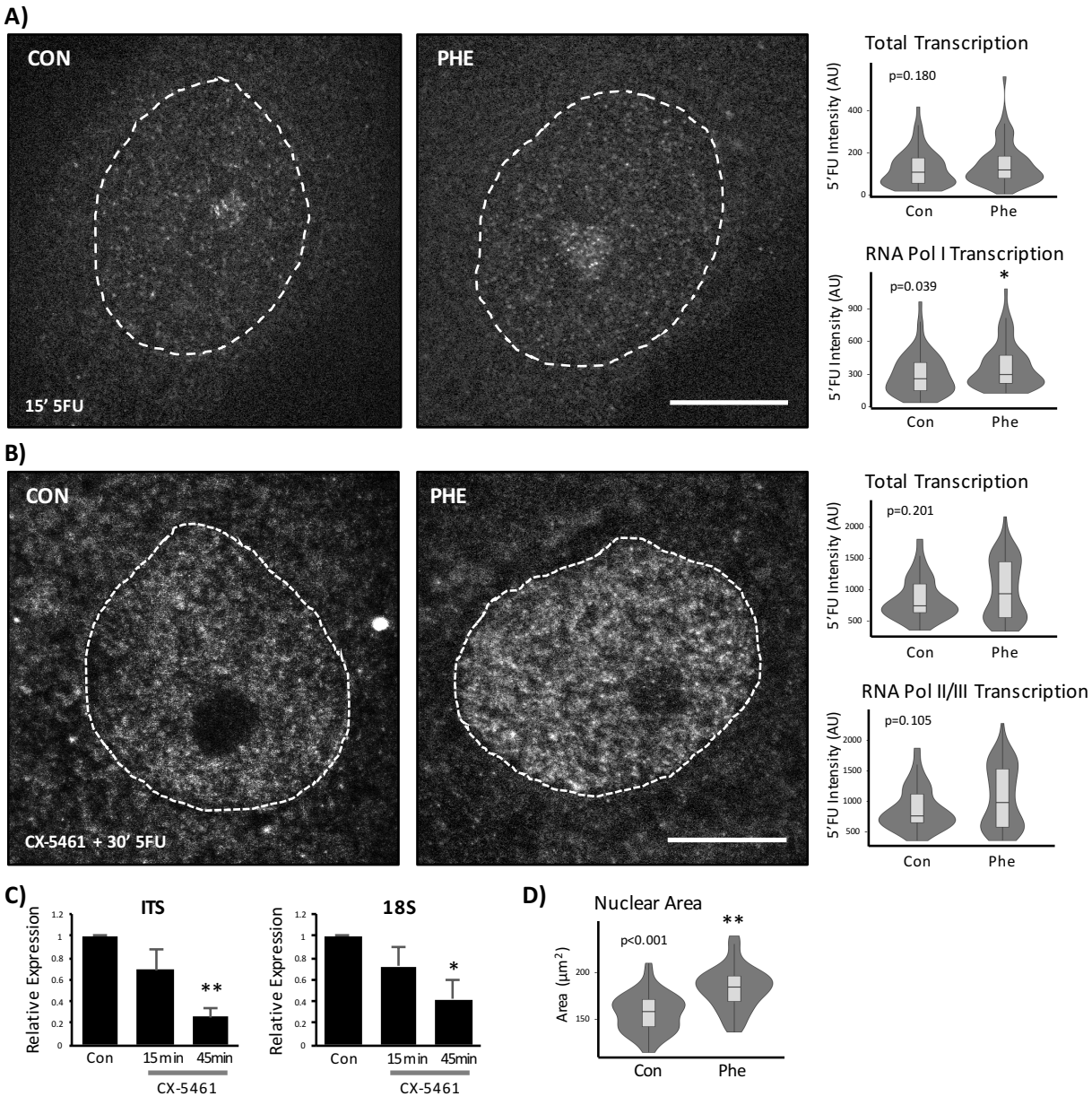

Figure 6-6: Hypertrophic cardiomyocytes have increases in global transcriptional activity. **A)** Neonatal rat ventricular myocytes were treated with phenylephrine (10μM, 48hr) to induce hypertrophy and treated with 5'fluorouridine to assess transcriptional activity. Representative images are shown *(left)*. 5'Fluorouridine intensities were measured across the entire nucleus (total transcription) or within nucleolus (marked by nucleolin, RNA Pol I transcription) *(right)*. *Control: n=61 nuclei; Phenylephrine: n=65 nuclei.* **B)** RNA polymerase II and III actvities were measured by inhibiting RNA polymerase I activity. We observe 19% and 23% increases in total and nucleoplasmic 5'fluorouridine intensities, respectively, though not significant. *Control: n=61 nuclei; Phenylephrine: n=60 nuclei.* **C)** CX-5461 treatment efficiency in inhibiting RNA polymerase I was confirmed by measuring ribosomal RNA expression, ITS (premature) and 18S (mature), at 15min (before addition of 5'fluorouridine) and 45min (time point at which cells were fixed for immunostaining). *15min: n=4; 45min: n=6.* **D)** Nuclear area increases in these samples by 17%. *Scale bar = 5μm. * p<0.05; ** p<0.001 [Mann-Whitney].*

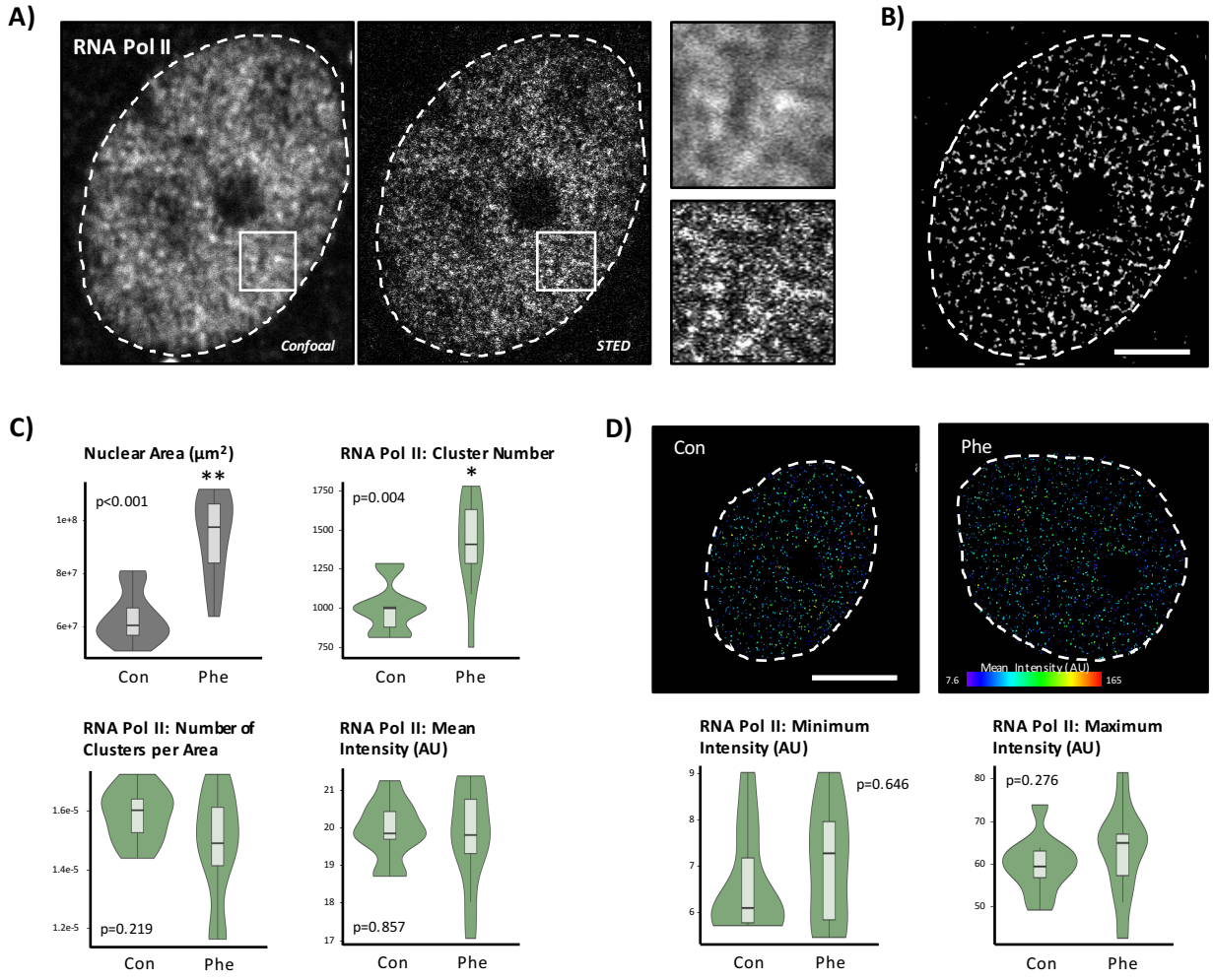

Figure 6-7: Properties of RNA polymerase II factories do not change in cultured hypertrophic cardiomyocytes. A) Neonatal rat ventricular myocytes were treated with phenylephrine, labeled with 5'fluorouridine and immunolabeled for active RNA polymerase II, phosphorylated at serine 2, and 5'fluorouridine incorporation for STED microscopy. *Left* image shows the confocal image of a control nucleus and with its corresponding super-resolution image on the *right*. Boxed regions highlight the level of detail that can be resolved with the STED microscope. **B)** For quantitative analyses of RNA polymerase II clusters, images were processed to remove noise. Afterwards, the remaining signal was used to quantify parameters of RNA polymerase II factories using Imaris program. *Scale bar = 3µm.* **C)** Nuclear area increases with hypertrophy; the number of clusters also increases. Cluster number was normalized to nuclear area and indicated no difference. Mean cluster intensity also does not differ. **D)** RNA polymerase II clusters are mapped and colored based on mean cluster intensity. Additional analyses examining the intensity ranges (measuring the minimum and maximum intensities per nucleus) demonstrate no change with hypertrophic agonist treatment. *Scale bar = 5µm. Control: n=10 nuclei; Phenylephrine: n=11 nuclei. * p<0.05; ** p<0.001 [Mann-Whitney].*

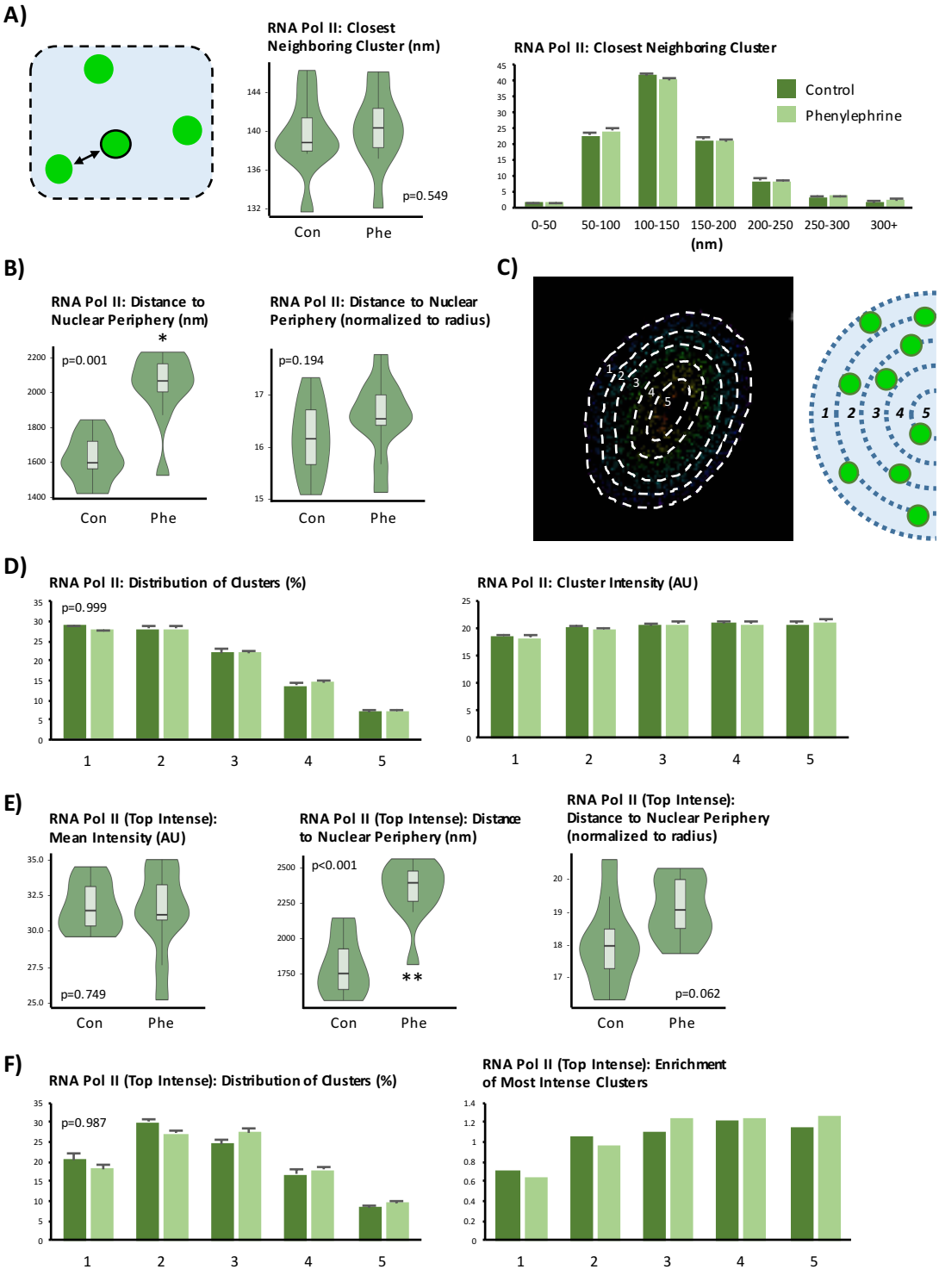
A)
RNA Pol II: Closest Neighboring Cluster (nm)
p=0.549
Con
Phe
RNA Pol II: Closest Neighboring Cluster
Control
Phenylephrine
0-50
50-100
100-150
150-200
200-250
250-300
300+
(nm)
B)
RNA Pol II: Distance to Nuclear Periphery (nm)
p=0.001
*
Con
Phe
RNA Pol II: Distance to Nuclear Periphery (normalized to radius)
p=0.194
Con
Phe
C)
1
2
3
4
5
D)
RNA Pol II: Distribution of Clusters (%)
p=0.999
RNA Pol II: Cluster Intensity (AU)
E)
RNA Pol II (Top Intense): Mean Intensity (AU)
p=0.749
Con
Phe
RNA Pol II (Top Intense): Distance to Nuclear Periphery (nm)
p<0.001
**
Con
Phe
RNA Pol II (Top Intense): Distance to Nuclear Periphery (normalized to radius)
p=0.062
Con
Phe
F)
RNA Pol II (Top Intense): Distribution of Clusters (%)
p=0.987
RNA Pol II (Top Intense): Enrichment of Most Intense Clusters

Figure 6-8: Cardiac transcription factories remain stable after hypertrophic stress. A) To assess anatomical distribution of cardiac transcription factories, we analyzed the distances to the closest neighboring cluster. Cartoon illustrates RNA polymerase II clusters in green. For each cluster, the distance to the nearest neighbor is recorded as indicated. The spacing between RNA polymerase II clusters does not change with hypertrophy. **B)** Positioning of transcription factories is also assessed with respect to the nuclear envelope. While the absolute distance to the periphery increases, the normalized distances show no change (normalized to radial distance to account for differences in nuclear size). **C)** To examine the distribution of clusters across the nucleus, we divided the nucleus into 5 bins based on the maximum and minimum distances to the periphery for each nucleus and then assessed cluster number and cluster intensity for each bin (*1* is closest to and *5* is furthest from periphery). **D)** The distribution of percent of total clusters per nucleus found within each bin is plotted *(left)* along with the mean intensities of the clusters at each bin *(right)*. **E)** For each nucleus, the clusters were ranked by mean intensity and the top 20% were used for analysis. The average of intensity of the top-ranked clusters does not differ, but the absolute distance to the periphery increases. When normalizing peripheral distance, there is an increase in distance from the periphery though not significant (highly intense clusters found more centrally). **F)** The positioning across the nucleus of the most intense clusters shows no change in distribution after hypertrophic stress. Enrichment was determined by comparing the fraction of the most intense clusters to the fraction of total clusters for each bin. *Control: n=10 nuclei; Phenylephrine: n=11 nuclei. * p<0.05; ** p<0.001 [Mann-Whitney; for cluster distribution, Chi-squared].*

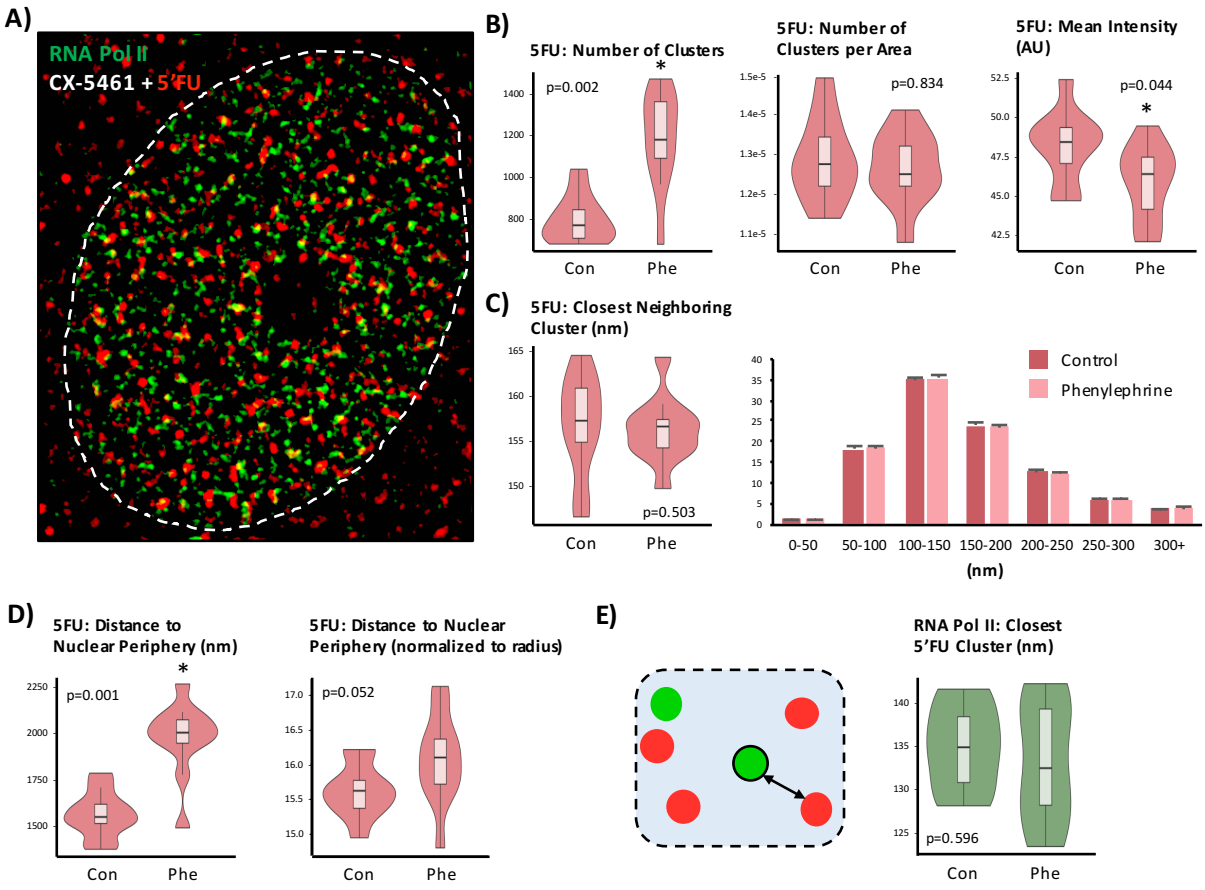

Figure 6-9: Labeling of nascent transcripts reflects increases in transcription factory activity with hypertrophy. A) Here, analyses integrate 5'fluorouridine measurements, a direct readout of RNA polymerase activity. Neonatal myocytes were treated with CX-5461 and then supplemented with 5'fluorouridine for 30min. **B)** Like RNA polymerase II, the absolute number of 5'fluorouridine clusters increases though not when normalized to nuclear area. The mean cluster intensity is significantly reduced. **C)** The average spacing between nearest neighboring 5'fluorouridine clusters does not change *(left)*, nor does the the distribution *(right)*. **D)** The distance of 5'fluorouridine clusters to the nuclear periphery increases and this trend remains when normalizing the distances to radius. **E)** The distance of closest neighboring 5'fluorouridine *(red)* with respect to RNA polymerase II cluster *(green)* does not change, though the trend shows a decrease in distance. *Control: n=10 nuclei; Phenylephrine: n=11 nuclei. * p<0.05 [Mann-Whitney].*

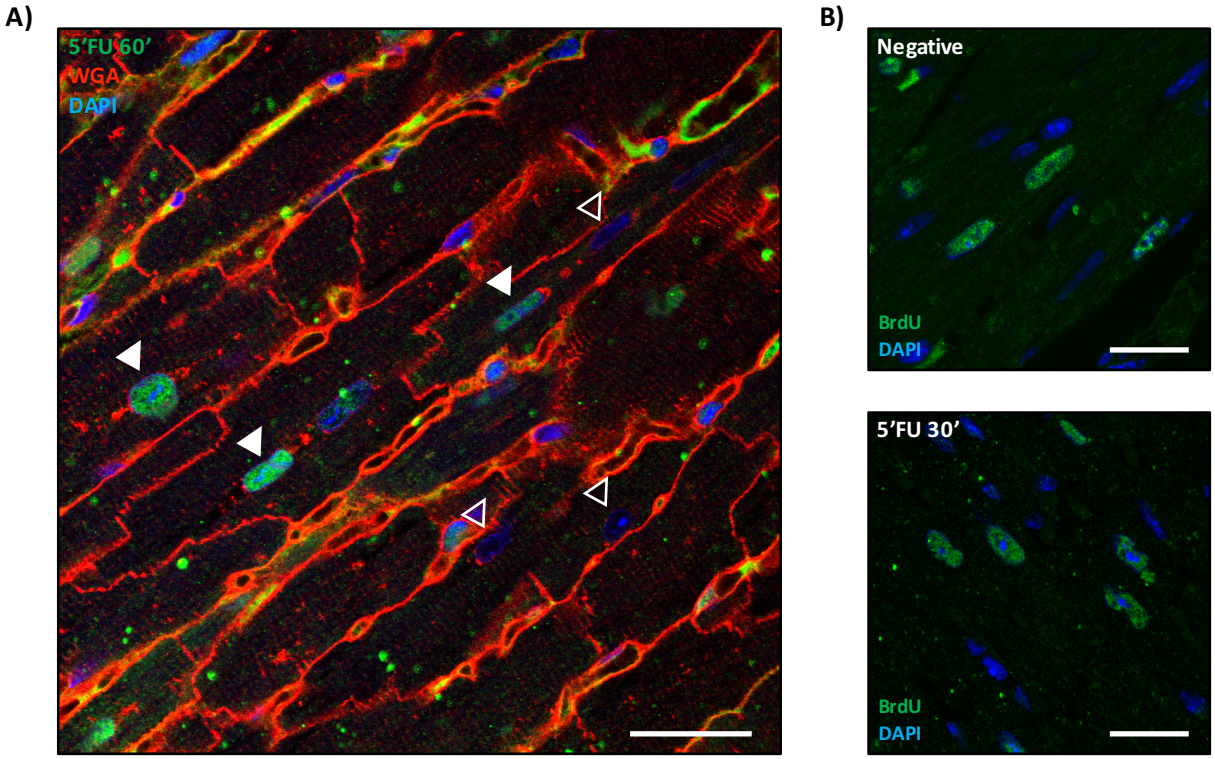

Figure 6-10: 5'Fluorouridine labeling in the adult mouse heart. A) Based off of successful outcomes of the *in situ* labeling in cultured cells, we proposed to perform the 5'fluorouridine labeling assay *in vivo* with implications of detecting transcriptional activity in the adult heart to characterize transcriptional responses due to stress with respect to cardiac anatomy. Adult mice were given an intraperitoneal injection of 0.4M 5'fluorouridine for different lengths of time (time points attempted ranged from 5min to 24hr) and then hearts were collected, fixed and prepared for histology. Immunofluorescence labeling was carried out, and a representative image is shown. We noticed differential patterns of 5'fluorouridine signal throughout the heart. Some nuclei were positive (closed arrows) while others were negative (open arrows). These results raised interesting questions regarding the contributions of nuclei in multinucleated cells that could be addressed using this assay. **B)** We performed that same labeling in control animals that did not receive any injection *(top)* and found positive signal in nuclei with similar intensities to 5'fluorouridine-injected animals *(bottom)*. We carried out extensive troubleshooting to resolve this false positive issue, including changing antibody species (5'fluorouridine was not recognized with these antibodies) and different sample processing methods (frozen vs paraffin-embedded tissue, storage of tissues in separate containers, whole animal fixation), as well as administration of 5'fluorouridine via osmotic pumps. This assay can be a powerful tool in understanding the heart's transcriptional response to stress. *Scale bar = 25μm.*

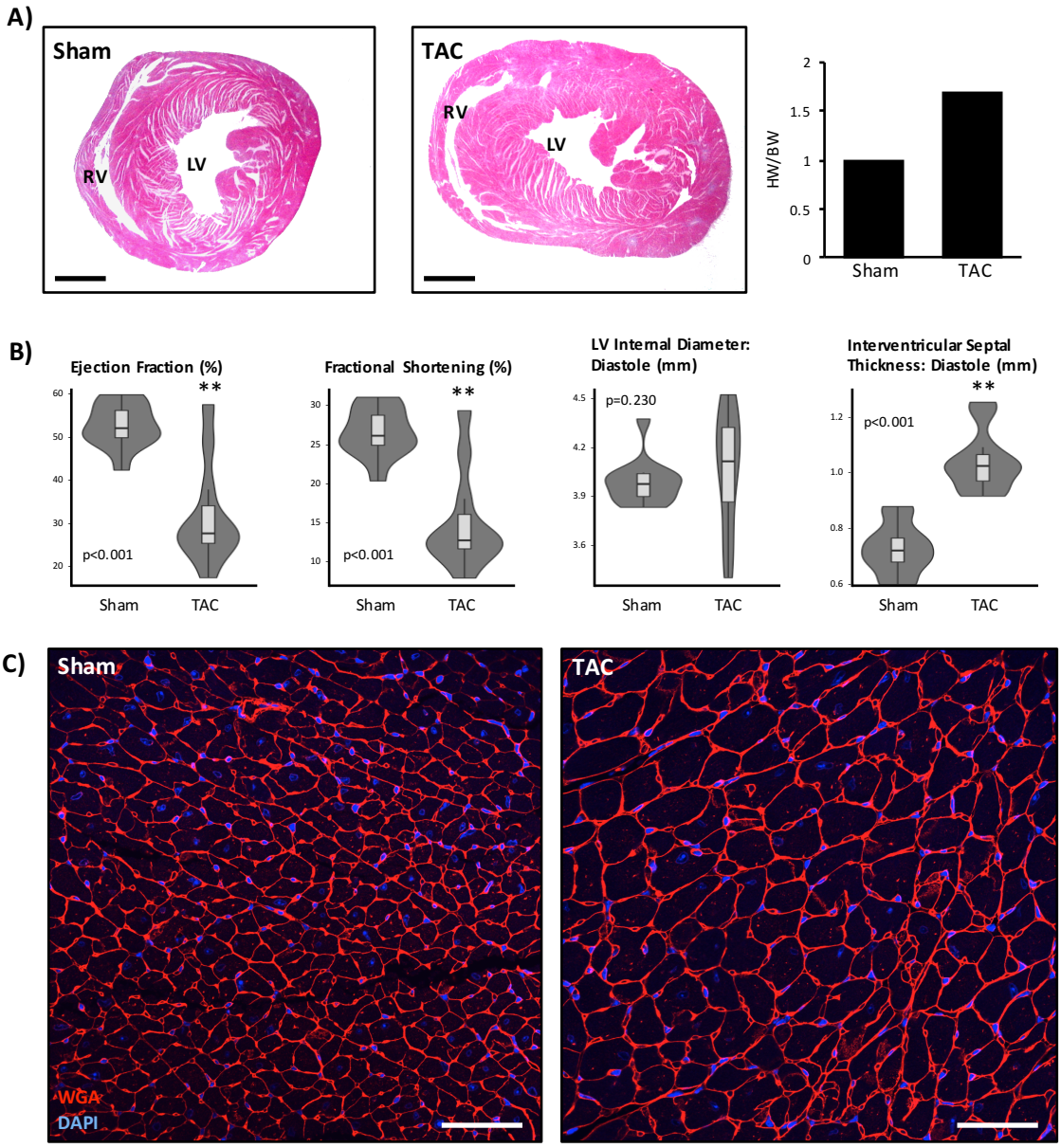

Figure 6-11: Transverse aortic constriction model of heart failure. A) Adult C57/Bl6 mice underwent transverse aortic constriction (TAC) surgery, and cardiac function was monitored by echocardiography until development of heart failure (<25% ejection fraction, <20% fractional shortening). Heart failure developed ~6weeks post-TAC surgery. Representative tissues sections show the enlargement of the heart after TAC, and quantifications show an increase in heart weight to body weight ratio. *Sham: n=2; TAC: n=2. Scale bar = 1mm.* **B)** Summary of cardiac function (ejection fraction and fractional shortening) and dimensions (left ventricular internal diameter and interventricular septal thickness) measured by echocardiography show that mice subjected to TAC developed heart failure. *Sham: n=12; TAC: n=11.* **C)** Wheat germ agglutinin (WGA) labeling of membranes shows increases in cardiomyocyte cross-sectional area. *Scale bar = 50μm. ** p<0.001 [Mann-Whitney].*

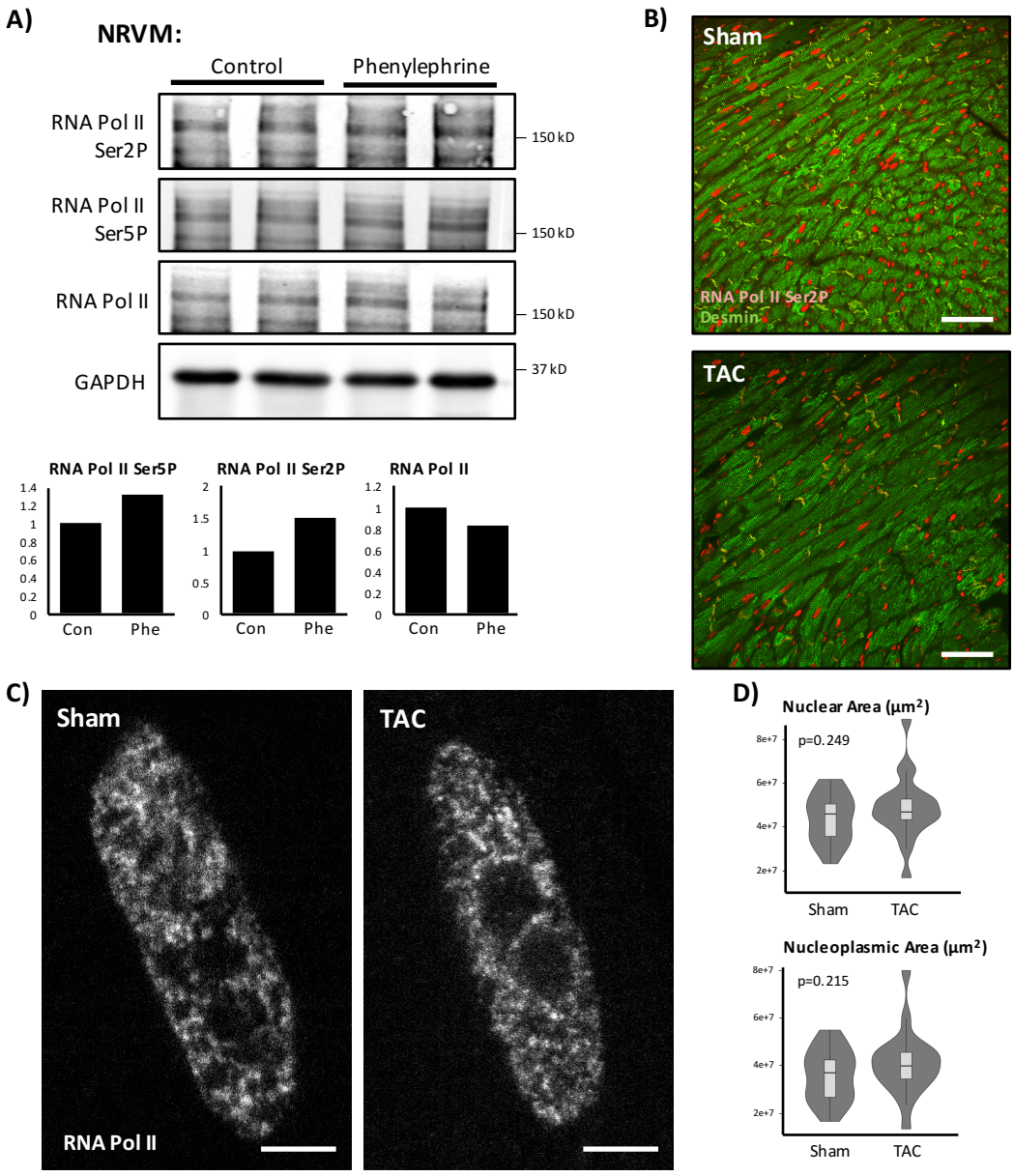

Figure 6-12: RNA polymerase II factories in failing hearts are mapped by STED microscopy. **A)** Hypertrophic cardiomyocytes show increased activation of RNA polymerase II, indicated by increases in serine 5 and serine 2 phosphorylated forms (normalized to Gapdh expression). *Molecular weights for RNA polymerase II ~220kDa, GAPDH ~37kDa.* **B)** Cardiac transcription factories were mapped using active RNA polymerase II in heart tissue sections from sham and TAC mice. Analyses specifically looked at cardiomyocyte transcription factories, and thus colabeling with cardiomyocyte marker, desmin, was used to differentiate nuclei of cardiomyocytes from other cell types in the heart. *Scale bar = 50µm.* **C)** Representative STED images of nuclei from control and failing hearts are shown. *Scale bar = 3µm.* **D)** The nuclei that were analyzed had similar nuclear and nucleoplasmic areas. Nucleoplasmic regions were determined based on presence of RNA polymerase II signal. Regions devoid of signal were regions associated with nucleoli or the characteristic cardiomyocyte heterochromatin chromocenter. *Sham: n=21 nuclei; TAC: n=20 nuclei. [Mann-Whitney]. (Imaging experiments, with different sets of sham/TAC hearts, were repeated >3 times. Representative analyses are presented here.)*

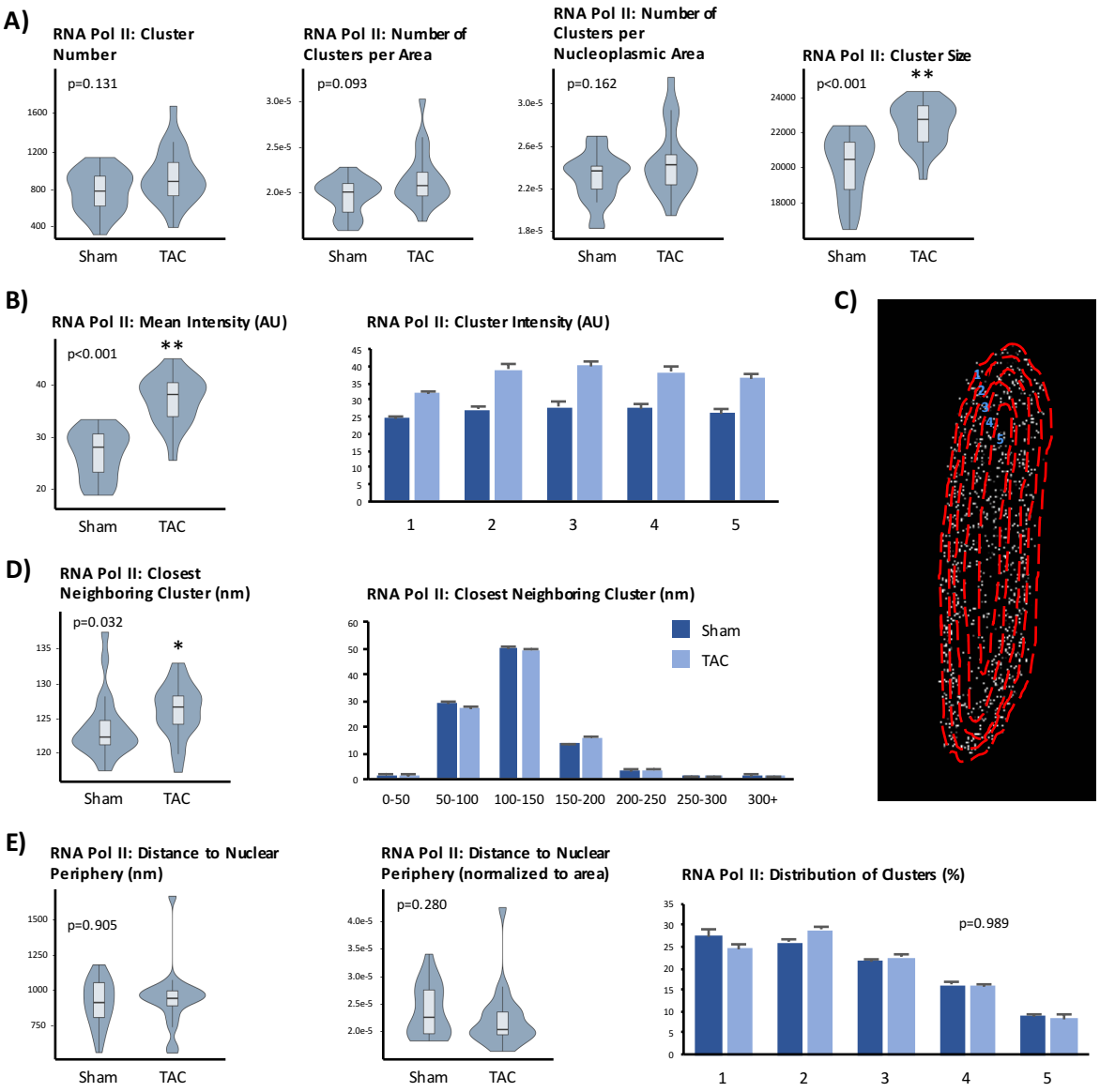

Figure 6-13: RNA polymerase II distribution does not change in the adult heart, supporting organization of transcription factories. A) RNA polymerase II density (number of factories per nuclear area) is not affected after pressure-overload stress, although cluster size increases. **B)** Mean intensity of total clusters increases, and this increase in intensity occurs uniformly across the nucleus as indicated by average of mean cluster intensity at each bin. **C)** To normalize nuclear distances, the difference between maximum and minimum distances to the nuclear periphery was used to generate 5 bins (as performed as in Figure 6-8C). The image illustrates this approach. **D)** The average distances between closest neighboring RNA polymerase II clusters, and the distribution of these distances, show minimal change in spacing. Note that while the average distance to the closest neighboring cluster is significant, the difference is only ~2nm (123.5nm to 125.8nm). **E)** The distances of the center of each cluster to the nuclear periphery also does not change. Cluster distances to periphery were normalized to area in the *middle* graph. Due to the heterogeneity in nuclear shapes, radial distance was not an appropriate variable to use for normalization. Altogether, these measurements suggest that the RNA polymerase II factories are fixed compartments. *Sham: n=21 nuclei; TAC: n=20 nuclei. * p<0.05; ** p<0.001 [Mann-Whitney; for cluster distribution, Chi-squared].*

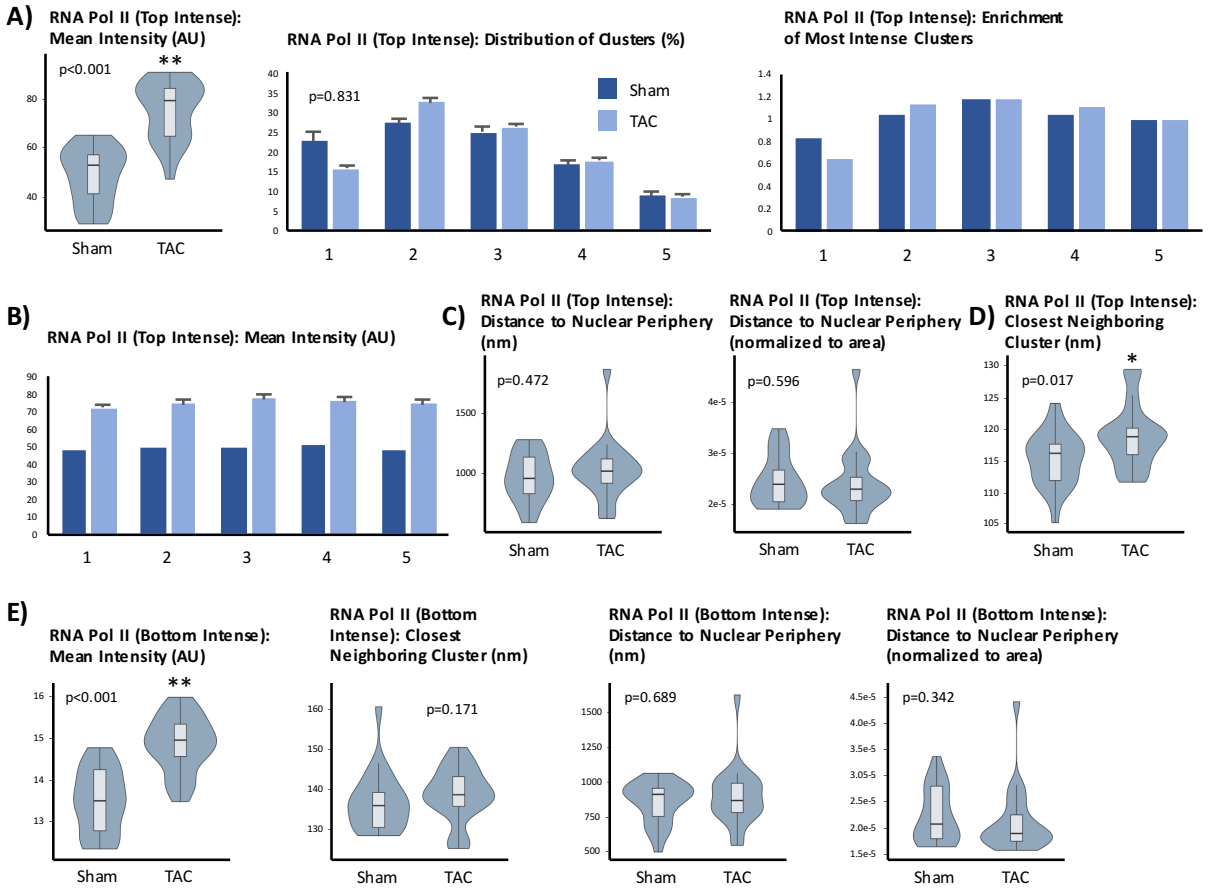

Figure 6-14: RNA polymerase II molecules are recruited to transcription factories in the stressed heart. A) Clusters were ranked based on mean intensity and then the top 20% were examined. The intensity of the highest ranked significantly increases but their distribution remains the same. Furthermore, examination of cluster enrichment (fraction of top intense clusters divided by fraction of total clusters per bin) suggests that there is a reduction in highly intense clusters from the nuclear periphery. **B)** The distribution of cluster intensities shows that intensity increases occur throughout the nucleus. **C)** Cluster distances to the nuclear periphery are plotted, both absolute distance and distance normalized to area, and do not differ between groups. **D)** Examination of top intense clusters also shows increased spacing between close RNA polymerase II neighbors (115.2nm to 118.8nm). **E)** The bottom 20%-ranked clusters have increases in mean intensity without changes to spatial organization in the nucleus. *Sham: n=21 nuclei; TAC: n=20 nuclei. * p<0.05; ** p<0.001 [Mann-Whitney; for cluster distribution, Chi-squared].*

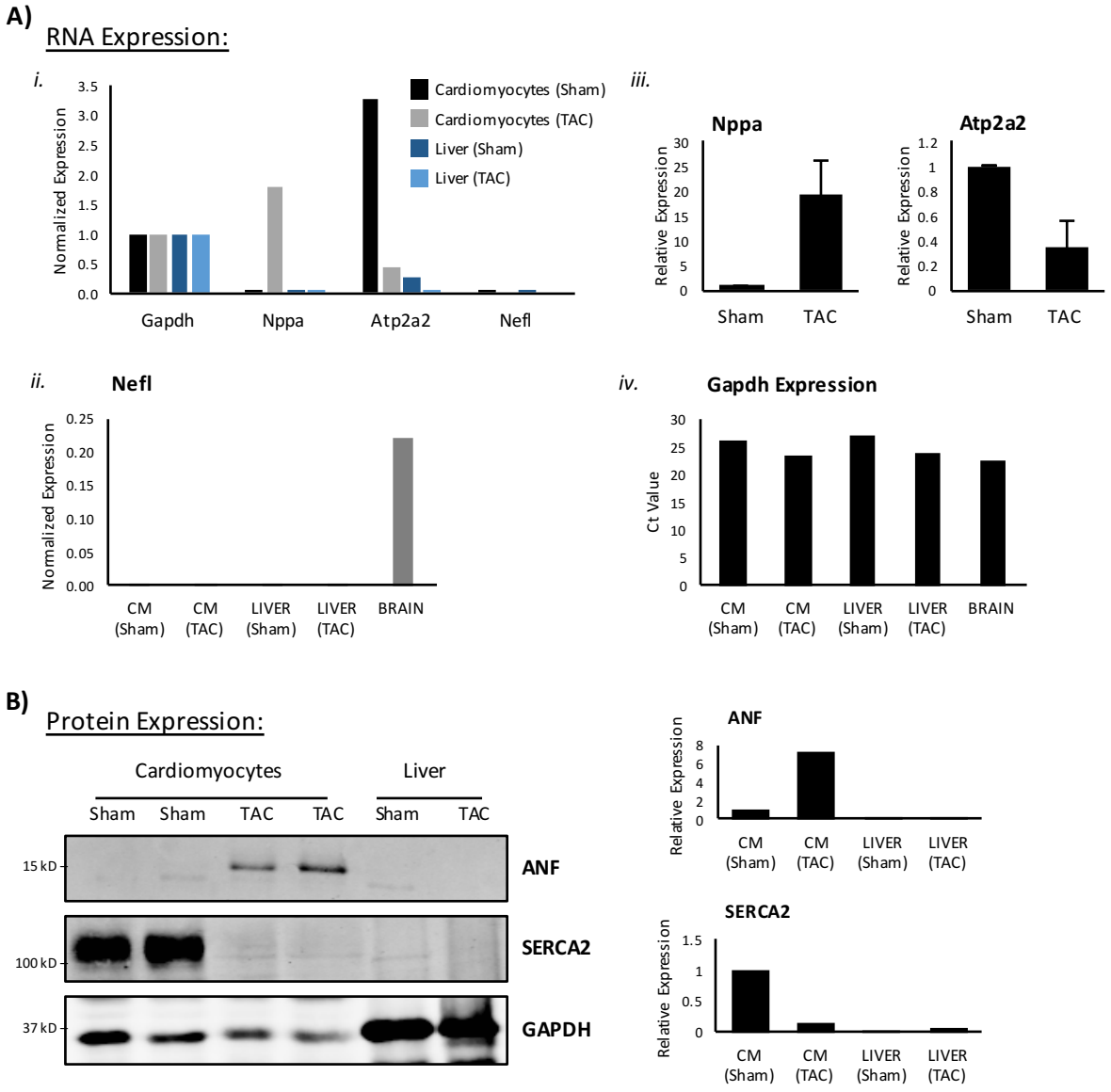

Figure 6-15: Validation of cardiac-specific changes in gene expression. A) RNA expression levels of four genes to be further analyzed by DNA FISH are validated. These genes were chosen to represent four categories of expression responses due to stress (activation, silencing, remain active and remain silent) and serve as models to understand genomic organization in cardiomyocytes. Nppa and Atp2a2 expression (normalized to Gapdh) occurs in a cardiac-specific manner; the liver expression is shown for comparison *(i)*. Nefl expression, a neuronal gene, serves as a negative control in both heart and liver tissues (normalized to Gapdh expression) *(ii)*. Changes in expression of Nppa and Atp2a2 after TAC are shown *(iii)*, along with raw expression of Gapdh *(iv)*. Ct values measure RNA abundance, with lower Ct values indicative of higher expression. **B)** The changes in expression on the level of RNA reflect the changes in protein abundance. Quantifications of western blots are shown on *right*. *Molecular weights for ANF ~17kDa, SERCA2 ~110kDa, GAPDH ~37kDa.*

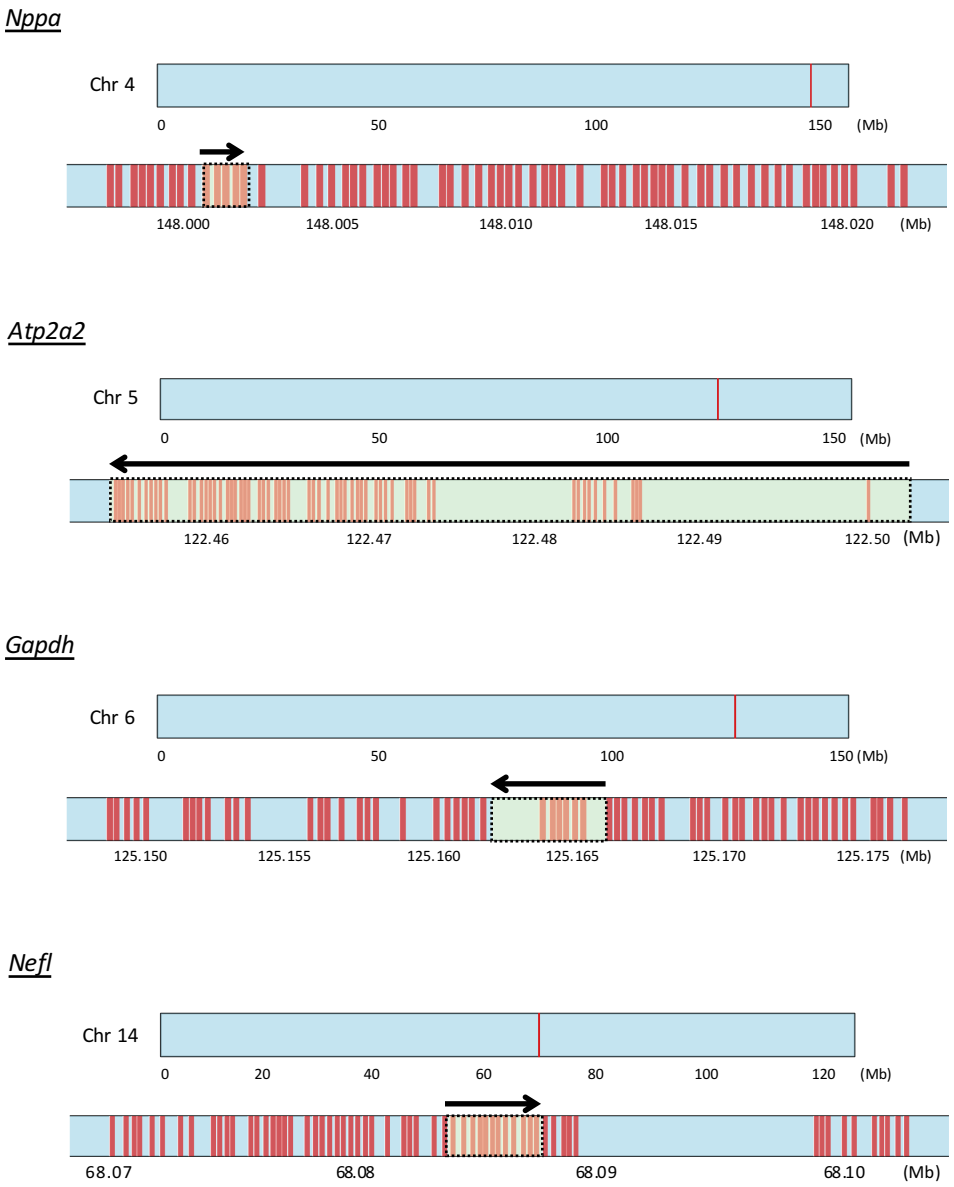

Figure 6-16: Design of DNA FISH probes. DNA FISH probes were designed using HD FISH, which utilizes PCR-based products (~200bp) targeting the mouse genome to tile the region of interest [28]. We probed at least 20kb regions around different categories of genes based on their response to pressure overload stress: upregulated (Nppa), downregulated (Atp2a2), active (Gapdh) and inactive (Nefl). We used the mm10 reference mouse genome to design primer sets targeting the following loci: Nppa Chr4:147,997,910-148,021,634 (64 primer sets); Atp2a2 Chr5:122,453,757-122,499,765 (51 primer sets); Gapdh Chr6:125,148,520-125,176,210 (60 primer sets); Nefl Chr14:68,069,935-68,102,872 (62 primer sets). For each gene, the location of chromosome that is targeted is marked *(top)* and zoomed in is the region labeled by FISH with the gene locus is highlighted by green box (arrow indicates direction of transcription) *(bottom)*. Red bars map out the regions targeted by FISH primers sets.

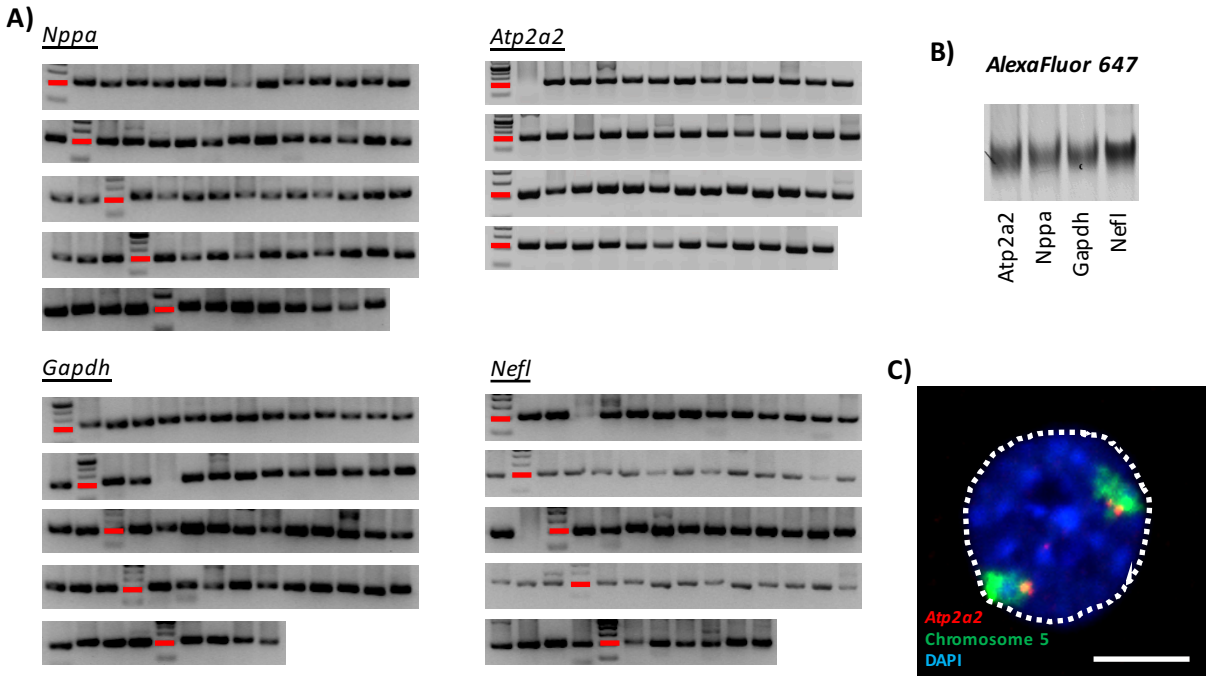

Figure 6-17: Generation of DNA FISH probes. A) PCR products were run on gel to confirm amplification of probes (each lane represents a different primer set). Most primers sets successfully amplified mouse 3T3 DNA. These products were pooled together to generate fluorescent probes. *Red bars indicate 200bp band of DNA ladder.* **B)** Pooled PCR products were fluorescently labeled with AlexaFluor 647 and run on gel. We successfully detected fluorescent signal at 200bp. **C)** We confirmed fluorescent signal for Atp2a2 in nuclei of mouse embryonic fibroblasts by colabeling for chromosome 5 and showing the direct association of the gene with its corresponding chromosome territory. *Scale bar = 5μm.*

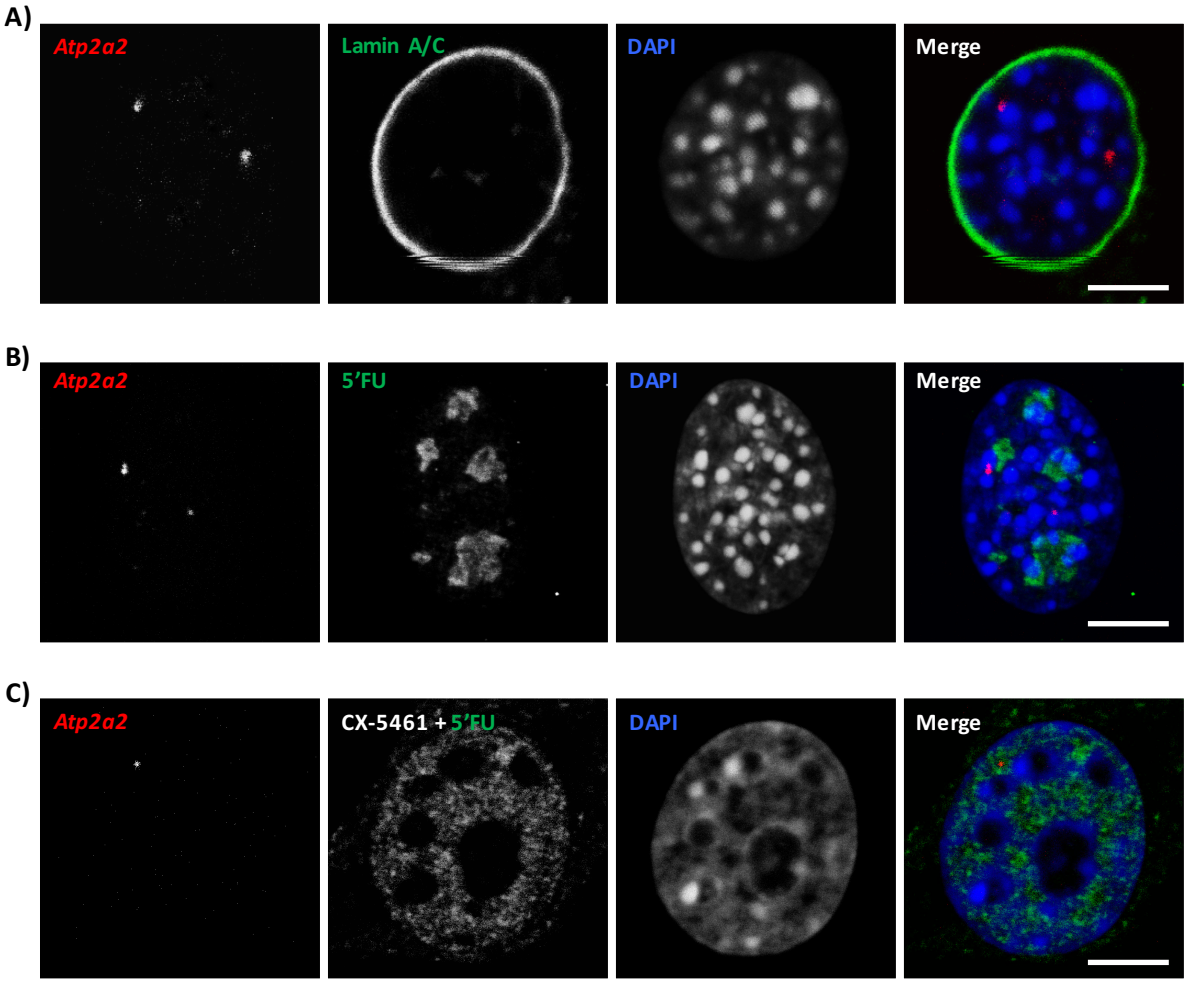

Figure 6-18: DNA FISH maps gene loci with respect to different nuclear territories. Mouse embryonic fibroblasts were labeled with the Atp2a2 DNA FISH probe. Localization of the gene can be assessed with respect to the nuclear lamina **(A)** and regions of active transcription, indicated by 5'fluorouridine labeling **(B, C)**. *Scale bar = 5μm.*

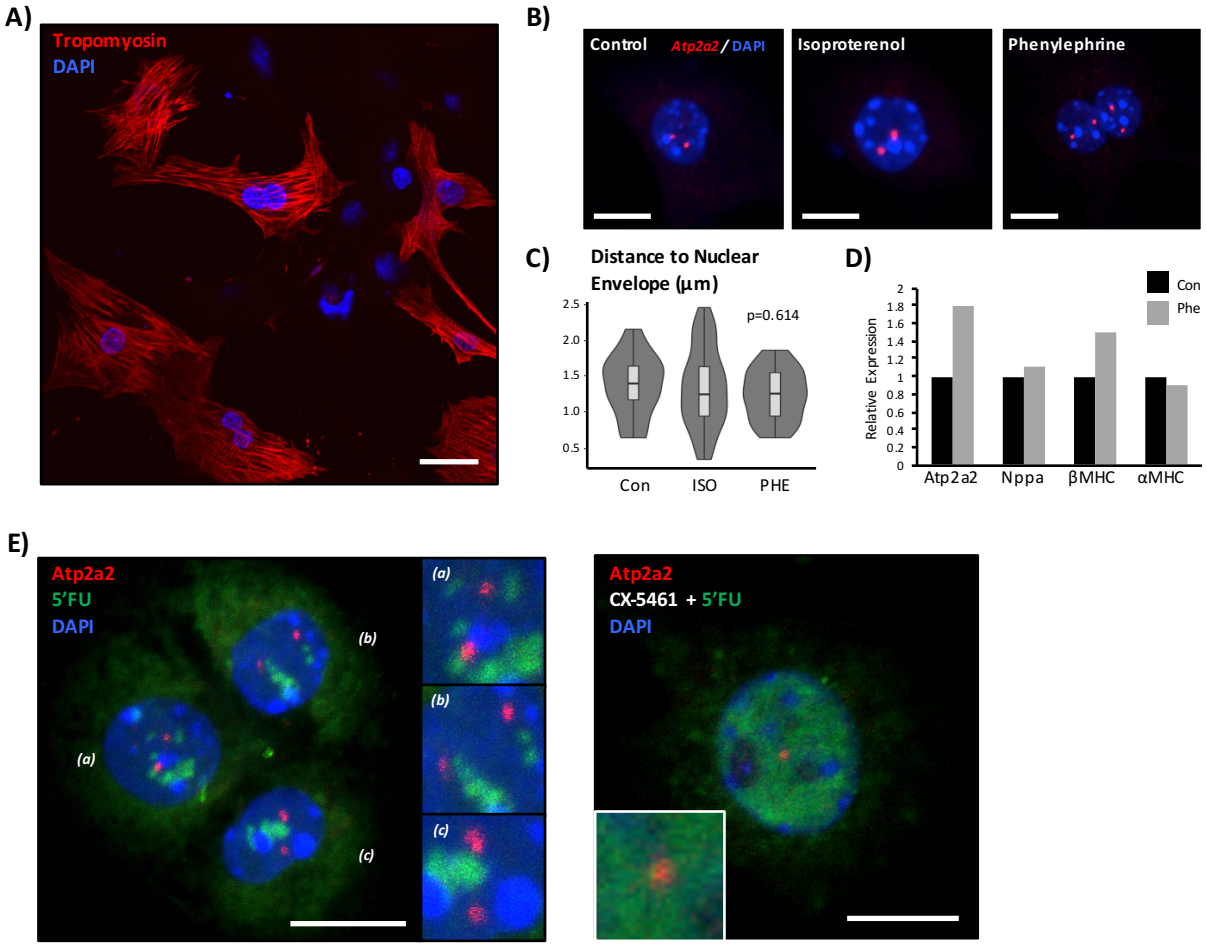

Figure 6-19: Atp2a2 localization upon agonist treatment in neonatal mouse myocytes does not change. A) Isolated neonatal mouse myocytes (positively labeled with tropomyosin to distinguish cardiomyocytes from non-cardiomyocytes) were used as a model to understand nuclear architecture and gene expression. Because we had set up the design of mouse FISH probes and *in situ* labeling of transcriptional activity, using 5'fluorouridine, we selected this model to proceed with our study. *Scale bar 25µm.* **B)** Representative images of Atp2a2 labeling in neonatal mouse cardiomyocytes show successful labeling of both loci after hypertrophic agonist treatment (48hr 1µM isoproterenol [ISO], 48hr 10µM phenylephrine [PHE]). *Scale bar 10µm.* **C)** Imaris software was used to measure the shortest distance of FISH loci to the nuclear periphery for each locus. No significant changes were observed *[one-way ANOVA]. Control: n=8 nuclei, 16 loci; ISO: n=20 nuclei, 42 loci; Phe: n=15 nuclei, 29 loci.* **D)** Gene expression measurements recapitulate expected trends of pathological gene expression, with the exception of Atp2a2 which was upregulated (opposite of what we expected). We later found that neonatal mouse myocytes may not be the best models to study pathological hypertrophy since they are still developing [39]. **E)** Atp2a2 were mapped with respect to sites of active transcription (30min 5'fluorouridine labeling), total transcription *(left)* and RNA polymerase II mediated transcription *(right)*. Scale *bar 10µm.*

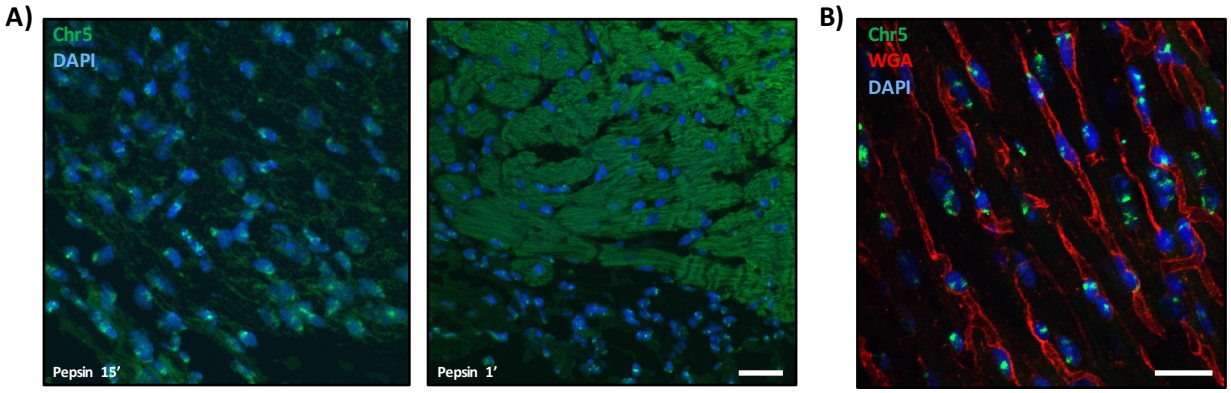

Figure 6-20: Chromosome labeling in the adult mouse heart. A) In order to troubleshoot the DNA FISH labeling protocol in adult heart tissue sections, we started with commercial chromosome 5 paints (Cytocell). Many protocols typically use heat or enzymatic digestion steps for antigen retrieval. Because the heart is a dense tissue, we initially tried pepsin digestion to achieve high labeling efficiency. While the digestion effectively allowed for chromosome labeling, we thought it would be problematic in our analyses where we want to preserve cellular and nuclear integrity to better understand *in situ* nuclear architecture. Tissue integrity can be noted by tissue autofluorescence from the green channel observed in heart sections digested for different times. **B)** We switched over to use buffers from a commercially available tissue pretreatment kit for FISH (Cytocell) and used a heat antigen retrieval approach. This approach worked well for chromosome paints. For DNA FISH of individual genes, the efficiency was much lower, but we were confident that tissue structure was maintained. *Scale bar = 25μm.*

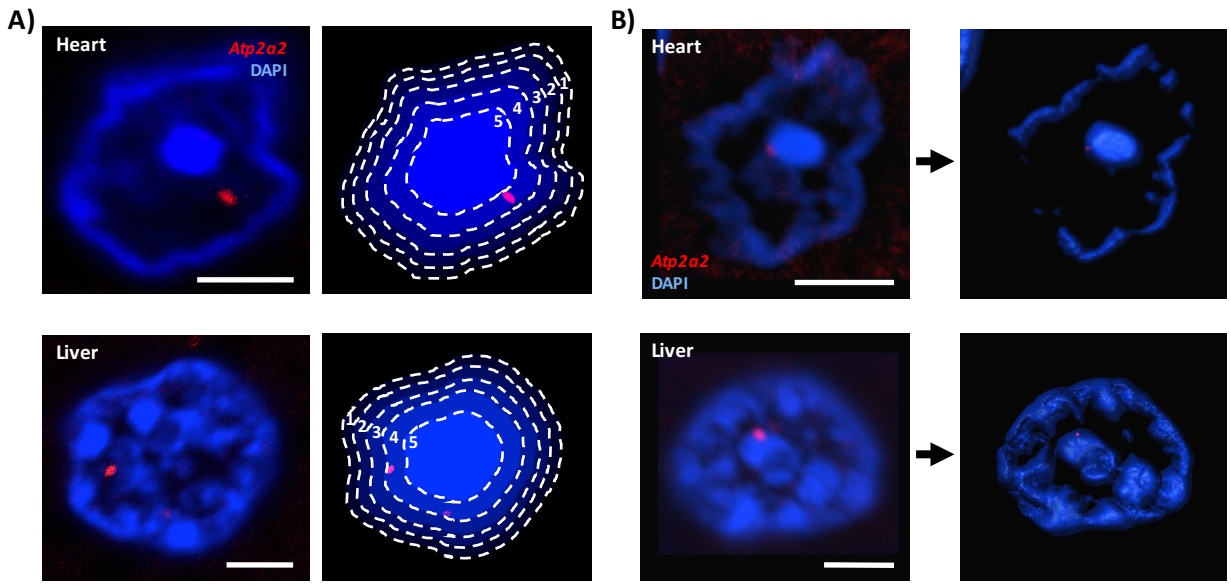

Figure 6-21: DNA FISH analysis with respect to nuclear landmarks. A) DNA FISH measurements to the nuclear periphery were normalized for shape and size between nuclei by using DAPI to bin the nucleus into 5 equal area annuli, allowing for the same probability of finding a locus in any given bin [30]. Afterwards, loci were assigned a bin location (1 near the periphery to 5 at the center) for analysis. We used a Chi-squared test to compare distributions between sham and TAC conditions. **B)** To measure the distance to heterochromatin, a DAPI intensity threshold was used in Imaris software to create a surface. The closest distance of the FISH spot to outer DAPI surface was measured. If loci were found in the surface (within the heterochromatin), they were assigned a distance of 0. We have previously confirmed that these intense DAPI signals corresponds with constitutive heterochromatin, marked by H3K9me3. The average distances were compared using a Mann-Whitney test while the percent of loci that colocalized were analyzed using a Chi-squared test. *Scale bar = 3μm.*

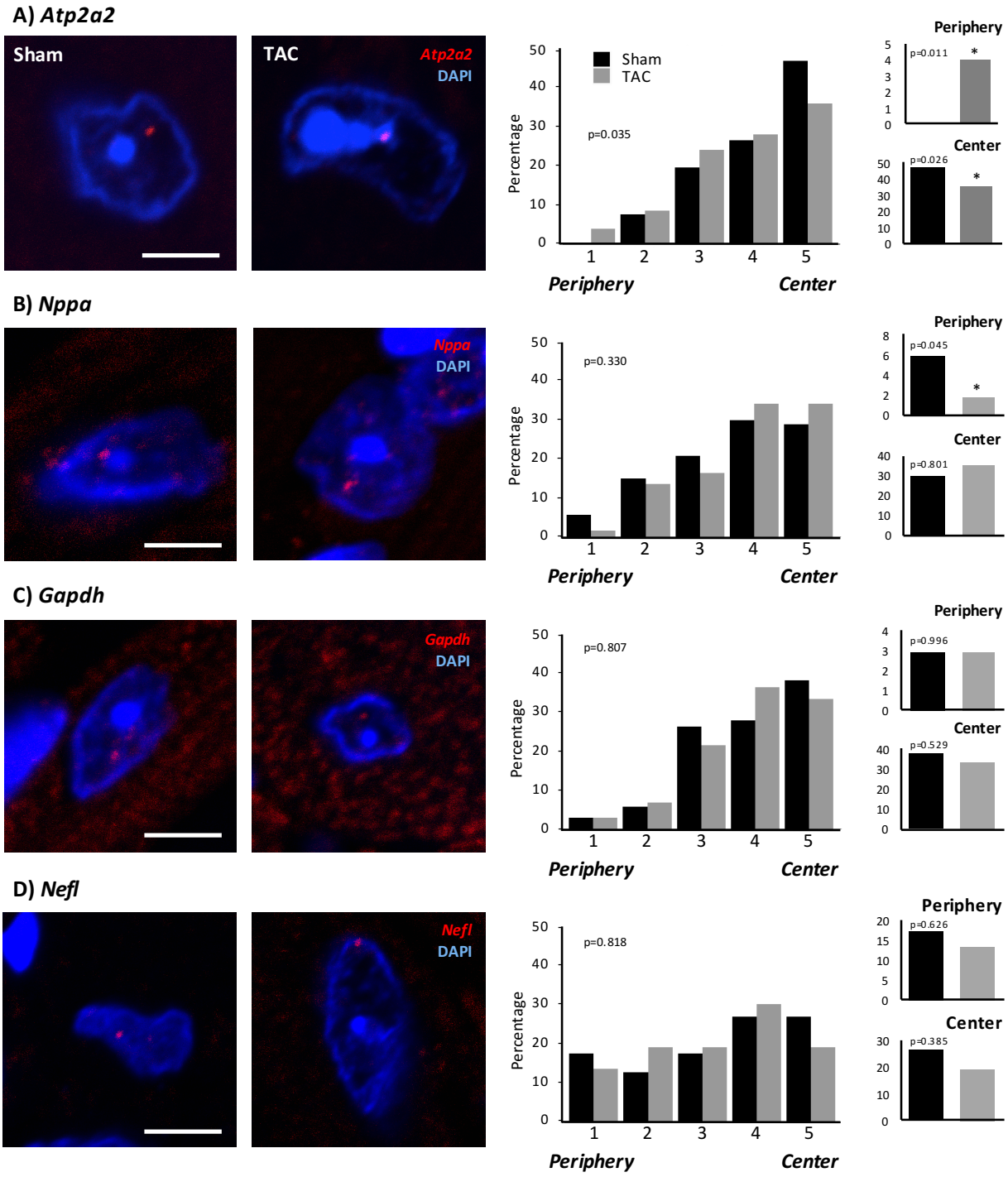
A) Atp2a2
Sham
TAC
Atp2a2
DAPI
Sham
TAC
p=0.035
Percentage
Periphery
Center
p=0.011
p=0.026
B) Nppa
Nppa
DAPI
p=0.330
p=0.045
p=0.801
C) Gapdh
Gapdh
DAPI
p=0.807
p=0.996
p=0.529
D) Nefl
Nefl
DAPI
p=0.818
p=0.626
p=0.385

Figure 6-22: Cardiac gene localization is associated with differential expression in the failing heart. DNA FISH was performed in adult mice, either control or those that had developed heart failure. Heart tissue sections were labeled for the following genes Atp2a2 **(A)**, Nppa **(B)**, Gapdh **(C)** and Nefl **(D)**. WGA counterstain was used to differentiate cardiomyocyte versus non-cardiomyocyte nuclei in the tissue. To assess the nuclear positioning of these genes, cardiomyocyte nuclei were binned into 5 concentric regions of equal area, and loci were assigned a bin (1, periphery to 5, center). The entire distribution is shown, with bins 1 (Periphery) and 5 (Center) highlighted on the *right*. Quantitation is compiled from different labeling experiments from 2-3 different hearts per treatment. *Atp2a2: Sham n=159, TAC n=280; Nppa: Sham n=77, TAC n=176; Gapdh: Sham n=69, TAC n=103; Nefl: Sham n=64, TAC n=37. Scale bar = 5μm. * p<0.05 [Chi-squared].*

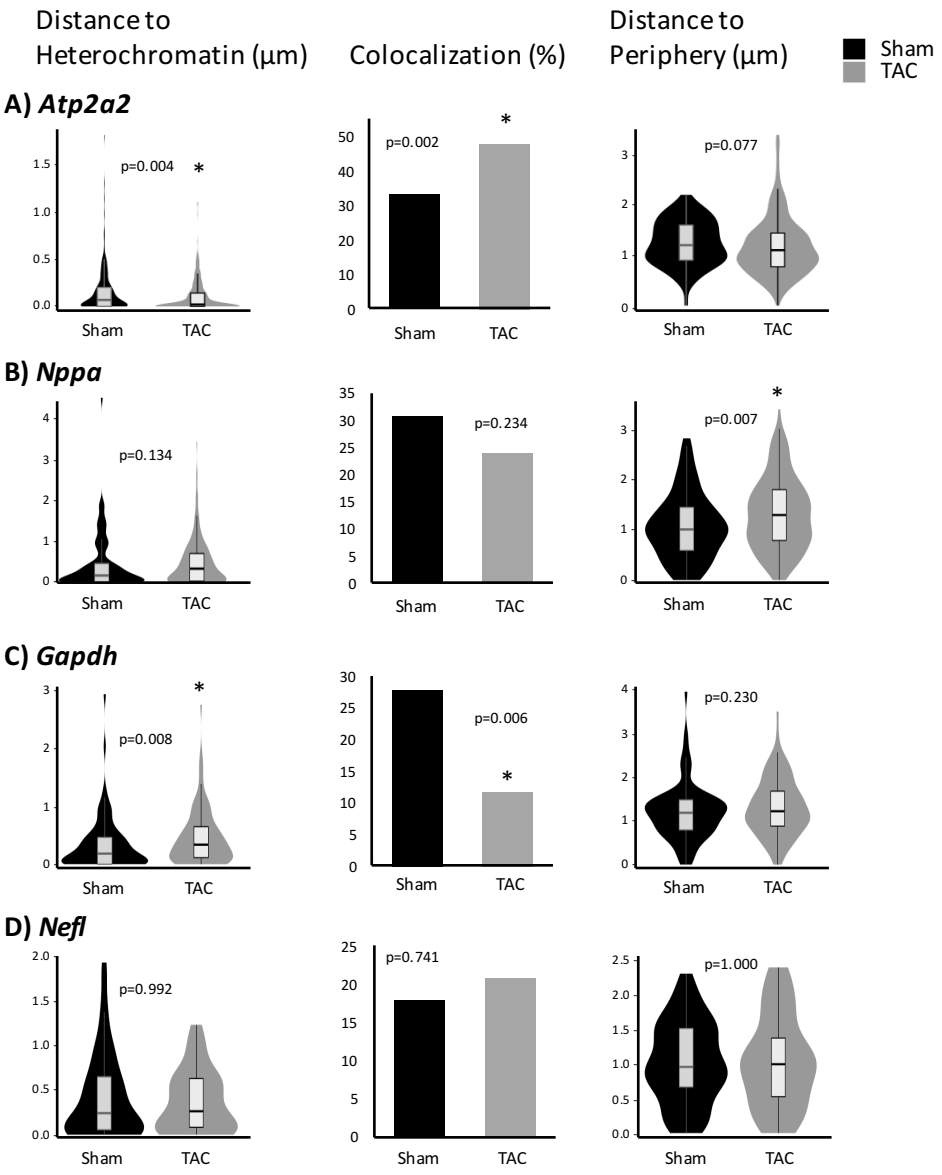

Figure 6-23: Gene association with heterochromatin and the nuclear envelope in cardiomyocyte nuclei. The distribution of absolute distances to heterochromatin are shown on *left*. As described in Figure 6-21B, DAPI intensity was used to threshold the most intensely labeled regions, designed as heterochromatin (DAPI intense regions colocalize with heterochromatin mark H3K9me3, data not shown). For the loci with distances of 0 (associate directly with heterochromatin), the fraction that colocalize are shown in *center*. In addition to performing the binned assessments of radial positioning of genes, we have plotted the absolute distances to the nuclear periphery (note that these are absolute distances and do not account for differences in nuclear shape or area) *(right)*. *Atp2a2: Sham n=71, TAC n=191; Nppa: Sham n=92, TAC n=179; Gapdh: Sham n=80, TAC n=105; Nefl: Sham n=67, TAC n=39. * p<0.05 [Mann-Whitney; for colocalization, Chi-squared].*

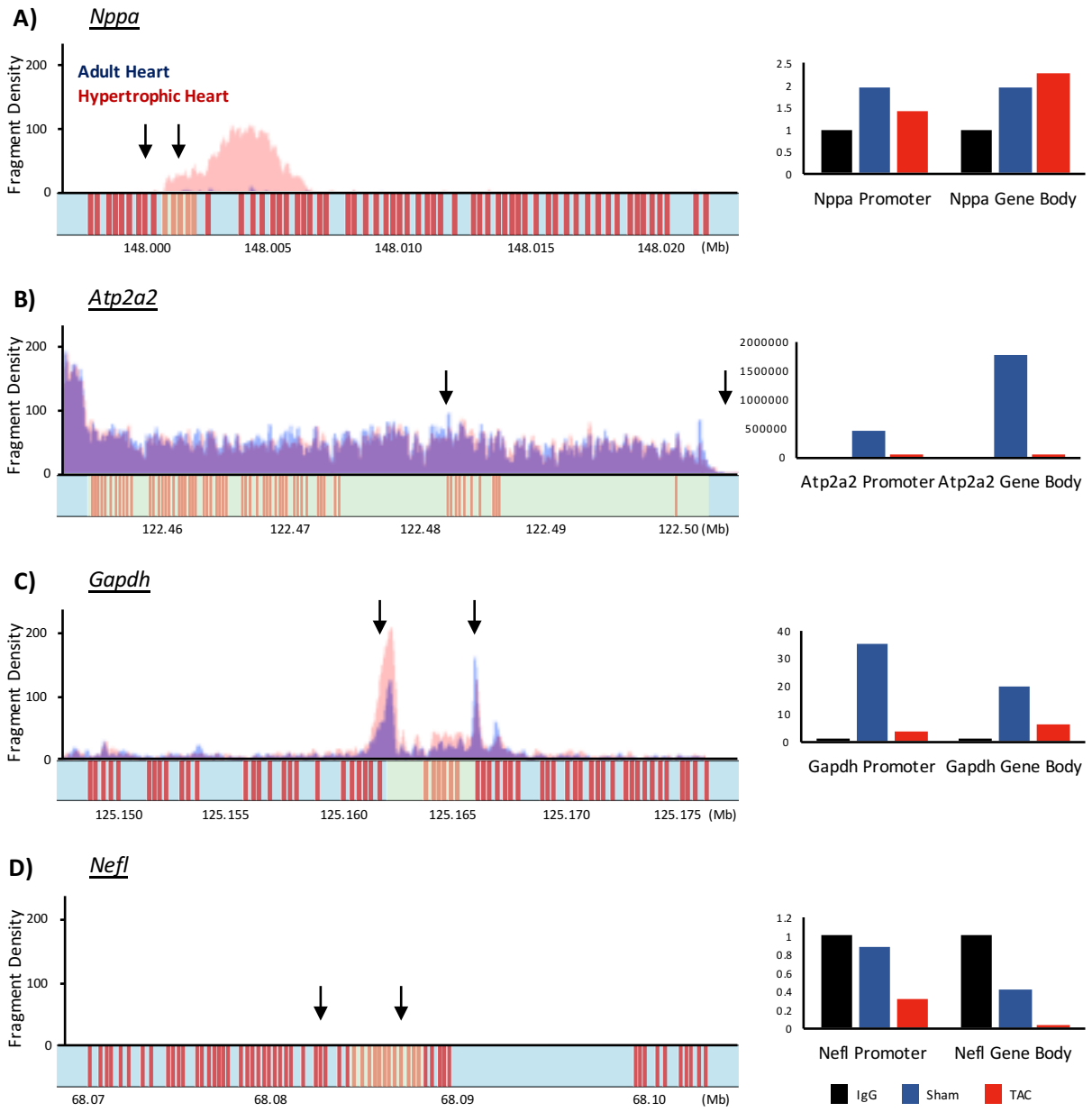

Figure 6-24: RNA polymerase II occupancy confers relationship between gene expression and association with transcription factories. *Left:* To determine association of genes with transcription factories, we converted the coordinates of our primers from mm10 to mm9 (using liftOver tool) to compare to published RNA polymerase II ChIP-seq (active RNA polymerase II, phosphorylated at serine 2) performed in hearts of sham and TAC mice (4 days after surgery) [40]. We have mapped above the signal from the ChIP-seq (sham in blue, TAC in red) at the regions we have targeted by DNA FISH. Fragment density indicates the number of mapped fragments per bin. *Right:* We next used ChIP-PCR to validate these findings in our mice that were in heart failure. ChIP-PCR was performed on isolated cardiomyocytes pooled from 6-7mice/group. IPs were normalized to input and fold enrichment over IgG is shown. Location of the primers used for promoter and gene body regions are indicated by arrows. Our results show increased enrichment of RNA polymerase II at the Nppa gene body, decreased enrichment at Atp2a2 and Gapdh genes and no enrichment at the Nefl gene.

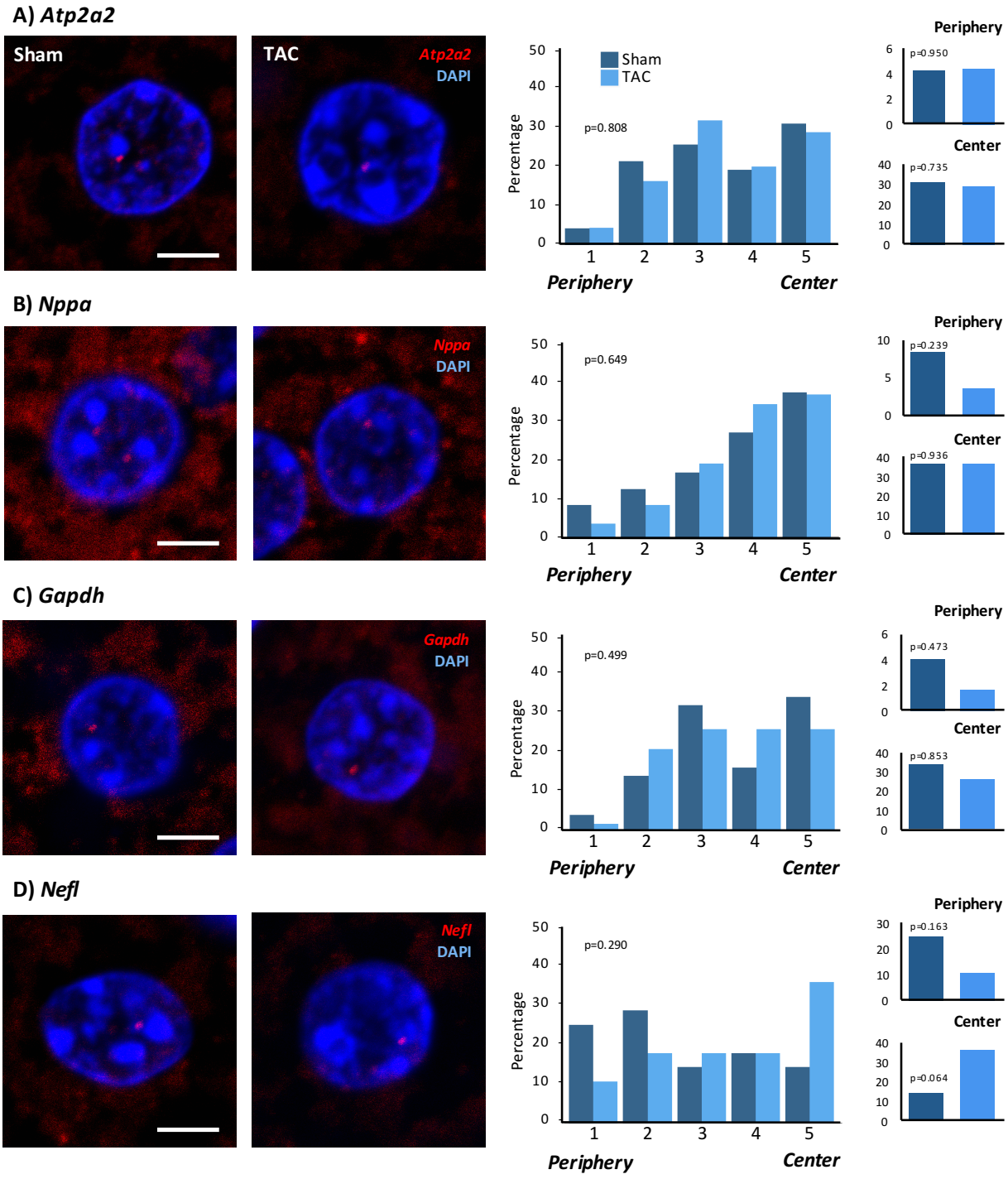
A) Atp2a2
Sham
TAC
Atp2a2
DAPI
Sham
TAC
p=0.808
Percentage
Periphery
Center
p=0.950
p=0.735
B) Nppa
Nppa
DAPI
p=0.649
p=0.239
p=0.936
C) Gapdh
Gapdh
DAPI
p=0.499
p=0.473
p=0.853
D) Nefl
Nefl
DAPI
p=0.290
p=0.163
p=0.064

Figure 6-25: Distribution of DNA FISH loci in liver nuclei is unaffected after pressure-overload stress. DNA FISH labeling in liver tissue from mice with heart failure was used to assess the tissue-specificity of genomic architecture. Furthermore, based on DAPI patterns, liver nuclei have very different nuclear shape and architecture. The distributions of Atp2a2 **(A)**, Nppa **(B)**, Gapdh **(C)** and Nefl **(D)** are not affected by TAC surgery. Quantitation is compiled from different labeling experiments from 2 different mice per treatment. *Atp2a2: Sham n=97, TAC n=137; Nppa: Sham n=49, TAC n=86; Gapdh: Sham n=50, TAC n=58; Nefl: Sham n=28, TAC n=28. Scale bar = 5μm. P values were calculated using Chi-squared test.*

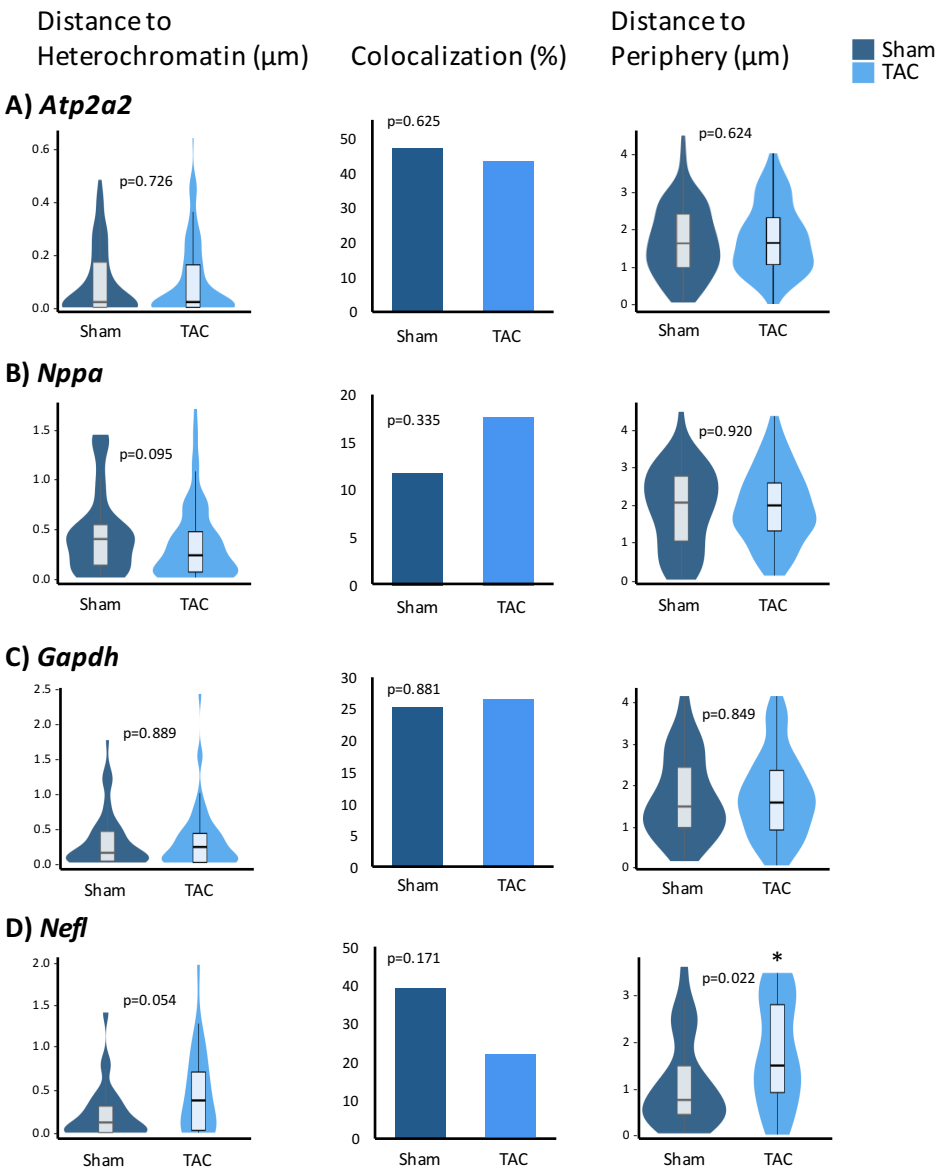

Figure 6-26: Gene association with heterochromatin and the nuclear envelope in hepatocyte nuclei. As done for in the heart, the distances with respect to heterochromatin are plotted. The distribution of absolute distances is shown on the *left* and the fraction that colocalize are shown in the *middle.* The absolute distances to the nuclear periphery are shown on *right.* TAC surgery does not impact gene localization in the liver. However, the distance to the nuclear periphery does increase for Nefl, which may be explained by effects of TAC at nearby genomic loci in the liver. *Atp2a2: Sham n=94, TAC n=140; Nppa: Sham n=52, TAC n=85; Gapdh: Sham n=52, TAC n=61; Nefl: Sham n=28, TAC n=28. * p<0.05 [Mann-Whitney; for colocalization, Chi-squared test was used].*

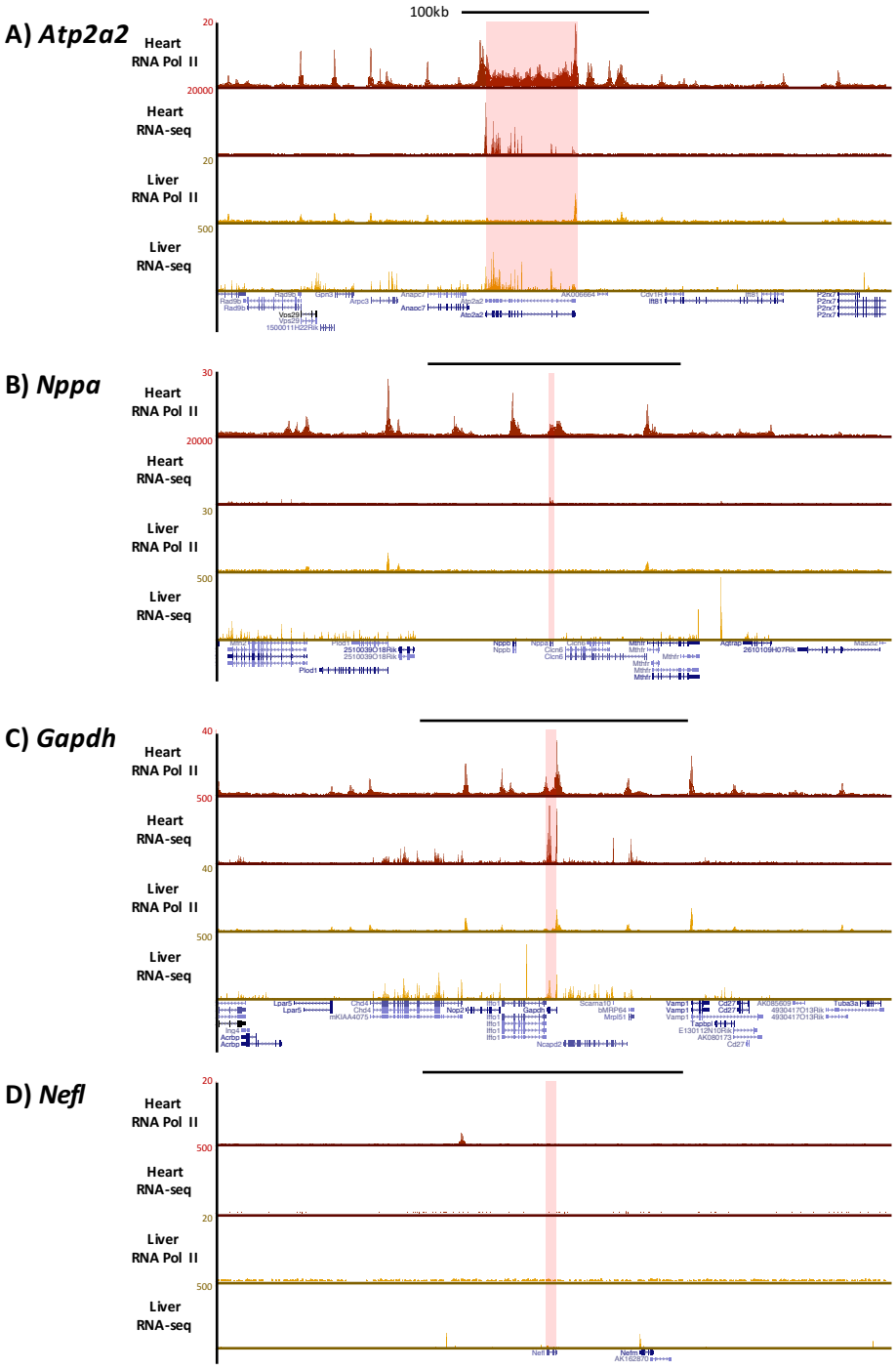
A) Atp2a2
100kb
Heart RNA Pol II
Heart RNA-seq
Liver RNA Pol II
Liver RNA-seq
B) Nppa
C) Gapdh
D) Nefl

Figure 6-27: Transcriptional activity, marked by RNA polymerase II enrichment and RNA-seq, at flanking sites in basal heart and liver. We used mm9 coordinates in the UCSC genome browser to examine RNA polymerase II occupancy and RNA-seq signal surrounding the genes analyzed by DNA FISH (gene bodies highlighted by pink box) to assess their environment on a linear scale for transcriptional activity. Nppa has RNA polymerase II peaks at regions outside of the gene in the basal heart, and these may influence its positioning in the nucleus despite the gene being silent. We see smaller RNA-seq signal in the liver surrounding Nppa and Atp2a2. These genes were chosen because of their cardiac specificity. It is still to be determined how much influence the smaller expression peaks have on locus positioning. On the other hand, Nefl is isolated in transcriptionally silent regions, which may explain its stronger associations with heterochromatin and nuclear envelope. Localization on a linear scale is one approach to determine nearby activity, but it is also important to take into account the 3D environment and transcriptional activity of interacting regions outside of the ~200kb region shown here.

(1) Do transcription factories exist in cardiomyocytes? Are they maintained after stress?

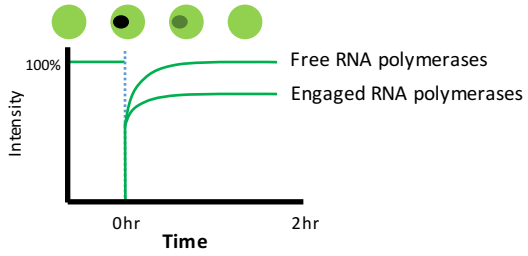

(2) How does stress affect transcription factory activity?

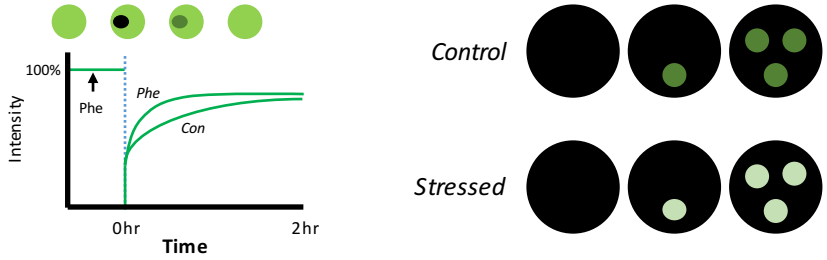

Figure 6-28: Fluorescence Recovery After Photobleaching (FRAP) can reveal transcription factory properties. Our STED results suggest that RNA polymerase II is fixed into factories. This was demonstrated by showing that the distribution of active RNA polymerase II is not affected with stress. To validate these properties, I propose to perform a FRAP experiment in cultured cardiomyocytes that will express GFP-tagged RNA polymerase II (tagged at its CTD domain; GFP-Pol II). We can address 2 questions: *1)* do transcription factories exist in cardiomyocytes, and are they maintained after stress? and *2)* does stress affect activity? *Top:* If RNA polymerases do form compartments, this would suggest that they are engaged. If we bleach a region of the nucleus, these polymerases would not be displaced and the intensity recovery would not reach 100%. On the other hand, if transcription factories are nonexistent in cardiomyocytes, then we expect them to freely diffuse (similar to a GFP-only control) and to recover total signal in our region of interest. *Bottom:* The second part addresses our observation from microscopy showing that there are significant increases in cluster intensity. This would suggest RNA polymerase II clusters are being recruited to factories. To test this, we would treat cells with phenylephrine, a hypertrophic agonist, and then perform FRAP soon after. I would expect, based on our current model, that the rate of increase in intensity of the bleached region would be faster in the hypertrophic cells (also illustrated on *right*).

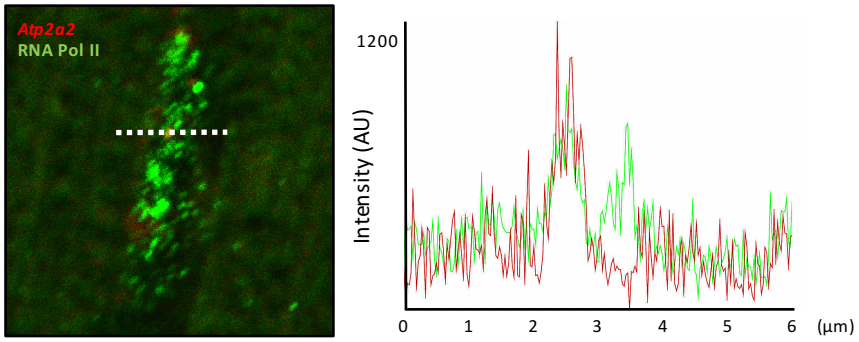

Figure 6-29: Association of gene expression with localization at RNA polymerase II factories. We initiated analyses examining localization of DNA FISH signal to RNA polymerase II factories with images taken by confocal microscopy. Due to the size constraints of the nucleus and the abundance of RNA polymerase II molecules, this analysis requires super-resolution methods to better resolve RNA polymerase II clusters. Above is a representative image of a nucleus from the sham heart, with an intensity scan across the indicated region. This approach indicates colocalization (FISH signal peak is ~800nm in width), though more precise quantitative measurements will be necessary to uncover spatial information that can be used to compare between conditions. Currently, we are working on acquiring this data using STED imaging.

Chapter 6: References

1. Rosa-Garrido M, Karbassi E, Monte E, Vondriska TM. Regulation of chromatin structure in the cardiovascular system. Circ J. 2013;77(6):1389-98. PubMed PMID: 23575346; PMCID: PMC3704339.
2. Franklin S, Chen HD, Mitchell-Jordan S, Ren SX, Wang YB, Vondriska TM. Quantitative Analysis of the Chromatin Proteome in Disease Reveals Remodeling Principles and Identifies High Mobility Group Protein B2 as a Regulator of Hypertrophic Growth. Molecular & Cellular Proteomics. 2012;11(6). doi: ARTN M111.014258 10.1074/mcp.M111.014258. PubMed PMID: WOS:000306408500019.
3. Monte E, Rosa-Garrido M, Karbassi E, Chen H, Lopez R, Rau CD, Wang J, Nelson SF, Wu Y, Stefani E, Lusis AJ, Wang Y, Kurdistani SK, Franklin S, Vondriska TM. Reciprocal Regulation of the Cardiac Epigenome by Chromatin Structural Proteins Hmgb and Ctcf: IMPLICATIONS FOR TRANSCRIPTIONAL REGULATION. J Biol Chem. 2016;291(30):15428-46. doi: 10.1074/jbc.M116.719633. PubMed PMID: 27226577; PMCID: PMC4957031.
4. Cutilletta AF, Rudnik M, Zak R. Muscle and non-muscle cell RNA polymerase activity during the development of myocardial hypertrophy. J Mol Cell Cardiol. 1978;10(8):677-87. PubMed PMID: 151746.
5. Dixon JR, Jung I, Selvaraj S, Shen Y, Antosiewicz-Bourget JE, Lee AY, Ye Z, Kim A, Rajagopal N, Xie W, Diao Y, Liang J, Zhao H, Lobanenkov VV, Ecker JR, Thomson JA, Ren B. Chromatin architecture reorganization during stem cell differentiation. Nature. 2015;518(7539):331-6. doi: 10.1038/nature14222. PubMed PMID: 25693564; PMCID: PMC4515363.

6. Arvey A, Agius P, Noble WS, Leslie C. Sequence and chromatin determinants of cell-type-specific transcription factor binding. Genome Res. 2012;22(9):1723-34. doi: 10.1101/gr.127712.111. PubMed PMID: 22955984; PMCID: PMC3431489.
7. Thurman RE, Rynes E, Humbert R, Vierstra J, Maurano MT, Haugen E, Sheffield NC, Stergachis AB, Wang H, Vernot B, Garg K, John S, Sandstrom R, Bates D, Boatman L, Canfield TK, Diegel M, Dunn D, Ebersol AK, Frum T, Giste E, Johnson AK, Johnson EM, Kutyavin T, Lajoie B, Lee BK, Lee K, London D, Lotakis D, Neph S, Neri F, Nguyen ED, Qu H, Reynolds AP, Roach V, Safi A, Sanchez ME, Sanyal A, Shafer A, Simon JM, Song L, Vong S, Weaver M, Yan Y, Zhang Z, Zhang Z, Lenhard B, Tewari M, Dorschner MO, Hansen RS, Navas PA, Stamatoyannopoulos G, Iyer VR, Lieb JD, Sunyaev SR, Akey JM, Sabo PJ, Kaul R, Furey TS, Dekker J, Crawford GE, Stamatoyannopoulos JA. The accessible chromatin landscape of the human genome. Nature. 2012;489(7414):75-82. doi: 10.1038/nature11232. PubMed PMID: 22955617; PMCID: PMC3721348.
8. Schneider R, Grosschedl R. Dynamics and interplay of nuclear architecture, genome organization, and gene expression. Genes Dev. 2007;21(23):3027-43. doi: 10.1101/gad.1604607. PubMed PMID: 18056419.
9. Cremer T, Cremer C. Chromosome territories, nuclear architecture and gene regulation in mammalian cells. Nat Rev Genet. 2001;2(4):292-301. doi: 10.1038/35066075. PubMed PMID: 11283701.
10. Cremer T, Cremer M. Chromosome Territories. Csh Perspect Biol. 2010;2(3). doi: ARTN a003889 10.1101/cshperspect.a003889. PubMed PMID: WOS:000279881700015.
11. Lieberman-Aiden E, van Berkum NL, Williams L, Imakaev M, Ragoczy T, Telling A, Amit I, Lajoie BR, Sabo PJ, Dorschner MO, Sandstrom R, Bernstein B, Bender MA, Groudine M, Gnirke A, Stamatoyannopoulos J, Mirny LA, Lander ES, Dekker J. Comprehensive mapping of long-range interactions reveals folding principles of the human genome. Science.

2009;326(5950):289-93. doi: 10.1126/science.1181369. PubMed PMID: 19815776; PMCID: PMC2858594.

12. Dixon JR, Selvaraj S, Yue F, Kim A, Li Y, Shen Y, Hu M, Liu JS, Ren B. Topological domains in mammalian genomes identified by analysis of chromatin interactions. Nature. 2012;485(7398):376-80. doi: 10.1038/nature11082. PubMed PMID: 22495300; PMCID: PMC3356448.
13. Rieder D, Trajanoski Z, McNally JG. Transcription factories. Front Genet. 2012;3:221. doi: 10.3389/fgene.2012.00221. PubMed PMID: 23109938; PMCID: PMC3478587.
14. Hozak P, Cook PR, Schofer C, Mosgoller W, Wachtler F. Site of transcription of ribosomal RNA and intranucleolar structure in HeLa cells. J Cell Sci. 1994;107 (Pt 2):639-48. PubMed PMID: 8207086.
15. Kimura H, Sugaya K, Cook PR. The transcription cycle of RNA polymerase II in living cells. J Cell Biol. 2002;159(5):777-82. doi: 10.1083/jcb.200206019. PubMed PMID: 12473686; PMCID: PMC2173384.
16. Jackson DA, Hassan AB, Errington RJ, Cook PR. Visualization of focal sites of transcription within human nuclei. EMBO J. 1993;12(3):1059-65. PubMed PMID: 8458323; PMCID: PMC413307.
17. Iborra FJ, Pombo A, Jackson DA, Cook PR. Active RNA polymerases are localized within discrete transcription 'factories' in human nuclei (vol 109, pg 1427, 1996). Journal of Cell Science. 1998;111:2280-. PubMed PMID: WOS:000075436700021.
18. Osborne CS, Chakalova L, Brown KE, Carter D, Horton A, Debrand E, Goyenechea B, Mitchell JA, Lopes S, Reik W, Fraser P. Active genes dynamically colocalize to shared sites of ongoing transcription. Nat Genet. 2004;36(10):1065-71. doi: 10.1038/ng1423. PubMed PMID: 15361872.
19. Zhao ZW, Roy R, Gebhardt JC, Suter DM, Chapman AR, Xie XS. Spatial organization of RNA polymerase II inside a mammalian cell nucleus revealed by reflected light-sheet

superresolution microscopy. Proc Natl Acad Sci U S A. 2014;111(2):681-6. doi: 10.1073/pnas.1318496111. PubMed PMID: 24379392; PMCID: PMC3896202.

20. Guelen L, Pagie L, Brasset E, Meuleman W, Faza MB, Talhout W, Eussen BH, de Klein A, Wessels L, de Laat W, van Steensel B. Domain organization of human chromosomes revealed by mapping of nuclear lamina interactions (vol 453, pg 948, 2008). Nature. 2013;500(7461):242-. doi: 10.1038/nature12316. PubMed PMID: WOS:000322825500042.
21. Zullo JM, Demarco IA, Pique-Regi R, Gaffney DJ, Epstein CB, Spooner CJ, Luperchio TR, Bernstein BE, Pritchard JK, Reddy KL, Singh H. DNA sequence-dependent compartmentalization and silencing of chromatin at the nuclear lamina. Cell. 2012;149(7):1474-87. doi: 10.1016/j.cell.2012.04.035. PubMed PMID: 22726435.
22. Reddy KL, Zullo JM, Bertolino E, Singh H. Transcriptional repression mediated by repositioning of genes to the nuclear lamina. Nature. 2008;452(7184):243-7. doi: 10.1038/nature06727. PubMed PMID: 18272965.
23. Kind J, Pagie L, Ortabozkoyun H, Boyle S, de Vries SS, Janssen H, Amendola M, Nolen LD, Bickmore WA, van Steensel B. Single-cell dynamics of genome-nuclear lamina interactions. Cell. 2013;153(1):178-92. doi: 10.1016/j.cell.2013.02.028. PubMed PMID: 23523135.
24. Kehat I, Accornero F, Aronow BJ, Molkentin JD. Modulation of chromatin position and gene expression by HDAC4 interaction with nucleoporins. J Cell Biol. 2011;193(1):21-9. doi: 10.1083/jcb.201101046. PubMed PMID: 21464227; PMCID: PMC3082185.
25. Mitchell-Jordan S, Chen HD, Franklin S, Stefani E, Bentolila LA, Vondriska TM. Features of endogenous cardiomyocyte chromatin revealed by super-resolution STED microscopy. Journal of Molecular and Cellular Cardiology. 2012;53(4):552-8. doi: 10.1016/j.yjmcc.2012.07.009. PubMed PMID: WOS:000308679700010.
26. Casafont I, Navascues J, Pena E, Lafarga M, Berciano MT. Nuclear organization and dynamics of transcription sites in rat sensory ganglia neurons detected by incorporation of 5'-

fluorouridine into nascent RNA. Neuroscience. 2006;140(2):453-62. doi: 10.1016/j.neuroscience.2006.02.030. PubMed PMID: 16563640.

27. Drygin D, Lin A, Bliesath J, Ho CB, O'Brien SE, Proffitt C, Omori M, Haddach M, Schwaebe MK, Siddiqui-Jain A, Streiner N, Quin JE, Sanij E, Bywater MJ, Hannan RD, Ryckman D, Anderes K, Rice WG. Targeting RNA polymerase I with an oral small molecule CX-5461 inhibits ribosomal RNA synthesis and solid tumor growth. Cancer Res. 2011;71(4):1418-30. doi: 10.1158/0008-5472.CAN-10-1728. PubMed PMID: 21159662.
28. Bienko M, Crosetto N, Teytelman L, Klemm S, Itzkovitz S, van Oudenaarden A. A versatile genome-scale PCR-based pipeline for high-definition DNA FISH. Nat Methods. 2013;10(2):122-4. doi: 10.1038/nmeth.2306. PubMed PMID: 23263692; PMCID: PMC3735345.
29. Solovei I, Cremer M. 3D-FISH on cultured cells combined with immunostaining. Methods Mol Biol. 2010;659:117-26. doi: 10.1007/978-1-60761-789-1_8. PubMed PMID: 20809307.
30. Therizols P, Illingworth RS, Courilleau C, Boyle S, Wood AJ, Bickmore WA. Chromatin decondensation is sufficient to alter nuclear organization in embryonic stem cells. Science. 2014;346(6214):1238-42. doi: 10.1126/science.1259587. PubMed PMID: WOS:000346189000060.
31. Brandenburger Y, Arthur JF, Woodcock EA, Du XJ, Gao XM, Autelitano DJ, Rothblum LI, Hannan RD. Cardiac hypertrophy in vivo is associated with increased expression of the ribosornal gene transcription factor UBF. Febs Lett. 2003;548(1-3):79-84. doi: 10.1016/S0014-5793(03)00744-0. PubMed PMID: WOS:000184536100015.
32. Goodfellow SJ, Graham EL, Kantidakis T, Marshall L, Coppins BA, Oficjalska-Pham D, Gerard M, Lefebvre O, White RJ. Regulation of RNA Polymerase III Transcription by Maf1 in Mammalian Cells (vol 378, pg 481, 2008). J Mol Biol. 2013;425(6):1099-. doi: 10.1016/j.jmb.2012.12.006. PubMed PMID: WOS:000316841100011.

33. Kimura H, Sugaya K, Cook PR. The transcription cycle of RNA polymerase II in living cells. Journal of Cell Biology. 2002;159(5):777-82. doi: 10.1083/jcb.200206019. PubMed PMID: WOS:000179814700006.

34. Jackson DA, Hassan AB, Errington RJ, Cook PR. Visualization of Focal Sites of Transcription within Human Nuclei. Embo Journal. 1993;12(3):1059-65. PubMed PMID: WOS:A1993KR53900027.

35. Wansink DG, Schul W, van der Kraan I, van Steensel B, van Driel R, de Jong L. Fluorescent labeling of nascent RNA reveals transcription by RNA polymerase II in domains scattered throughout the nucleus. J Cell Biol. 1993;122(2):283-93. PubMed PMID: 8320255; PMCID: PMC2119648.

36. Rajabi M, Kassiotis C, Razeghi P, Taegtmeyer H. Return to the fetal gene program protects the stressed heart: a strong hypothesis. Heart Failure Reviews. 2007;12(3-4):331-43. doi: 10.1007/s10741-007-9034-1. PubMed PMID: WOS:000248170900017.

37. Cahoy JD, Emery B, Kaushal A, Foo LC, Zamanian JL, Christopherson KS, Xing Y, Lubischer JL, Krieg PA, Krupenko SA, Thompson WJ, Barres BA. A transcriptome database for astrocytes, neurons, and oligodendrocytes: a new resource for understanding brain development and function. J Neurosci. 2008;28(1):264-78. doi: 10.1523/JNEUROSCI.4178-07.2008. PubMed PMID: 18171944.

38. Finlan LE, Sproul D, Thomson I, Boyle S, Kerr E, Perry P, Ylstra B, Chubb JR, Bickmore WA. Recruitment to the nuclear periphery can alter expression of genes in human cells. Plos Genetics. 2008;4(3). doi: ARTN e1000039 10.1371/journal.pgen.1000039. PubMed PMID: WOS:000255407300013.

39. Deng XF, Rokosh DG, Simpson PC. Autonomous and growth factor-induced hypertrophy in cultured neonatal mouse cardiac myocytes. Comparison with rat. Circ Res. 2000;87(9):781-8. PubMed PMID: 11055982.

40. Sayed D, He MZ, Yang Z, Lin L, Abdellatif M. Transcriptional Regulation Patterns Revealed by High Resolution Chromatin Immunoprecipitation during Cardiac Hypertrophy. Journal of Biological Chemistry. 2013;288(4):2546-58. doi: 10.1074/jbc.M112.429449. PubMed PMID: WOS:000314211500040.
41. Moller S, Bernardi M. Interactions of the heart and the liver. Eur Heart J. 2013;34(36):2804-11. doi: 10.1093/eurheartj/eht246. PubMed PMID: 23853073.
42. Lee H, Adams WJ, Alford PW, McCain ML, Feinberg AW, Sheehy SP, Goss JA, Parker KK. Cytoskeletal prestress regulates nuclear shape and stiffness in cardiac myocytes. Exp Biol Med (Maywood). 2015;240(11):1543-54. doi: 10.1177/1535370215583799. PubMed PMID: 25908635; PMCID: PMC4778402.
43. Kempe H, Schwabe A, Cremazy F, Verschure PJ, Bruggeman FJ. The volumes and transcript counts of single cells reveal concentration homeostasis and capture biological noise. Mol Biol Cell. 2015;26(4):797-804. doi: 10.1091/mbc.E14-08-1296. PubMed PMID: 25518937; PMCID: PMC4325848.
44. Zhurinsky J, Leonhard K, Watt S, Marguerat S, Bahler J, Nurse P. A Coordinated Global Control over Cellular Transcription. Curr Biol. 2010;20(22):2010-5. doi: 10.1016/j.cub.2010.10.002. PubMed PMID: WOS:000284923700024.
45. Kirby TJ, Patel RM, McClintock TS, Dupont-Versteegden EE, Peterson CA, McCarthy JJ. Myonuclear transcription is responsive to mechanical load and DNA content but uncoupled from cell size during hypertrophy. Molecular Biology of the Cell. 2016;27(5):788-98. doi: 10.1091/mbc.E15-08-0585. PubMed PMID: WOS:000370817000007.
46. Sayed D, Yang Z, He MZ, Pfleger JM, Abdellatif M. Acute Targeting of General Transcription Factor IIB Restricts Cardiac Hypertrophy via Selective Inhibition of Gene Transcription. Circ-Heart Fail. 2015;8(1):138-U228. doi: 10.1161/Circheartfailure.114.001660. PubMed PMID: WOS:000348145400018.

47. Sano M, Wang SC, Shirai M, Scaglia F, Xie M, Sakai S, Tanaka T, Kulkarni PA, Barger PM, Youker KA, Taffet GE, Hamamori Y, Michael LH, Craigen WJ, Schneider MD. Activation of cardiac Cdk9 represses PGC-1 and confers a predisposition to heart failure. EMBO J. 2004;23(17):3559-69. doi: 10.1038/sj.emboj.7600351. PubMed PMID: 15297879; PMCID: PMC516624.

48. Klotz S, Jan Danser AH, Burkhoff D. Impact of left ventricular assist device (LVAD) support on the cardiac reverse remodeling process. Prog Biophys Mol Biol. 2008;97(2-3):479-96. doi: 10.1016/j.pbiomolbio.2008.02.002. PubMed PMID: 18394685.

49. Batalov I, Feinberg AW. Differentiation of Cardiomyocytes from Human Pluripotent Stem Cells Using Monolayer Culture. Biomark Insights. 2015;10(Suppl 1):71-6. doi: 10.4137/BMI.S20050. PubMed PMID: 26052225; PMCID: PMC4447149.

50. Chen B, Gilbert LA, Cimini BA, Schnitzbauer J, Zhang W, Li GW, Park J, Blackburn EH, Weissman JS, Qi LS, Huang B. Dynamic imaging of genomic loci in living human cells by an optimized CRISPR/Cas system. Cell. 2013;155(7):1479-91. doi: 10.1016/j.cell.2013.12.001. PubMed PMID: 24360272; PMCID: PMC3918502.

51. Li G, Ruan X, Auerbach RK, Sandhu KS, Zheng M, Wang P, Poh HM, Goh Y, Lim J, Zhang J, Sim HS, Peh SQ, Mulawadi FH, Ong CT, Orlov YL, Hong S, Zhang Z, Landt S, Raha D, Euskirchen G, Wei CL, Ge W, Wang H, Davis C, Fisher-Aylor KI, Mortazavi A, Gerstein M, Gingeras T, Wold B, Sun Y, Fullwood MJ, Cheung E, Liu E, Sung WK, Snyder M, Ruan Y. Extensive promoter-centered chromatin interactions provide a topological basis for transcription regulation. Cell. 2012;148(1-2):84-98. doi: 10.1016/j.cell.2011.12.014. PubMed PMID: 22265404; PMCID: PMC3339270.

52. Fanucchi S, Shibayama Y, Burd S, Weinberg MS, Mhlanga MM. Chromosomal Contact Permits Transcription between Coregulated Genes. Cell. 2013;155(3):606-20. doi: 10.1016/j.cell.2013.09.051. PubMed PMID: WOS:000326571800015.

53. Croft JA, Bridger JM, Boyle S, Perry P, Teague P, Bickmore WA. Differences in the localization and morphology of chromosomes in the human nucleus. Journal of Cell Biology. 1999;145(6):1119-31. doi: DOI 10.1083/jcb.145.6.1119. PubMed PMID: WOS:000080945700001.

54. Hofmann WA, Stojiljkovic L, Fuchsova B, Vargas GM, Mavrommatis E, Philimonenko V, Kysela K, Goodrich JA, Lessard JL, Hope TJ, Hozak P, de Lanerolle P. Actin is part of pre-initiation complexes and is necessary for transcription by RNA polymerase II. Nature Cell Biology. 2004;6(11):1094-U18. doi: 10.1038/ncb1182. PubMed PMID: WOS:000224816700014.

55. Solovei I, Kreysing M, Lanctot C, Kosem S, Peichl L, Cremer T, Guck J, Joffe B. Nuclear Architecture of Rod Photoreceptor Cells Adapts to Vision in Mammalian Evolution. Cell. 2009;137(2):356-68. doi: 10.1016/j.cell.2009.01.052. PubMed PMID: WOS:000265456800027.

Future Directions

In this project, we took different approaches to investigate the factors that control cardiac gene expression to understand the fundamental question of how a cell achieves its identity. There is evidence that some such factors, including cellular environment, cell contacts, extracellular matrix and mechanical forces, affect stem cell differentiation (1) and that these signals are eventually relayed to the nucleus to regulate gene expression through effects on chromatin structure (2). With cellular differentiation, the nucleus undergoes changes in architecture and chromatin landscape (3-5). Here, we describe the roles of established epigenetic regulators in cardiac development in molding global genomic structure to influence transcription. From our analyses of the hybrid mouse diversity panel, we demonstrate that there is no single gene marker of cardiac disease: instead a network of genes influences phenotypic responses to pathological stress, with differential modulation of chromatin structure as an underlying mechanism.

We describe features of cardiac gene regulation and demonstrate that transcriptional activity is organized into factories. This provides insight into chromatin architecture, describing a role for transcription in recruiting regions of the genome in 3D to discrete sites, and suggests that destabilization of transcription factories may trigger pathological changes in gene expression. Further investigation on whether cardiac genes always associate with the same sets of genes in a factory (using chromatin interaction analysis by paired-end tag sequencing (6)) and identification of other protein components and transcription factors involved (through immunoprecipitation and mass spec approaches) will pinpoint key structural elements and cardiomyocyte-specific features required for the maintenance of the transcriptome. HMGB2 is an important regulator of cardiac gene expression and is enriched at cardiac enhancers (7). Exploration of HMGB2's function would provide insight into whether its influence on cardiac

transcription is through direct association with cardiac transcription factories. In our study, we show that gene positioning with respect to silencing compartments (e.g. nuclear lamina and heterochromatin) correlates with differential expression. We need to explore the 3D genomic context of these loci to integrate the regulation of local interactions, using chromatin conformation capture approaches (8) and DamID to map lamina-associating domains (9), in adult cardiomyocytes to understand global nuclear architecture with single locus resolution.

Another fundamental challenge is to characterize cardiac transcriptional activity and gene regulation *in vivo*. Approaches using 5'fluorouridine, or other similar analogues to selectively label for RNA, would allow us to describe nuclear function with transcription as a direct readout, on a cell-by-cell basis and with respect to cardiac anatomy in healthy and disease states (Are given sections of the myocardium more susceptible to changes in activity, if at all, with stress? Or, are all cells of the heart equally affected by a given stress?). Additionally, due to the nature of most studies being based on populations of cells (either mixed populations from entire tissue or isolated cardiomyocytes), very little is known regarding the contributions of multinucleation and ploidy to RNA and protein synthesis in the cardiomyocyte (10). A transcription run-on assay would provide a measure of activity for each cardiac nucleus within the cell and help address whether both are active or if there is differential activity. It may be that one is quiescent and may become active upon stress—these changes may be triggered near sites in the heart that sense the most mechanical stress or they may be dependent on cellular environment and paracrine signaling. The transcriptional responses to stress may also be influenced by genetics and thus be mouse strain dependent, contributing to the phenotypic differences in susceptible versus resistant strains.

The hybrid mouse diversity panel has been a powerful tool that can be used to model the diversity of the human population and understand the genetic influences of heart failure

susceptibility. This resource can be used to describe shared foundations of global cardiac genomic architecture across different mouse strains and the differences that may contribute to disease development. Interestingly, strains of mice already show differences in DNA methylation at the basal state (11), but how these variations in DNA modifications, along with other protein factors, interact to create a genomic structure that is both sufficient to confer specific cell type and also contribute to diverse expression profiles is an interesting question. Through understanding this foundation, we can use these features of global architecture to classify the basis of disease susceptibility. We showed that genetics cannot directly predict gene expression and in the final chapter we show that chromatin architecture can be indicative of gene expression. Characterizing the effects of genetic variability on this architecture can better elucidate the contributions of DNA sequence and chromatin proteins to affect global architecture and gene expression. I would hypothesize mice that are more susceptible to developing heart failure have higher DNA plasticity. By identifying how readily pathological genes are turned on, as a result of situation within local and global chromatin environments, in different strains of mice, we can reveal key features important for setting the basis for cardiac gene expression. Some of these frameworks may be weaker than others, allowing for a more rapid response to stress. On the other hand, having compliant chromatin architecture may allow for better adaptability to stress. Further dissection of different mouse strains can elucidate the properties of chromatin architecture and cardiac transcription factories that affect disease susceptibility. This project has identified chromatin structural genes potentially important for mediating cardiac gene expression, established a role for chromatin as a contributor of transcriptome diversity and provided direct evidence for changes in chromatin structure due to pathological stress. As emphasized with the hybrid mouse diversity panel studies, there is no single factor determining cardiac phenotype but a combination of gene interactions that may be driven by a common chromatin regulatory mechanism.

Future Directions: References

1. Clause KC, Liu LJ, Tobita K. Directed stem cell differentiation: the role of physical forces. Cell Commun Adhes. 2010;17(2):48-54. doi: 10.3109/15419061.2010.492535. PubMed PMID: 20560867; PMCID: PMC3285265.
2. Spencer VA, Xu R, Bissell MJ. Extracellular matrix, nuclear and chromatin structure, and gene expression in normal tissues and malignant tumors: a work in progress. Adv Cancer Res. 2007;97:275-94. doi: 10.1016/S0065-230X(06)97012-2. PubMed PMID: 17419950; PMCID: PMC2912285.
3. Dixon JR, Jung I, Selvaraj S, Shen Y, Antosiewicz-Bourget JE, Lee AY, Ye Z, Kim A, Rajagopal N, Xie W, Diao Y, Liang J, Zhao H, Lobanenkov VV, Ecker JR, Thomson JA, Ren B. Chromatin architecture reorganization during stem cell differentiation. Nature. 2015;518(7539):331-6. doi: 10.1038/nature14222. PubMed PMID: 25693564; PMCID: PMC4515363.
4. Meshorer E, Misteli T. Chromatin in pluripotent embryonic stem cells and differentiation. Nat Rev Mol Cell Biol. 2006;7(7):540-6. doi: 10.1038/nrm1938. PubMed PMID: 16723974.
5. Pajerowski JD, Dahl KN, Zhong FL, Sammak PJ, Discher DE. Physical plasticity of the nucleus in stem cell differentiation. Proc Natl Acad Sci U S A. 2007;104(40):15619-24. doi: 10.1073/pnas.0702576104. PubMed PMID: 17893336; PMCID: PMC2000408.
6. Li G, Ruan X, Auerbach RK, Sandhu KS, Zheng M, Wang P, Poh HM, Goh Y, Lim J, Zhang J, Sim HS, Peh SQ, Mulawadi FH, Ong CT, Orlov YL, Hong S, Zhang Z, Landt S, Raha D, Euskirchen G, Wei CL, Ge W, Wang H, Davis C, Fisher-Aylor KI, Mortazavi A, Gerstein M, Gingeras T, Wold B, Sun Y, Fullwood MJ, Cheung E, Liu E, Sung WK, Snyder M, Ruan Y. Extensive promoter-centered chromatin interactions provide a topological basis for transcription regulation. Cell. 2012;148(1-2):84-98. doi: 10.1016/j.cell.2011.12.014. PubMed PMID: 22265404; PMCID: PMC3339270.

7. Monte E, Rosa-Garrido M, Karbassi E, Chen H, Lopez R, Rau CD, Wang J, Nelson SF, Wu Y, Stefani E, Lusis AJ, Wang Y, Kurdistani SK, Franklin S, Vondriska TM. Reciprocal Regulation of the Cardiac Epigenome by Chromatin Structural Proteins Hmgb and Ctcf: IMPLICATIONS FOR TRANSCRIPTIONAL REGULATION. J Biol Chem. 2016;291(30):15428-46. doi: 10.1074/jbc.M116.719633. PubMed PMID: 27226577; PMCID: PMC4957031.
8. Lieberman-Aiden E, van Berkum NL, Williams L, Imakaev M, Ragoczy T, Telling A, Amit I, Lajoie BR, Sabo PJ, Dorschner MO, Sandstrom R, Bernstein B, Bender MA, Groudine M, Gnirke A, Stamatoyannopoulos J, Mirny LA, Lander ES, Dekker J. Comprehensive mapping of long-range interactions reveals folding principles of the human genome. Science. 2009;326(5950):289-93. doi: 10.1126/science.1181369. PubMed PMID: 19815776; PMCID: PMC2858594.
9. Guelen L, Pagie L, Brasset E, Meuleman W, Faza MB, Talhout W, Eussen BH, de Klein A, Wessels L, de Laat W, van Steensel B. Domain organization of human chromosomes revealed by mapping of nuclear lamina interactions (vol 453, pg 948, 2008). Nature. 2013;500(7461):242-. doi: 10.1038/nature12316. PubMed PMID: WOS:000322825500042.
10. Bensley JG, De Matteo R, Harding R, Black MJ. Three-dimensional direct measurement of cardiomyocyte volume, nuclearity, and ploidy in thick histological sections. Sci Rep. 2016;6:23756. doi: 10.1038/srep23756. PubMed PMID: 27048757; PMCID: PMC4822151.
11. Chen HD, Orozco LD, Wang J, Rau CD, Rubbi L, Ren SX, Wang YB, Pellegrini M, Lusis AJ, Vondriska TM. DNA Methylation Indicates Susceptibility to Isoproterenol-Induced Cardiac Pathology and Is Associated With Chromatin States. Circulation Research. 2016;118(5):786-97. doi: 10.1161/Circresaha.115.305298. PubMed PMID: WOS:000371747700007.